S-CUBED

SSS-R-84-6534

RESIDUAL STRESSES AND THERMO-MECHANICAL BEHAVIOR OF METAL-MATRIX COMPOSITES

Final Report
(DRAFT)

M. H. Rice
G. A. Gurtman

"The views and conclusions contained in this document are those of the authors and should not be interpreted as necessarily representing the official policies, either expressed or implied, of the Defense Advanced Research Projects Agency or the U.S. Government."

Naval Research Laboratory
Washington, D. C.

January, 1984

P. O. Box 1620, La Jolla, California 92038-1620
(619) 453-0060

ARPA Order No: 4555
Contract No: N00014-82-C-2322
Contract Dates: July 1982 through July 1983
Principal Investigator: Dr. M. H. Rice
(619)453-0060 X472

UNCLASSIFIED
ITY CLASSIFICATION OF THIS PAGE

5606[illegible]

REPORT DOCUMENTATION PAGE

EPORT SECURITY CLASSIFICATION	1b. RESTRICTIVE MARKINGS
ECURITY CLASSIFICATION AUTHORITY	3. DISTRIBUTION/AVAILABILITY OF REPORT APPROVED FOR PUBLIC RELEASE DISTRIBUTION UNLIMITED
ECLASSIFICATION/DOWNGRADING SCHEDULE	
RFORMING ORGANIZATION REPORT NUMBER(S) SSS-R-84-6534	5. MONITORING ORGANIZATION REPORT NUMBER(S)
AME OF PERFORMING ORGANIZATION S-CUBED	6b. OFFICE SYMBOL (If applicable)
	7a. NAME OF MONITORING ORGANIZATION Naval Research Laboratory
DDRESS (City, State and ZIP Code) P.O. Box 1620 La Jolla, CA 92038-1620	7b. ADDRESS (City, State and ZIP Code) Naval Research Laboratory Washington, D.C. 20375
AME OF FUNDING/SPONSORING RGANIZATION Naval Research Laboratory	8b. OFFICE SYMBOL (If applicable)
	9. PROCUREMENT INSTRUMENT IDENTIFICATION NUMBER Proposal No. 8610463/R1
DDRESS (City, State and ZIP Code) Naval Research Laboratory Washington, D.C. 20375	10. SOURCE OF FUNDING NOS.

PROGRAM ELEMENT NO.	PROJECT NO.	TASK NO.	WORK UNIT NO.

ITLE (Include Security Classification)
ESIDUAL STRESSES AND THERMO-MECHANICAL BE-AVIOR OF METAL-MATRIX COMPOSITES

ERSONAL AUTHOR(S)
M. H. Rice, G. A. Gurtman

TYPE OF REPORT	13b. TIME COVERED	14. DATE OF REPORT (Yr., Mo., Day)	15. PAGE COUNT
Final (Draft)	FROM 7/82 TO 7/83	1984, January 27	176

UPPLEMENTARY NOTATION

COSATI CODES		
ELD	GROUP	SUB. GR.

18. SUBJECT TERMS (Continue on reverse if necessary and identify by block number)
Metal-matrix composites; Silicon-carbide/Aluminum; Graphite/Alumimun; Cross-plied laminate; Tungsten/Aluminum; Residual stresses

BSTRACT (Continue on reverse if necessary and identify by block number)

(U) A plastic-flow code was used to calculate microscopic stress-temperature histories in metal-matrix composites during a cooling and reheating cycle. Stress results are given for graphite/aluminum, tungsten/aluminum and silicon-carbide aluminum composites. For the graphite/aluminum material a parametric study was carried out on the effect of variations in various fiber properties on the calculated stresses. A computer code is presented for calculating the thermo-elastic properties of cross-plied laminates from those of the inidividual plies on from the fiber and matrix properties appropriate to each ply. Modifications to a code (PRUFC) developed previously for computing the properties of a unidirectionally reinforced composite from those of the fiber and matrix components are described. A formally exact two-dimensional Fourier-series solution is presented for determining the stresses and deformation of a plate subjected to an arbitrary, transverse temperature distribution. Numerical results are given for several temperature profiles, including a discontinuous step-function distribution.

ISTRIBUTION/AVAILABILITY OF ABSTRACT LASSIFIED/UNLIMITED ☒ SAME AS RPT. ☐ DTIC USERS ☐	21. ABSTRACT SECURITY CLASSIFICATION Unclassified
NAME OF RESPONSIBLE INDIVIDUAL M. H. Rice	22b. TELEPHONE NUMBER (Include Area Code) (619)453-0060X473
	22c. OFFICE SYMBOL

FORM 1473, 83 APR EDITION OF 1 JAN 73 IS OBSOLETE.

UNCLASSIFIED
SECURITY CLASSIFICATION OF THIS PAGE

Block 18. (continued)

Thermal deformation
Thermo-elastic properties

ACKNOWLEDGEMENT

The authors wish to thank Lt. Col. L. Jacobson of the Defense Advanced Research Projects Agency for his support in initiating the work described herein. We are also grateful to Dr. S. C. Sanday and Mr. T. A. Hahn for providing technical direction and guidance throughout the course of this program.

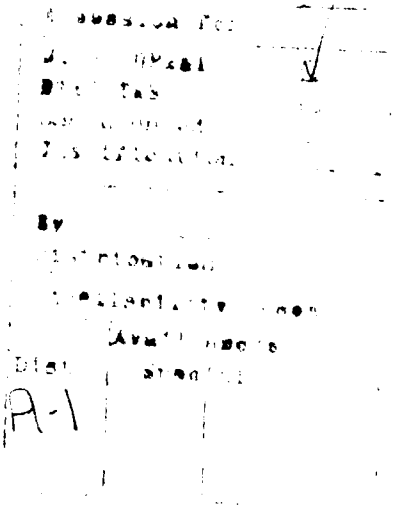

(This Page Left Blank)

TABLE OF CONTENTS

LIST OF FIGURES

LIST OF FIGURES (cont'd)

LIST OF FIGURES (cont'd)

LIST OF FIGURES (cont'd)

LIST OF FIGURES (cont'd)

LIST OF FIGURES (cont'd)

(This Page Left Blank)

LIST OF TABLES

(This Page Left Blank)

1. INTRODUCTION

One of the primary tasks in the present effort was the use of the S-CUBED plastic-flow code to calculate for typical metal-matrix composites the residual microscopic stresses which would result from given fabrication and/or processing cycles. Such calculations have been done for graphite/aluminum, tungsten/aluminum and silicon-carbide/aluminum unidirectionally reinforced fibrous composites. In particular, a rather extensive series of parametric calculations was performed for the graphite/aluminum case to determine the changes in the aluminum matrix residual stresses which would result from variations and/or uncertainties in the thermoelastic properties of the graphite fibers.

The S-CUBED plastic-flow code, which uses the concentric-cylinder approximation for unidirectional composites, is described in detail in Ref. 1. Briefly, the equations of elastic-plastic flow are integrated numerically as the composite is cooled from an initial stress-free state and then reheated. The fibers are assumed to remain perfectly elastic throughout the cooling and heating cycle, and they may be treated as being anisotropic-transversely isotropic. The matrix material is assumed to be isotropic and is allowed to undergo plastic flow when its stress state reaches the yield surface. The magnitude of the yield stress may depend both on the temperature and the degree of plastic flow.

Results of the parametric study of a graphite/aluminum-2024 composite are given in Section 2, where stress-temperature histories are given for the axial stress, hoop stress, and fiber-matrix interfacial radial stress. The temperature cycle used for these calculations is a cooling from a consolidation temperature of 930°F to a minimum temperature of -240°F and then reheating until the aluminum matrix again reaches the yield surface. Results are given both for the T0 temper (slow cooling) and the T4 temper (rapid quench) thermoelastic properties and yield strength models used for 6061 and 2024 aluminums are detailed in Appendix A.

Results of two calculations on a tungsten/aluminum composite are given in Section 3, and similar calculations on a silicon carbide/aluminum composite are described in Section 4.

In Section 5, a computational method is presented for determining the elastic moduli and thermal expansion characteristics of cross-plied laminates from the properties of the individual unidirectionally reinforced composite plies. Calculated results as a function of lay-up angle are given for a laminate made up of graphite/aluminum layers. A computer code has been constructed for treating a laminate with plies in up to three different directions. The properties of the individual plies may be calculated directly from the fiber and matrix properties if desired. The code also provides values for the intra-ply thermal stress derivatives about an initial stress-free state. A FORTRAN listing of the code is given in Appendix B.

A consideration of numerical results from a finite-element code calculation as given in a recent report by Hashin and Humphreys (Ref. 2) has led to a revision of the PRUFC code. This code was recently developed at S-CUBED for calculating the properties of unidirectional fibrous composites from those of the constituents (Ref. 3). In Section 6, various ways of obtaining the transverse properties of a composite within the context of the concentric-cylinder approximation used in the PRUFC code are examined and compared with the results of a more nearly exact (but much more expensive to run) finite-element code computation. A comparison of residual stresses calculated with the S-CUBED plastic-flow code (concentric-cylinder approximation) with those obtained from the finite-element method is also given in Section 6. The agreement is quite good.

In Section 7, a two-dimensional Fourier-series solution is presented for the stresses and thermal deformations in an elastic plate subjected to an arbitrary transverse temperature distribution.

A summary and some general conclusions are offered in Section 8.

2. GRAPHITE/ALUMINUM PARAMETER STUDY

A series of calculations was performed to determine the sensitivity of the matrix residual stresses to variations in various fiber properties. Eignteen different sets of graphite fiber properties were used. For each set of fiber properties, results were obtained for a slow cooling (T0 temper) and a rapid quench (T4 temper) of the 2024 aluminum matrix from an initial consolidation temperature of 930°F to a minimum temperature of -240°F. The fiber properties are tabulated in Table 2.1, and the thermoelastic properties and yield-stress models used for the 2024 aluminum are summarized in Appendix A. The room temperature thermoelastic properties of the composite as calculated with the latest version of the PRUFC code (Section 6) for each set of fiber properties are given in Table 2.2, the values being appropriate to the case where the aluminum matrix is not on its yield surface.

2.1 CALCULATIONAL RESULTS

Plots of the volume-averaged (matrix) axial stress, volume-averaged hoop stress, and the radial stress at the fiber-matrix interface as a function of temperature are given as Figures 2.1 through 2.42. The temperature cycle is a reheating from -240°F after a slow (T0) or fast (T4) cooldown from an initial consolidation temperature of 930°F. For this high initial temperature, the matrix is completely yielded after only a few degrees (<30°F) of cooling, and the changes in the stress state upon further cooling are due primarily to the variation of yield strength with temperature and plastic flow. Upon reheating from -240°F, however, the matrix immediately drops below the yield surface; and the variation in stress with temperature is then governed by the (reversible) equations of thermoelasticity. As the reheating continues, the matrix will eventually again reach its yield surface, as indicated by the open circles on the reheating curves. The plots are

TABLE 2.1

FIBER PROPERTIES USED IN THE PARAMETRIC RESIDUAL-STRESS STUDY
OF A GRAPHITE/ALUMINUM 2024 UNIDIRECTIONALLY REINFORCED COMPOSITE

Calc. No.	1	2	3	4	5	6	7	8	9	10	11	12	13	14	15	16	17	18
n_f*	0.45	=**	=	=	=	=	=	=	=	=	=	=	=	=	0.37	=	0.30	0.60
E_x(Msi)	1	=	=	=	=	=	=	=	=	=	=	=	1.5	2.0	1.25	=	1.5	=
E_z(Msi)	35	=	=	=	=	=	=	=	=	=	50	100	50	=	35	=	50	=
ν_{xy}†	0.3	=	=	=	=	=	=	=	0.4	0.5	0.4	=	=	=	0.45	=	0.4	=
ν_{xz}	0.3	=	=	=	=	=	0.4	0.5	0.4	=	=	=	=	=	0.41	=	0.4	=
α_x(10^{-6}°F^{-1})	5	=	=	10	15	20	15	=	=	=	=	=	=	=	2.7	15	=	=
α_z(10^{-6}°F^{-1})	0.5	-1	-1.5	-1	=	=	=	=	=	=	=	=	=	=	-0.57	=	-1	=

* n_f is the fiber volume fraction.

** The "equal" sign indicates a value the same as that in the preceding column.

† For the Poisson's ratios, the second subscript is the direction of the applied stress (fibers parallel to the z-axis).

TABLE 2.2

ROOM-TEMPERATURE G/AL 2024 COMPOSITE PROPERTIES AS CALCULATED WITH THE PRUFC CODE (ELASTIC MATRIX) FOR EACH SET OF FIBER PROPERTIES AS GIVEN IN TABLE 2.1

Calc. No	1	2	3	4	5	6	7	8	9	10	11	12	13	14	15	16	17	18
Vol. Frac.	0.45	=	=	=	=	=	=	=	=	=	=	=	=	=	0.37	=	0.30	0.60
E_x(Msi)	4.75	=	=	=	=	=	=	4.74	4.75	4.78	=	4.82	5.32	5.81	5.83	=	6.89	4.05
E_z(Msi)	21.53	=	=	=	=	=	=	21.55	21.53	=	28.28	50.78	28.28	=	19.57	=	22.36	34.21
ν_{xy}	0.300	=	=	=	=	=	0.298	0.296	0.322	0.349	0.329	0.341	0.334	0.338	0.336	=	=	0.330
ν_{xz}	0.326	=	=	=	=	=	0.340	0.355	0.341	0.343	0.341	=	0.345	0.347	0.342	=	0.339	0.353
$\alpha_x(10^{-6}{}^\circ F^{-1})$	13.69	13.98	14.08	14.70	15.43	16.15	15.38	15.33	15.34	15.30	15.64	16.05	15.54	15.46	13.12	14.97	15.15	15.68
$\alpha_z(10^{-6}{}^\circ F^{-1})$	3.72	2.62	2.26	2.61	=	2.60	=	2.59	2.60	=	1.74	0.53	1.74	=	3.76	3.82	3.41	0.64
G_{xy}(Mxi)	1.83	=	=	=	=	=	=	=	1.80	1.77	1.80	=	1.99	2.17	2.18	=	2.58	1.52

terminated at this point due to the limitations of the present version of the S-CUBED plastic-flow code. Physically, if the reheating were continued beyond the yield point, the slope of the stress-temperature curves would exhibit a discontinuous sharp decrease in absolute magnitude with a subsequent return to zero stress at the melt point. As long as the temperature at the upper yield point is not exceeded, subsequent cooling will cause the stresses to retrace the original heating path from -240°F. (The possible effect of creep on the matrix residual stresses is not treated here.)

The effect on the matrix stress of a variation of the axial coefficient of thermal expansion for the fibers is shown in Figures 2.1 through 2.6. Neither the axial, hoop, nor interfacial radial stress shows a marked variation for the range $\alpha_z = 0.5 \times 10^{-6}$ $°F^{-1}$ to $\alpha_z = -1.5 \times 10^{-6} °F^{-1}$ for the fiber expansion coefficient. The reversible, elastic portion of the axial stress shows the greatest dependency.

The effect of a variation in the fibers transverse coefficient of thermal expansion on the matrix stresses is depicted in Figures 2.7 through 2.12. The axial stress does not exhibit a strong dependency, but the hoop and interfacial radial stresses show a marked variation. Perhaps it is not surprising that as the fiber's transverse expansion coefficient approaches that of the matrix, the hoop and radial residual stresses become small. Here it should be pointed out that a negative (compressive) interfacial radial stress would increase the effective fiber-matrix bond strength; hence a moderately large negative value might be desirable.

A variation of the fiber's Poisson's ratios, as shown in Figures 2.13 through 2.18, has only a minute effect on all three of the calculated stress-temperature histories.

An increase in the fiber's axial elastic modulus from 50 Msi to 100 Msi, Figures 2.19 through 2.24, does produce a more rapid decrease in the matrix axial stress upon reheating from -240°F but

has a completely negligible effect on the hoop and interfacial radial stress-temperature histories.

A parametric variation in the transverse elastic modulus of the fibers leads to the calculated results for the matrix stresses plotted in Figures 2.25 through 2.30. Doubling the fiber modulus from 1 Msi to 2 Msi has a negligible effect on the axial matrix stresses, and the effect on the calculated hoop and interfacial radial stresses is also small.

For the calculations discussed above, the fiber volume fraction in all cases is $n_f = 0.45$. In Figures 2.31 through 2.36, results are plotted for a fiber volume fraction of $n_f = 0.37$ for two values of the fiber's transverse thermal expansion coefficient. As was the case with Calculations 2, 4 and 6, the larger value of the transverse expansion coefficient produces a significant decrease in the magnitudes of the hoop stresses and interfacial radial stresses.

Results for two different fiber volume fractions of $n_f = 0.30$ and $n_f = 0.60$ are plotted in Figures 2.37 through 2.42. The residual stresses are somewhat higher in magnitude for the larger volume fraction.

2.2 SUMMARY AND CONCLUSIONS

In general, for all of the fiber parameter variations discussed above, the calculations indicate that the axial matrix stress at room temperature after a rapid quench from 930°F to -240°F (T4 temper) will lie in the range from about 30 ksi to 40 ksi (tensile) and that the matrix will remain elastic up to about 600°F upon reheating. The residual hoop stress at room temperature in all cases is tensile and ranges from about 10 ksi to 20 ksi in magnitude if the fiber's transverse coefficient of thermal expansion is taken to be less than or equal to that of the matrix ($\sim 12.4 \times 10^{-6} °F^{-1}$ for 2024 aluminum at room temperature). Further, the interfacial

radial stress between the fiber and matrix is compressive as long as the fiber's transverse expansion coefficient does not exceed that of the matrix, the magnitude ranging from about 2 ksi to 10 ksi over the range of material parameters used in these calculations. This would appear to be a significant result, since a compressive interfacial stress is desirable as an aid in maintaining the integrity of the fiber-matrix bond. This bond is critical, since it is the source of the (localized) shear forces which are ultimately responsible for equilibrating axial strain between the fiber and matrix components.

For the slow cool to -240°F (T0 temper) the axial residual stresses at room temperature for all cases considered here are very close to zero, a situation which would appear to be desirable if the composite is to be subjected to subsequent mechanical loading. Because of the reduced yield strength of the T0 temper with respect to that of the T4, however, the matrix will again reach its yield point after reheating to between 200°F and 300°F. Even though the axial stress at room temperature is much lower for the T0 temper than the T4, the hoop stress will still be about 5 ksi to 10 ksi in tension for the range of fiber parameters considered. As long as the fiber's transverse expansion coefficient is less than that of the matrix, the interfacial radial stresses would still be compressive according to the calculations, the magnitudes being in the range from 2 ksi to about 8 ksi.

A room temperature axial residual stress of 30 ksi to 40 ksi in the matrix as calculated for the T4 temper would be undesirable if the composite were to be subjected to large tensile loads. This is due to the fact that the matrix would reach the yield surface, with a consequent degradation of the axial modulus, at a lower applied load than it would if the matrix stress were initially near zero. For compressive loads about the ambient state, however, an initial tensile residual stress might be useful. In any case, it is not immediately apparent how the room temperature residual stress for the T4 temper might be reduced. Continued heating beyond the

yield point of ~600°F would result in a stress temperature path that must ultimately pass through zero stress at the melt point. A recooling from any point on this path segment would result in a (reversible) elastic curve for the axial stress that would lie to the right of the initial heating curve from -240°F, and consequently the room temperature axial residual stress would be higher than it was before. This might be alleviated however, if creep of the matrix material was taken into account.

Some reduction of the axial residual stress would be achieved by cooling below -240°F initially. No explicit calculation was done, but it appears from an extrapolation of the curves presented here that cooling to ~-320°F (liquid nitrogen) would reduce the axial residual stress by about 5 ksi or 10 ksi.

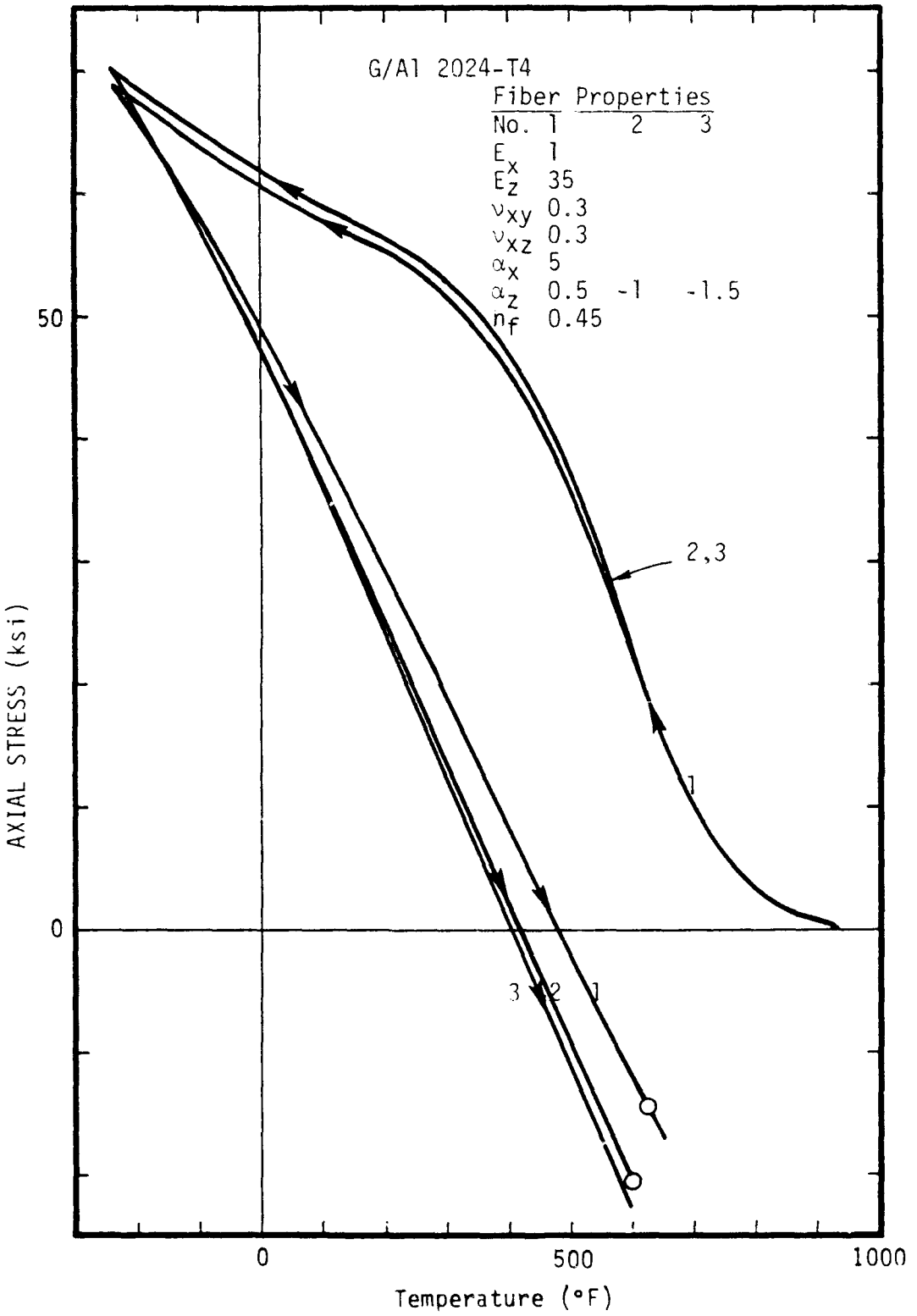

Figure 2.1. Volume-averaged axial stress versus temperature for the matrix of a graphite/aluminum composite (rapid cooling).

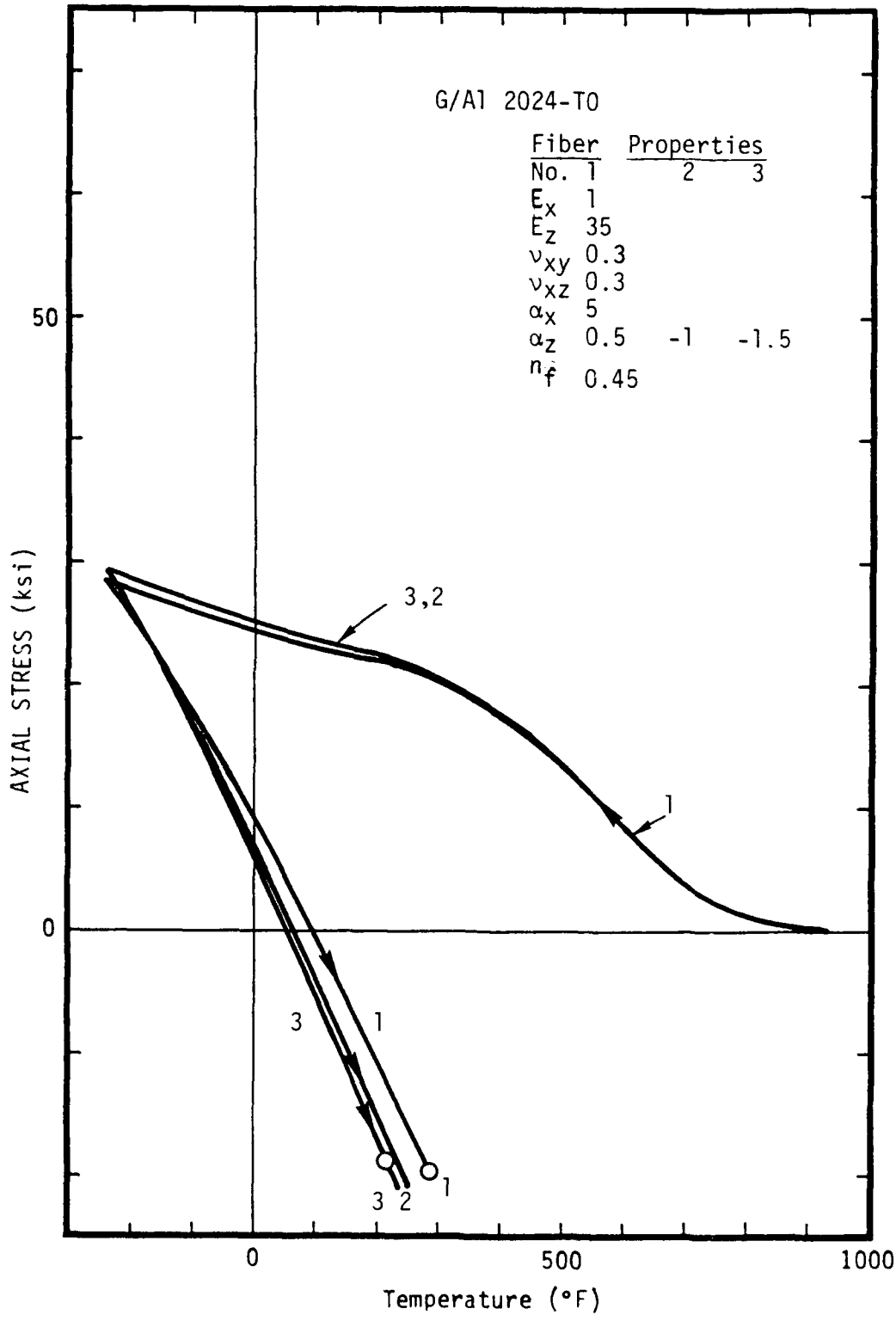

Figure 2.2. Volume-averaged axial stress versus temperature for the matrix of a graphite/aluminum composite (slow cooling).

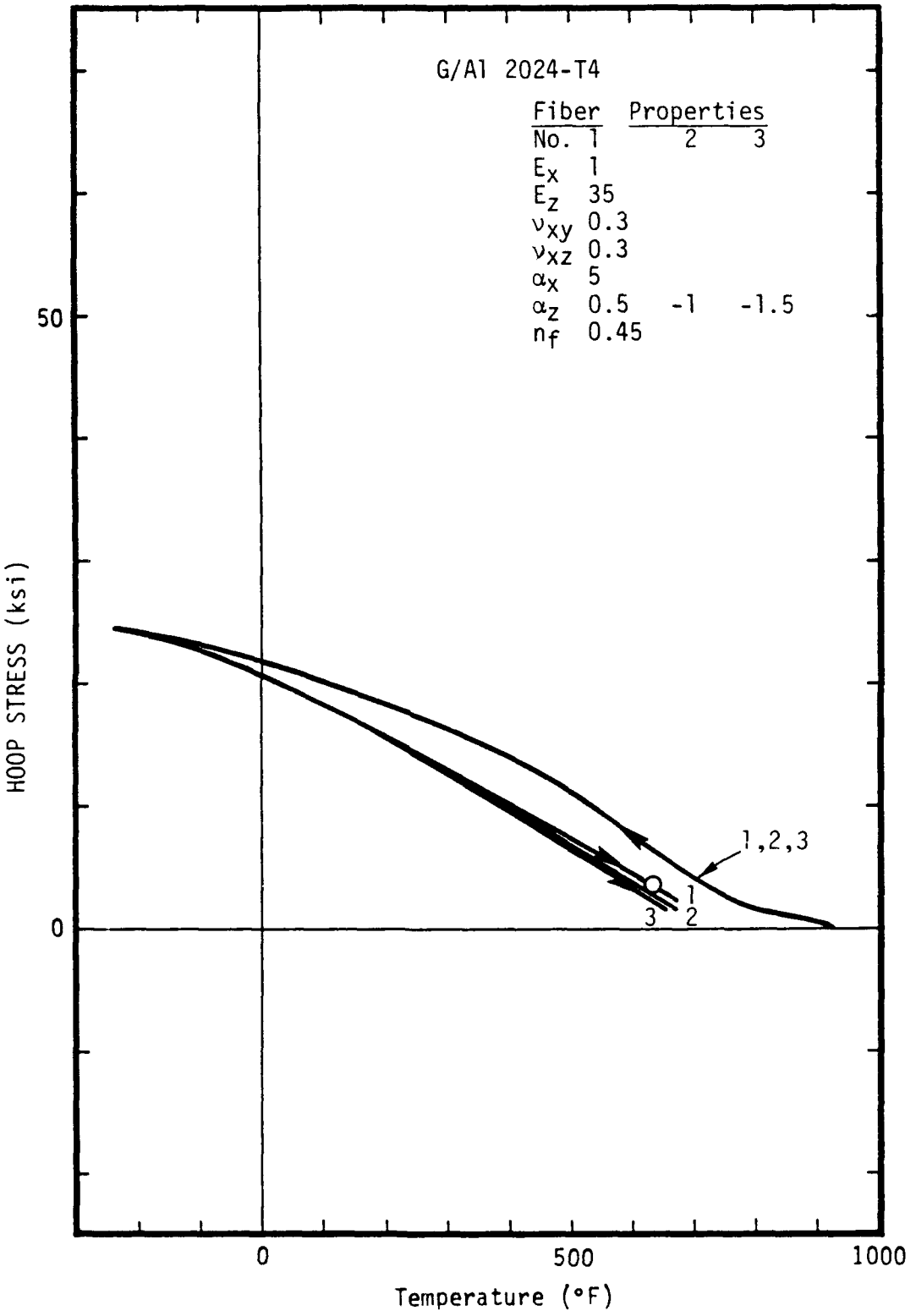

Figure 2.3. Volume-averaged hoop stress versus temperature for the matrix of a graphite/aluminum composite (rapid cooling).

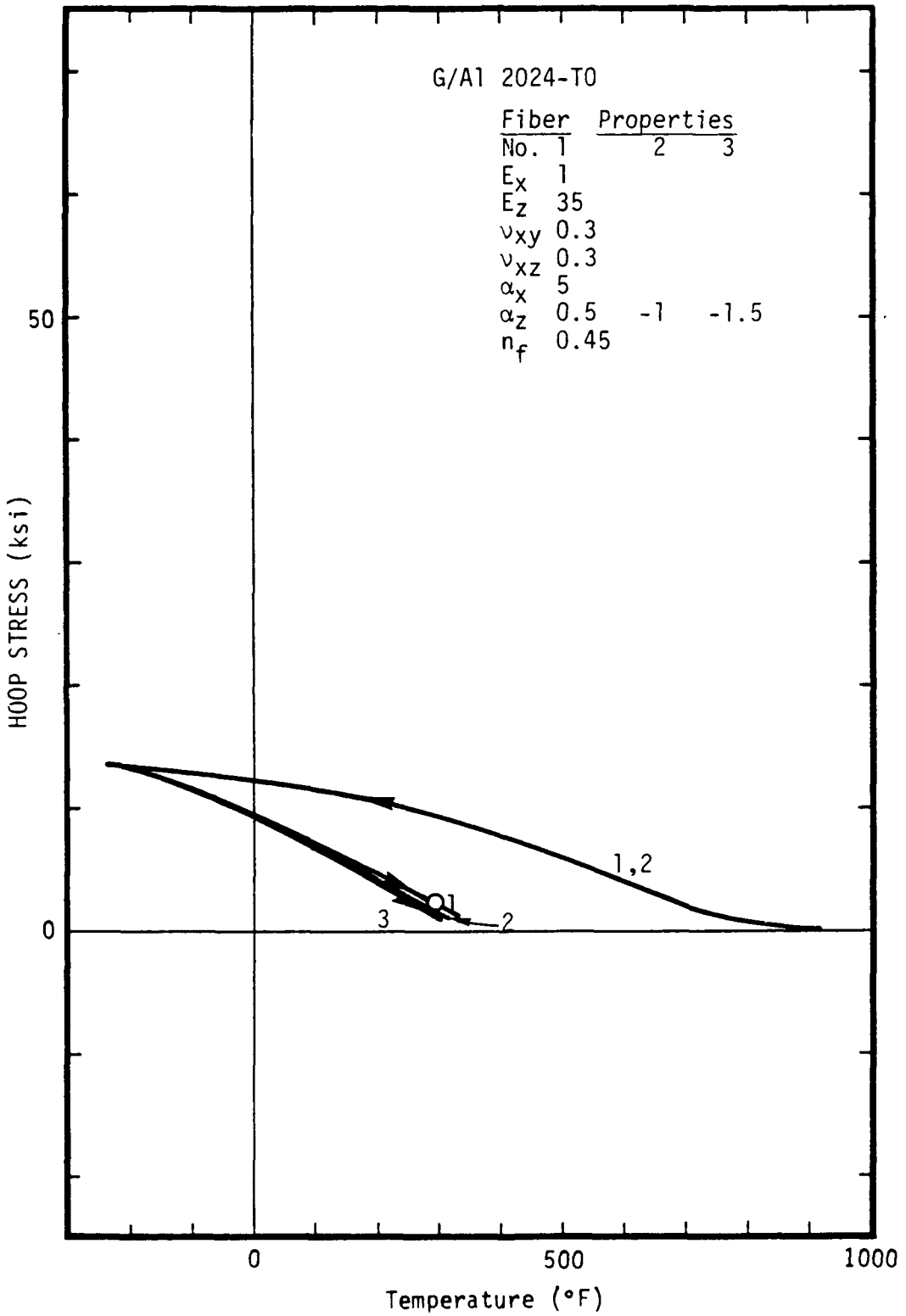

Figure 2.4. Volume-averaged hoop stress versus temperature for the matrix of a graphite/aluminum composite (slow cooling).

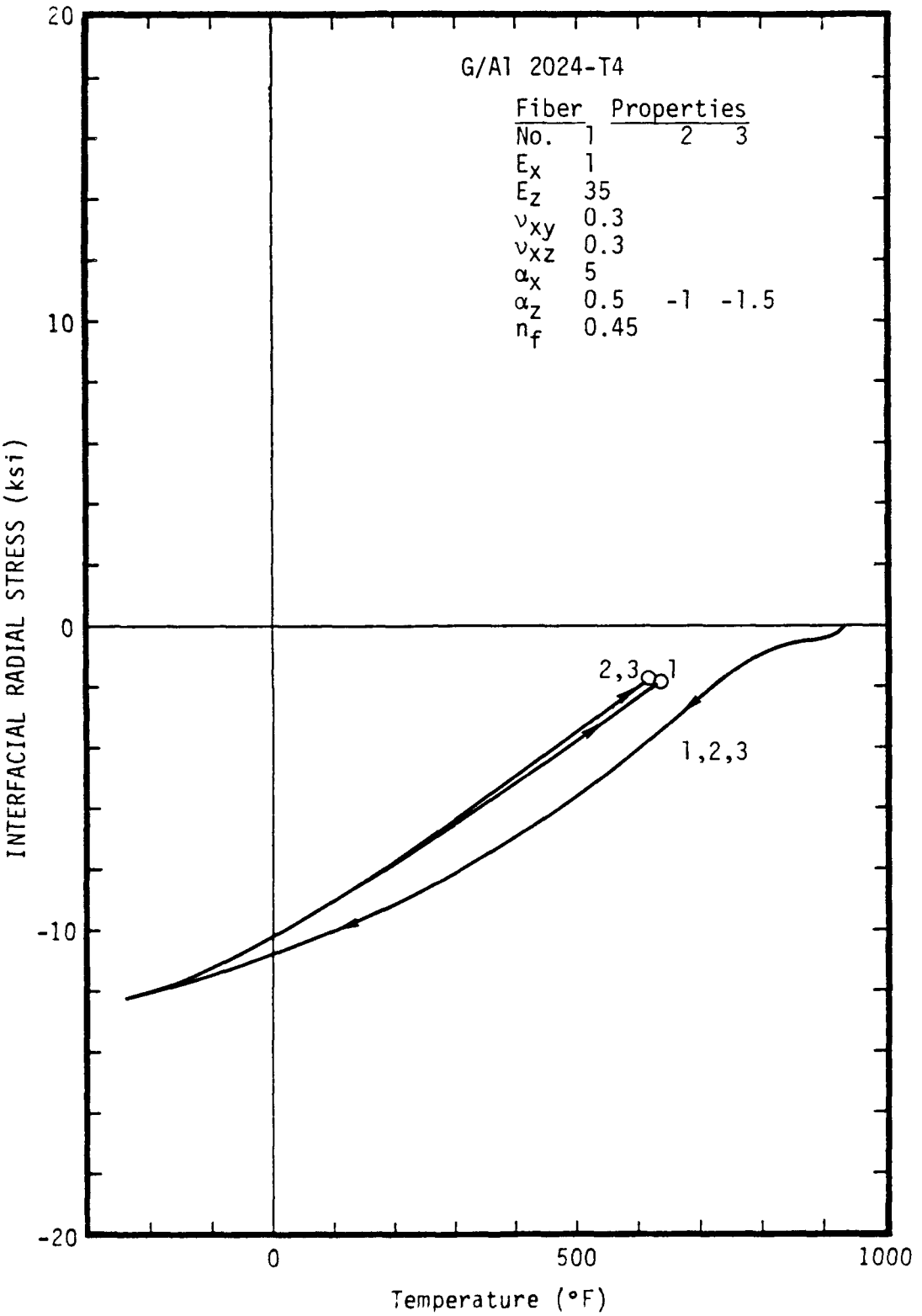

Figure 2.5. Radial stress versus temperature at the fiber-matrix interface of a graphite/aluminum composite (rapid cooling).

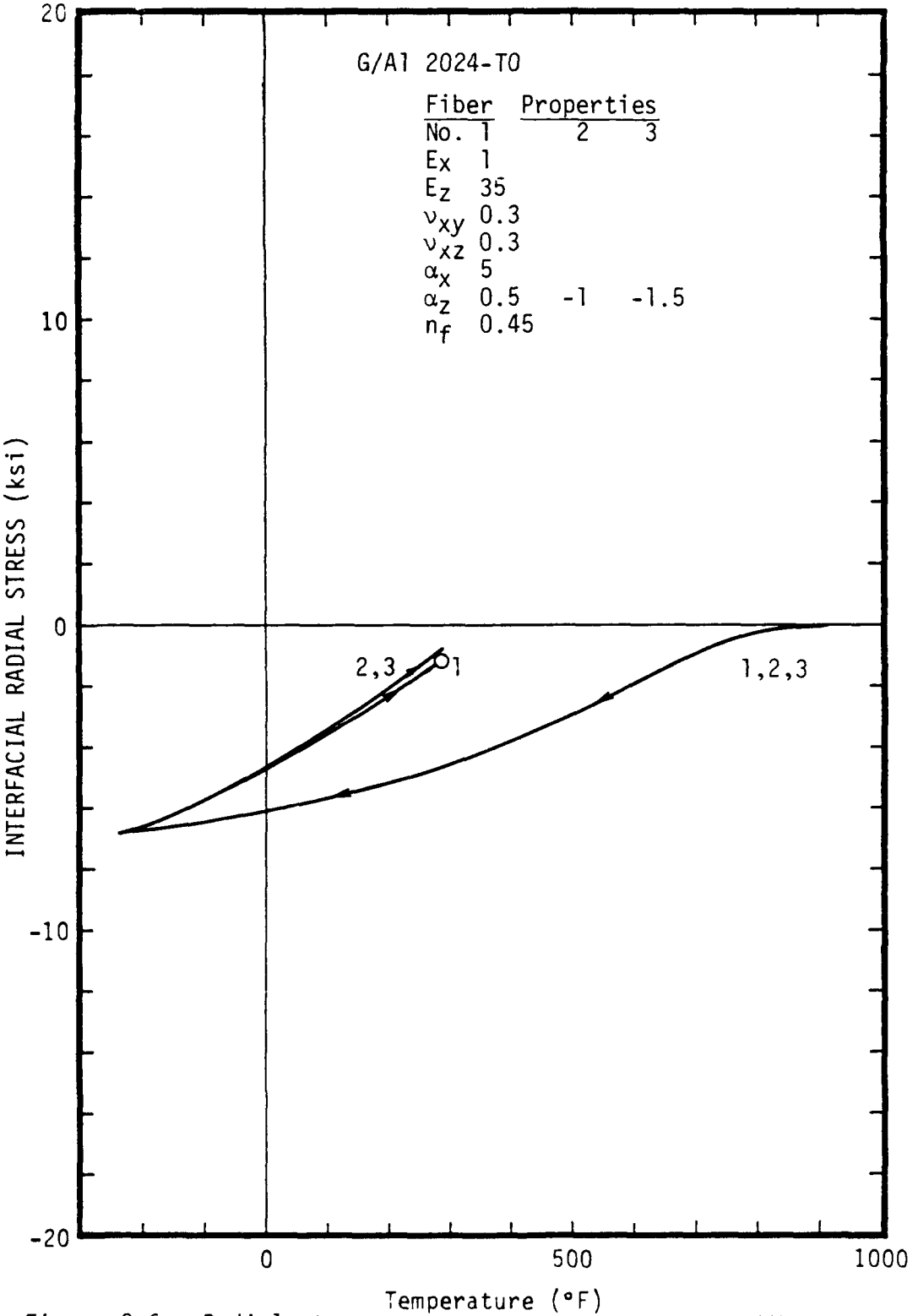

Figure 2.6. Radial stress versus temperature at the fiber-matrix interface of a graphite/aluminum composite (slow cooling).

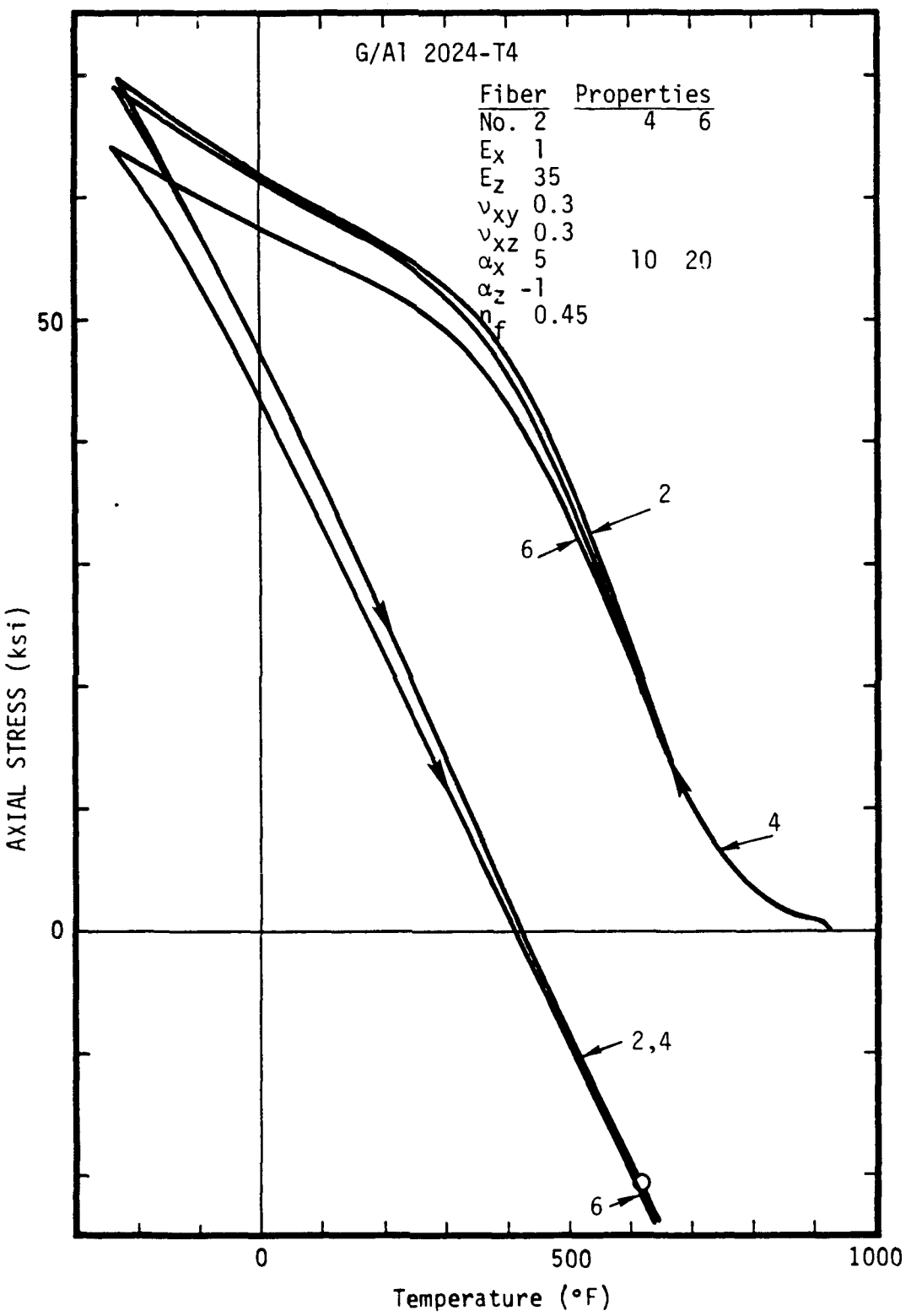

Figure 2.7. Volume-averaged axial stress versus temperature for the matrix of a graphite/aluminum composite (rapid cooling).

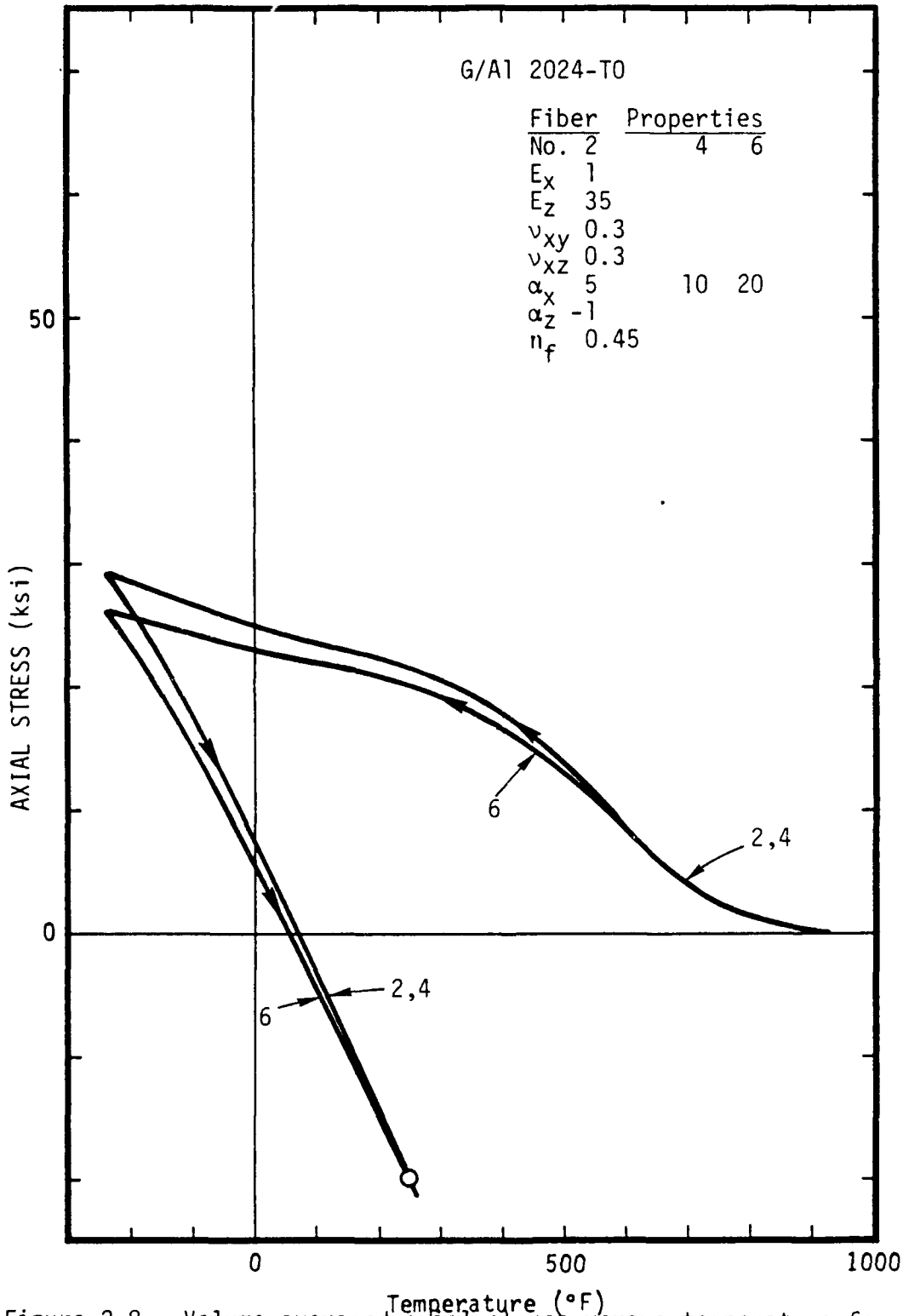

Figure 2.8. Volume-averaged axial stress versus temperature for the matrix of a graphite/aluminum composite (slow cooling).

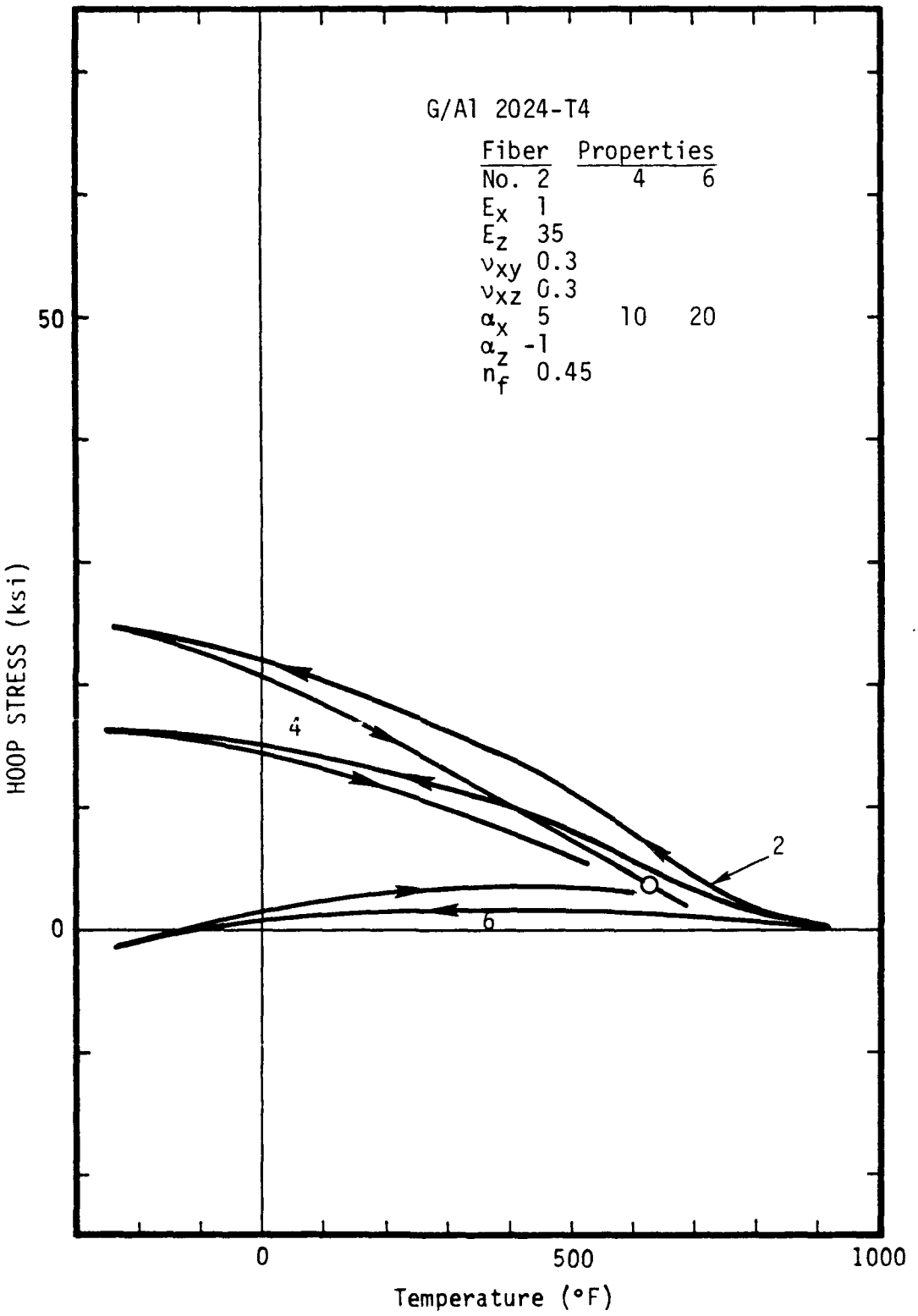

Figure 2.9. Volume-averaged hoop stress versus temperature for the matrix of a graphite/aluminum composite (rapid cooling).

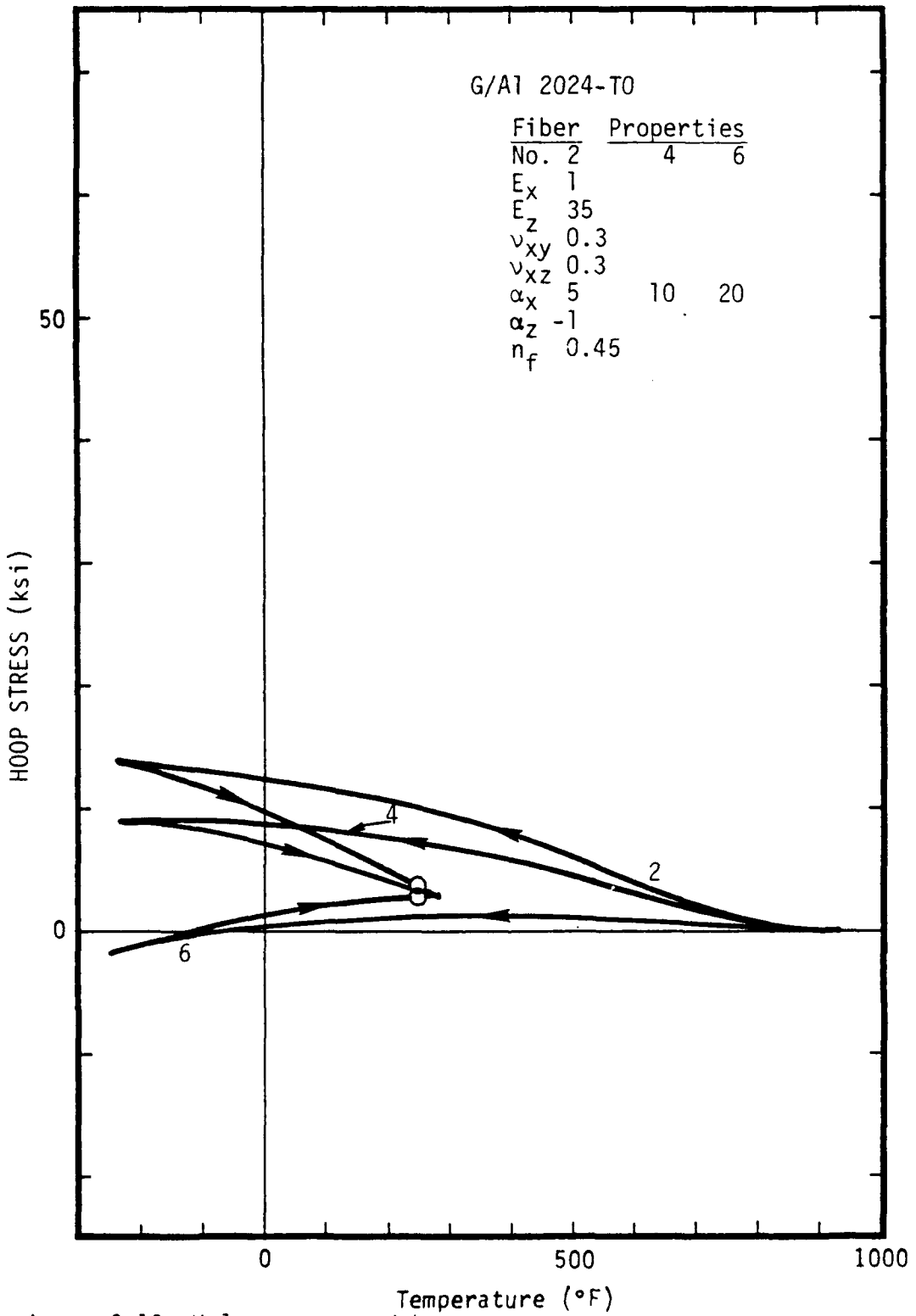

Figure 2.10. Volume-averaged hoop stress versus temperature for the matrix of a graphite/aluminum composite (slow cooling).

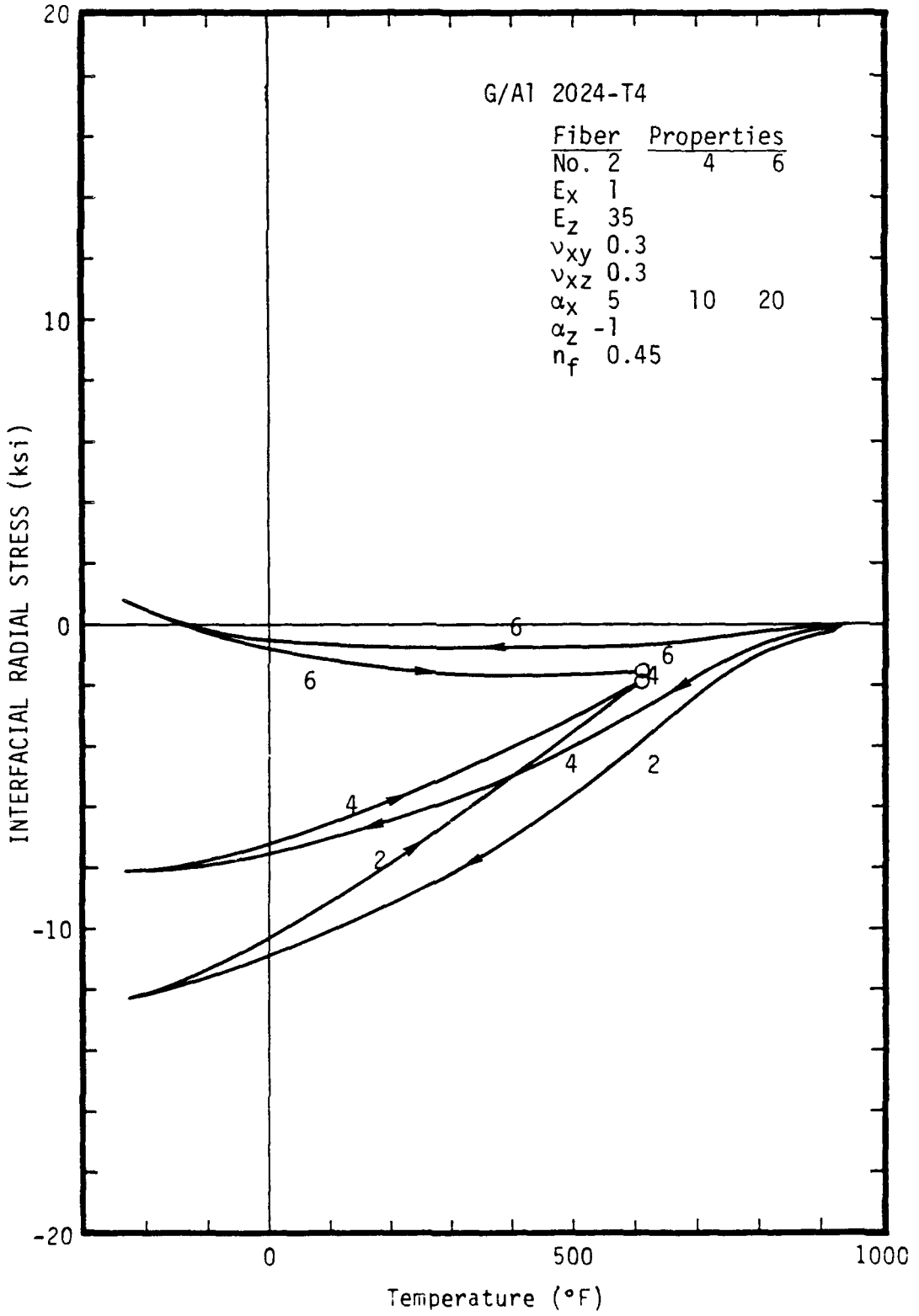

Figure 2.11. Radial stress versus temperature at the fiber-matrix interface of a graphite/aluminum composite (rapid cooling).

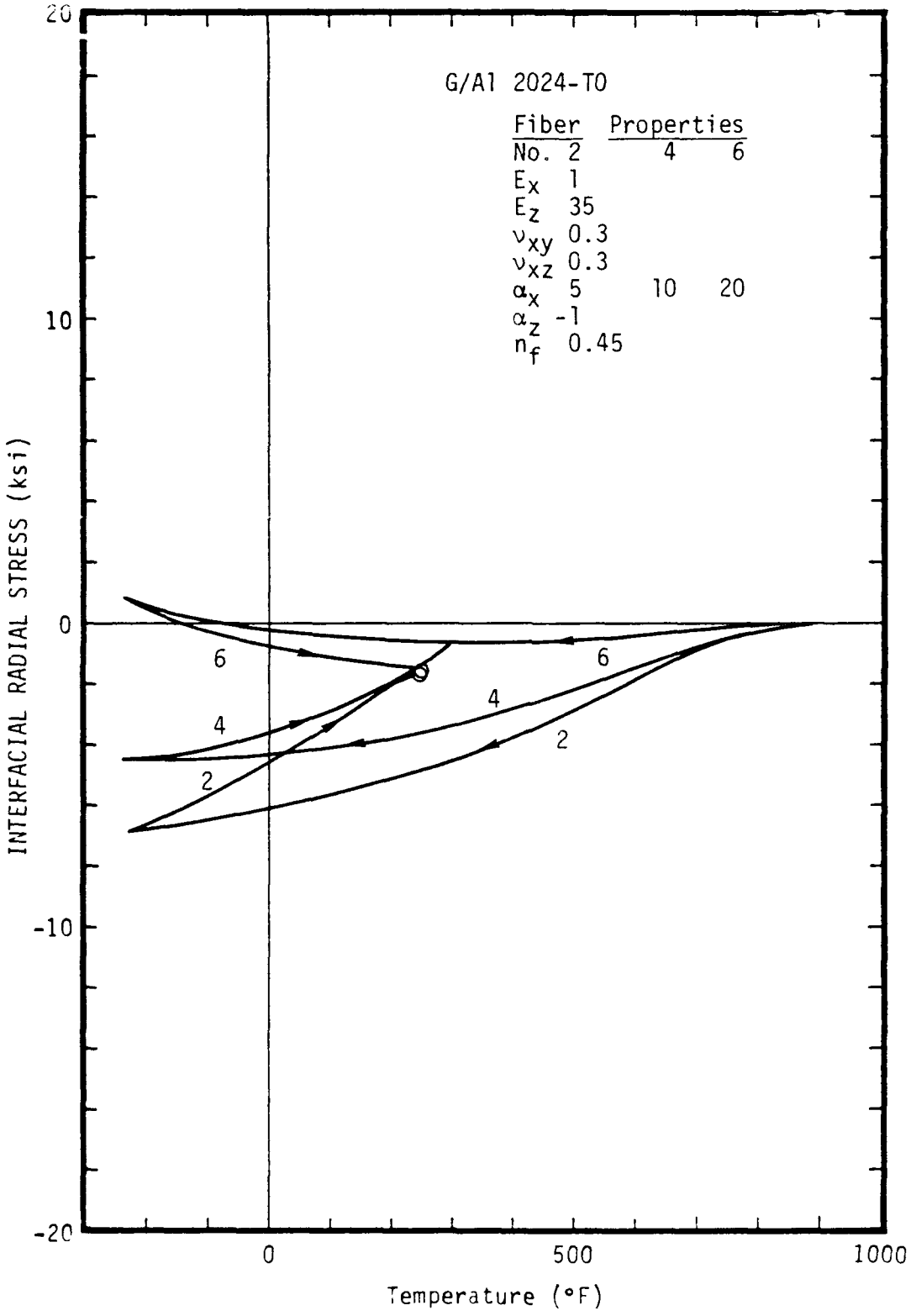

Figure 2.12. Radial stress versus temperature at the fiber-matrix interface of a graphite/aluminum composite (slow cooling).

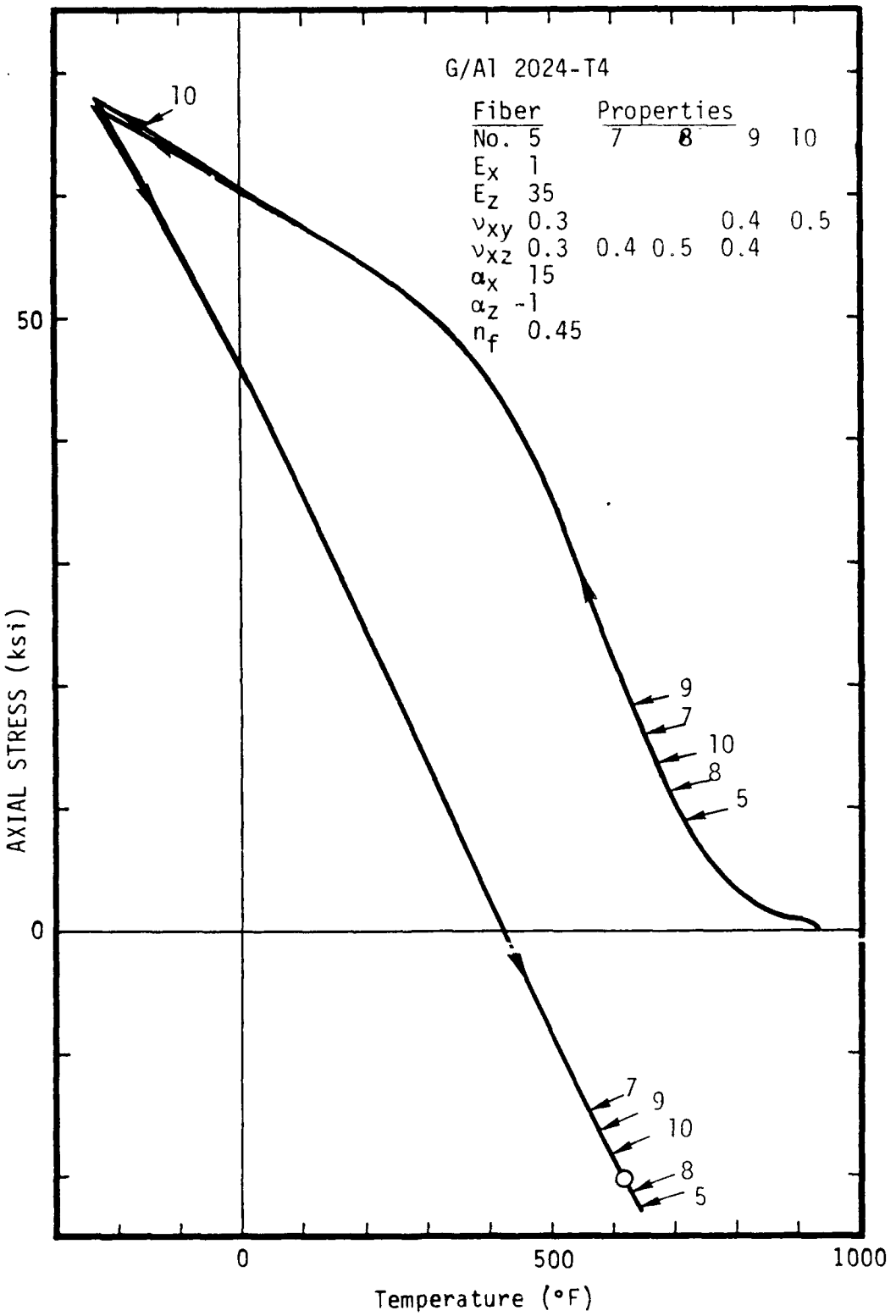

Figure 2.13. Volume-averaged axial stress versus temperature for the matrix of a graphite/aluminum composite (rapid cooling).

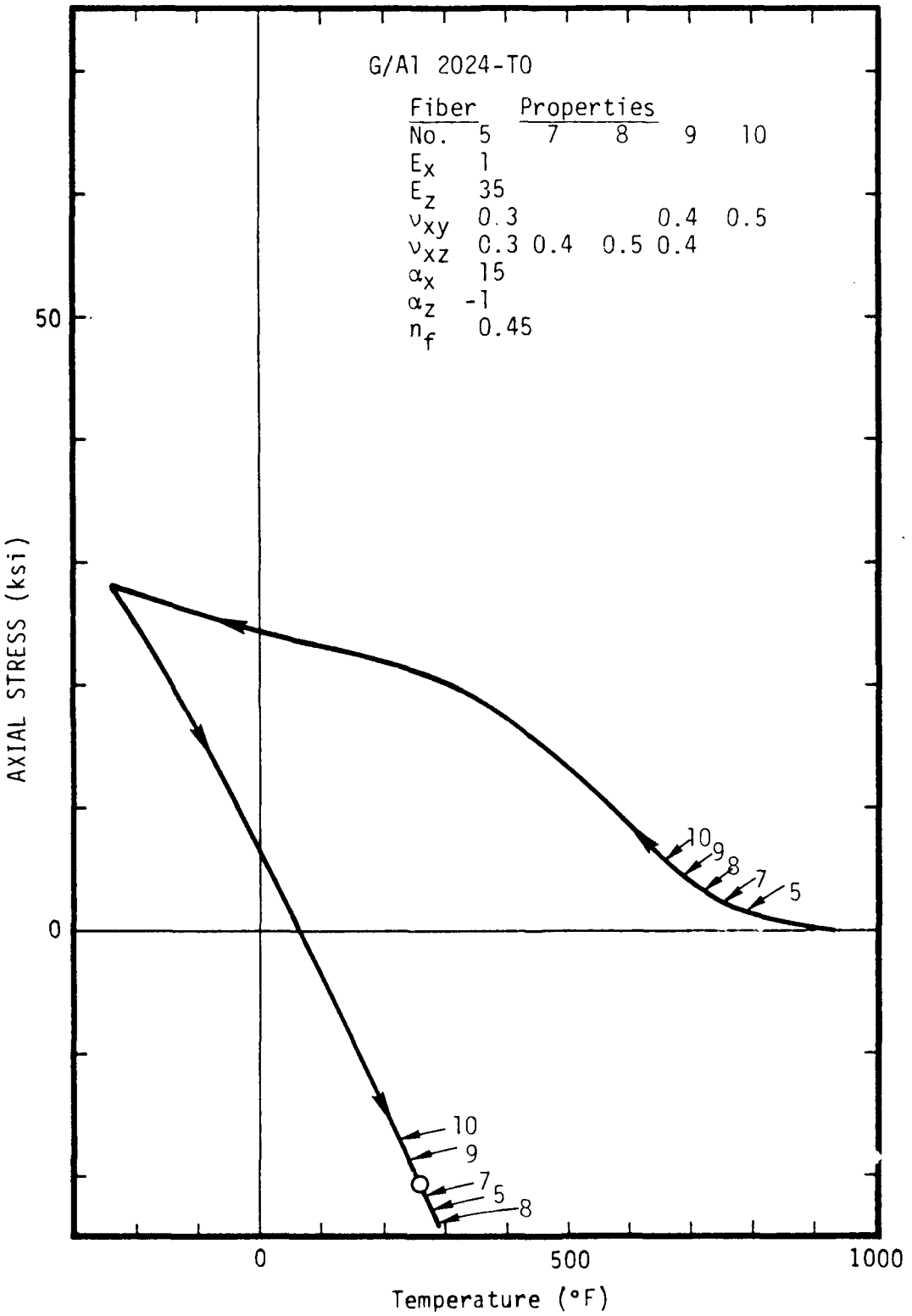

Figure 2.14. Volume-averaged axial stress versus temperature for the matrix of a graphite/aluminum composite (slow cooling).

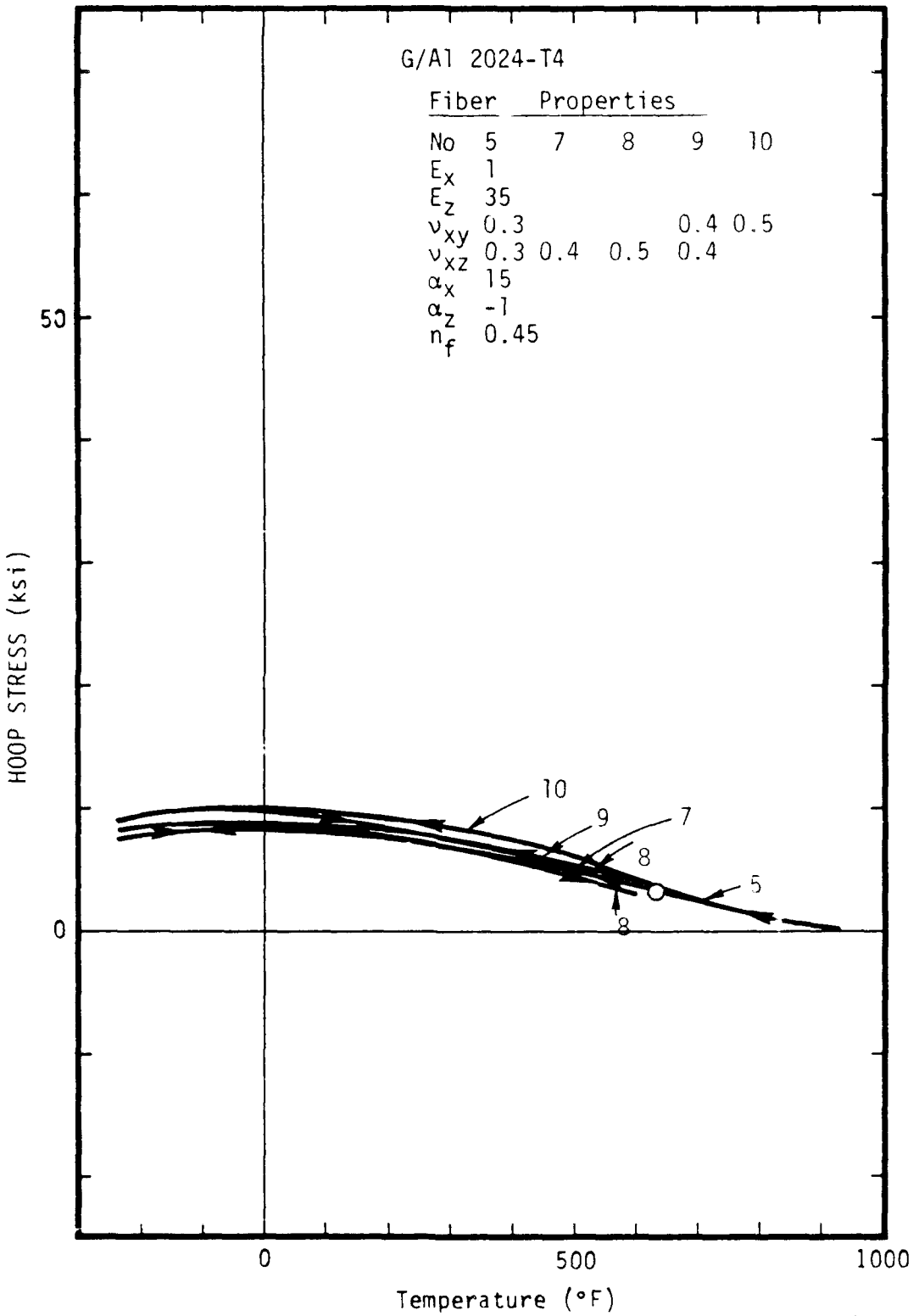

Figure 2.15. Volume-averaged hoop stress versus temperature for the matrix of a graphite/aluminum composite (rapid cooling).

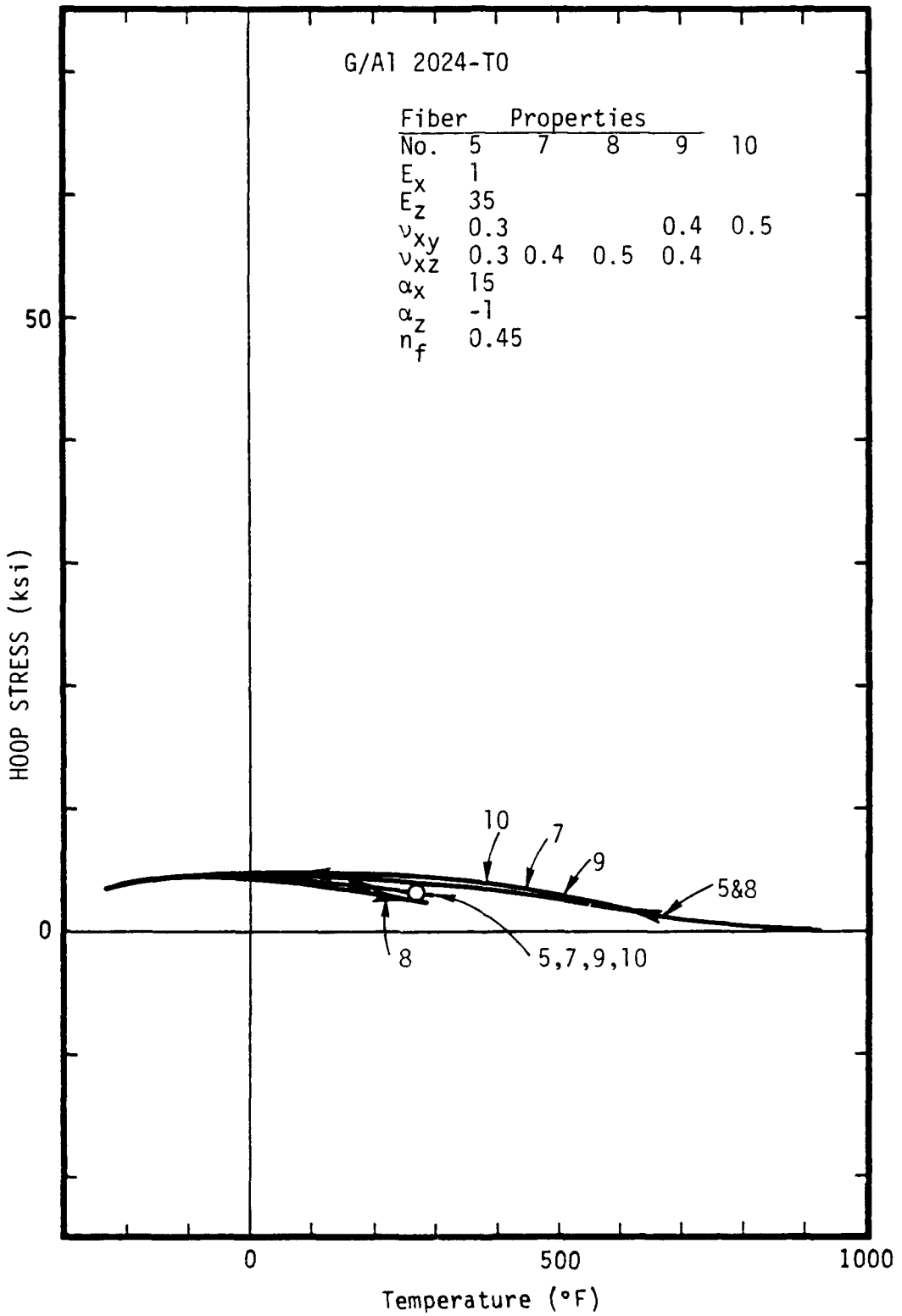

Figure 2.16. Volume-averaged hoop stress versus temperature for the matrix of a graphite/aluminum composite (slow cooling).

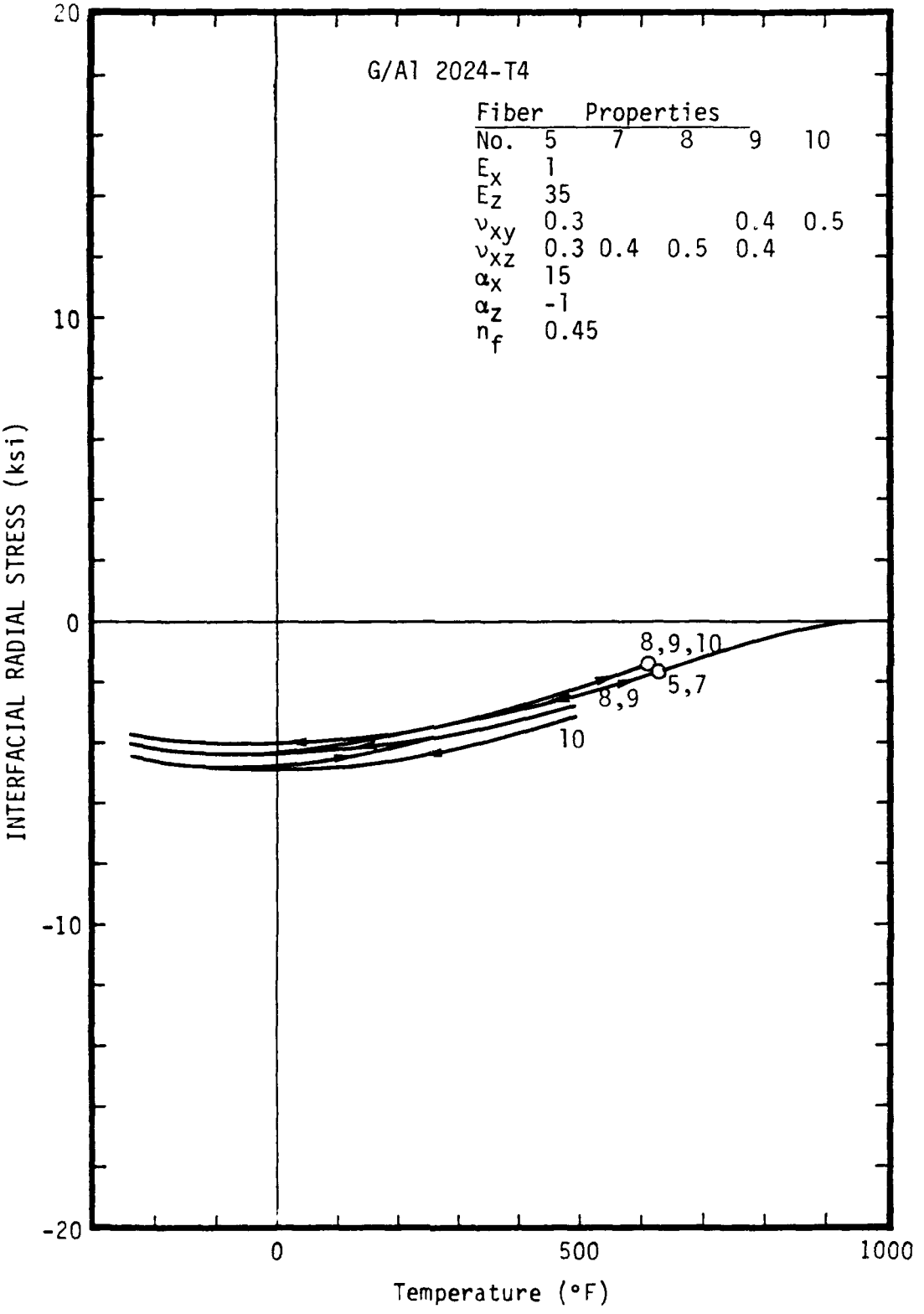

Figure 2.17. Radial stress versus temperature at the fiber-matrix interface of a graphite/aluminum composite (rapid cooling).

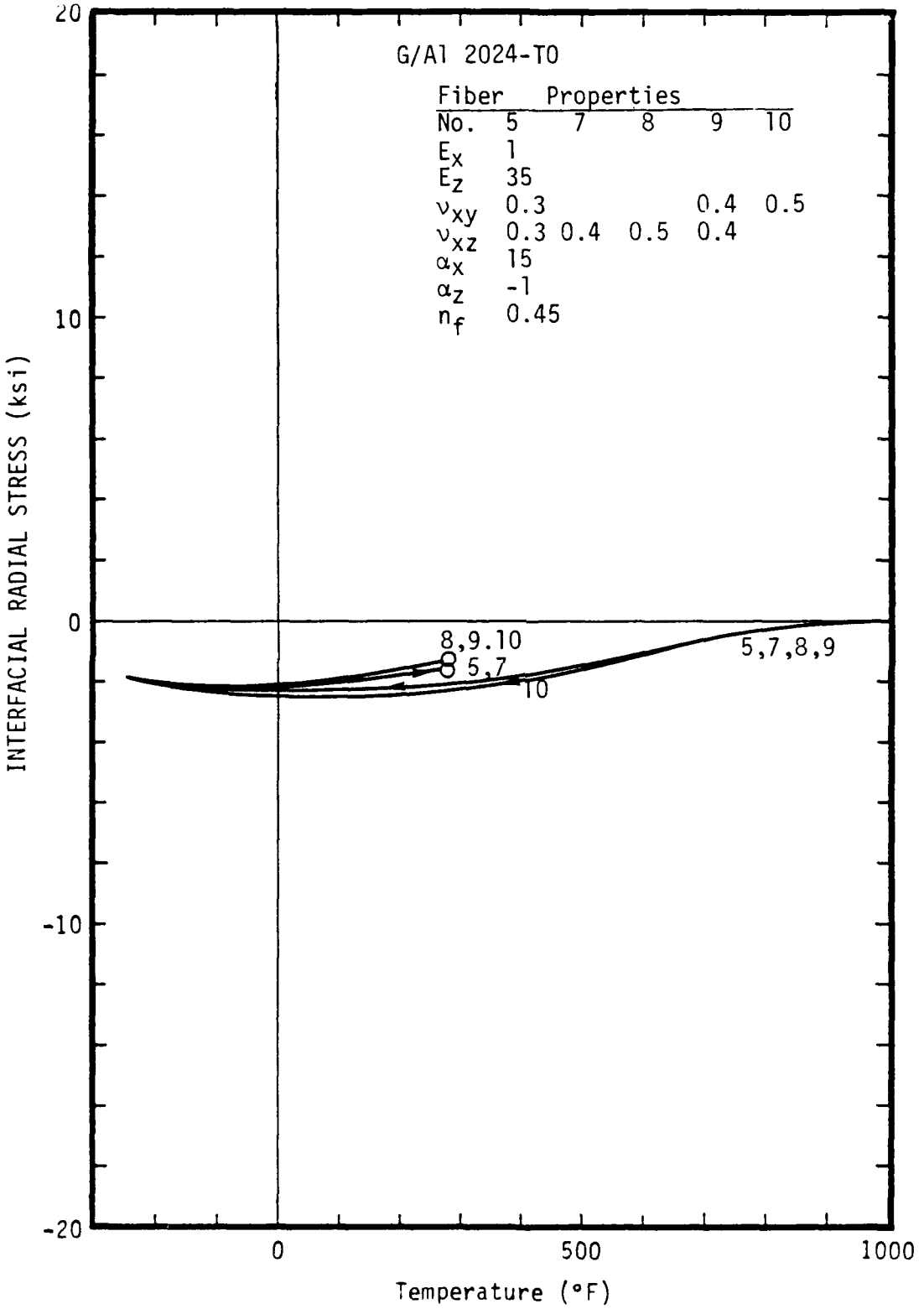

Figure 2.18. Radial stress versus temperature at the fiber-matrix interface of a graphite/aluminum composite (slow cooling).

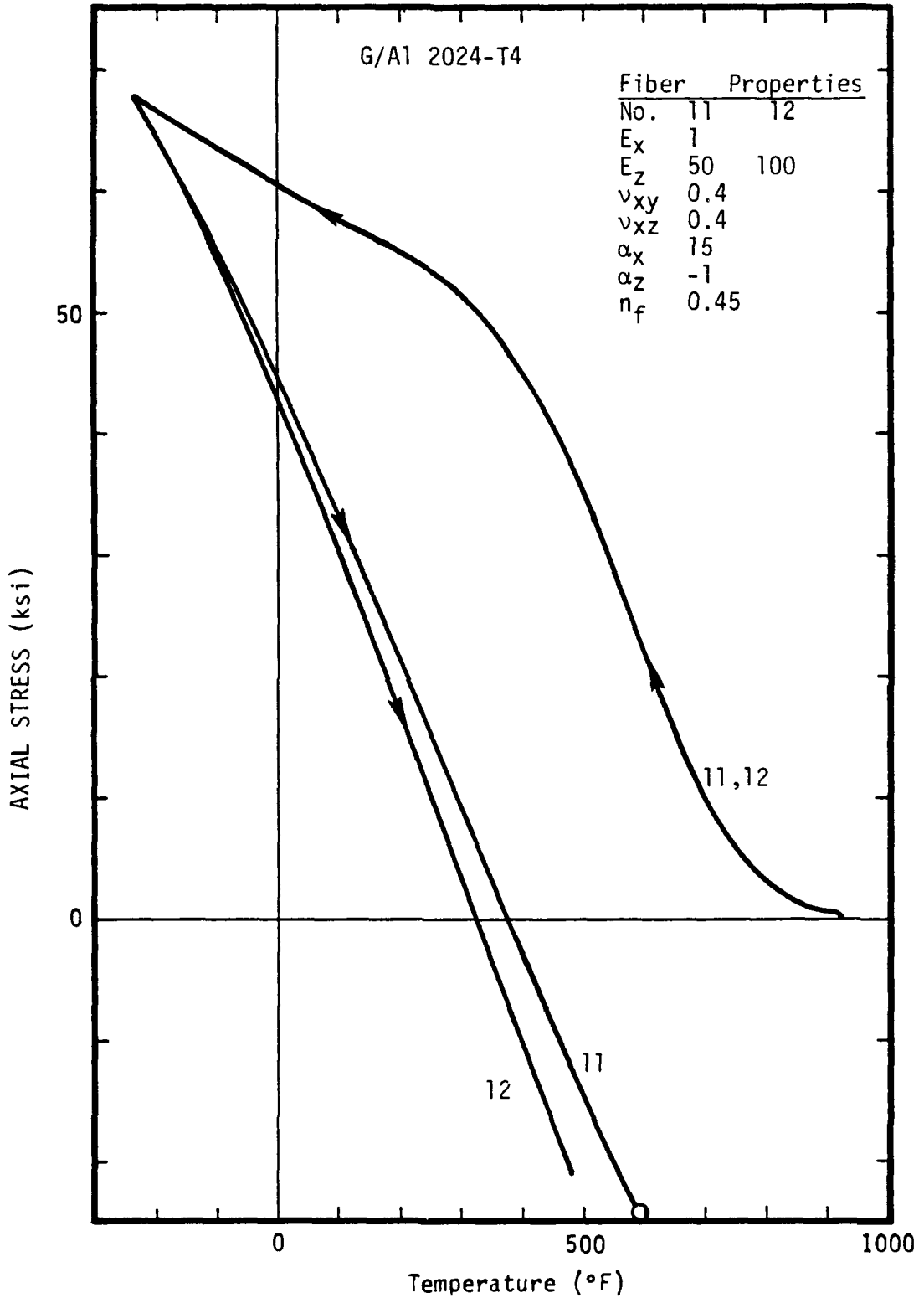

Figure 2.19. Volume-averaged axial stress versus temperature for the matrix of a graphite/aluminum composite (rapid cooling).

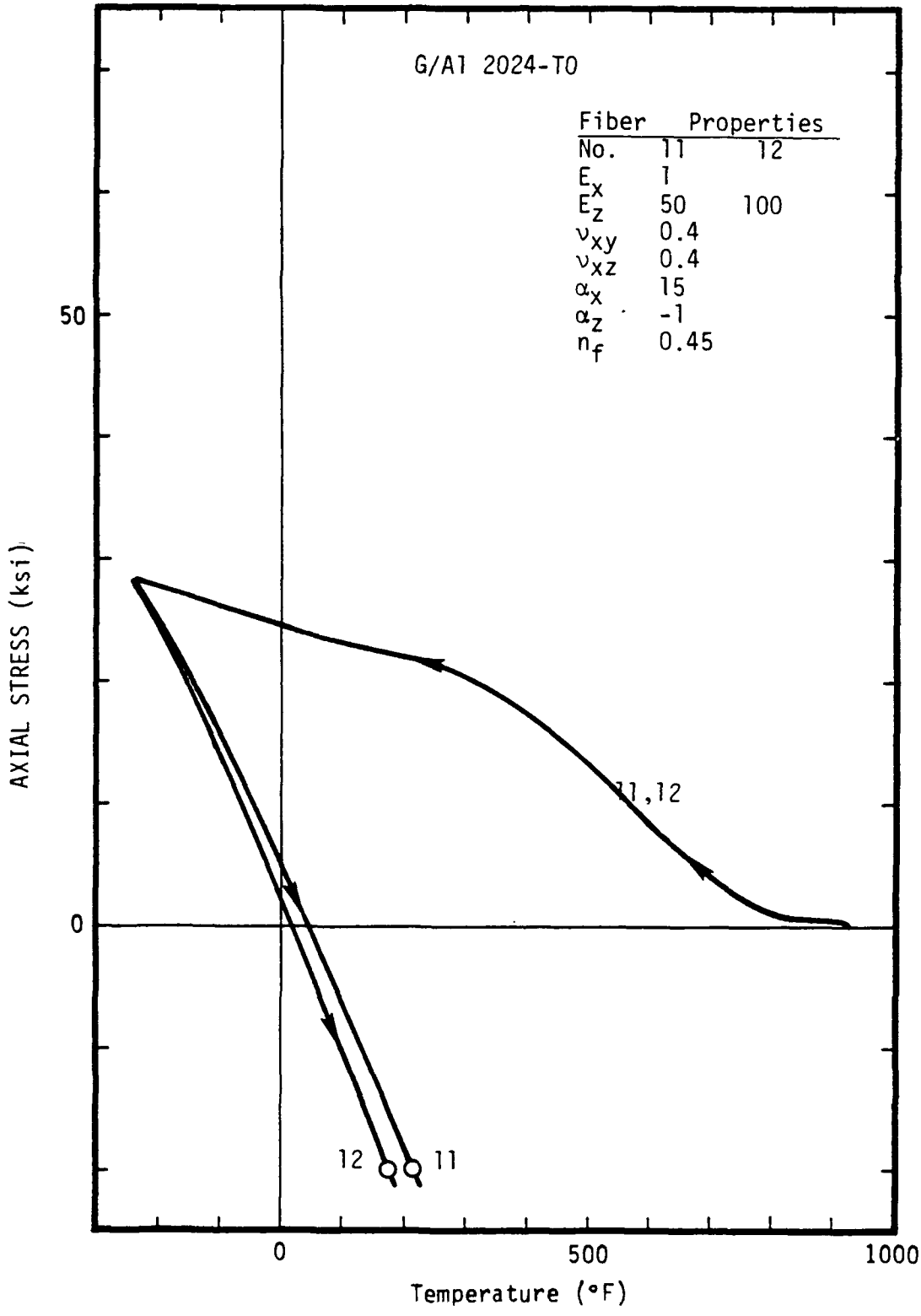

Figure 2.20. Volume-averaged axial stress versus temperature for the matrix of a graphite/aluminum composite (slow cooling).

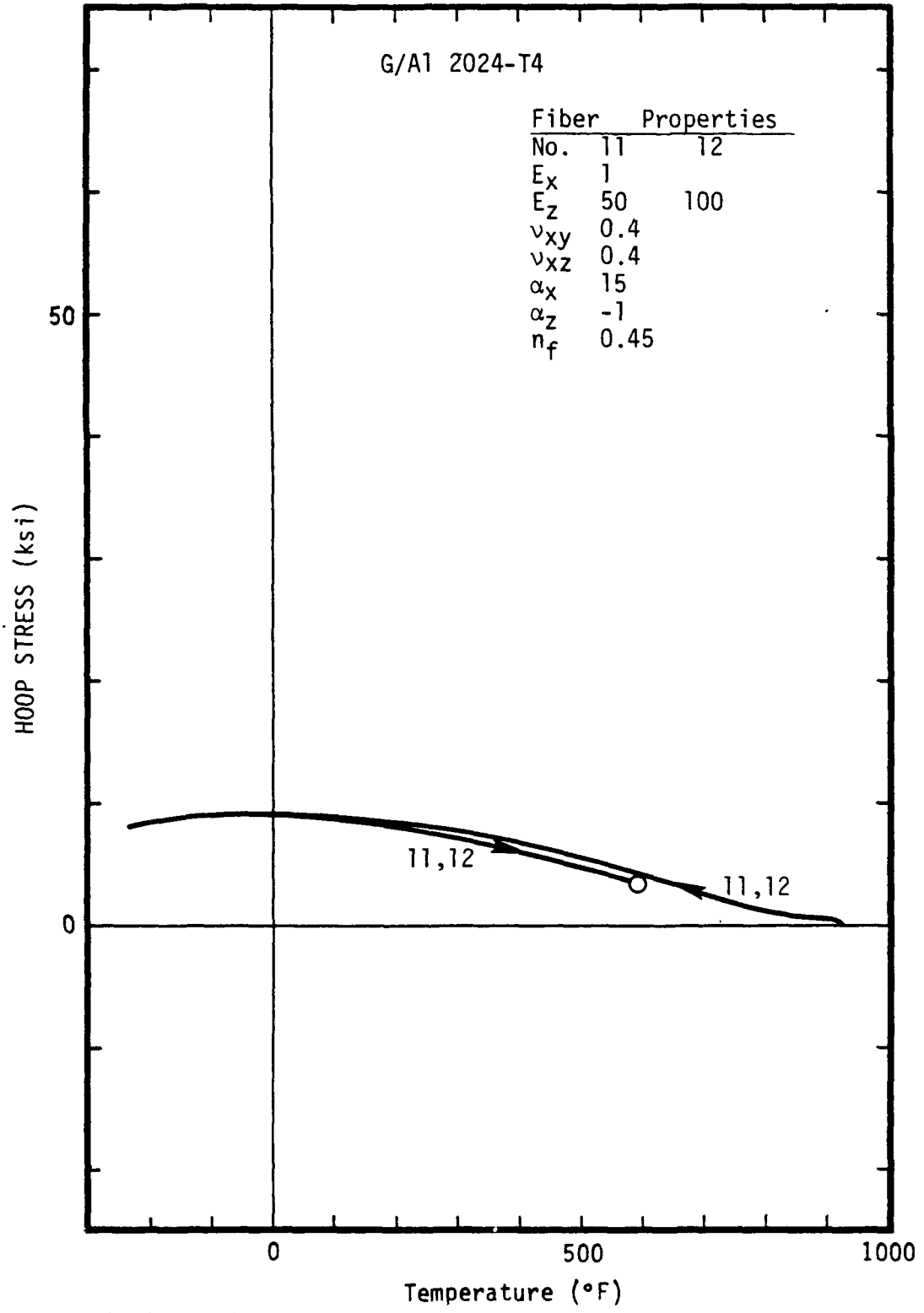

Figure 2.21. Volume-averaged hoop stress versus temperature for the matrix of a graphite/aluminum composite (rapid cooling).

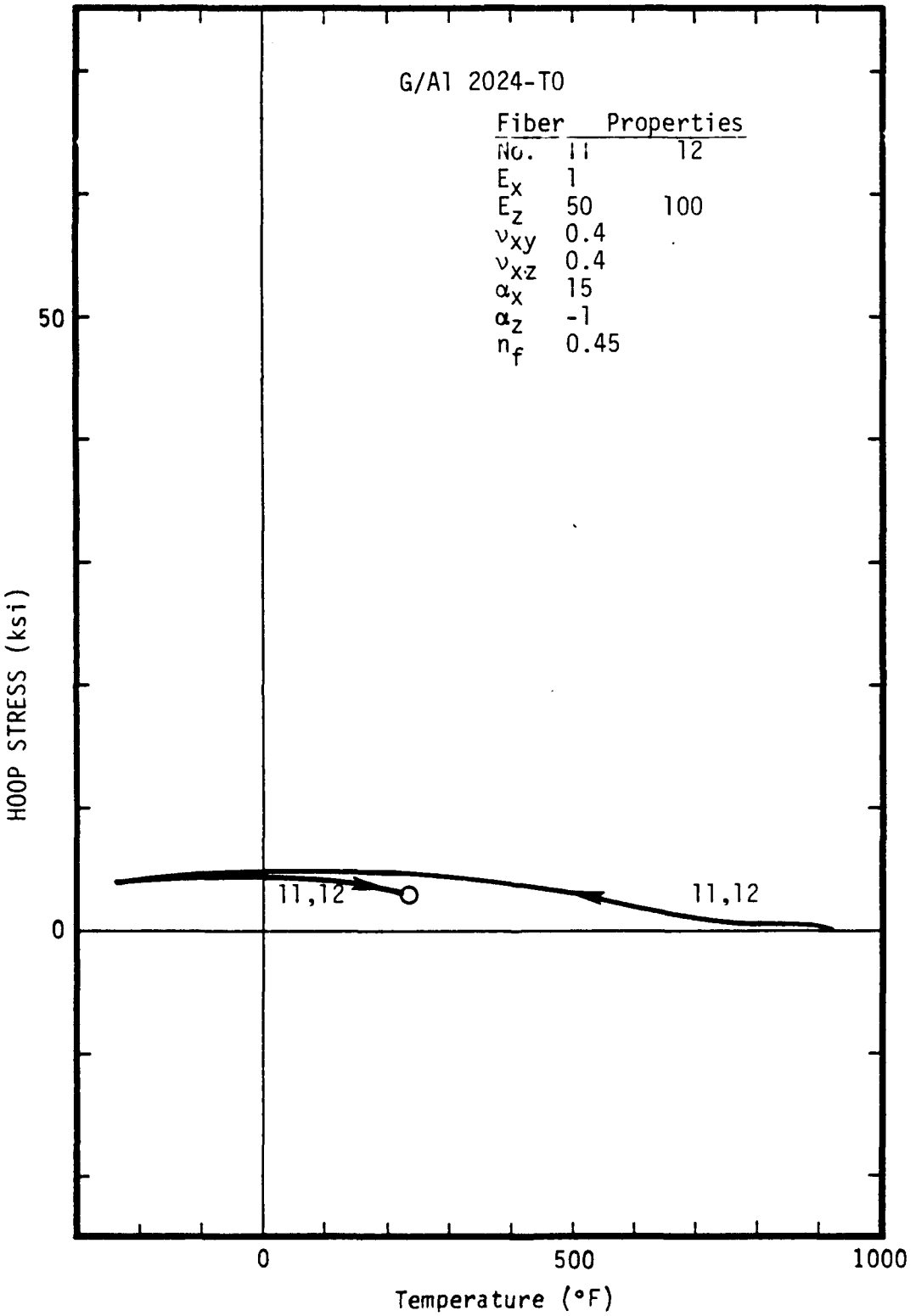

Figure 2.22. Volume-averaged hoop stress versus temperature for the matrix of a graphite/aluminum composite (slow cooling).

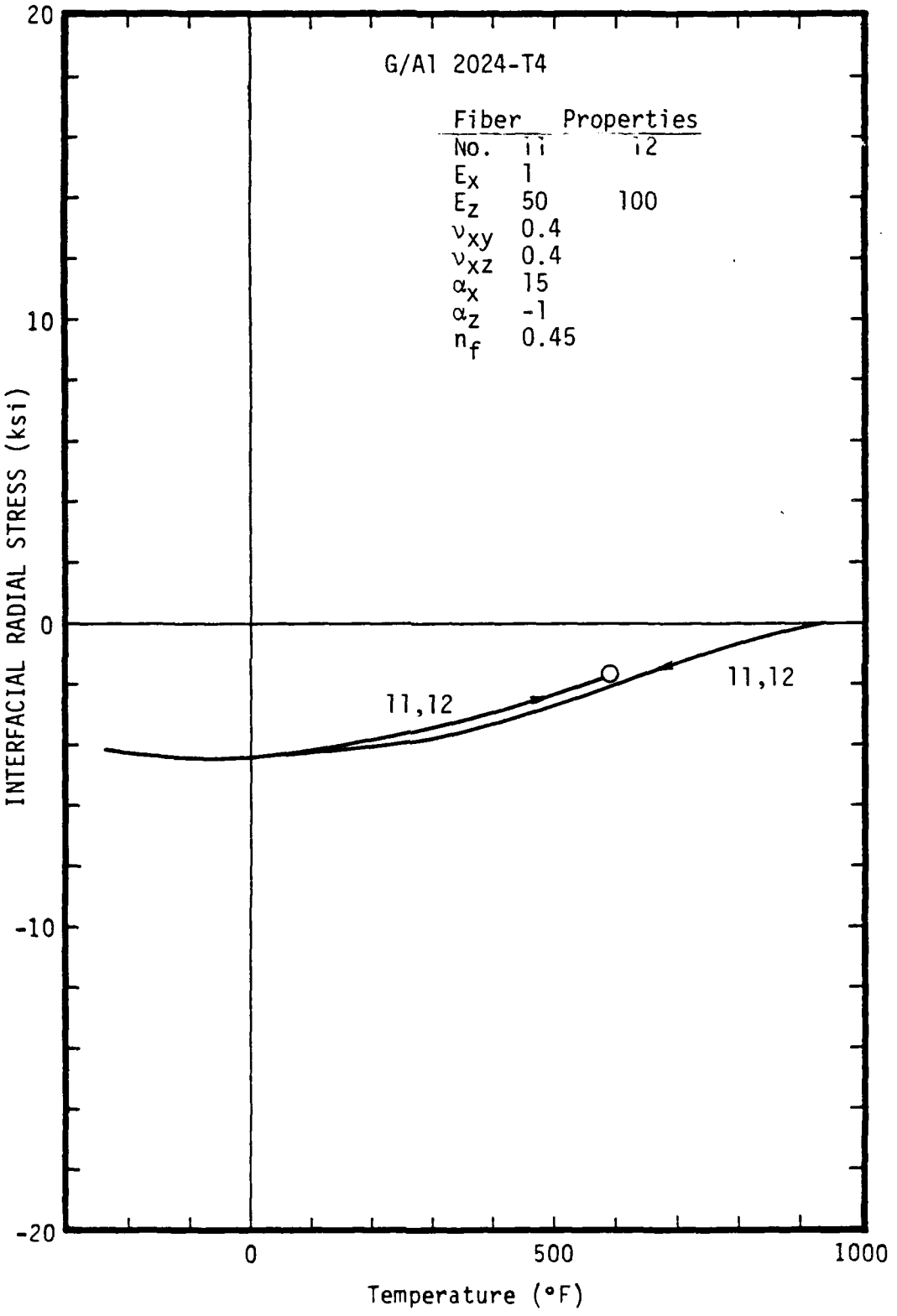

Figure 2.23. Radial stress versus temperature at the fiber-matrix interface of a graphite/aluminum composite (rapid cooling).

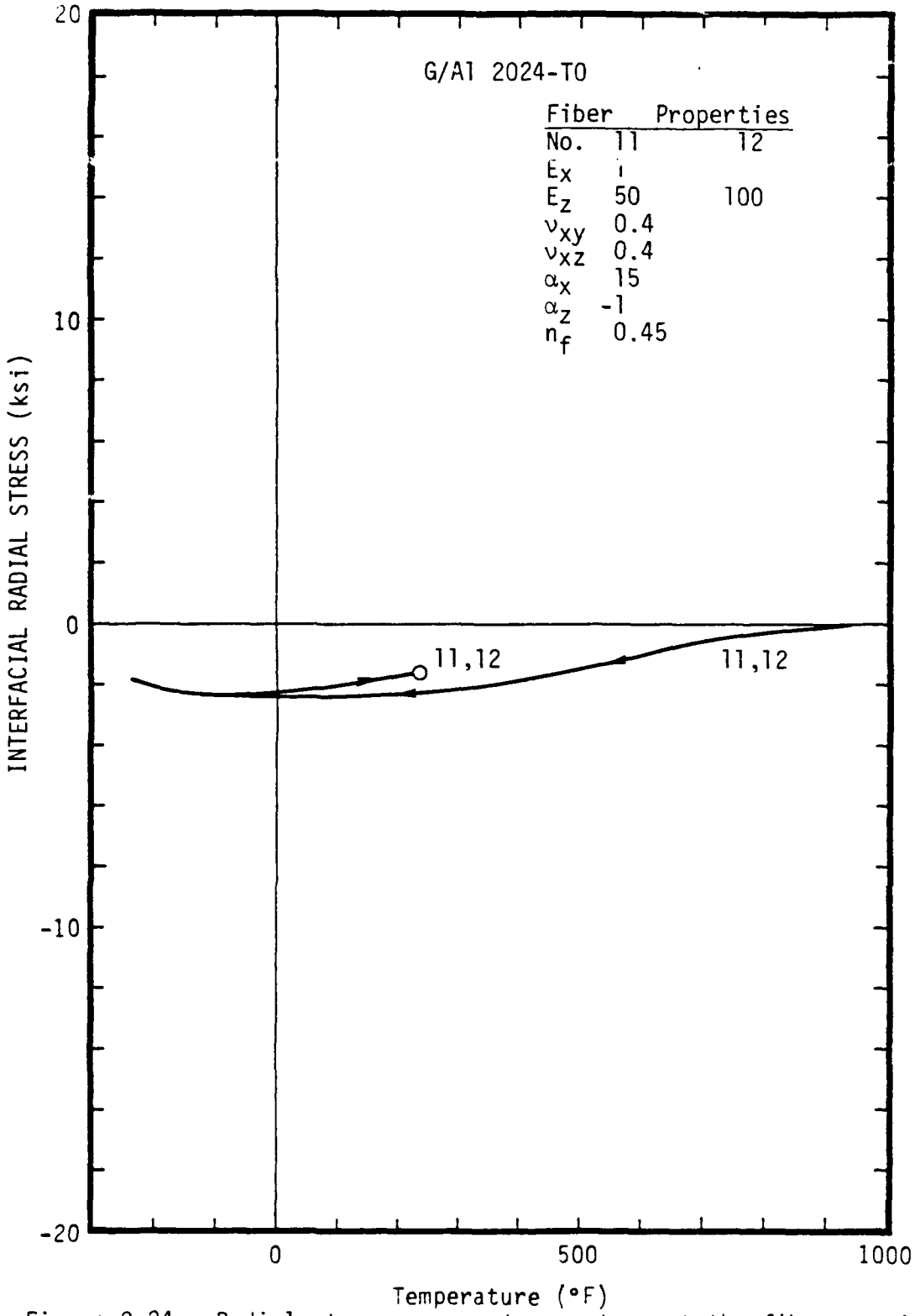

Figure 2.24. Radial stress versus temperature at the fiber-matrix interface of a graphite/aluminum composite (slow cooling).

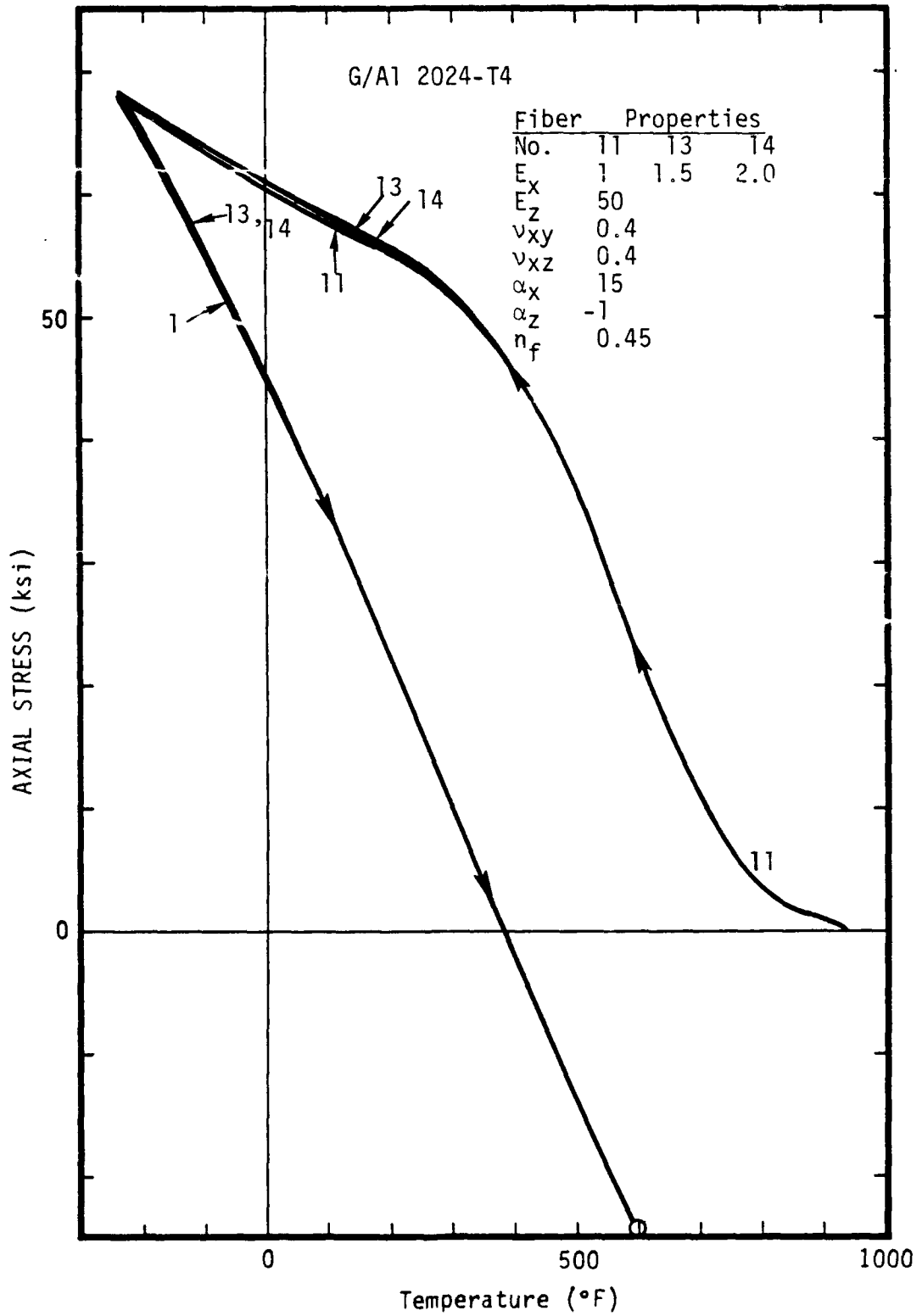

Figure 2.25. Volume-averaged axial stress versus temperature for the matrix of a graphite/aluminum composite (rapid cooling).

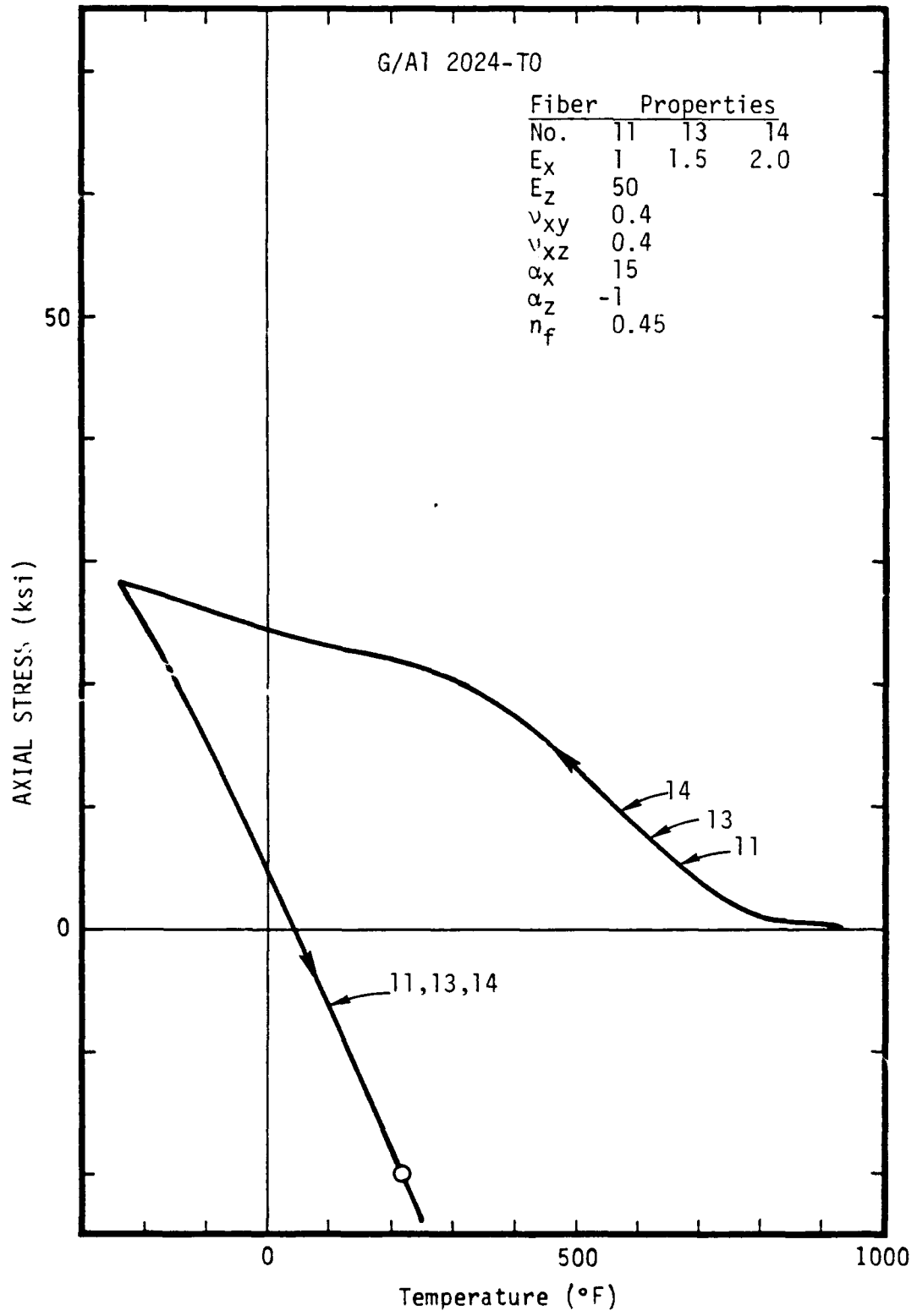

Figure 2.26. Volume-averaged axial stress versus temperature for the matrix of a graphite/aluminum composite (rapid cooling).

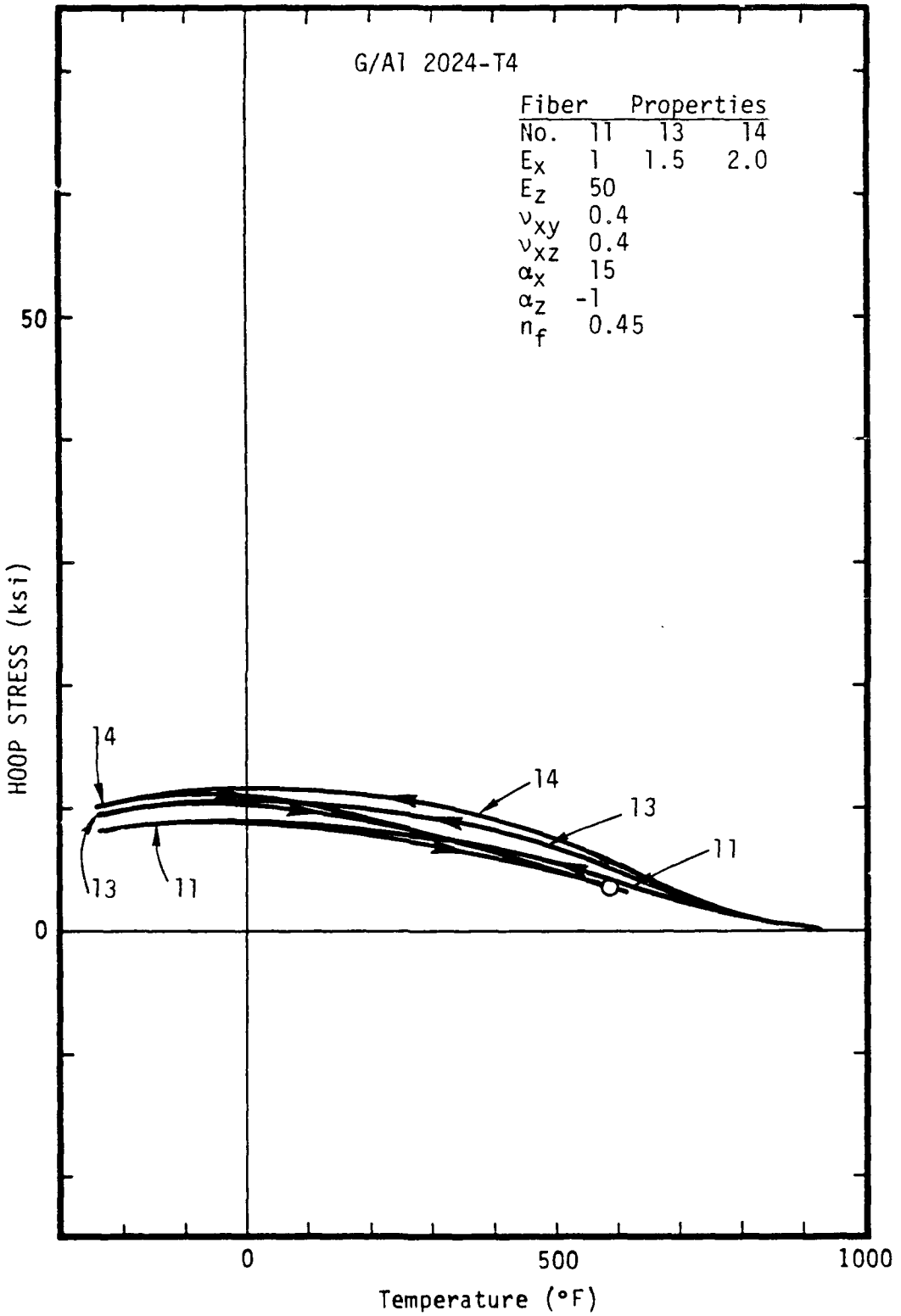

Figure 2.27. Volume-averaged hoop stress versus temperature for the matrix of a graphite/aluminum composite (rapid cooling).

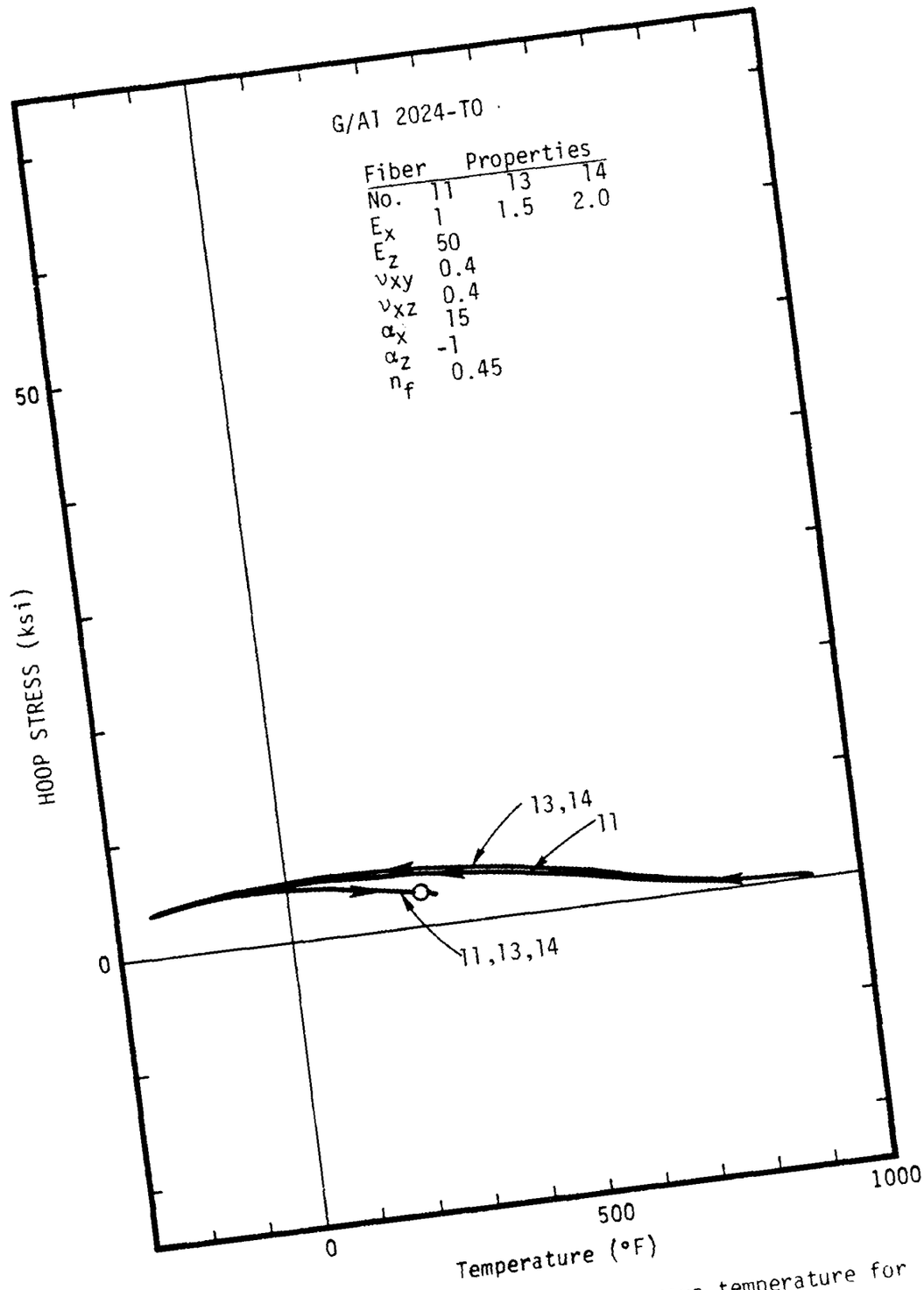

Figure 2.28. Volume-averaged hoop stress versus temperature for the matrix of a graphite/aluminum composite (slow cooling).

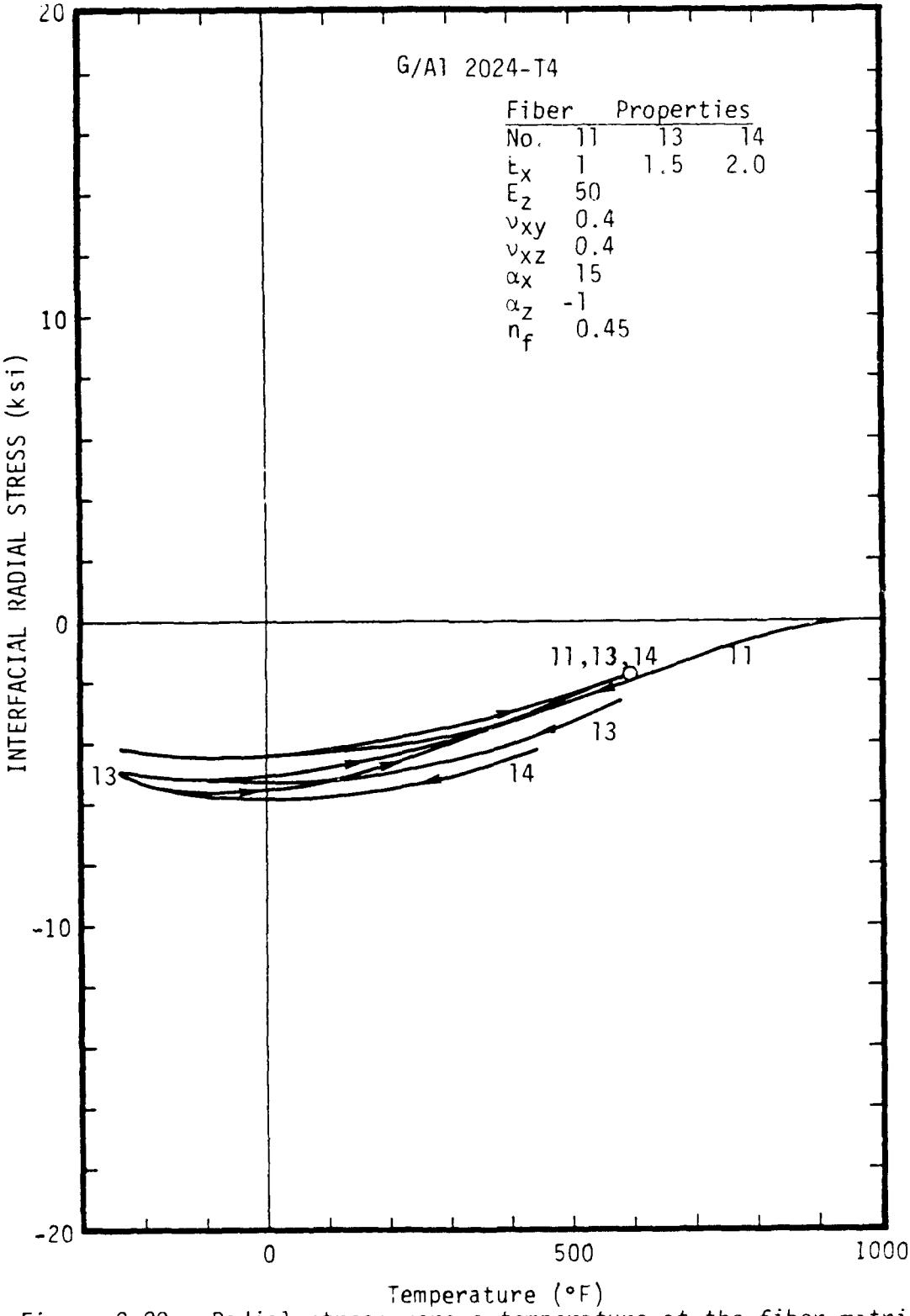

Figure 2.29. Radial stress versus temperature at the fiber-matrix interface of a graphite/aluminum composite (rapid cooling).

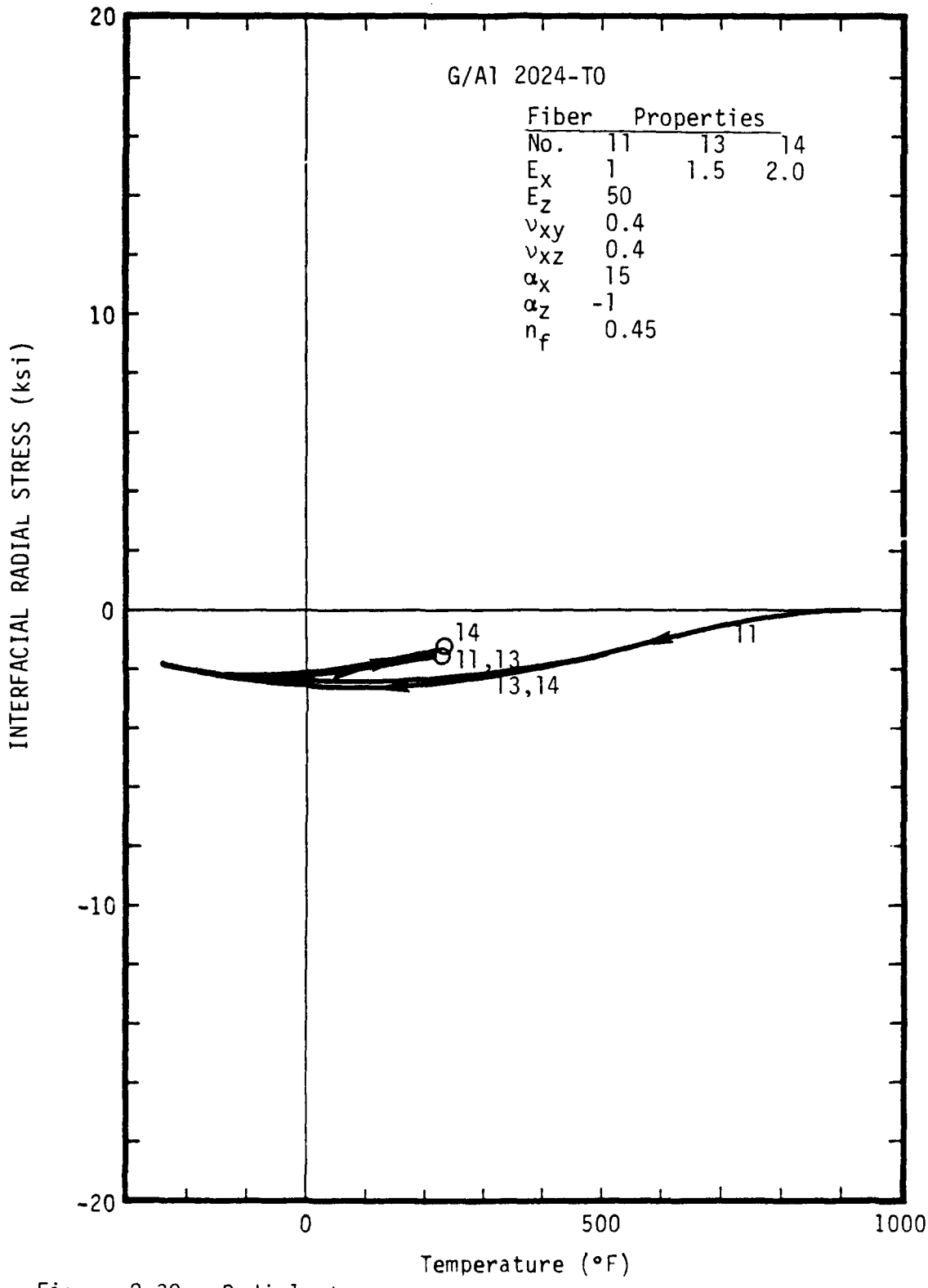

Figure 2.30. Radial stress versus temperature at the fiber-matrix interface of a graphite/aluminum composite (slow cooling).

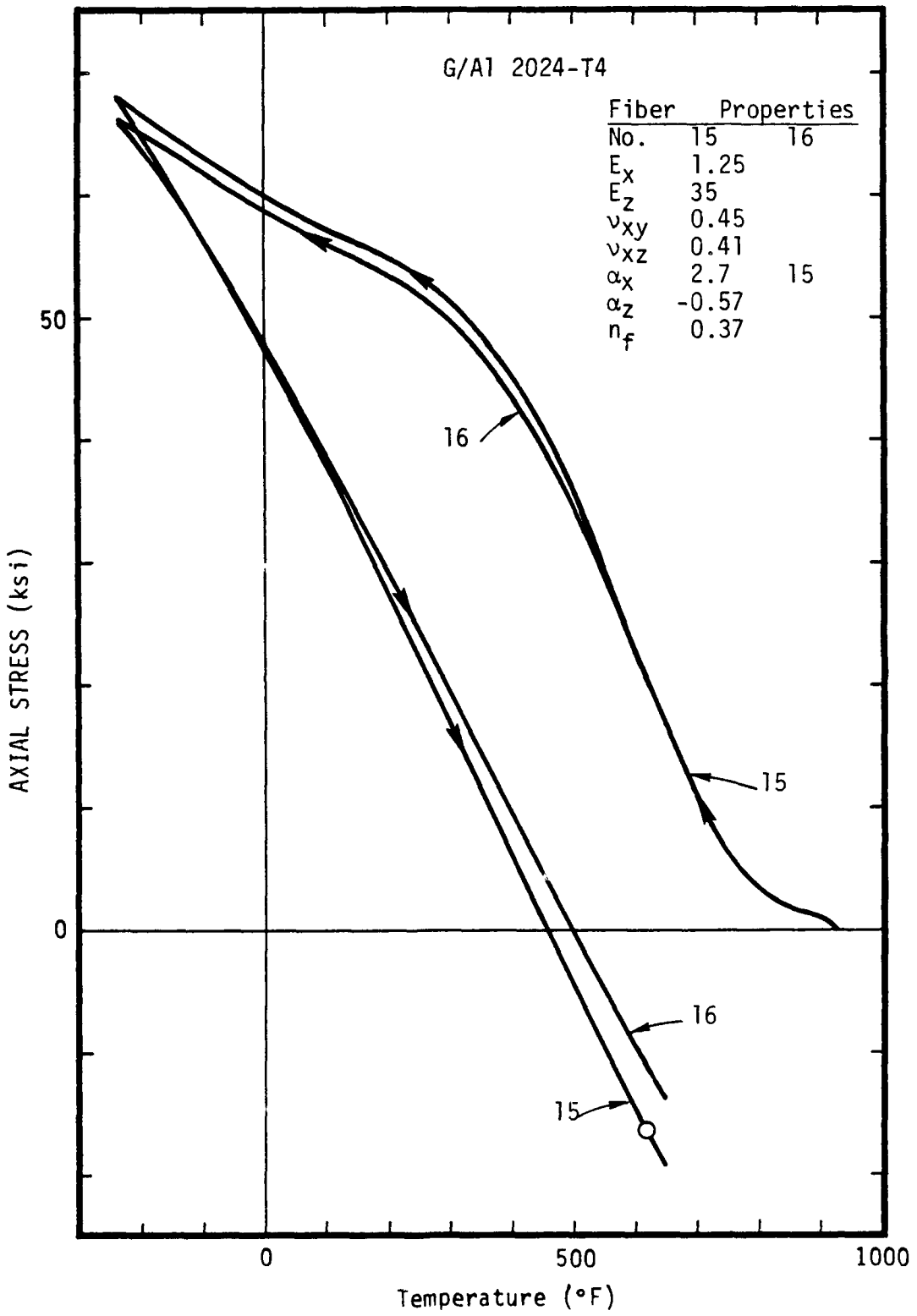

Figure 2.31. Volume-averaged axial stress versus temperature for the matrix of a graphite/aluminum composite (rapid cooling).

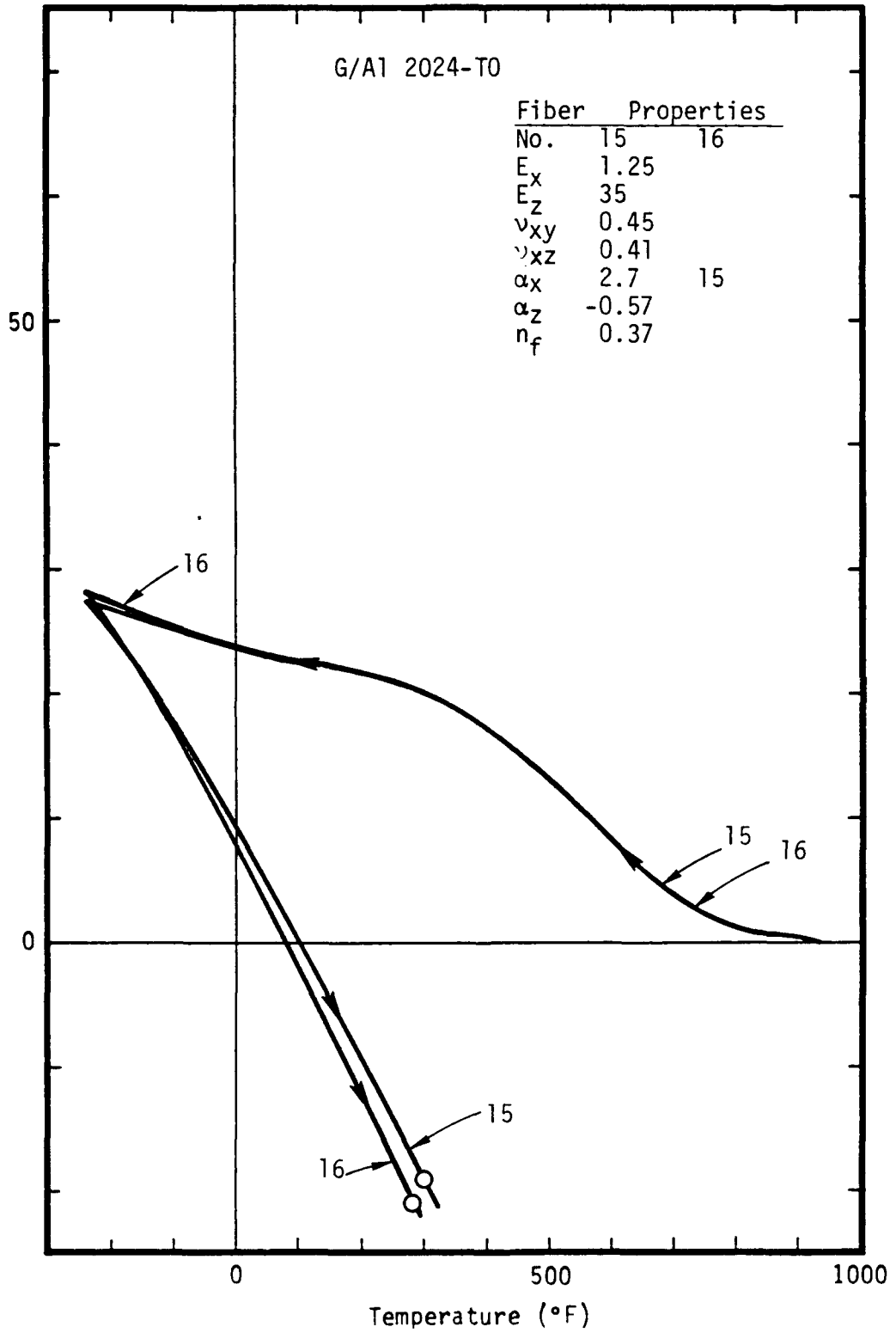

Figure 2.32. Volume-averaged axial stress versus temperature for the matrix of a graphite/aluminum composite (slow cooling).

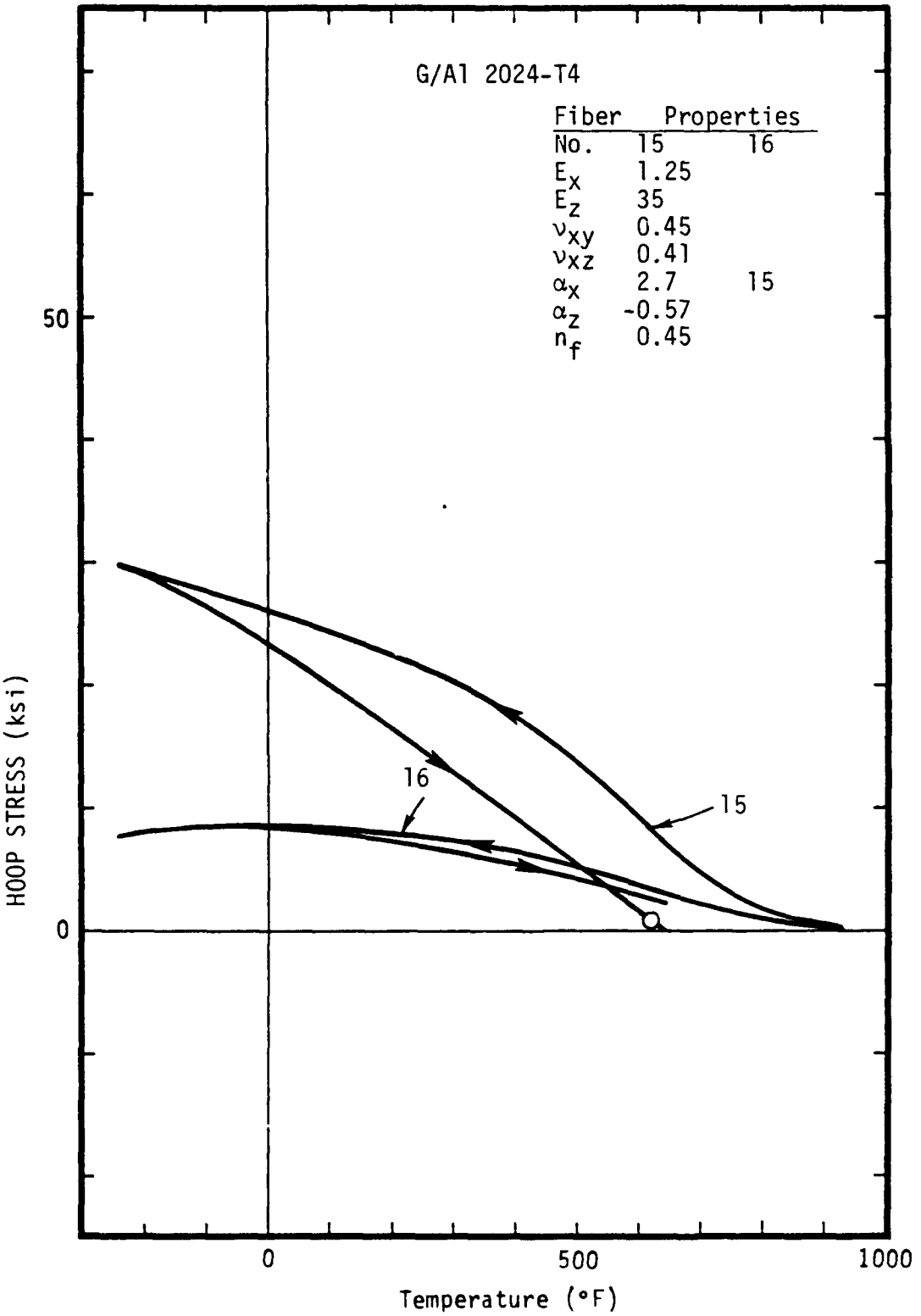

Figure 2.33. Volume-averaged hoop stress versus temperature for the matrix of a graphite/aluminum composite (rapid cooling).

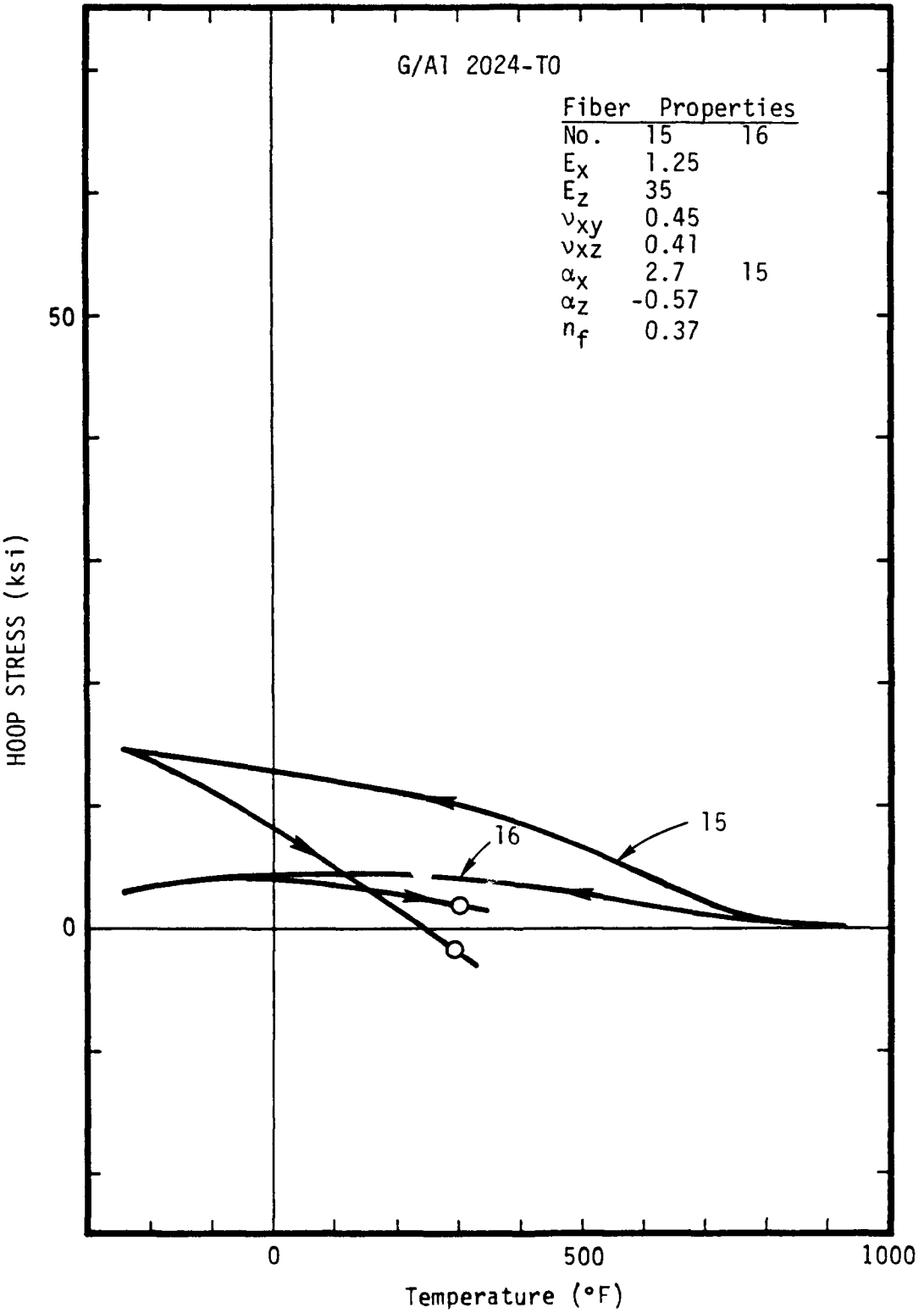

Figure 2.34. Volume-averaged hoop stress versus temperature for the matrix of a graphite/aluminum composite (slow cooling).

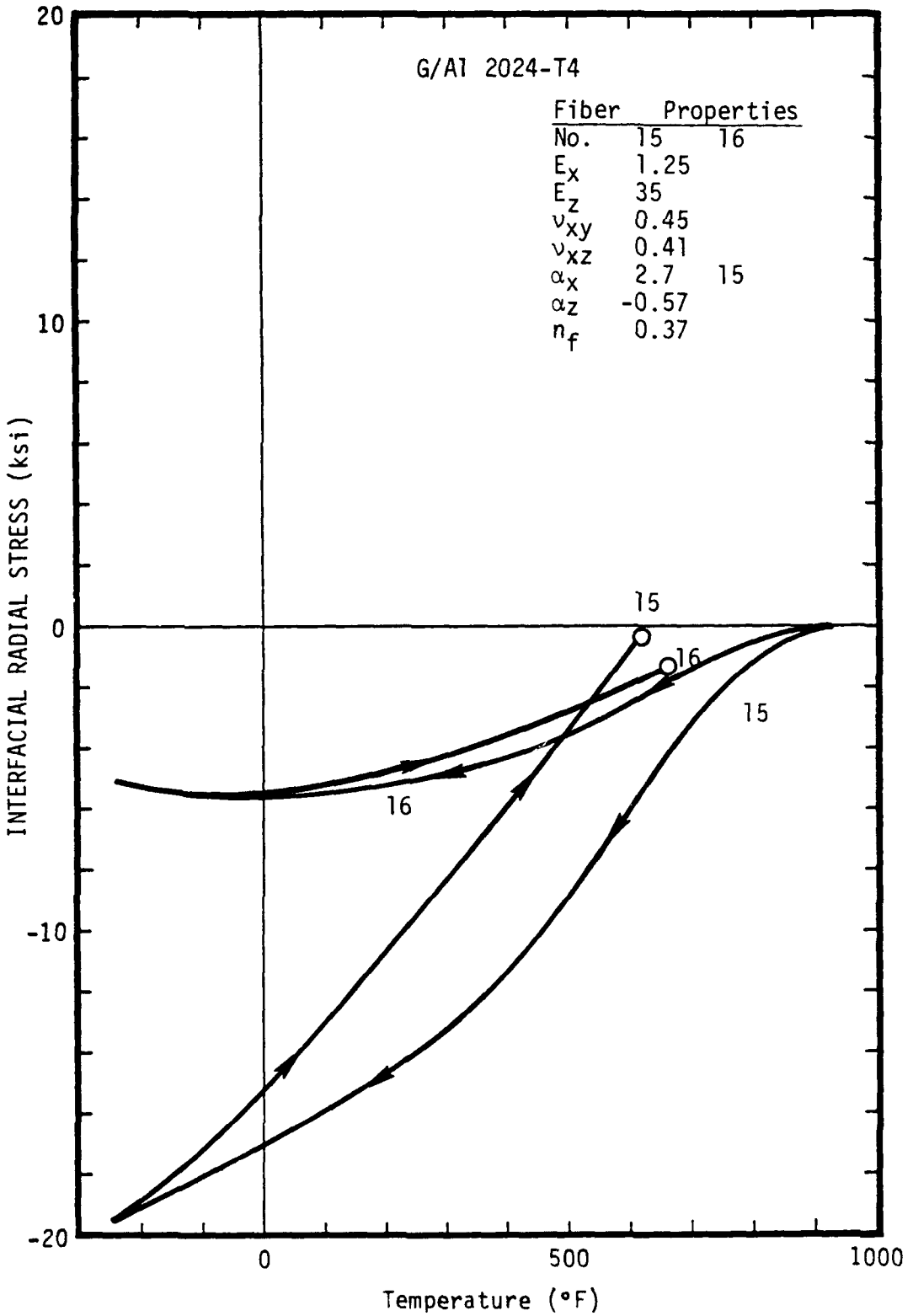

Figure 2.35. Radial stress versus temperature at the fiber-matrix interface of a graphite/aluminum composite (rapid cooling).

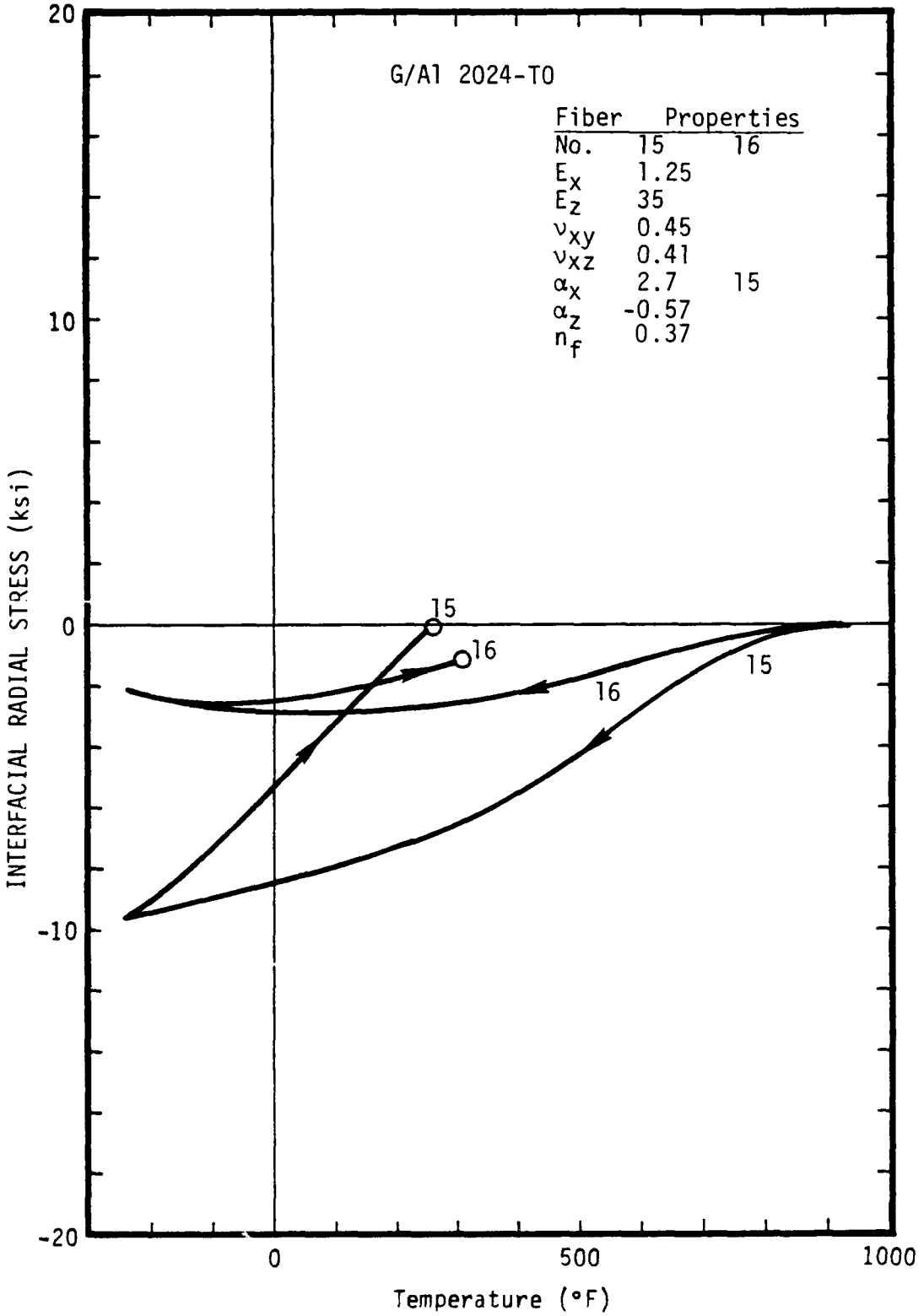

Figure 2.36. Radial stress versus temperature at the fiber-matrix interface of a graphite/aluminum composite (slow cooling).

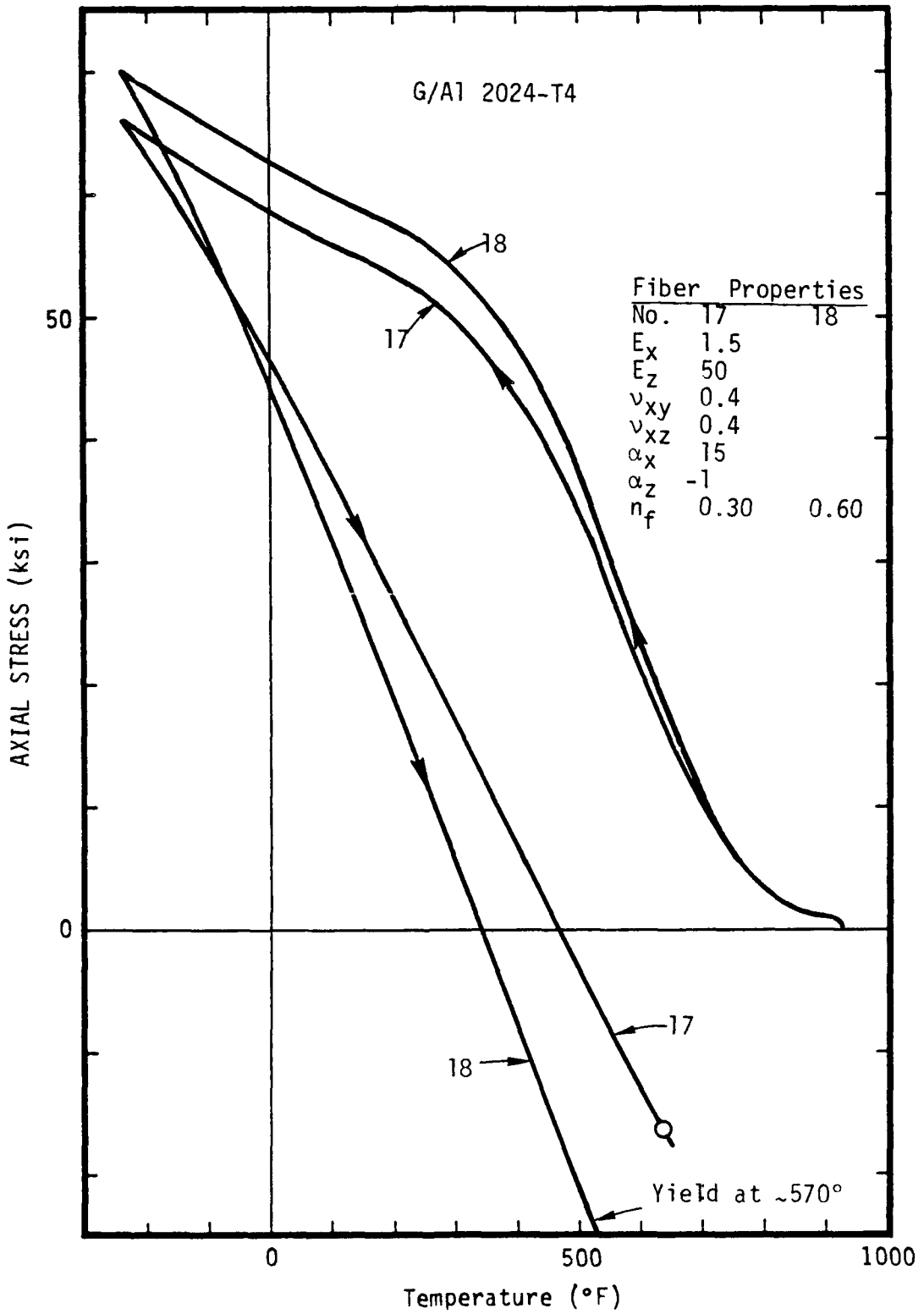

Figure 2.37. Volume-averaged axial stress versus temperature for the matrix of a graphite/aluminum composite (rapid cooling).

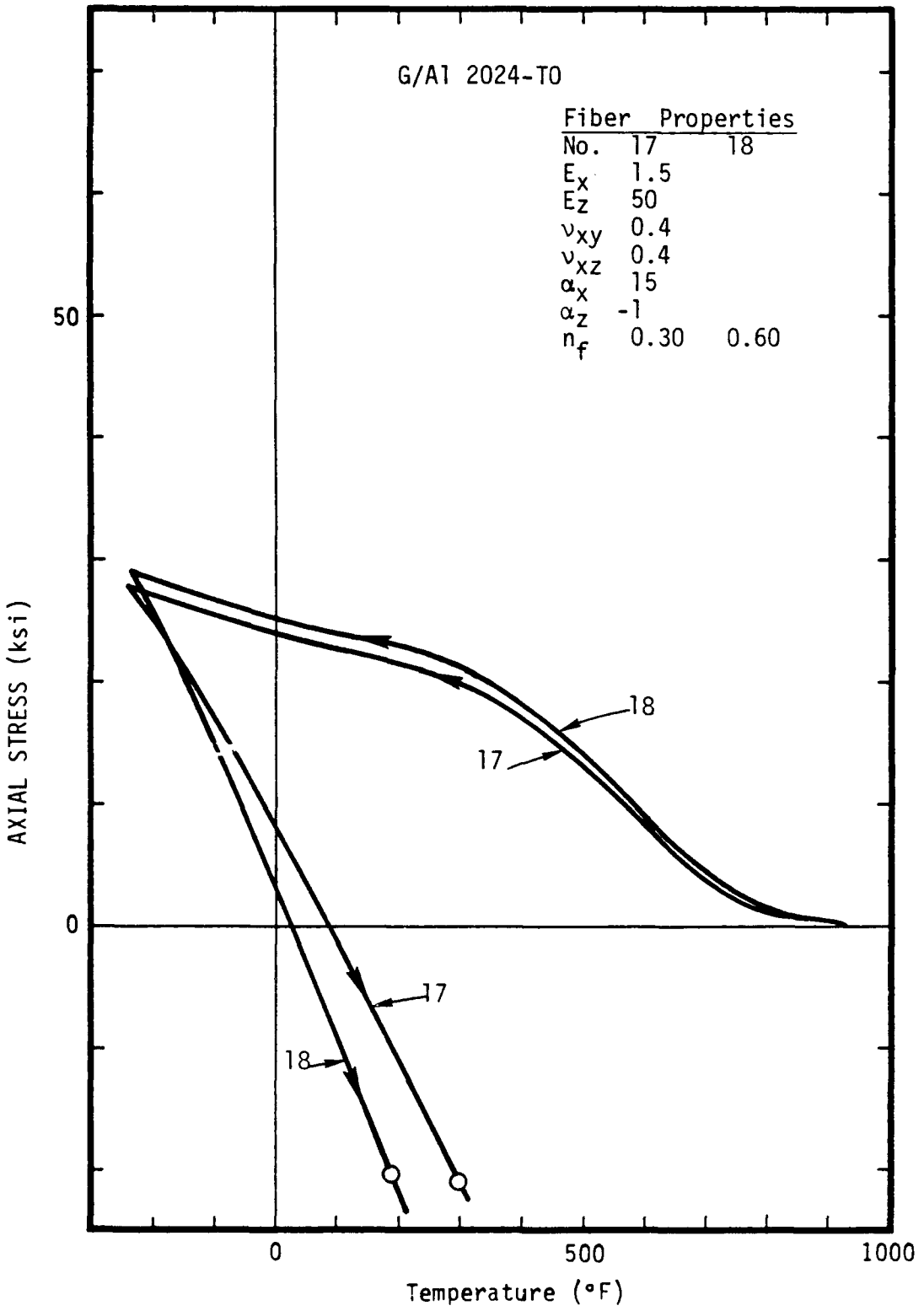

Figure 2.38. Volume-averaged axial stress versus temperature for the matrix of a graphite/aluminum composite (slow cooling).

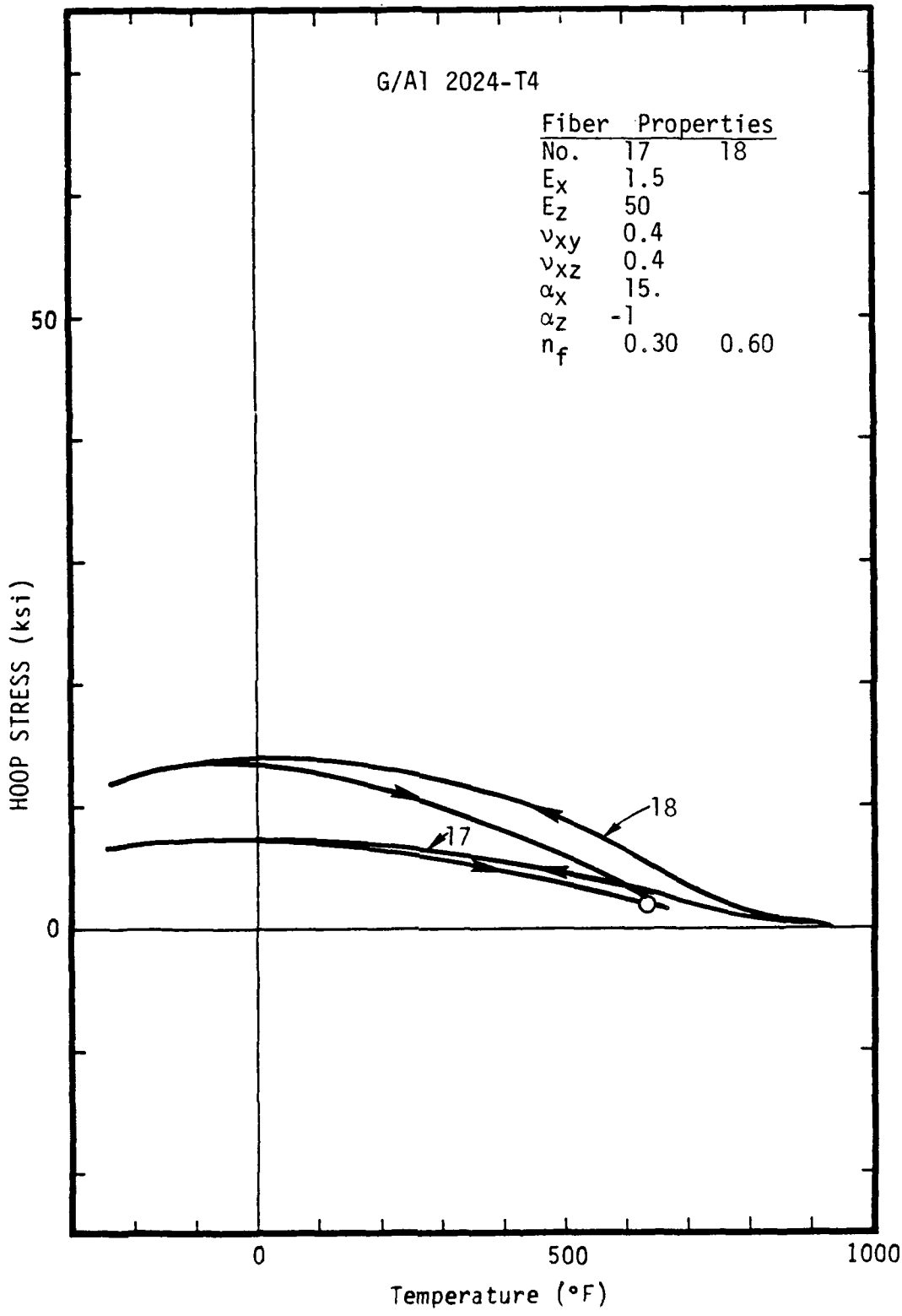

Figure 2.39. Volume-averaged hoop stress versus temperature for the matrix of a graphite/aluminum composite (rapid cooling).

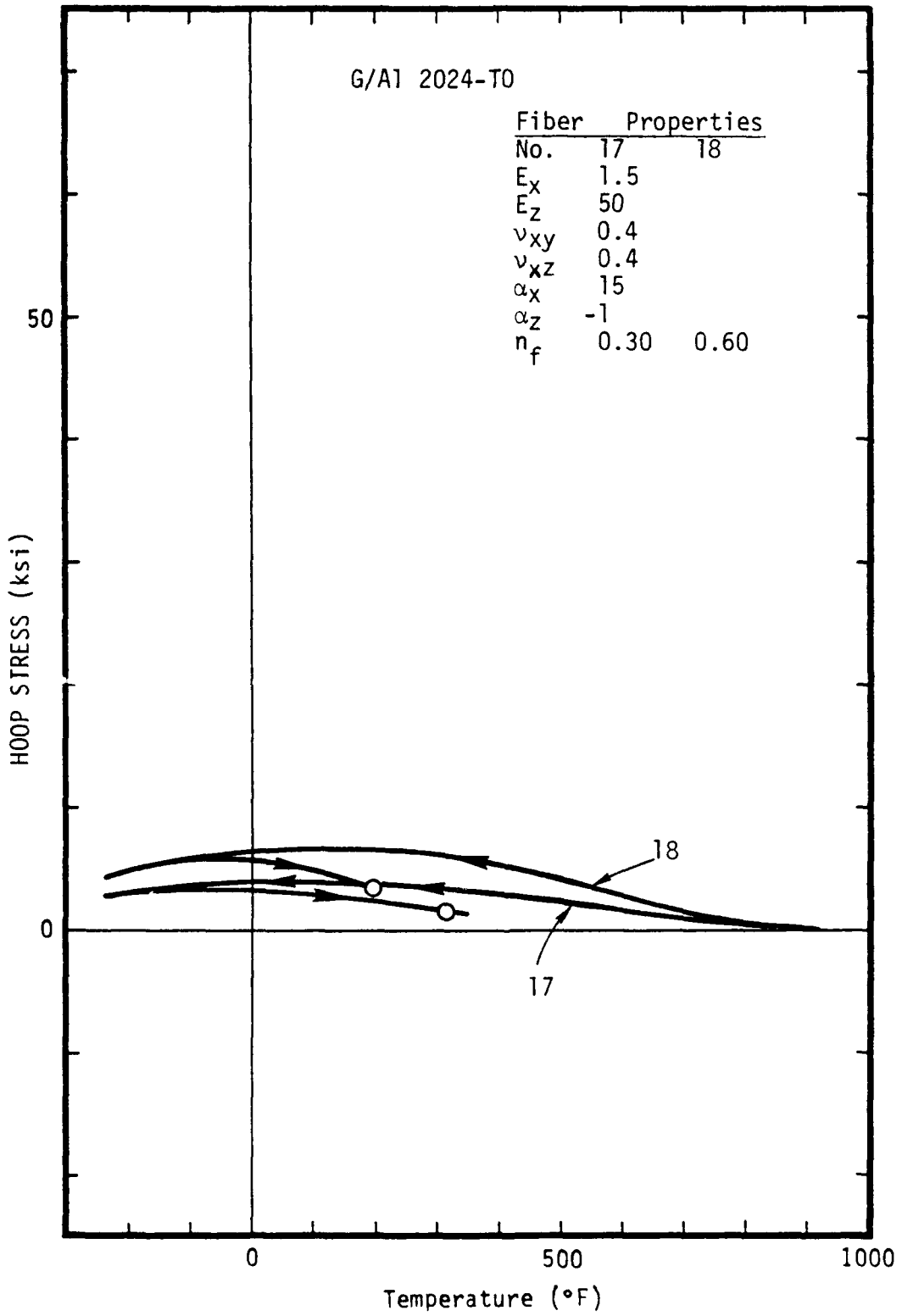

Figure 2.40. Volume-averaged hoop stress versus temperature for the matrix of a graphite/aluminum composite (slow cooling).

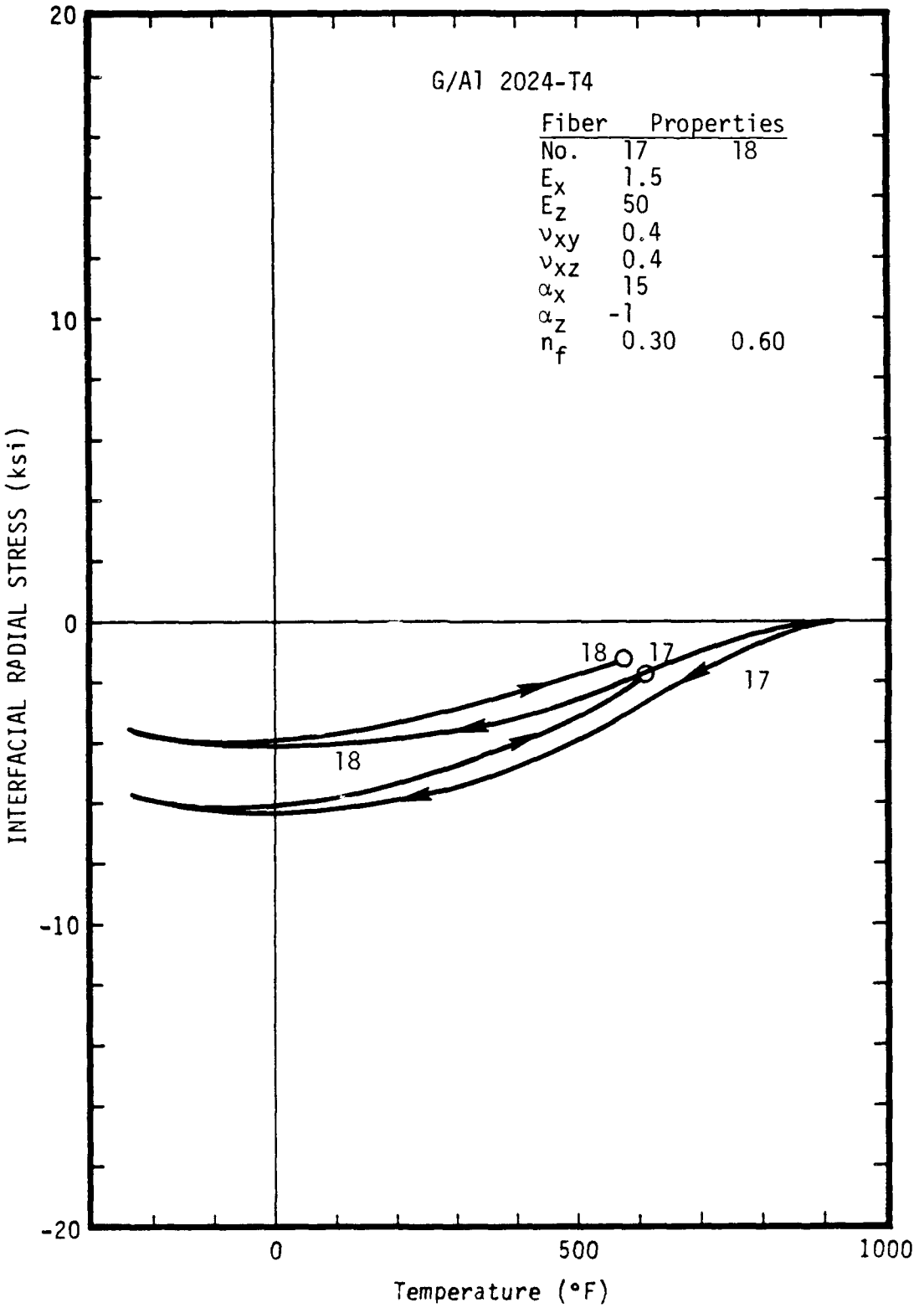

Figure 2.41. Radial stress versus temperature at the fiber-matrix interface of a graphite/aluminum composite (rapid cooling).

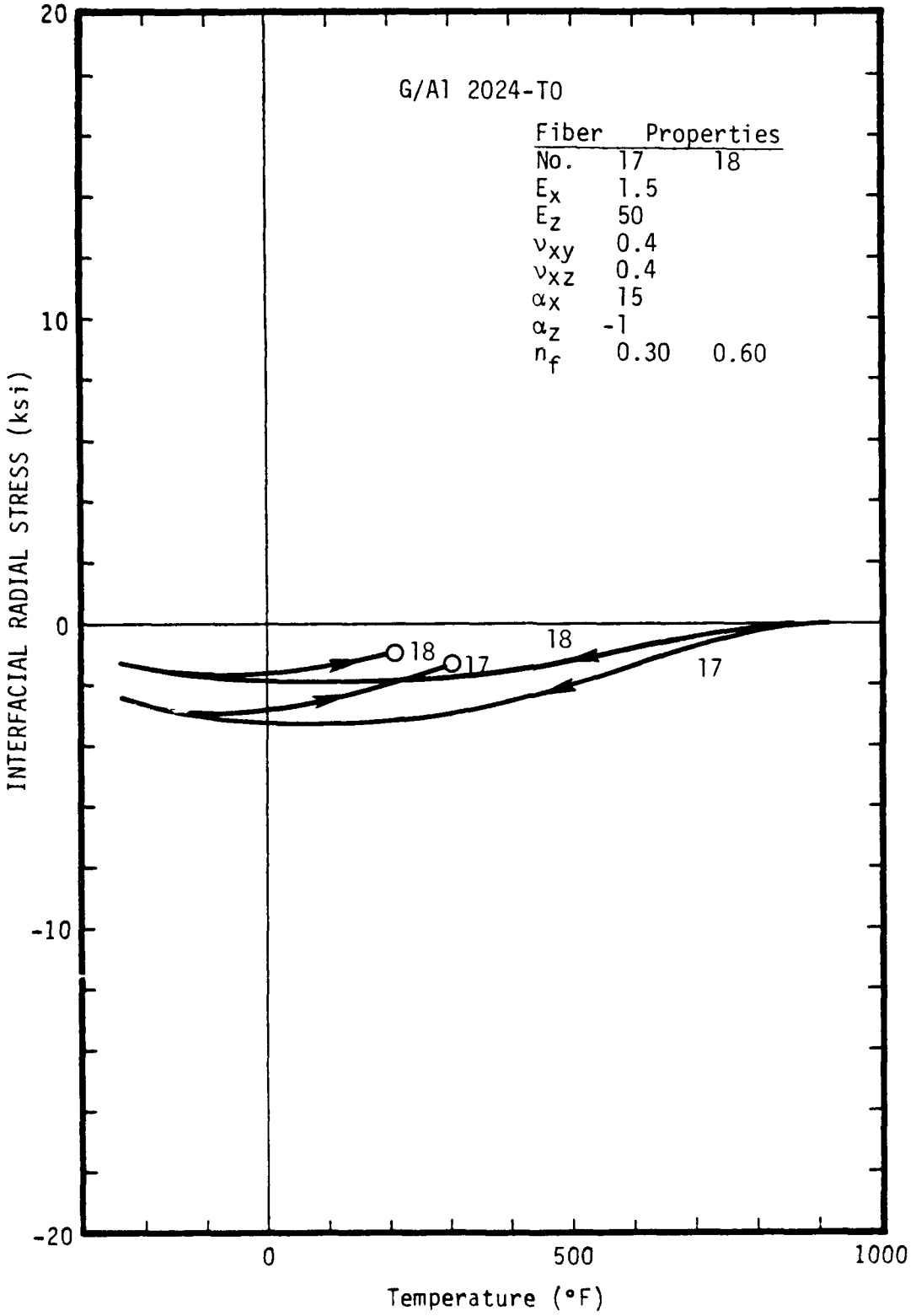

Figure 2.42. Radial stress versus temperature at the fiber-matrix interface of a graphite/aluminum composite (slow cooling).

(This Page Left Blank)

3. TUNGSTEN/ALUMINUM RESIDUAL STRESSES

Calculated axial and hoop stresses (volume averaged) in the aluminum matrix are given in Figures 3.1 and 3.2 for a composite which is 45 percent by volume of tungsten fibers and in Figures 3.3 and 3.4 for a 55 percent fiber loading. The temperature cycle is a cooling from a consolidation temperature of 930°F to a minimum temperature of -240°F followed by a reheating. The open circles on the reheating curves mark the temperature at which the stress state in the matrix again reaches the yield surface. As was the case for the graphite/aluminum calculations in Section 2, the matrix reaches the yield surface after only a few degrees of cooling (< 50°F) from the initial value of 930°F. The subsequent increase in stress is due to the temperature and plastic-flow dependence of the yield strength.

The material properties and yield-strength models for the 2024 aluminum are given in Appendix A. The tungsten fibers are assumed to be elastic over the entire temperature range, the following values being used for the tungsten's elastic modulus, Poisson's ratio and linear coefficient of thermal expansion:

$E = 59$ Msi

$\nu = 0.28$

$\alpha = 2.5 \times 10^{-6}$ in/in/°F .

The properties of the composite as calculated with the PRUFC code are given in Table 3.1 below.

TABLE 3.1 CALCULATED THERMOELASTIC PROPERTIES OF A TUNGSTEN/AL2024 COMPOSITE

n_f	0.45	0.55
E_x(Msi)	17.74	20.69
E_z(Msi)	32.33	37.18
ν_{xy}	0.434	0.428
ν_{xz}	0.305	0.300
$\alpha_z(10^{-6}°F^{-1})$	8.48	7.34
$\alpha_z(10^{-6}°F^{-1})$	4.34	3.82
G_{xy}(Msi)	6.19	7.24
G_{xz}(Msi)	7.63	8.98

For the TO temper (slow cooling from 930°F) the residual axial and hoop stresses are close to zero after reheating to room temperature from -240°F. Because of the low yield strength, however, the matrix will again reach the yield surface at about 150°F. For the T4 temper (rapid quench), the higher yield strength allows the matrix to remain elastic up to about 500°F. The high value of the axial residual stress at room temperature, however, would be undesirable if the composite is to be subjected to large tensile loads.

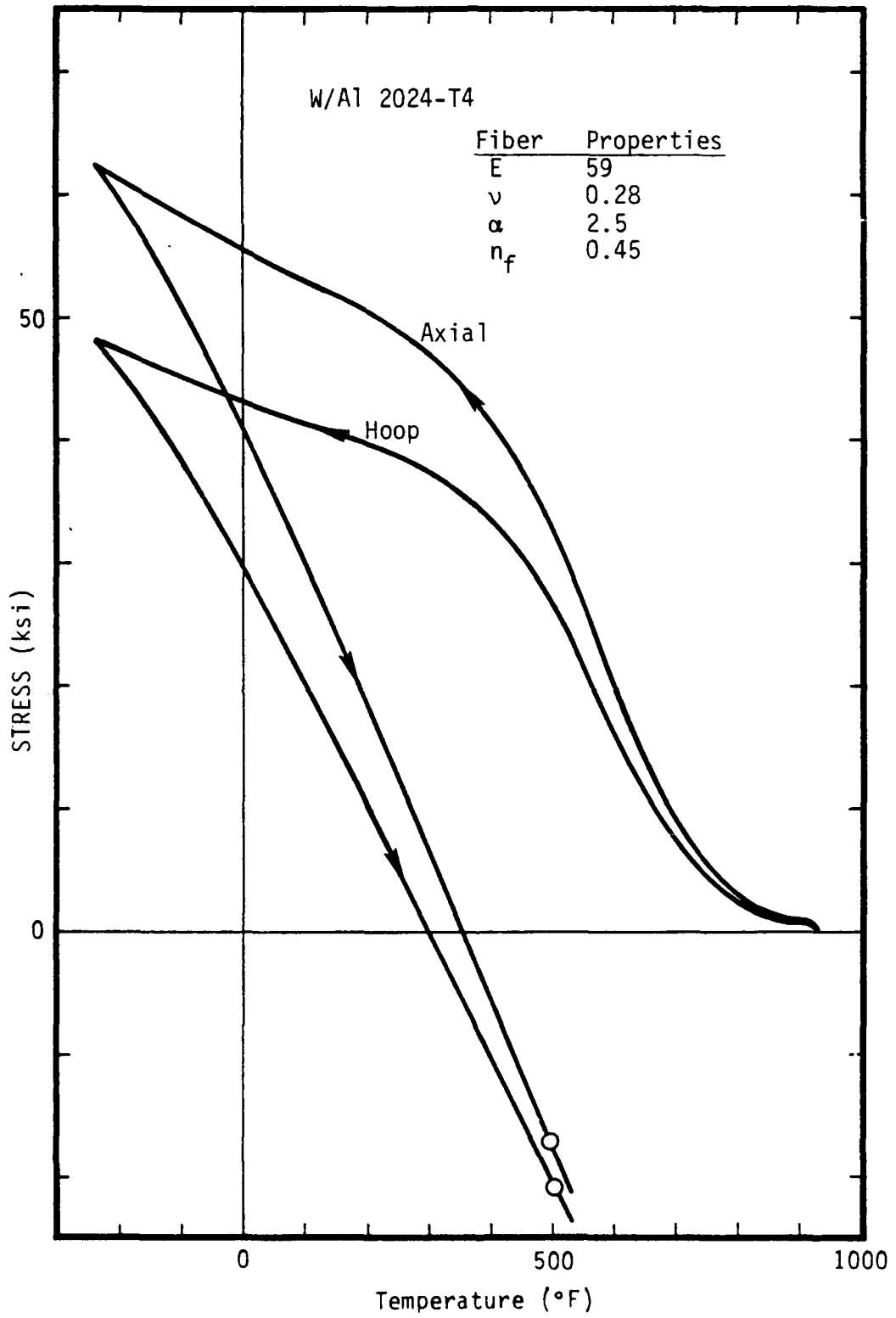

Figure 3.1. Volume-averaged axial and hoop stresses versus temperature for the matrix of a tungsten/aluminum composite (rapid cooling).

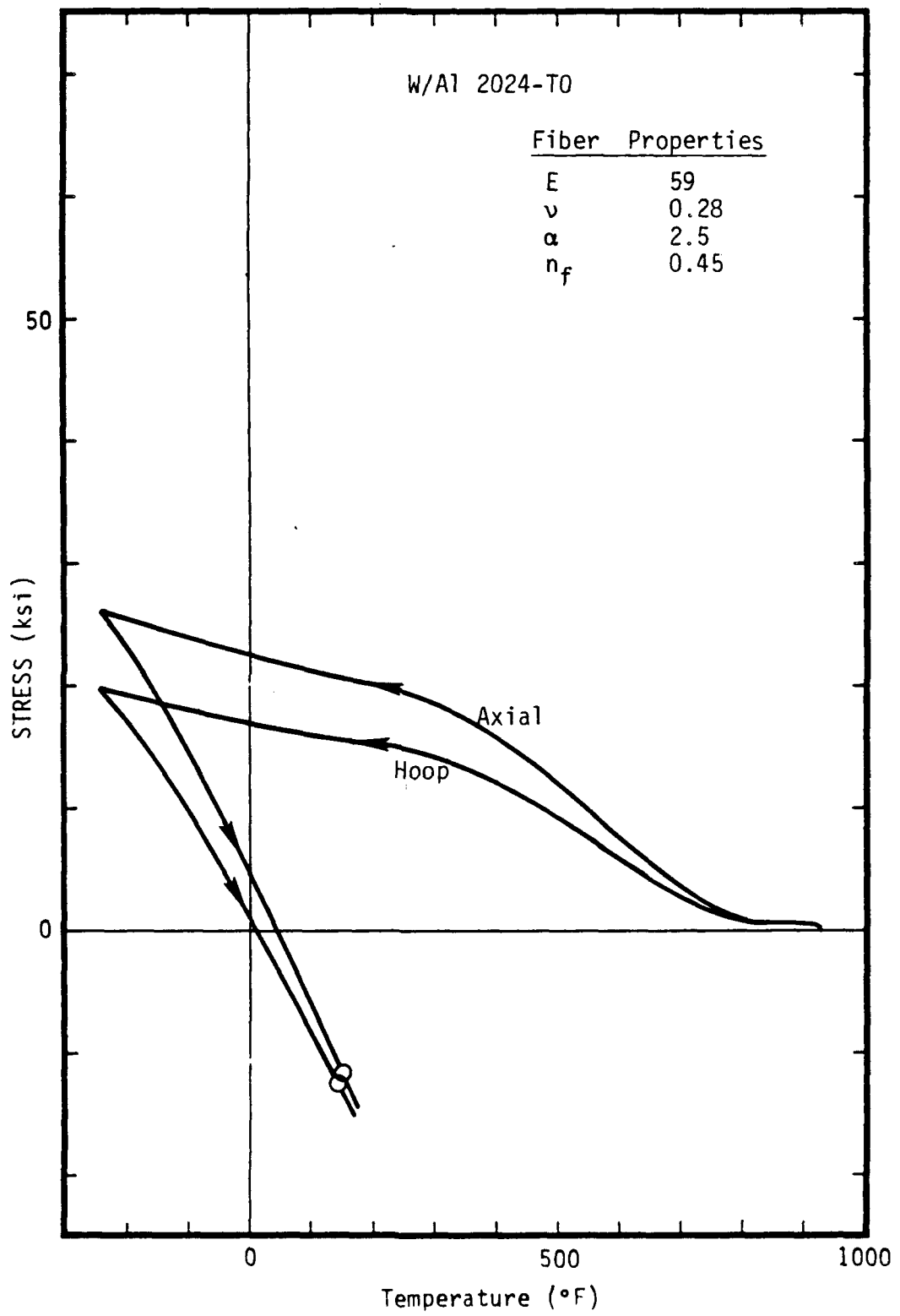

Figure 3.2. Volume-averaged axial and hoop stresses versus temperature for the matrix of a tungsten/aluminum composite (slow cooling).

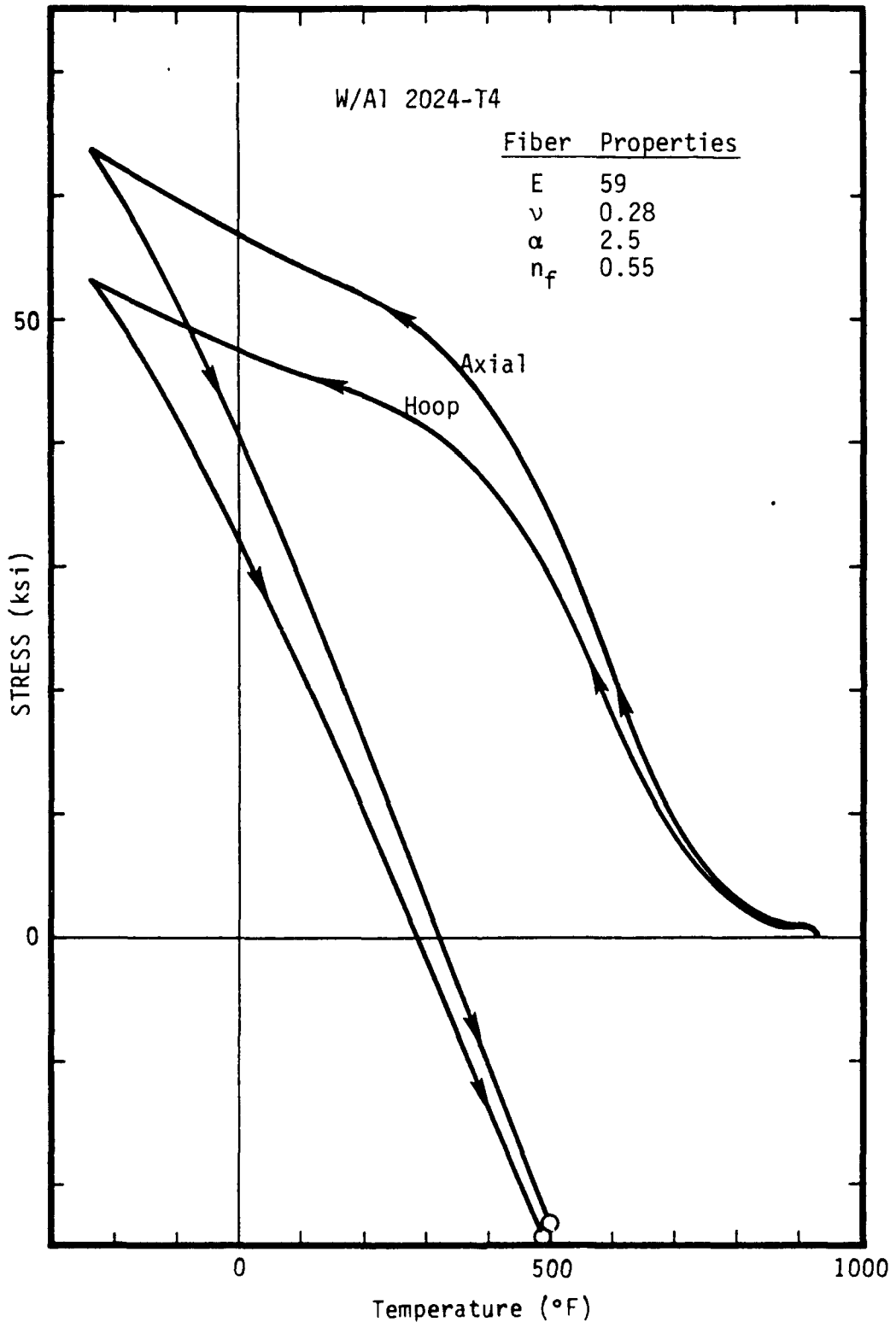

Figure 3.3. Volume-averaged axial and hoop stresses versus temperature for the matrix of a tungsten/aluminum composite (ranid cooling).

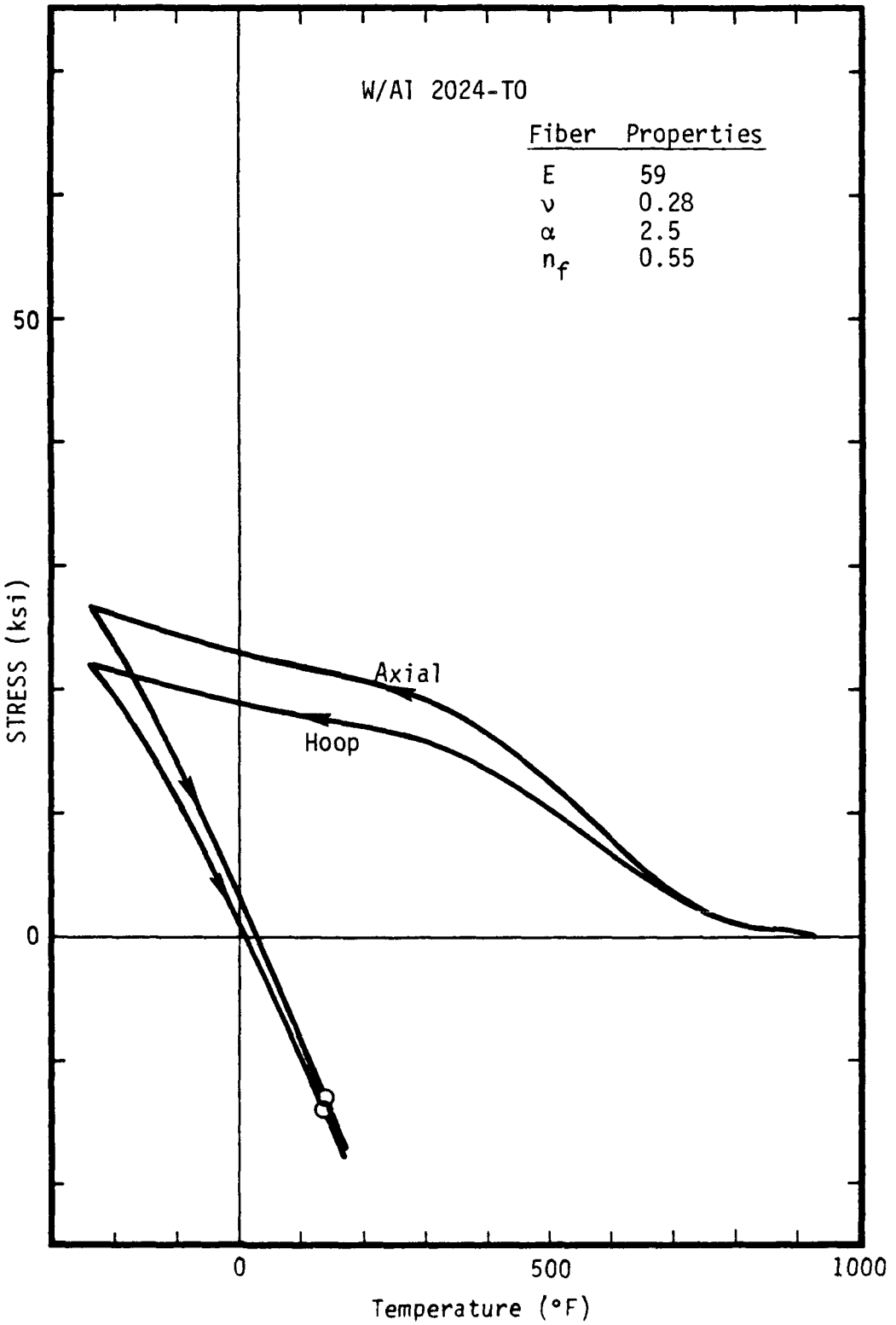

Figure 3.4. Volume-averaged axial and hoop stresses versus temperature for the matrix of a tungsten/aluminum composite (slow cooling).

4. SILICON CARBIDE/ALUMINUM RESIDUAL STRESSES

Several calculations have been done to determine the magnitudes of the residual stresses to be expected in a SiC/Al composite as a result of cooling from the consolidation to ambient temperature. The effect of these stresses on the elastic properties of unidirectional panels and cross-plied laminates is also considered. The results of this section have been submitted previously as an Interim Progress Report to the Naval Research Laboratory (Ref.4).

4.1 FIBER PROPERTIES

For bulk SiC, which we assume to be isotropic, the elastic (Young's) modulus and shear modulus were taken as (Ref. 5):

$$E = 68 \text{ Msi}$$
$$G = 27 \text{ Msi} \quad .$$

The coefficient of thermal expansion was assumed to be

$$\alpha = 2.42 \times 10^{-6} \text{ in/in/}^{\circ}\text{F}^{-1}$$

which, from Ref 5, is appropriate for the temperature range considered here.

The SiC fibers, however, are not completely bulk material, but apparently contain a core of essentially zero strength material (carbon) whose diameter is about 1.3×10^{-3} in. as compared with an outer fiber diameter of about 5.6×10^{-3} in. The volume fraction of the carbon core is thus 0.054. The overall properties of a fiber were determined with the PRUFC Code (Ref. 3), in which the sheath of the concentric cylinder model was assigned properties appropriate to the bulk SiC, and the core was assigned elastic moduli a factor of 10^{-3} smaller (hollow cylinder approximation). The resulting calculated properties of the fiber, which now becomes anisotropic-transversely isotropic, are:

$$E_A = 64.33 \text{ Msi}$$

$$E_T = 60.56 \text{ Msi}$$

$$\nu_{TT} = 0.2400$$

$$\nu_{TA} = 0.2600$$

$$G_{AT} = 24.25 \text{ Msi}$$

$$\alpha_A = \alpha_T = 2.42 \times 10^{-6} {}^\circ F^{-1} \quad ,$$

where the Poisson's ratio ν_{TT} refers to the transverse contraction for an applied transverse stress, and ν_{TA} refers to the transverse contraction for an applied axial stress. As expected, because of the small volume fraction of the core, the net fiber properties differ only slightly from those of the bulk SiC.

The material properties and yield-strength models for the aluminum 6061 matrix are given in Appendix A.

4.2 RESIDUAL STRESS RESULTS

Average axial stresses in the aluminum matrix of a SiC/Al composite are shown in Figure 4.1. Results are given for fiber volume fractions of 0.35 and 0.50 and for both the T0 and T4 aluminum tempers. The assumed thermal cycle process is a cooling from an initially stress-free state at 700°F to room temperature and then reheating.

As mentioned previously, the code uses a concentric-cylinder approximation to model the composite. For initial cooling from the stress-free state, both the inner cylinder (fiber) and the outer (matrix) are elastic. As cooling continues, the matrix material will in general reach its yield point, after which the Reuss equations for plastic flow (see, for example, Ref. 6) are integrated numerically to determine the distribution of stress in the outer (matrix) cylinder. In the code's present form the fiber is treated as linearly elastic over the entire temperature range.

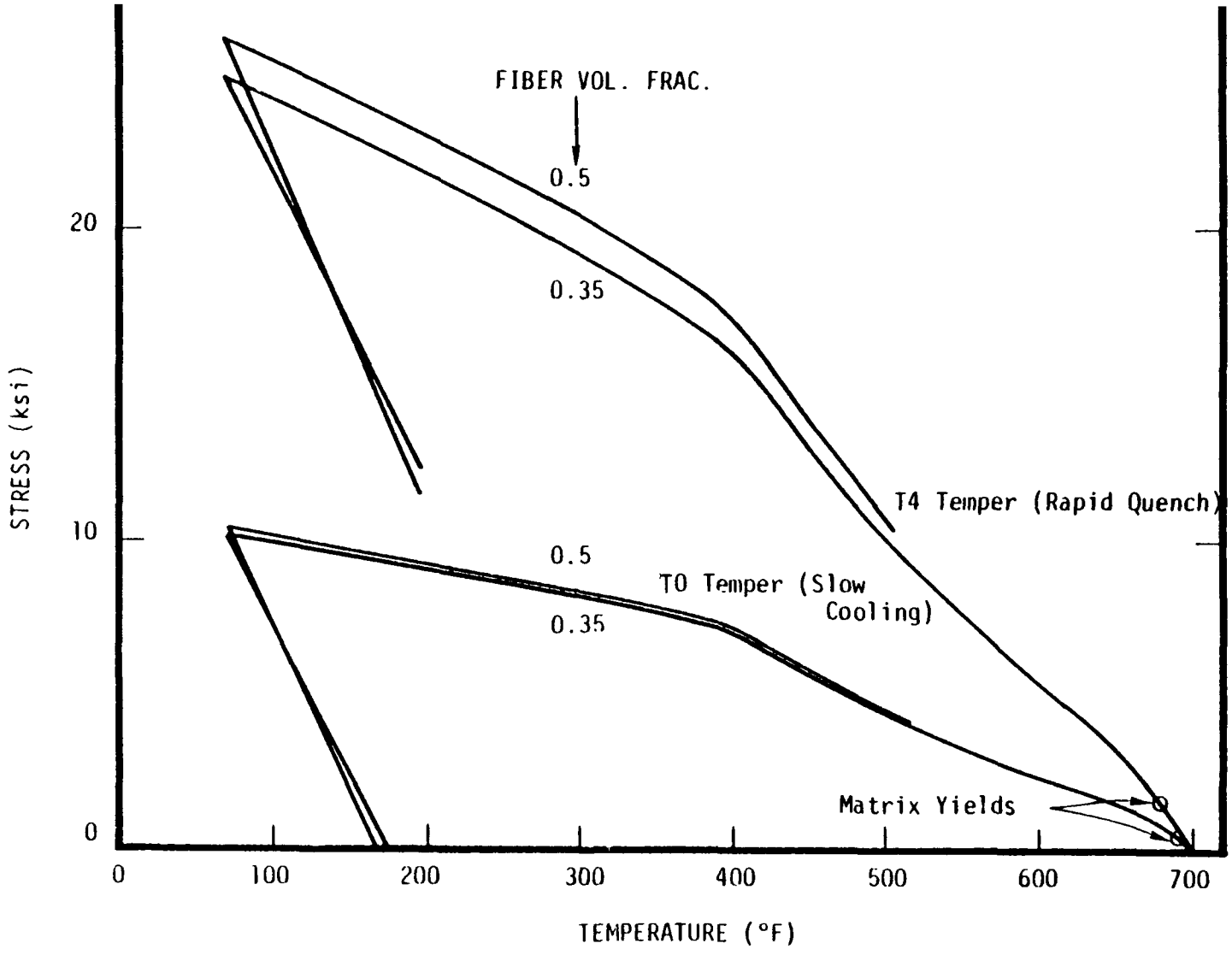

Figure 4.1. Calculated average axial stresses in the matrix of a SiC/Al 6061 composite as a function of temperature for different fiber volume fractions and matrix tempers. The assumed thermal cycle is a cooling to 70°F from a consolidation temperature of 700°F, and then a reheating from 70°F to indicate the rate of decrease of the residual stress.

For the cases depicted in Figure 4.1, about 20 degrees or less of cooling from the initial temperature of 700°F is sufficient to bring the aluminum matrix to its yield surface. The additional increase in axial stress for further cooling results from two causes: the increase of the matrix yield stress itself as a function of decreasing temperature, and a further increase due to plastic-flow work hardening. At the lowest temperature (70°F) the axial stress is a maximum, and its magnitude depends strongly on the effective temper of the aluminum. The calculation suggests that the maximum residual stress due to rapid quenching (T4 temper) would be over twice that of the slow-cooled or annealed state. If the composite is reheated from room temperature, the matrix material will fall off the yield surface, and as shown in Figure 4.1, the rate of decrease of stress in the elastic regime will be quite rapid. For the annealed case, a temperature increase of about 100°F would be sufficient to reduce the residual stresses to approximately zero.

It is anticipated that A357 aluminum casting alloy will also be used in the fabrication of these composites. No residual stress calculations for this material have been done as yet because we have been unable to locate yield strength information for the T0 and T4 tempers. No large differences with respect to the 6061 matrix are expected however, since the yield strength of the A357 alloy in the T6 temper is comparable to that of 6061-T6, and other mechanical properties also are not significantly different.

4.3 ELASTIC PROPERTIES OF A UNIAXIALLY REINFORCED LAMINATE

Since the coefficient of thermal expansion for the aluminum matrix is greater than that of the SiC fibers, the residual stresses in the matrix after cool-down will be tensile in the axial direction. (The calculated hoop stresses in the concentric cylinder model are also tensile, but the radial stress is compressive, so that there should be little tendency for debonding to occur between the matrix and fibers.) If the composite is not subjected to an

overall tensile axial stress, the matrix will remain on the yield surface and the effective axial elastic modulus will be lower than it would be in the absence of residual stresses.

The plastic-flow code as described in Ref. 1 has been augmented so that it is now possible to calculate the stresses as a function of axial strain following the cool-down procedure. The calculated overall axial stress as a function of axial strain at 70°F is plotted in Figure 4.2 for the 6061-T0 yield model after cooling from 700°F. Also shown is the straight-line stress-strain curve for an elastic matrix as calculated with the PRUFC code, and an experimental stress-strain curve obtained from AVCO (Ref. 7), the volume fraction of fibers in this case being 0.45. The experimental curve changes slope at about 90 ksi, and the slope of the higher-stress segment is in good agreement with that of the curve corresponding to the yielded matrix. The lower-stress portion of the experimental curve however, is in agreement with the stress-strain curve as calculated using an elastic matrix.

The overall axial stress for the composite is related to that in the fibers and matrix by

$$\sigma_z = n_f \sigma_{zf} + (1 - n_f)\sigma_{zm} \quad .$$

For this material one has, to good approximation,

$$\sigma_{zf} \simeq \frac{E_f}{E_m} \sigma_{zm}$$

for the fiber stress in terms of that in the matrix, where E_f and E_m are the respective fiber and matrix axial elastic moduli. For an elastic matrix of modulus E_m = 10 Msi, and an overall composite axial stress of 90 ksi, the matrix would experience a stress of 26 ksi, a value close to the nominal yield stress of 6061 aluminum in the T4 temper. On the other hand, if the break in the experimental curve at 90 ksi is to be interpreted as the transition point from an

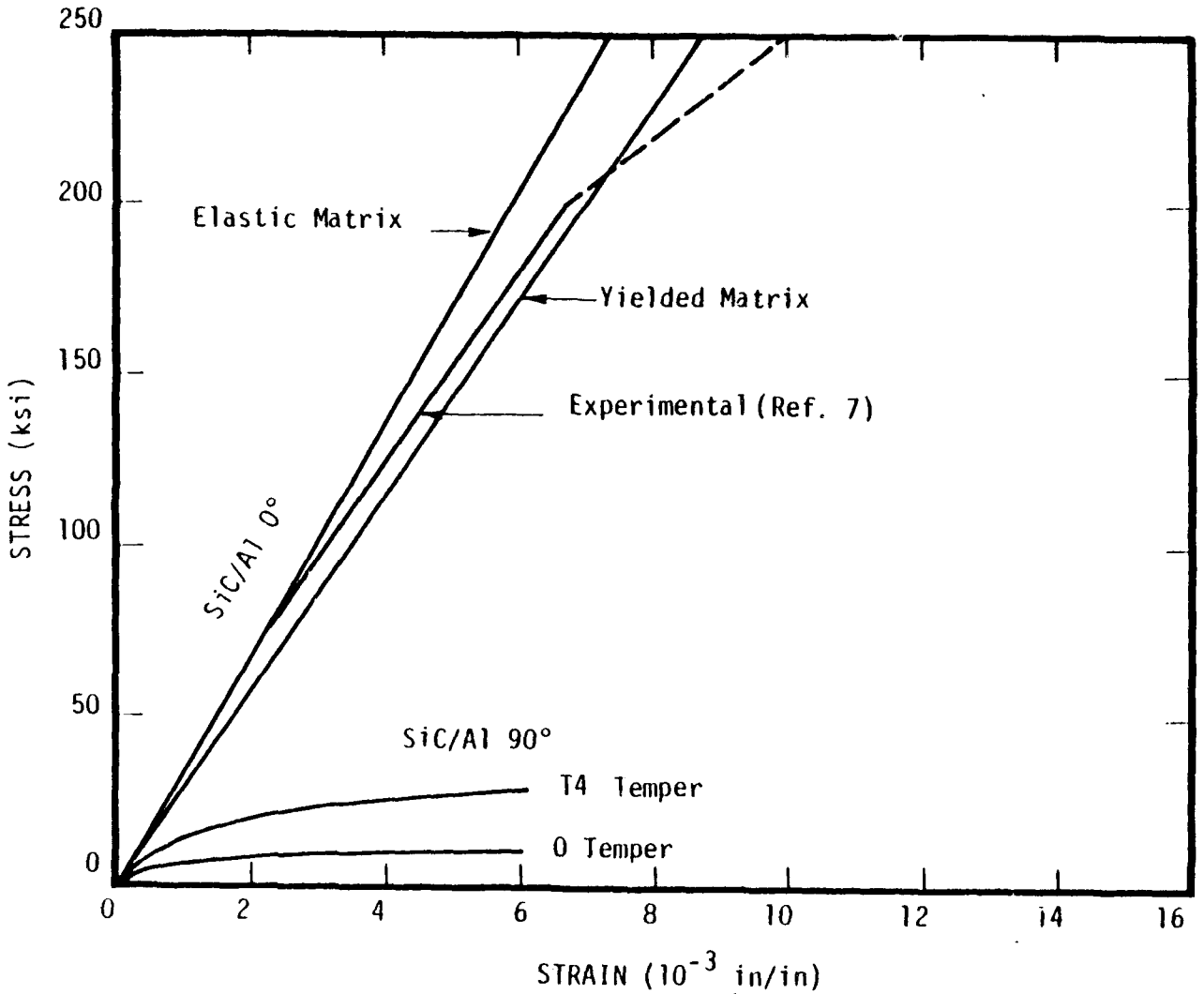

Figure 4.2. Comparison of calculated and experimental axial stress-strain curves for a 0.45 fiber volume-fraction SiC/Al 6061 composite. The curve for the yielded matrix corresponds to the TO temper model of Figure 4.1.

elastic to a plastic matrix, then the initial state of the matrix would have to be essentially stress-free, in marked disagreement with the calculated axial residual stress as shown in Figure 4.1.

The slope of the calculated stress-strain curve corresponding to a yielded matrix is 29.3 Msi, which is close to the value

$$n_f E_f = (0.45)(64.33) = 28.9 \text{ Msi} \quad ,$$

which one would expect for the composite elastic modulus if the matrix modulus were zero. This result is to be expected, since at the yield surface the effective modulus of the matrix is approximately equal to the local slope of the yield-strength versus strain curve, which typically ranges from several hundred ksi to about 1 Msi (see Figures A.3 and A.4 of Appendix A). Since this slope for either the T0 or T4 temper is small as compared with the 64 Msi modulus of the fiber, the choice of tempers has a negligible effect on the calculated value of the effective axial modulus for the composite if the matrix is indeed on the yield surface.

The concentric-cylinder approximation used in the S-CUBED plastic-flow code does not lend itself to the calculation of the transverse stress-strain relations if the matrix is on the yield surface. From the PRUFC code, however, for an elastic matrix the calculated transverse modulus for the composite is

$$E_T = 17.1 \text{ Msi}$$

for a fiber volume fraction of 0.45. The mixture result for a simple series combination of the fiber and matrix materials,

$$\frac{1}{E_T^*} = \frac{0.45}{60.56} + \frac{0.55}{10}$$

gives the result

$$E_T^* = 16.0 \text{ Msi} \quad ,$$

quite close to the PRUFC result, so that the simple series combination might be expected to give a useful approximation to the transverse behavior, even if the matrix has yielded.

Note here that if the matrix material is at the yield surface due to the cool-down residual stresses, then the dominant residual stress is tension in the axial direction. Consequently, an applied transverse tension will pull the matrix off the yield surface and the initial transverse behavior will be elastic. Under an applied transverse compressive stress, the matrix would stay on the yield surface and flow plastically, resulting in a lower apparent modulus for the composite.

For the simple series combination, the overall strain is given by

$$\varepsilon = n_f \varepsilon_f + (1 - n_f)\varepsilon_m$$

in the transverse direction, or

$$\varepsilon = n_f \frac{\sigma}{E_f} + (1 - n_f)\varepsilon_m(\sigma) \quad .$$

The above relation was used to obtain the estimates for the 90 degree orientation composites as plotted in Figure 4.2.

4.4 LAMINATE PROPERTIES

The code constructed at S-CUBED (Appendix B) may be used to compute the elastic properties of a laminate with plies oriented in up to three different arbitrary directions. As input one may use either the elastic and thermal properties of each type of ply, or the volume fractions and individual properties of the fiber and matrix components for each type of ply. In the latter case the code computes the ply properties as per the method used in the PRUFC

code. With the fiber and matrix properties as input, the code was used to determine the elastic behavior of a $0^\circ/90^\circ/90^\circ/0^\circ$ laminate with each ply consisting of a 0.45 fiber volume-fraction SiC/Al composite. The resulting slope of tne initial elastic segment is indicated in Figure 4.3, both for an initial stress-free state and for tne case where tne matrix material is at the yield surface due to cool-down residual stresses. Fcr the 90° plies, the initial benavior, as discussed above, will be elastic even though the matrix is initially on the yield surface. It turns out that for these orientations, tne resulting elastic modulus of the composite laminate is very nearly the same as that of a simple combination of parallel springs. Thus, with equal volume fractions of the 0° and 90° plies, the laminate modulus corresponding to an elastic matrix is

$$(34.5 + 17.1)/2 = 25.8 \text{ Msi},$$

and for the yielded matrix it drops to

$$(29.3 + 17.1)/2 = 23.2 \text{ Msi}$$

as indicated in Figure 4.3. Eventually, the 90° plies, which had initially dropped off the yield surface, will once again reach the yield surface. Using an elastic-perfectly plastic model with a yield stress of 21 ksi (T4 temper), this is found to occur at an overall stress of about 28 ksi, at which point the slope of tne stress-strain curve will drop to about

$$29.3/2 = 14.6 \text{ ksi}$$

Tne resulting stress-strain relationship agrees well with a projected estimate from AVCO, as shown in Figure 4.3.

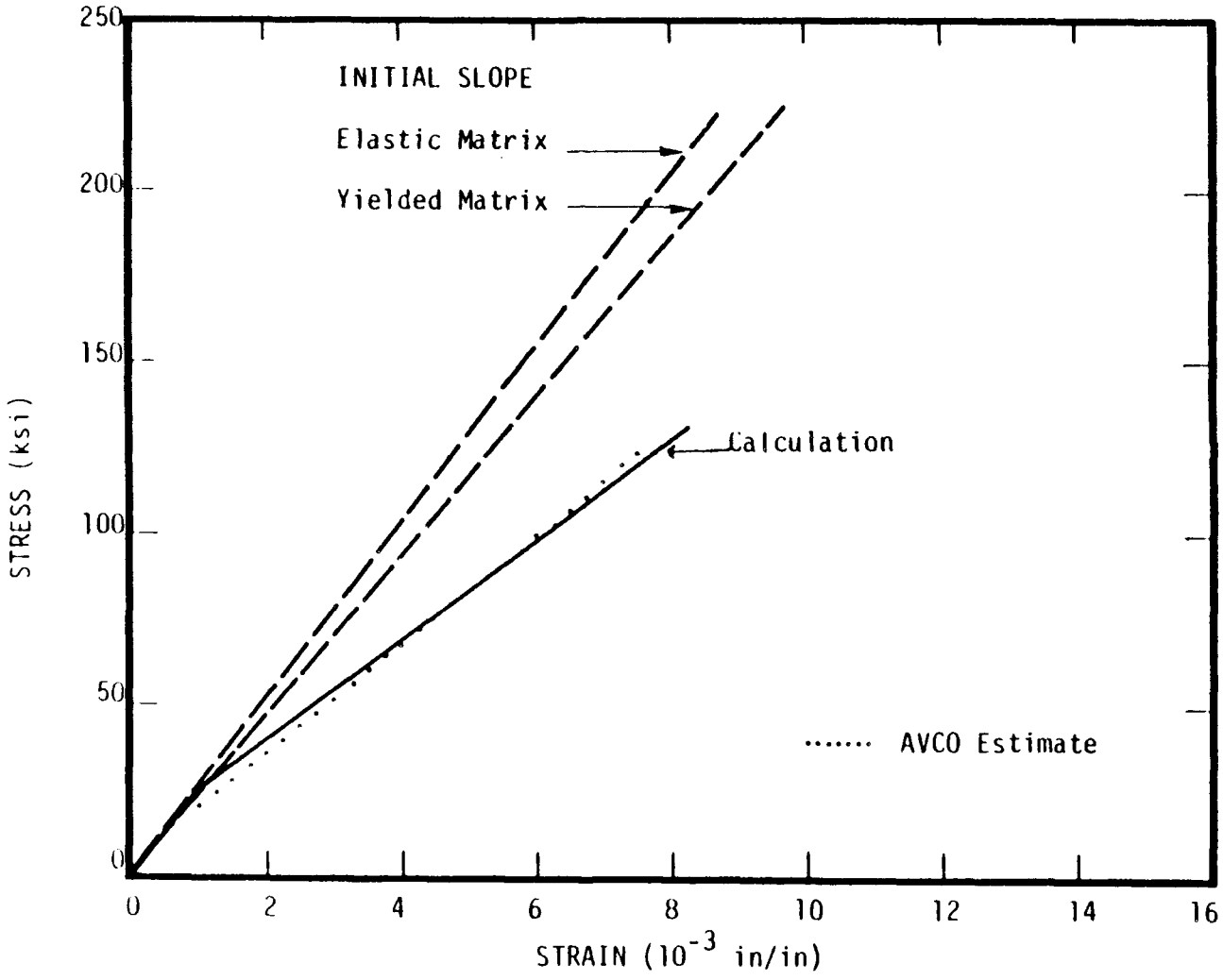

Figure 4.3. Calculated stress-strain relations for a 0°/90°/90°/0° laminate consisting of 0.45 fiber volume-fraction SiC/Al plies. Also shown is a projected estimate from AVCO (Ref. 7).

5. THERMOELASTIC PROPERTIES OF CROSS-PLY LAMINATES

Computational machinery is presented for determining the elastic moduli and thermal expansion characteristics of cross-plied laminates from the properties of the individual unidirectionally reinforced layers. Explicit formulas are given for the elastic constants and thermal expansion coefficients for a laminate with equal volume fractions of plies oriented in two directions. The computer code (Appendix B) in its present form may be used for plies oriented in up to three different directions. The code also provides the stress-temperature derivatives within each type of ply, appropriate to a uniform heating from an initial stress-free state.

5.1 TRANSFORMATION OF ELASTIC CONSTANTS

As a first step, it is necessary to obtain expressions for the elastic constants of a fiber-reinforced material in a coordinate system rotated with respect to that defined by the direction of the fibers. The stress-strain relations for a fiber-reinforced material assume the simplest form in the fiber coordinate system (FCS), i.e., that coordinate system in which one of the axes is in the direction of the fibers. If we take the z-axis as being parallel to the fibers, then the stresses are given in terms of the strains by the matrix relation

$$\begin{bmatrix} \sigma_{xx} \\ \sigma_{yy} \\ \sigma_{zz} \\ \sigma_{yz} \\ \sigma_{xz} \\ \sigma_{xy} \end{bmatrix} = \begin{bmatrix} C_{11} & C_{12} & C_{13} & 0 & 0 & 0 \\ C_{12} & C_{11} & C_{13} & 0 & 0 & 0 \\ C_{13} & C_{13} & C_{33} & 0 & 0 & 0 \\ 0 & 0 & 0 & 2C_{44} & 0 & 0 \\ 0 & 0 & 0 & 0 & 2C_{44} & 0 \\ 0 & 0 & 0 & 0 & 0 & 2C_{66} \end{bmatrix} \begin{bmatrix} \varepsilon_{xx} \\ \varepsilon_{yy} \\ \varepsilon_{zz} \\ \varepsilon_{yz} \\ \varepsilon_{xz} \\ \varepsilon_{xy} \end{bmatrix} \tag{5.1}$$

i.e.,

$$\sigma_{xx} = C_{11}\varepsilon_{xx} + C_{12}\varepsilon_{yy} + C_{13}\varepsilon_{zz} \quad ,$$
$$\sigma_{yz} = 2C_{44}\varepsilon_{yz} \quad , \quad \text{etc.}, \tag{5.2}$$

where the strains are defined by

$$\varepsilon_{ij} = \frac{1}{2}\left(\frac{\partial u_i}{\partial x_j} + \frac{\partial u_j}{\partial x_i}\right) \tag{5.3}$$

In what follows, the subscripts 1, 2, 3 will be used interchangeably with x, y, z, respectively, to denote the coordinate axes. In the usual case, where the material is not only orthotropic but also transversely isotropic,

$$C_{66} = \frac{1}{2}(C_{11} - C_{12}) \quad . \tag{5.4}$$

For the laminate analysis, we require the elastic constants of the ply in the rotated coordinate system x'y'z' as shown in Figure 5.1, obtained by a positive rotation ($\theta > 0$) about the x,x' axis, which is perpendicular to the face of the ply. The elastic constants C_{pq} are, of course, components of the fourtn rank tensor, C_{ijmn}, which relates the stresses to the strains,

$$\sigma_{ij} = C_{ijmn}\varepsilon_{mn} \quad , \tag{5.5}$$

using the summation convention m,n = 1,2,3 over repeated indices.

In general, the transformation to a new coordinate system is given by

$$C'_{pqkr} = \ell_{pi}\ell_{qj}\ell_{km}\ell_{rn}C_{ijmn} \quad , \tag{5.6}$$

where the ℓ_{ij} relate the components of a vector in the primed coordinate system to those in the unprimed; and in the present case (Figure 5.1), these quantities are given by the matrix

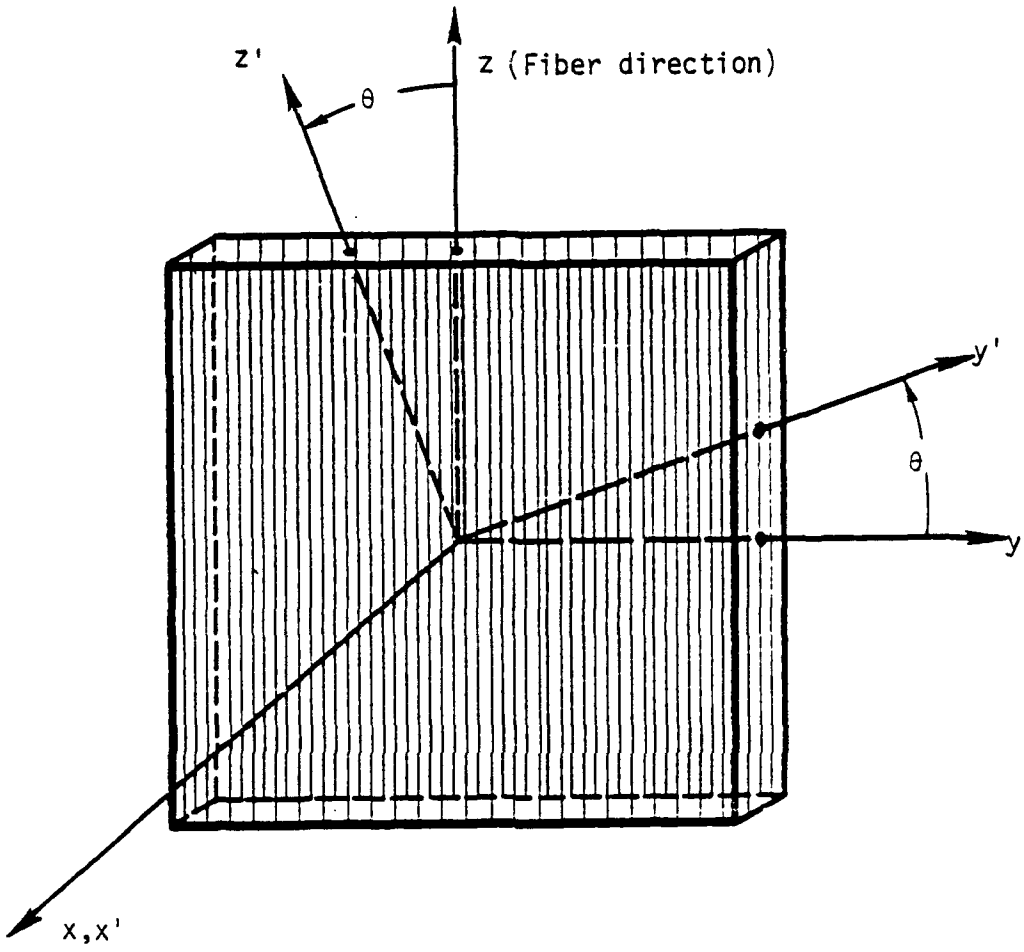

Figure 5.1 Coordinate system x'y'z' used for laminate analysis.

$$\left[\ell_{ij}\right] = \begin{bmatrix} \ell_{11} & \ell_{12} & \ell_{13} \\ \ell_{21} & \ell_{22} & \ell_{23} \\ \ell_{31} & \ell_{32} & \ell_{33} \end{bmatrix} = \begin{bmatrix} 1 & 0 & 0 \\ 0 & \cos\theta & \sin\theta \\ 0 & -\sin\theta & \cos\theta \end{bmatrix} . \tag{5.7}$$

In the FCS, the nonvanishing components of the tensor C_{ijkm} are given in terms of the elastic constants defined in Eq, (5.1) by

$$\begin{aligned} C_{11} &= C_{1111} = C_{2222} \\ C_{12} &= C_{1122} = C_{2211} \\ C_{13} &= C_{1133} = C_{2233} = C_{3311} = C_{3322} \\ C_{33} &= C_{3333} \\ C_{44} &= C_{2323} = C_{2332} = C_{3223} = C_{3232} \\ &= C_{1313} = C_{1331} = C_{3113} = C_{3131} \\ C_{66} &= C_{1212} = C_{1221} = C_{2112}\ C_{2121} \quad . \end{aligned} \tag{5.8}$$

Thus, tne calculation of a typical component in the new coordinate system requires the consideration of 21 terms. For example,

$$\begin{aligned} C'_{3333} = {} & \ell_{31}\ell_{31}\ell_{31}\ell_{31}C_{1111} + \ell_{32}\ell_{32}\ell_{32}\ell_{32}C_{2222} \\ & + \ell_{31}\ell_{31}\ell_{32}\ell_{32}C_{1122} + \ell_{32}\ell_{32}\ell_{31}\ell_{31}\ C_{2211} \\ & + \ \ldots \quad + \ldots \quad + \ldots \\ & + \ell_{32}\ell_{31}\ell_{31}\ell_{32}C_{2112} + \ell_{32}\ell_{31}\ell_{32}\ell_{31}C_{2121} \quad . \end{aligned} \tag{5.9}$$

Many of the terms are zero, however, because of the simple form of the transformation matrix, Eq. (5.7).

The result is that the stresses and strains in the primed coordinate system of Figure 5.1 are related by (note that the matrix is <u>not</u> symmetric)

$$\begin{bmatrix} \sigma'_{xx} \\ \sigma'_{yy} \\ \sigma'_{zz} \\ \sigma'_{yz} \\ \sigma'_{xz} \\ \sigma'_{xy} \end{bmatrix} = \begin{bmatrix} C'_{11} & C'_{12} & C'_{13} & 2C'_{14} & 0 & 0 \\ C'_{12} & C'_{22} & C'_{23} & 2C'_{24} & 0 & 0 \\ C'_{13} & C'_{23} & C'_{33} & 2C'_{34} & 0 & 0 \\ C'_{14} & C'_{24} & C'_{34} & 2C'_{44} & 0 & 0 \\ 0 & 0 & 0 & 0 & 2C'_{55} & 2C'_{56} \\ 0 & 0 & 0 & 0 & 2C'_{56} & 2C'_{66} \end{bmatrix} \begin{bmatrix} \varepsilon'_{xx} \\ \varepsilon'_{yy} \\ \varepsilon'_{zz} \\ \varepsilon'_{yz} \\ \varepsilon'_{xz} \\ \varepsilon'_{xy} \end{bmatrix} , \qquad (5.10)$$

where the new elastic constants are given in terms of the old by

$$C'_{11} = C_{11}$$

$$C'_{12} = C_{12}\cos^2\theta + C_{13}\sin^2\theta$$

$$C'_{13} = C_{12}\sin^2\theta + C_{13}\cos^2\theta \qquad (5.11)$$

$$C'_{14} = -C_{12}\sin\theta\cos\theta + C_{13}\sin\theta\cos\theta$$

$$C'_{22} = C_{11}\cos^4\theta + C_{33}\sin^4\theta + 2C_{13}\sin^2\theta\cos^2\theta + 4C_{44}\sin^2\theta\cos^2\theta$$

$$C'_{23} = (C_{11} + C_{33})\sin^2\theta\cos^2\theta + C_{13}(\sin^4\theta + \cos^4\theta) - 4C_{44}\sin^2\theta\cos^2\theta$$

$$C'_{24} = -C_{11}\sin\theta\cos^3\theta + C_{13}(\sin\theta\cos^3\theta - \sin^3\theta\cos\theta) + C_{33}\sin^3\theta\cos\theta + 2C_{44}(\sin\theta\cos^3\theta - \sin^3\theta\cos\theta)$$

$$C'_{33} = C_{33}\cos^4\theta + C_{11}\sin^4\theta + 2C_{13}\sin^2\theta\cos^2\theta + 4C_{44}\sin^2\theta\cos^2\theta$$

$$C'_{34} = -C_{11}\sin^3\theta\cos\theta + C_{33}\sin\theta\cos^3\theta + C_{13}(\sin^3\theta\cos\theta - \sin\theta\cos^3\theta) + 2C_{44}(\sin^3\theta\cos\theta - \sin\theta\cos^3\theta)$$

$$C'_{44} = (C_{11} + C_{33}) \sin^2\theta\cos^2\theta - 2C_{13}\sin^2\theta\cos^2\theta + C_{44}(\cos^2\theta - \sin^2\theta)^2$$

$$C'_{55} = C_{44}\cos^2\theta + C_{66}\sin^2\theta$$

$$C'_{56} = (C_{44} - C_{66}) \sin\theta\cos\theta$$

$$C'_{66} = C_{66}\cos^2\theta + C_{44}\sin^2\theta$$

The above results have been checked against those given by Hasnin[8] for an initial coordinate system in which the fibers are parallel to the x-axis.

The description in the primed coordinate system is completed by a consideration of the thermal stress parameters. In the fiber coordinate system the thermal stresses are given by

$$\begin{aligned} \sigma_{xx}^{(T)} &= \sigma_{yy}^{(T)} = -\gamma_1\Delta T \quad , \\ \sigma_{zz}^{(T)} &= -\gamma_3\Delta T \quad , \end{aligned} \tag{5.12}$$

where ΔT is the temperature increment, and the stress-temperature coupling coefficients are given in terms of the linear coefficients of thermal expansion by

$$\begin{aligned} \gamma_1 &= (C_{11} + C_{12})\alpha_x + C_{13}\alpha_z \\ \gamma_3 &= 2C_{13}\alpha_x + C_{33}\alpha_z \quad . \end{aligned} \tag{5.13}$$

The nonvanishing components of this second rank tensor in the primed coordinate system are

$$\begin{aligned} \gamma'_{11} &= \gamma_1 \\ \gamma'_{22} &= \gamma_1\cos^2\theta + \gamma_3\sin^2\theta \\ \gamma'_{33} &= \gamma_1\sin^2\theta + \gamma_3\cos^2\theta \\ \gamma'_{23} &= \gamma'_{32} = (\gamma_3 - \gamma_1) \sin\theta\cos\theta \end{aligned} \tag{5.14}$$

In summary, the stresses are given in terms of the strains in the rotated, or laminate coordinate system (LCS), by

$$\begin{aligned}
\sigma_{11} &= C_{11}\varepsilon_{11} + C_{12}\varepsilon_{22} + C_{13}\varepsilon_{33} + 2C_{14}\varepsilon_{23} - \gamma_{11}\Delta T \\
\sigma_{22} &= C_{12}\varepsilon_{11} + C_{22}\varepsilon_{22} + C_{23}\varepsilon_{33} + 2C_{24}\varepsilon_{23} - \gamma_{22}\Delta T \\
\sigma_{33} &= C_{13}\varepsilon_{11} + C_{23}\varepsilon_{22} + C_{33}\varepsilon_{33} + 2C_{34}\varepsilon_{23} - \gamma_{33}\Delta T \\
\sigma_{23} &= C_{14}\varepsilon_{11} + C_{24}\varepsilon_{22} + C_{34}\varepsilon_{33} + 2C_{44}\varepsilon_{23} - \gamma_{23}\Delta T \\
\sigma_{13} &= 2C_{55}\varepsilon_{13} + 2C_{56}\varepsilon_{12} \\
\sigma_{12} &= 2C_{56}\varepsilon_{13} + 2C_{66}\varepsilon_{12} \quad ,
\end{aligned} \tag{5.15}$$

where, for convenience, the primes have been omitted. If we consider the stresses as a six component column matrix, then the above relations can be written in matrix form as

$$\sigma = C\varepsilon - \gamma\,\Delta T \quad , \tag{5.16}$$

and the inverse relations giving the strains in terms of the stresses are

$$\varepsilon = C^{-1}\sigma + C^{-1}\gamma\,\Delta T \quad ,$$

or equivalently as

$$\varepsilon = S\sigma + \alpha\,\Delta T \quad , \tag{5.18}$$

i.e.,

$$\begin{aligned}
\varepsilon_{11} &= S_{11}\sigma_{11} + S_{12}\sigma_{22} + S_{13}\sigma_{33} + 2S_{14}\sigma_{23} + \alpha_{11}\Delta T \\
\varepsilon_{22} &= S_{12}\sigma_{11} + S_{22}\sigma_{22} + S_{23}\sigma_{33} + 2S_{24}\sigma_{23} + \alpha_{22}\Delta T \\
\varepsilon_{33} &= S_{13}\sigma_{11} + S_{23}\sigma_{22} + S_{33}\sigma_{33} + 2S_{34}\sigma_{23} + \alpha_{33}\Delta T \\
\varepsilon_{23} &= S_{14}\sigma_{11} + S_{24}\sigma_{22} + S_{34}\sigma_{33} + 2S_{44}\sigma_{23} + \alpha_{23}\Delta T \\
\varepsilon_{13} &= 2S_{55}\sigma_{13} + 2S_{56}\sigma_{12} \\
\varepsilon_{12} &= 2S_{56}\sigma_{13} + 2S_{66}\sigma_{12}
\end{aligned} \tag{5.19}$$

where the inverse S of the matrix C is easily obtained using the computer (note again that the matrix S and the matrix C are not symmetric when the strains are defined by Eq. (5.3)).

5.2 THERMAL EXPANSION COEFFICIENTS

Here we shall be concerned with the thermal expansion coefficients of a laminate containing equal volume fractions of plies with fibers oriented in one or the other of two directions. The z-axis of the laminate coordinate system is taken as the bisector of the angle between the fiber directions, as indicated in Figure 5.2.

The elastic constants in the LCS of a ply with fibers in the z_1 direction are given directly by the relations (5.11); and the elastic constants of a ply with fibers along z_2 may be obtained from the connections (5.11) by replacing sine by - sine, i.e.,

$$\begin{aligned} C_{14}^{(2)} &= - C_{14}^{(1)} \\ C_{24}^{(2)} &= - C_{24}^{(1)} \\ C_{34}^{(2)} &= - C_{34}^{(1)} \\ C_{56}^{(2)} &= - C_{56}^{(1)} \\ \gamma_{23}^{(2)} &= - \gamma_{23}^{(1)} \\ \alpha_{23}^{(2)} &= - \alpha_{23}^{(1)} \end{aligned} \quad , \tag{5.20}$$

all the other parameters being equal. If the laminate thickness (x-direction) is very much less than the lateral dimensions (y,z directions), then away from the edges the shear stresses between plies will vanish, and the appropriate boundary conditions for determining the thermal expansion coefficients are

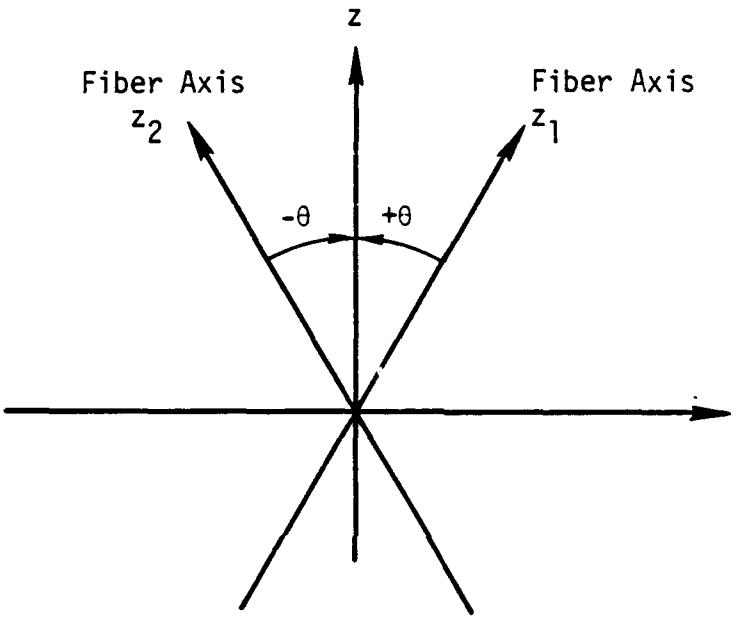

Figure 5.2. Laminate geometry.

$$\sigma_{xx}^{(1)} = \sigma_{xx}^{(2)} = 0 \tag{5.21}$$

$$\varepsilon_{zz}^{(1)} = \varepsilon_{zz}^{(2)} \tag{5.22}$$

$$\varepsilon_{yy}^{(1)} = \varepsilon_{yy}^{(2)} \tag{5.23}$$

$$\varepsilon_{yz}^{(1)} = \varepsilon_{yz}^{(2)} \tag{5.24}$$

and (equal volume fractions),

$$\sigma_{zz}^{(1)} + \sigma_{zz}^{(2)} = 0 \tag{5.25}$$

$$\sigma_{yy}^{(1)} + \sigma_{yy}^{(2)} = 0 \tag{5.26}$$

$$\sigma_{yz}^{(1)} + \sigma_{yz}^{(2)} = 0 \tag{5.27}$$

The conditions (5.22), (5.23), and (5.24) give the three equations,

$$(S_{23}^{(1)} + S_{23}^{(2)})\sigma_{yy}^{(1)} + (S_{33}^{(1)} + S_{33}^{(2)})\sigma_{zz}^{(1)} + 2(S_{34}^{(1)} + S_{34}^{(2)})\sigma_{yz}^{(1)} + (\alpha_{33}^{(1)} - \alpha_{33}^{(2)})\Delta T = 0 \tag{5.28}$$

$$(S_{22}^{(1)} + S_{22}^{(2)})\sigma_{yy}^{(1)} + (S_{23}^{(1)} + S_{23}^{(2)})\sigma_{zz}^{(1)} + 2(S_{24}^{(1)} + S_{24}^{(2)})\sigma_{yz}^{(1)} + (\alpha_{22}^{(1)} - \alpha_{22}^{(2)})\Delta T = 0 \tag{5.29}$$

$$(S_{24}^{(1)} + S_{24}^{(2)})\sigma_{yy}^{(1)} + (S_{34}^{(1)} + S_{34}^{(2)})\sigma_{zz}^{(1)} + 2(S_{44}^{(1)} + S_{44}^{(2)})\sigma_{yz}^{(1)} + (\alpha_{23}^{(1)} - \alpha_{23}^{(2)})\Delta T = 0 \tag{5.30}$$

where use nas been made of (5.21), (5.25), (5.26), and (5.27). Since

$$S_{34}^{(2)} = -S_{34}^{(1)}, \quad \alpha_{33}^{(2)} = \alpha_{33}^{(1)}, \text{ etc.},$$

the first two relations (5.28) and (5.29) give the intuitively obvious result

$$\sigma_{yy}^{(1)} = \sigma_{zz}^{(1)} = \sigma_{yy}^{(2)} = \alpha_{zz}^{(2)} = 0 \quad , \tag{5.31}$$

and the third condition (5.30) gives

$$4S_{44}^{(1)}\sigma_{yz}^{(1)} + 2\alpha_{23}^{(1)}\Delta T = 0 \quad . \tag{5.32}$$

The z-component of the thermal strain is just

$$\varepsilon_{zz} = \varepsilon_{zz}^{(1)} = 2S_{34}^{(1)}\sigma_{yz}^{(1)} + \alpha_{33}^{(1)} \Delta T \quad , \tag{5.33}$$

which with the use of (5.32) gives the desired result

$$\alpha_z = \frac{\varepsilon_{zz}}{\Delta T} = - \frac{S_{34}^{(1)}}{S_{44}^{(1)}} \alpha_{23}^{(1)} + \alpha_{33}^{(1)} \quad . \tag{5.34}$$

Similarly,

$$\varepsilon_{yy} = 2S_{24}^{(1)}\sigma_{yz}^{(1)} + \alpha_{22}^{(1)} \Delta T \tag{5.35}$$

which with the use of (5.32) gives

$$\alpha_y = \frac{\varepsilon_{yy}}{\Delta T} = - \frac{S_{24}^{(1)}}{S_{44}^{(1)}} \alpha_{23}^{(1)} + \alpha_{22}^{(1)} \quad ; \tag{5.36}$$

and finally, one obtains,

$$\alpha_x = - \frac{S_{14}^{(1)}}{S_{44}^{(1)}} \alpha_{23}^{(1)} + \alpha_{11}^{(1)} \tag{5.37}$$

Remember that in the above expressions the S_{ij} and α_{ij} are elements of the tensors in the <u>laminate</u> coordinate system.

The elements S_{ij} may be obtained in two ways: by computing the elements of the matrix C and taking the inverse, or by direct computation from the elements in the fiber coordinate system using the transformation Eqs. (5.11)

For example,

$$S'_{34} = -S_{11}\sin^3\theta\cos\theta + S_{33}\sin\theta\cos^3\theta + S_{13}(\sin^3\theta\cos\theta - \sin\theta\cos^3\theta) + 2S_{44}(\sin^3\theta\cos\theta - \sin\theta\cos^3\theta) \quad , \tag{5.38}$$

where

$$\begin{aligned} S_{11} &= 1/E_x = S_{22} \\ S_{12} &= -\nu_{xy}/E_x = S_{21} \\ S_{13} &= -\nu_{xz}/E_z = S_{31} = S_{23} = S_{32} \\ S_{33} &= 1/E_z \\ S_{44} &= 1/(4C_{44}) = 1/(4G_A) \\ S_{66} &= 1/(4C_{66}) = 1/(4G_T) \end{aligned} \tag{5.39}$$

are the nonvanishing components in the FCS in terms of the Young's moduli E_x, E_z and the Poisson's ratios ν_{xy}, ν_{xz} (contraction, force). The quantities G_A, G_T are the standard axial and transverse shear moduli.

5.3 ELASTIC PARAMETERS

The elastic (Young's) modulus in the z-direction for the laminate is obtained by applying the conditions

$$\varepsilon_{zz}^{(1)} = \varepsilon_{zz}^{(2)} = \varepsilon_0, \quad (\Delta T = 0) \tag{5.40}$$

$$\varepsilon_{yy}^{(1)} = \varepsilon_{yy}^{(2)} \tag{5.41}$$

$$\varepsilon_{yz}^{(1)} = \varepsilon_{yz}^{(2)} \tag{5.42}$$

$$\sigma_{xx}^{(1)} = \sigma_{xx}^{(2)} = 0 \tag{5.43}$$

$$\sigma_{yy}^{(1)} + \sigma_{yy}^{(2)} = 0 \tag{5.44}$$

$$\sigma_{yz}^{(1)} + \sigma_{yz}^{(2)} = 0 \tag{5.45}$$

where (5.44) and (5.45) imply equal volume fractions of the two types of ply.

The condition (5.41) gives

$$S_{22}^{(1)}\sigma_{yy}^{(1)} + S_{23}^{(1)}\sigma_{zz}^{(1)} + 2S_{24}^{(1)}\sigma_{23}^{(1)} = S_{22}^{(2)}\sigma_{yy}^{(2)} + S_{23}^{(2)}\sigma_{zz}^{(2)} + 2S_{24}^{(2)}\sigma_{23}^{(2)} \quad , \tag{5.46}$$

and (5.42) gives

$$S_{24}^{(1)}\sigma_{yy}^{(1)} + S_{34}^{(1)}\sigma_{zz}^{(1)} + 2S_{44}^{(1)}\sigma_{23}^{(1)} = S_{24}^{(2)}\sigma_{yy}^{(2)} + S_{34}^{(2)}\sigma_{zz}^{(2)} + 2S_{44}^{(2)}\sigma_{23}^{(2)} \quad , \tag{5.47}$$

where use has been made of (5.43). With the use of (5.44) and (5.45) the above relations become

$$(S_{22}^{(1)} + S_{22}^{(2)})\sigma_{yy}^{(1)} + S_{23}^{(1)}\sigma_{zz}^{(1)} - S_{23}^{(2)}\sigma_{zz}^{(2)} + 2(S_{24}^{(1)} + S_{24}^{(2)})\sigma_{23}^{(1)} = 0 \quad , \tag{5.48}$$

$$(S_{24}^{(1)} + S_{24}^{(2)})\sigma_{yy}^{(1)} + S_{34}^{(1)}\sigma_{zz}^{(1)} - S_{34}^{(2)}\sigma_{zz}^{(2)} + 2(S_{44}^{(1)} + S_{44}^{(2)})\sigma_{23}^{(1)} = 0 \quad ; \tag{5.49}$$

and (5.40) gives the two relations

$$S_{23}^{(1)}\sigma_{yy}^{(1)} + S_{33}^{(1)}\sigma_{zz}^{(1)} + 2S_{34}^{(1)}\sigma_{23}^{(1)} = \varepsilon_o \tag{5.50}$$

$$- S_{23}^{(2)}\sigma_{yy}^{(1)} + S_{33}^{(2)}\sigma_{zz}^{(2)} - 2S_{34}^{(2)}\sigma_{23}^{(1)} = \varepsilon_o \tag{5.51}$$

The relations (5.48), (5.49), (5.50), and (5.51) constitute a set of four equations in the four variables $\sigma_{yy}^{(1)}$, $\sigma_{zz}^{(1)}$, $\sigma_{zz}^{(2)}$, and $\sigma_{23}^{(1)}$.

Equation (5.48) simplifies to

$$2S_{22}^{(1)}\sigma_{yy}^{(1)} + S_{23}^{(1)}(\sigma_{zz}^{(1)} - \sigma_{zz}^{(2)}) = 0 \quad , \tag{5.52}$$

and (5.49) reduces to

$$S_{34}^{(1)}(\sigma_{zz}^{(1)} + \sigma_{zz}^{(2)}) + 4S_{44}^{(1)}\sigma_{23}^{(1)} = 0 \quad . \tag{5.53}$$

The relation (5.51) is also

$$- S_{23}^{(1)}\sigma_{yy}^{(1)} + S_{33}^{(1)}\sigma_{zz}^{(2)} + 2S_{34}^{(1)}\sigma_{23}^{(1)} = \varepsilon_0 \tag{5.54}$$

which when subtracted from (5.50) gives

$$2S_{23}^{(1)}\sigma_{yy}^{(1)} + S_{33}^{(1)}(\sigma_{zz}^{(1)} - \sigma_{zz}^{(2)}) = 0 \quad , \tag{5.55}$$

and a consideration of 5.52) and (5.55) gives the results,

$$\begin{aligned} \sigma_{yy}^{(1)} &= \sigma_{yy}^{(2)} = 0 \\ \sigma_{zz}^{(1)} &= \sigma_{zz}^{(2)} \quad , \end{aligned} \tag{5.56}$$

which, it must be admitted, seem very appropriate.

The relation (5.53) then becomes

$$2S_{34}^{(1)}\sigma_{zz}^{(1)} + 4S_{44}^{(1)}\sigma_{23}^{(1)} = 0 \tag{5.57}$$

and (5.54) is now

$$S_{33}^{(1)}\sigma_{zz}^{(1)} + 2S_{34}^{(1)}\sigma_{23}^{(1)} = \varepsilon_0 \tag{5.58}$$

The above two relations yield the desired result,

$$\frac{\sigma_{zz}^{(1)}}{\varepsilon_0} = S_{33}^{(1)} - \frac{S_{34}^{(1)2}}{S_{44}^{(1)}} = 1 \tag{5.59}$$

or

$$\frac{1}{E_z} = S_{33}^{(1)} - \frac{S_{34}^{(1)2}}{S_{44}^{(1)}} \tag{5.60}$$

for the reciprocal of Young's modulus E_z.

The elastic modulus in the y-direction follows from the conditions

$$\varepsilon_{yy}^{(1)} = \varepsilon_{yy}^{(2)} = \varepsilon_o \tag{5.61}$$

$$\varepsilon_{zz}^{(1)} = \varepsilon_{zz}^{(2)} \tag{5.62}$$

$$\varepsilon_{yz}^{(1)} = \varepsilon_{yz}^{(2)} \tag{5.63}$$

$$\sigma_{xx}^{(1)} = \sigma_{xx}^{(2)} = 0 \tag{5.64}$$

and for equal volume fractions,

$$\sigma_{zz}^{(1)} + \sigma_{zz}^{(2)} = 0 \tag{5.65}$$

$$\sigma_{yz}^{(1)} + \sigma_{yz}^{(2)} = 0 \quad . \tag{5.66}$$

Doing the same algebra as above for E_z gives the desired relation

$$\frac{1}{E_y} = S_{22}^{(1)} - \frac{S_{24}^{(1)\,2}}{S_{44}^{(1)}} \tag{5.67}$$

for the reciprocal of the Young's modulus.

In a similar fashion, one obtains for the elastic modulus in the direction perpendicular to the laminate,

$$\frac{1}{E_x} = S_{11}^{(1)} - \frac{S_{14}^{(1)\,2}}{S_{44}^{(1)}} \quad . \tag{5.68}$$

The corresponding Poisson's ratios are easily obtained from the above results. For the case of an applied stress in the z direction,

$$\begin{aligned} \varepsilon_{xx} &= S_{13}\sigma_{zz} + 2S_{14}\sigma_{23} \\ \varepsilon_{zz} &= S_{33}\sigma_{zz} + 2S_{34}\sigma_{23} \end{aligned} \tag{5.69}$$

which with the use of (5.57) gives

$$\nu_{xz} = - \frac{S_{13}S_{44} - S_{14}S_{34}}{S_{33}S_{44} - S_{34}^2} \quad . \tag{5.70}$$

Likewise,

$$\varepsilon_{yy} = S_{23}\sigma_{zz} + 2S_{24}\sigma_{23} \quad , \tag{5.71}$$

and

$$\nu_{yz} = - \frac{S_{23}S_{44} - S_{24}S_{34}}{S_{33}S_{44} - S_{34}^2} \quad . \tag{5.72}$$

In order to obtain an expression for the in-plane shear modulus, we apply the conditions:

$$\varepsilon_{yz}^{(1)} = \varepsilon_{yz}^{(2)} = \varepsilon_o \tag{5.73}$$

$$\varepsilon_{zz}^{(1)} = \varepsilon_{zz}^{(2)} \tag{5.74}$$

$$\varepsilon_{yy}^{(1)} = \varepsilon_{yy}^{(2)} \tag{5.75}$$

$$\sigma_{xx}^{(1)} = \sigma_{xx}^{(2)} = 0 \tag{5.76}$$

$$\sigma_{zz}^{(1)} + \sigma_{zz}^{(2)} = 0 \tag{5.77}$$

$$\sigma_{yy}^{(1)} + \sigma_{yy}^{(2)} = 0 \tag{5.78}$$

The condition (5.74) yields with the use of (5.76), (5.77), and (5.78),

$$S_{23}\sigma_{yy}^{(1)} + S_{33}\sigma_{zz}^{(1)} + S_{34}^{(1)}(\sigma_{yz}^{(1)} + \sigma_{yz}^{(2)}) = 0 \qquad (5.79)$$

and (5.75) gives

$$S_{22}\sigma_{yy}^{(1)} + S_{23}\sigma_{zz}^{(1)} + S_{24}^{(1)}(\sigma_{yz}^{(1)} + \sigma_{yz}^{(2)}) = 0 \qquad (5.80)$$

The superscript is omitted in the above expression if the quantity has tne same numerical value for both types of ply (θ and - θ fiber orientation).

From (5.73) we obtain two relations

$$S_{24}^{(1)}\sigma_{yy}^{(1)} + S_{34}^{(1)}\sigma_{zz}^{(1)} + 2S_{44}\sigma_{yz}^{(1)} = \varepsilon_o \qquad (5.81)$$

$$S_{24}^{(2)}\sigma_{yy}^{(2)} + S_{34}^{(2)}\sigma_{zz}^{(2)} + 2S_{44}\sigma_{yz}^{(2)} = \varepsilon_o \quad . \qquad (5.82)$$

Subtracting (5.82) from (5.81) leads to the conclusion that

$$\sigma_{yz}^{(1)} = \sigma_{yz}^{(2)} \quad , \qquad (5.83)$$

whereas adding (5.82) and (5.81) gives the useful relation,

$$S_{24}^{(1)}\sigma_{yy}^{(1)} + S_{34}^{(1)}\sigma_{zz}^{(1)} + 2S_{44}\sigma_{yz}^{(1)} = \varepsilon_o \qquad (5.84)$$

which together with (5.79) and (5.80) form a set of three simultaneous linear equations in the variables $\sigma_{yy}^{(1)}$, $\sigma_{zz}^{(1)}$, and $\sigma_{yz}^{(1)}$. These may be solved numerically to obtain the in-plane shear modulus

$$C_{44}^{(eff)} = \frac{\sigma_{yz}^{(1)}}{2\varepsilon_o} \quad . \qquad (5.85)$$

5.4 NUMERICAL RESULTS

Calculated results for several parameters as a function of tne lay-up angle θ (Figure 5.2) are presented for a laminate whose plies consist of 30 percent by volume graphite fibers in a 2024 aluminum

matrix. The input parameters for the fibers and matrix, as given in Table 5.1 below, are the same as those used by Hashin and Humphreys[2] in a recent report.

TABLE 5.1
INPUT ELASTIC CONSTANTS FOR FIBER AND MATRIX

Elastic Constant	T-50 Graphite Fiber	2024-T4 Al Matrix
E_z(GPa)	388.2	72.4
E_x(GPa)	7.6	72.4
G_{44}(GPa)	14.9	27.2
G_{66}(GPa)	2.6	27.2
ν_{xz}**	0.41	0.33
ν_{xy}	0.45	0.33
$\alpha_z(°C^{-1})$	-0.68×10^{-6}	22.5×10^{-6}
$\alpha_x(°C^{-1})$	9.74×10^{-6}	22.5×10^{-6}

**The subscripts are (contraction, force).

The PRUFC code[3] was used to calculate the elastic properties of a ply in the fiber coordinate system, with the results as given in Table 5.2 (the PRUFC code was subsequently revised as discussed in Section 6).

The linear thermal expansion coefficients for the laminate, as calculated with Eqs. (5.34), (5.36), and (5.37) are plotted as a function of ply angle in Figure 5.3. It will be noted that the axial thermal expansion has a minimum at about 20 deg (40 deg total angle between fiber directions). It is also comforting to note that the calculated results exhibit the required symmetry about 45 degrees.

TABLE 5.2
INPUT ELASTIC PROPERTIES FOR A FIBER REINFORCED PLY
(30 percent by volume of fibers)

Elastic Constant	Value
E_z(GPa)	167.18
E_x(GPa)	37.11
C_{44}(GPa)	22.82
C_{66}(GPa)	12.68
ν_{xz}	0.33840
ν_{xy}	0.46294
$\alpha_z(^\circ C^{-1})$	6.29×10^{-6}
$\alpha_x(^\circ C^{-1})$	25.66×10^{-6}
C_{11}(GPa)	50.85
C_{12}(GPa)	25.48
C_{13}(GPa)	25.83
C_{33}(GPa)	184.66

The elastic moduli along the three laminate axes are plotted in Figure 5.4, and two Poisson's ratios are given in Figure 5.5 as a function of lay-up angle. The in-plane shear modulus for the laminate is shown in Figure 5.6.

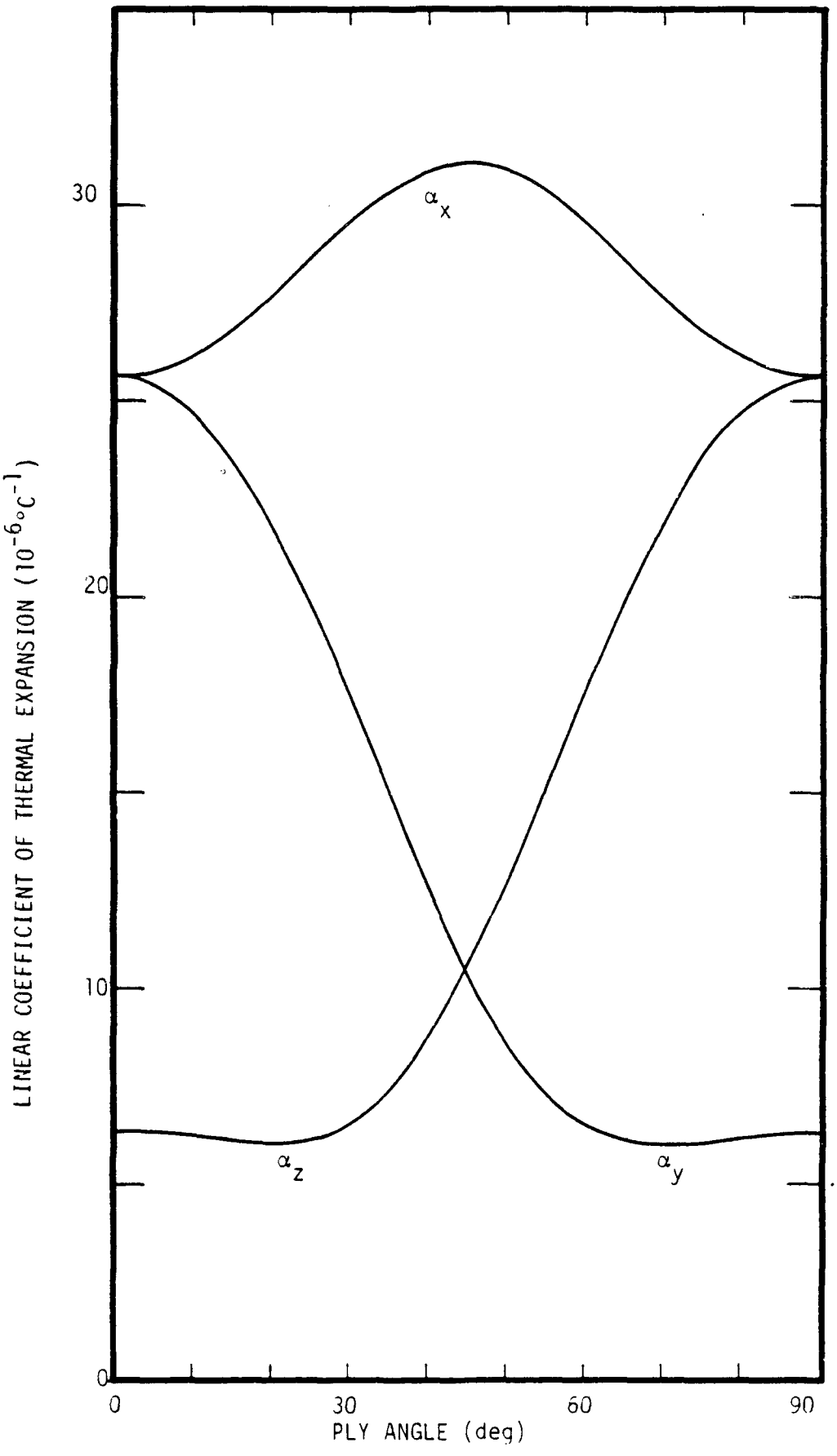

Figure 5.3. Calculated linear thermal expansion coefficients for a cross-ply metal-matrix laminate as a function of lay-up angle.

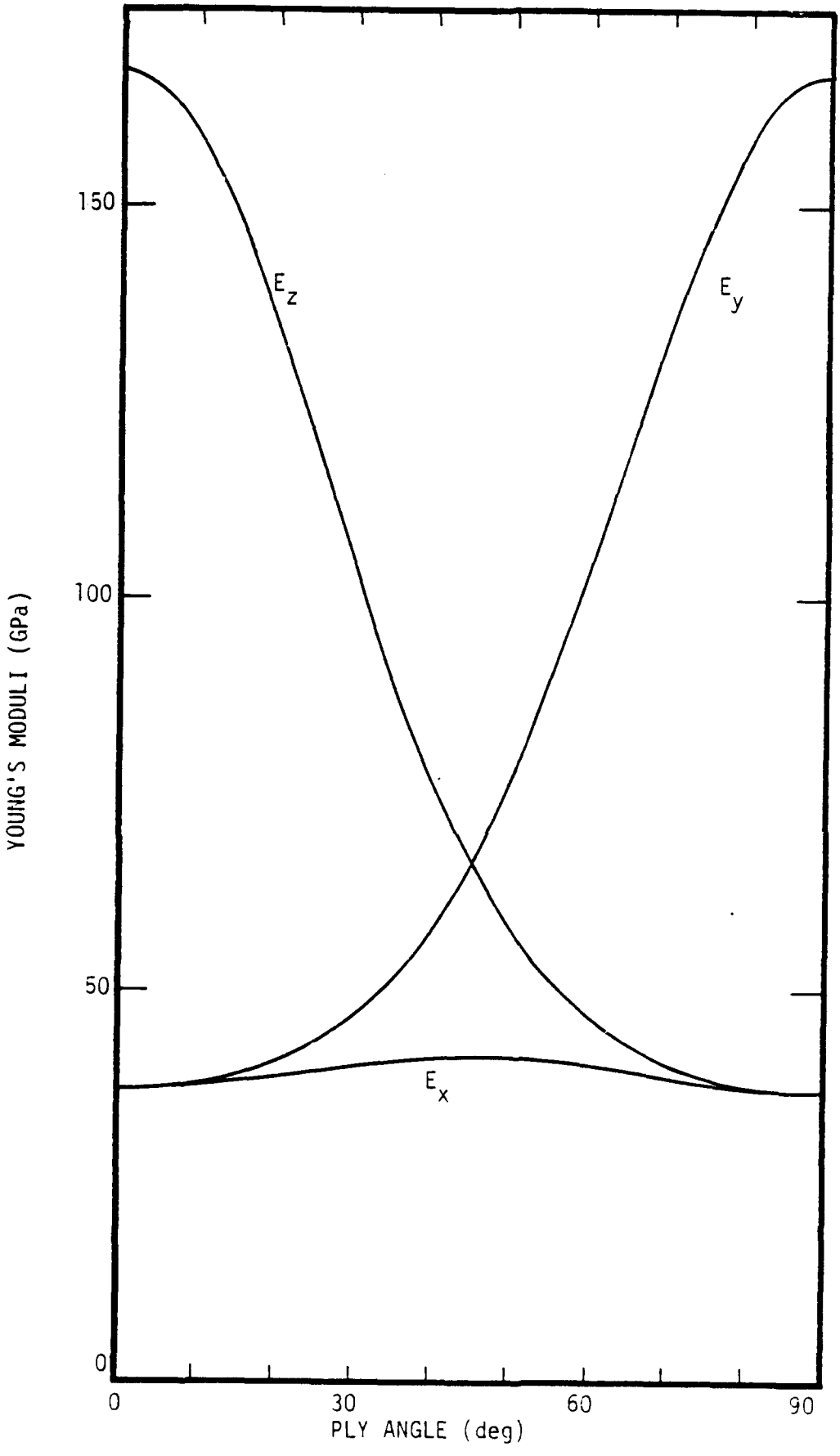

Figure 5.4. Calculated elastic (Young's) moduli for a metal-matrix laminate as a function of lay-up angle.

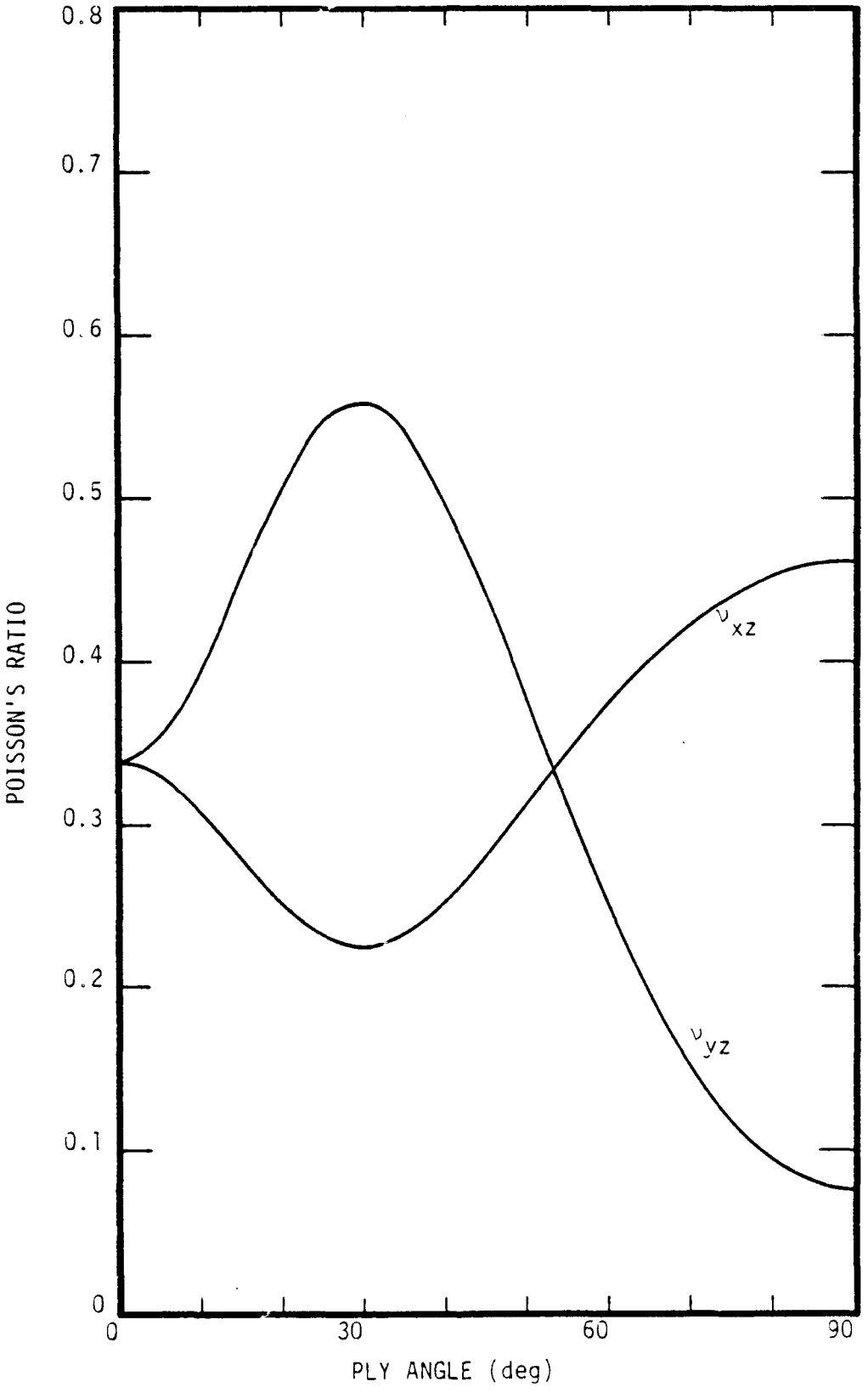

Figure 5.5. Two calculated Poisson's ratios for a metal-matrix laminate as a function of lay-up angle.

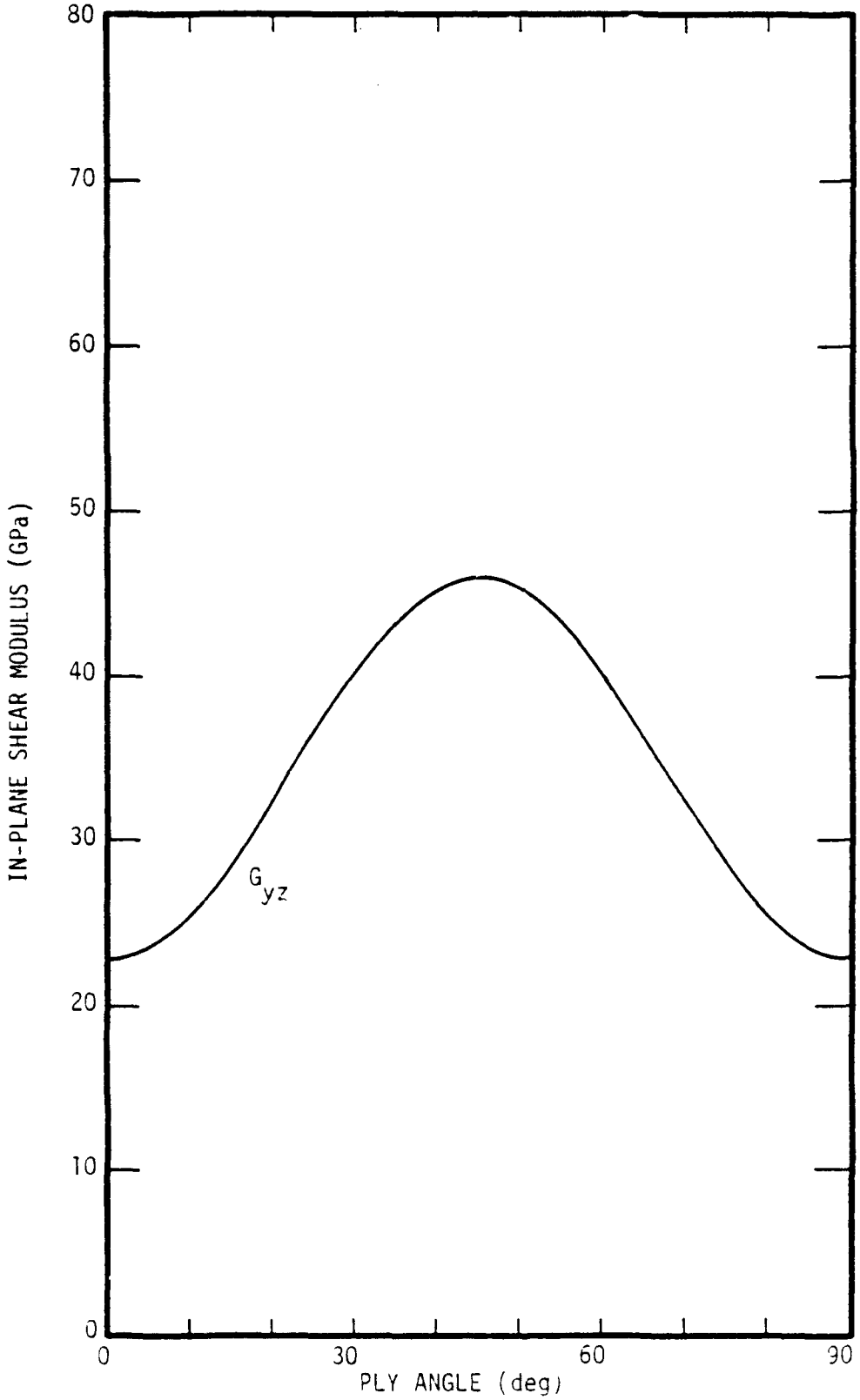

Figure 5.6. Calculated in-plane shear modulus for a metal-matrix laminate as a function of lay-up angle.

(This Page Left Blank)

6. TRANSVERSE ELASTIC PROPERTIES OF A UNIDIRECTIONALLY REINFORCED COMPOSITE AND THE PRUFC CODE

In a recent report,[2] Hashin and Humphreys present numerical results for a typical graphite/aluminum composite as calculated using a finite-element code (ANSYS) to determine the stress-strain state in the unit cell of a model in which the fibers are arranged in a perfect hexagonal array. The advantage of their method is that it is expected to give a very accurate representation of the behavior of a composite in terms of the properties of the fiber and matrix components. The disadvantage is, as stated in the report, "The ANSYS computer code, ..., is very expensive to run for such cases." Consequently, it is of interest to compare these finite element results with those obtained with PRUFC[3] and the S-CUBED plastic-flow code,[1] which are inexpensive to run but use the concentric-cylinder approximation.

We present first a comparison of calculated elastic properties of a graphite/aluminum composite as obtained from the properties of the constituents. In the example given in Ref. 2, the properties of the fiber and aluminum matrix are as given in Table 6.1.

A comparison of the composite parameters as calculated with PRUFC and those calculated by Hashin and Humphreys for a 30 percent by volume of fibers is given in Table 6.2 below. Also given are values obtained from the "Composite Cylinder Assemblage" (CCA) model of a composite (Hashin, Ref. 8).

The only significant differences are in the transverse properties E_T, G_{TT}, and ν_{TT} (only two of which are independent, because of the transverse isotropy). Not all the transverse properties differ, however. If one considers the transverse bulk modulus k whose reciprocal is given by

$$\frac{1}{k} = \frac{2\varepsilon_x}{\sigma_0} = 2\left[\frac{1 - \nu_{TT}}{E_T} - \frac{2\nu_{AT}^2}{E_A}\right] , \qquad (6.1)$$

$$\sigma_x = \sigma_y = \sigma_0, \ \varepsilon_z = 0 ,$$

TABLE 6.1

CONSTITUENT PROPERTIES FOR A GRAPHITE/ALUMINUM COMPOSITE

Elastic Constant	T-50 Graphite Fiber	2024-T4 Al Matrix
E_A(GPa)	388.2	72.4
E_T(GPa)	7.6	72.4
G_{AT}(GPa)	14.9	27.2
G_{TT}(GPa)	2.6	27.2
ν_{AT}*	0.41	0.33
ν_{TT}	0.45	0.33
$\alpha_A(°C^{-1})$	-0.68×10^{-6}	22.5×10^{-6}
$\alpha_T(°C^{-1})$	9.74×10^{-6}	22.5×10^{-6}

A = Axial (Longitudinal)

T = Transverse

*This Poisson's ratio is the transverse contraction for an axial stress.

TABLE 6.2

CALCULATED PROPERTIES FOR A GRAPHITE/ALUMINUM COMPOSITE
(30 Percent by Volume of Fibers)

Elastic Constant	PRUFC	Finite-Element Method	CCA
E_A(GPa)	167.18	167.14*	--
E_T(GPa)	33.06	42.26	41.78
G_{TT}(GPa)	10.86	15.13	14.99
G_{AT}(GPa)	22.82	23.20	22.87
ν_{TT}	0.522	0.396	0.394
ν_{AT}	0.338	0.340	0.338
$\alpha_A(°C^{-1})$	6.29×10^{-6}	6.36×10^{-6}	6.36×10^{-6}
$\alpha_T(°C^{-1})$	25.65×10^{-6}	25.69×10^{-6}	25.65×10^{-6}

the values as obtained by the PRUFC code and the finite element method are, respectively,

$$k = 38.19 \text{ GPa (PRUFC)}$$
$$k = 38.73 \text{ GPa (F.E.)} \quad ,$$

a good agreement. The difficulty is that the concentric-cylinder approximation to a composite does not provide a unique definition of the transverse shear modulus.

In the PRUFC code as documented in Ref. 3, the transverse shear modulus is obtained from a consideration of the deformation of concentric cylinders subjected to a stress field at its outer surface the same as that acting on a fictitious cylindrical surface in a homogeneous material subjected to the stress field

$$\sigma_{xx} = -\sigma_{yy} = \sigma_0 = \text{const.}$$
$$\varepsilon_z = 0 \quad .$$

(see Appendix B of Reference 9). For the fictitious, homogeneous cylinder, of course, the resulting strain will be uniform throughout its volume and is related to the stress field by

$$\sigma_0 = 2G_{TT}\varepsilon_{xx} \quad , \tag{6.2}$$

involving only the transverse shear modulus, G_{TT}. For the concentric cylinder, however, for which an exact solution of the equations of elasticity is available,[9] the effective strain $\delta x/x$ (see Figure 6.1) at the outer surface will, in general, no longer be constant but will vary with the angle θ. In fact, for some combinations of properties and fiber volume fractions, the effective strain $\delta x/x$ may go from positive to negative as $\theta \to 90$ degrees. Thus, if the relation (6.2) above is used to obtain the shear modulus from the concentric-cylinder model, the value of ε_{xx} used must be some sort of average. The same problem of nonuniqueness

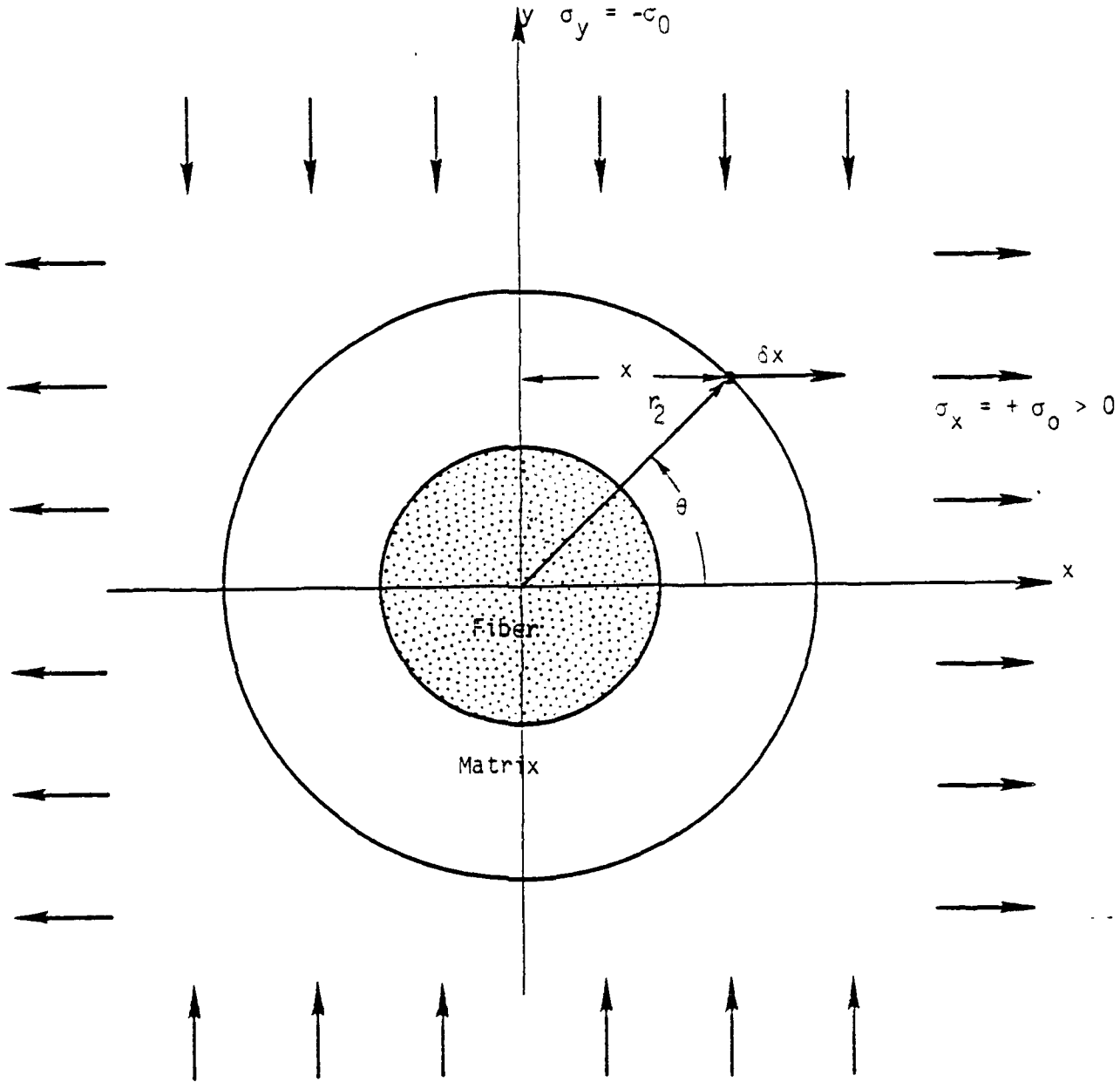

Figure 6.1 Concentric cylinder geometry.

occurs with Hashin's CCA model,[8] the value for the transverse shear modulus quoted in Table 6.2 being the greater of calculated upper and lower bounds (see page 295 of Reference 8).

In the original version of PRUFC, a volume weighted average was used for ε_{xx} in Eq. (6.2) to obtain the transverse shear modulus, i.e.,

$$\bar{\varepsilon}_{xx} = \frac{4}{\pi r_2^2} \int_0^{r_2} \left(\frac{\delta x}{x}\right) x\,dy \quad , \tag{6.3}$$

δx being the displacement at the outer surface $r = r_2$. This procedure results in the values for the transverse properties given in Table 6.2. Since the transverse shear modulus obtained in this manner is significantly below that as calculated by the finite-element method, which is presumably the better value, several other averaging alternatives have been examined. Results are given in Figure 6.2, where the shear modulus is plotted versus fiber volume fraction.

The use of

$$\bar{\varepsilon}_{xx} = \left(\frac{\delta x}{x}\right)_{\theta = 0} \tag{6.4}$$

results in a decrease in the calculated shear modulus relative to the volume weighted average (6.3), and a greater discrepancy with Hashin and Humphrey's result for the 30 percent composite. A closer agreement with the finite element result is obtained if one uses the linear average

$$\bar{\varepsilon}_{xx} = \frac{1}{r_2} \int_0^{r_2} \frac{\delta x}{x}\,dy \quad , \tag{6.5}$$

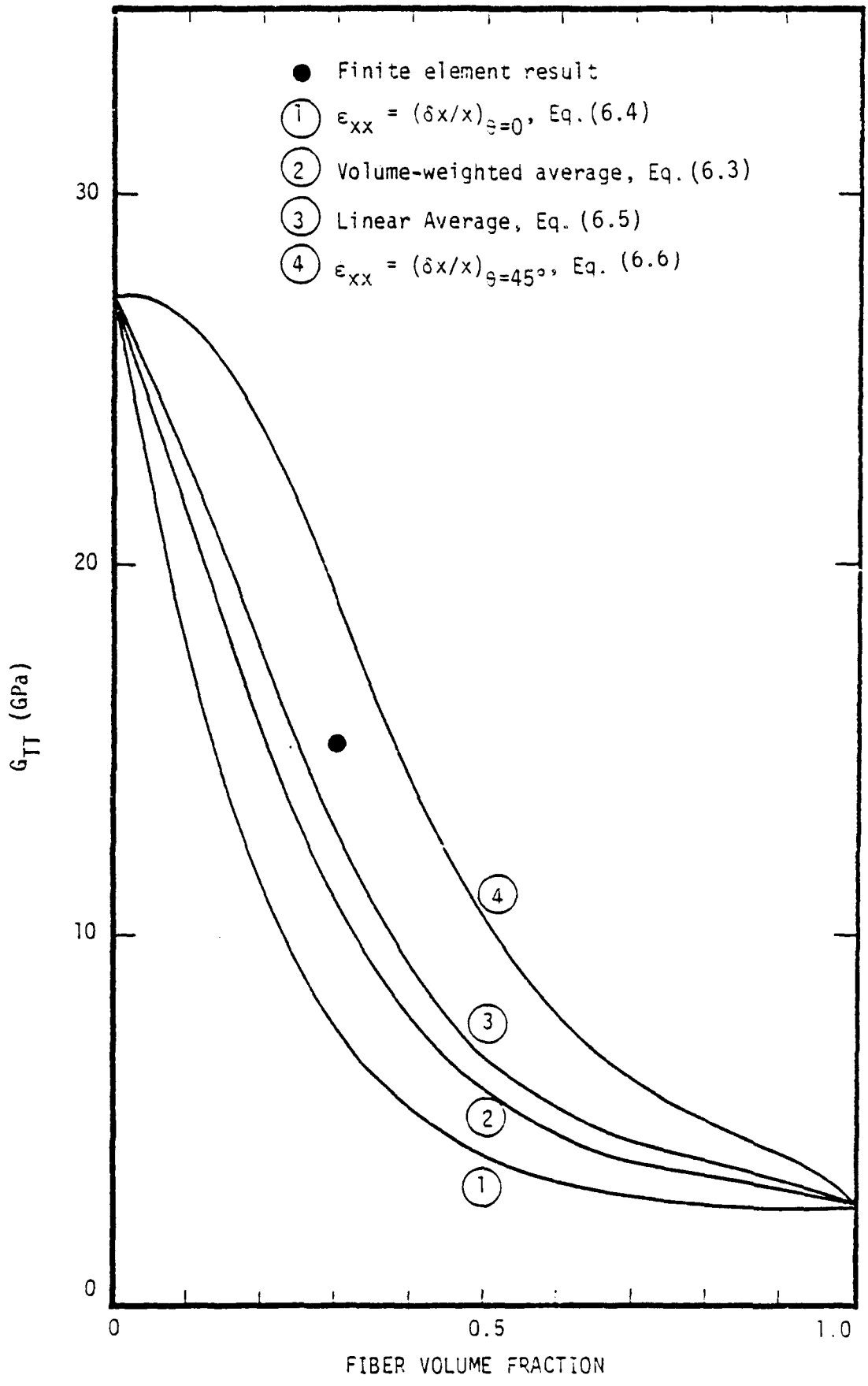

Figure 6.2. PRUFC results for the transverse shear modulus of a graphite/aluminum composite as a function of fiber volume fraction for various possible averaging procedures using stress boundary conditions. Also shown is the finite-element result of Hashin and Humphreys[2] for 30 percent by volume of fibers.

but the PRUFC calculation is still low. Finally, the use of

$$\bar{\varepsilon}_{xx} = \left(\frac{\delta x}{x}\right)_{\theta=45^\circ} \tag{6.6}$$

in Eq.(6.2) results in a PRUFC shear modulus greater than that obtained with the finite element method. The use of $(\delta x/x)$ at 45° suggests itself because this is also the value of

$$\frac{1}{2}\left(\frac{\delta x}{x} - \frac{\delta y}{y}\right) \quad ,$$

which turns out to be independent of θ. Calculated results for ν_{xy} and $\bar{E}_x$ using the various values of $\bar{\varepsilon}_{xx}$ are given in Figures 6.3 and 6.4.

An alternative approach is to specify the displacement on the outer surface of the concentric cylinder model and to solve the equations of elasticity for the resulting stress field. As outlined in Ref. 9, the radial and hoop displacements are of the form

$$U^{(\alpha)}(r,\theta) = u^{(\alpha)}(r)\cos 2\theta \tag{6.7}$$

$$V^{(\alpha)}(r,\theta) = v^{(\alpha)}(r)\sin 2\theta \quad , \tag{6.8}$$

and the condition now that the displacements on the outer surface,

$$\frac{\delta x}{x} = -\frac{\delta y}{y} = \varepsilon_0 = \text{constant} \tag{6.9}$$

be the same as that on a cylindrical surface within a homogeneous material subjected to the uniform strain field $\varepsilon_{xx} = -\varepsilon_{yy} = \varepsilon_0$, is satisfied by requiring that

$$v^{(2)}(r_2) = -u^{(2)}(r_2) \quad . \tag{6.10}$$

The stress boundary conditions (B.9) and (B.10) of Ref. 9 are replaced by

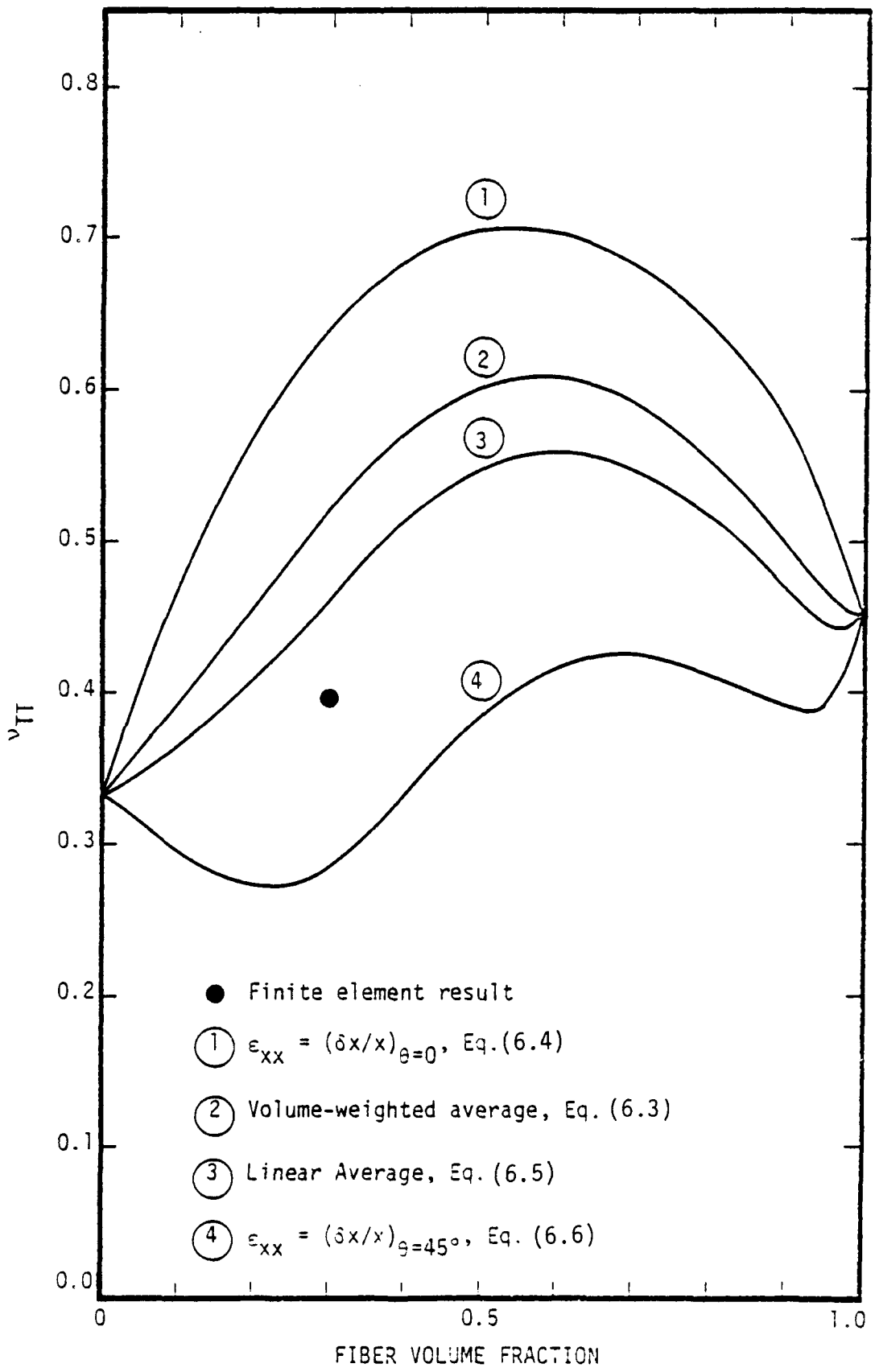

Figure 6.3. PRUFC results for the transverse Poisson's ratio of a graphite/aluminum composite as a function of fiber volume fraction for various possible averaging procedures using stress boundary conditions. Also shown is the finite-element result of Hashin and Humphreys[12] for 30 percent by volume of fibers.

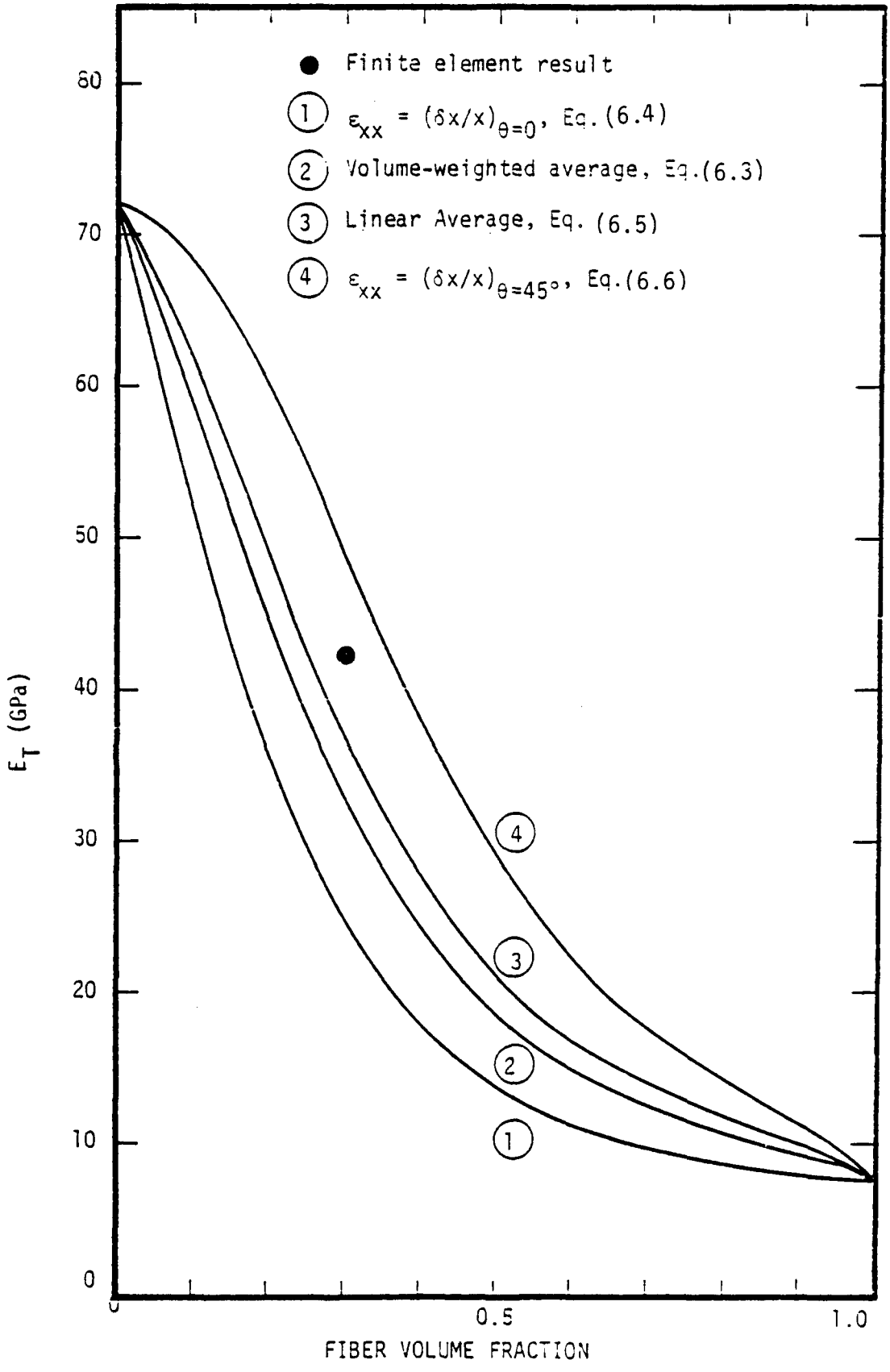

Figure 6.4. PRUFC results for the transverse elastic modulus of a graphite/aluminum composite as a function of fiber volume fraction for various possible averaging procedures using stress boundary conditions. Also shown is the finite-element result of Hashin and Humphreys[2] for 30 percent by volume of fibers.

$$u^{(2)}(r_2) = \varepsilon_0 \quad , \tag{6.11}$$

$$v^{(2)}(r_2) = -\varepsilon_0 \quad , \tag{6.12}$$

the other conditions, (B.5) - (B.8) remaining the same. Equations (6.11) and (6.12) follow from the relations for the cartesian components of displacement in terms of the radial and hoop components,

$$\delta x = u(r) \cos 2\theta \cos\theta - v(r) \sin 2\theta \sin\theta \tag{6.13}$$

$$\delta y = u(r) \cos 2\theta \sin\theta + v(r) \sin 2\theta \cos\theta \quad . \tag{6.14}$$

As before, the boundary conditions lead to a set of six linear equations for the coefficients of the elastic solutions, Eqs.(B.27) of Ref. 9, the bottom two rows of the matrix K being replaced by

$$\begin{aligned}
&K_{51} = 1, \quad K_{52} = 1, \quad K_{53} = 1, \\
&K_{54} = 1, \quad K_{55} = 0, \quad K_{56} = 0 \quad , \\
&K_{61} = -1, \quad K_{62} = -\frac{1}{2}\frac{(3 + \eta^{(2)})}{\eta^{(2)}} \quad , \\
&K_{61} = -\frac{1}{2}(1 - \eta^{(2)}), \quad K_{64} = 1 \quad , \\
&K_{65} = 0, \quad K_{66} = 0 \quad ,
\end{aligned} \tag{6.15}$$

where the applied strain and outer radius have been normalized to $\varepsilon = 1$, $r_2 = 1$. The coefficient K_{23} as given in Ref. 9 is in error. It should be

$$K_{23} = -\frac{1}{2}(1 - \eta^{(2)})\frac{1}{r_1} \quad .$$

From Eq. (B.13) of Ref. 9, the radial stress at the surface of the outer shell is given by

$$\sigma_{rr}^{(2)}(1,\theta) = [C_{11}^{(2)}(A_2 + 3B_2 - C_2 - 3D_2) - C_{12}^{(2)}] \cos 2\theta \qquad (6.16)$$

$$\equiv \sigma_{rro} \cos 2\theta$$

and from (B.15) the shear stress is

$$\sigma_{r\theta}^{(2)}(1,\theta) = C_{66}^{(2)}\left[- A_2 - \frac{3}{2}\frac{(3 + \eta^{(2)})}{\eta^{(2)}} B_2 \right. \qquad (6.17)$$

$$\left. + \frac{1}{2}(1 - \eta^{(2)})C_2 - 3D_2 - 1\right] \sin 2\theta$$

$$\equiv \sigma_{r\theta o} \sin 2\theta$$

(Actually, the above quantities are stresses per unit of applied strain, σ/ε_0). As in Eq. (6.2) above, the transverse shear modulus will be obtained from the relation

$$\bar{\sigma}_{xx} = 2G_{TT}\varepsilon_0 \qquad (6.18)$$

where $\bar{\sigma}_{xx}$ is some sort of average at the outer surface. In arriving at an average, we consider the x-component of the surface traction rather than $\sigma_{xx}(r,\theta)$ itself. In general, the force per unit area on a surface with normal unit vector $\hat{n}$ is given by

$$\vec{f} = \hat{n} \cdot \vec{\vec{\sigma}} \quad , \qquad (6.19)$$

and for the cylindrical surface $\hat{n} = \hat{r}$ so that

$$\vec{f} = \hat{r}\sigma_{rr} + \hat{\theta}\sigma_{r\theta} \quad , \qquad (6.20)$$

and the x-component is

$$f_x = \sigma_{rr}\cos\theta - \sigma_{r\theta} \sin\theta \qquad (6.21)$$

(Note that σ_{xx} itself also depends upon $\sigma_{\theta\theta}$). The stress per projected area perpendicular to the x-axis is

$$f_x^* = f_x r_2 \frac{d\theta}{dy} \tag{6.22}$$

and the linear average is then given by

$$\bar{\sigma}_{xx} = \bar{f}_x^* = \int_0^1 (\sigma_{rr}\cos\theta - \sigma_{r\theta}\sin\theta) \frac{d\theta}{dy}\, dy \quad , \tag{6.23}$$

since $r_2 = 1$, and the result is

$$\bar{\sigma}_{xx} = \frac{1}{3}\sigma_{rro} - \frac{2}{3}\sigma_{r\theta o} \tag{6.24}$$

where σ_{rro} and $\sigma_{r\theta o}$ are defined by (6.16) and (6.17).

A comparison of the calculated transverse shear modulus using the linear-average, displacement boundary conditions with that from the linear-average, stress boundary conditions is given in Figure 6.5. Also plotted is the arithmetic mean of the two shear moduli, which although still high with respect to the finite element result appears to be the most plausible way to obtain the transverse properties using the concentric-cylinder approximation, and the PRUFC code has been revised accordingly. A comparison of results for the 30 percent composite using the revised PRUFC code with those obtained by the finite-element method is given in Table 6.3.

Hashin and Humphreys[2] also present calculated results for a thermal process in which the yield strength of the aluminum matrix material in a 30 percent composite is exceeded. The yield-strength model they used is given as Figure 6.6, which is reproduced from Ref. 2. This isotropic hardening model was used in the S-CUBED residual stress code[1] along with the fiber and matrix properties as given in Table 6.1, and two of the calculations were repeated. Figure 6.7 gives the axial strain as calculated with the S-CUBED model[1] for a 30 percent composite, initially stress free at 371°C, as it is cooled to room temperature and reheated. Using the isotropic hardening model of Figure 6.6, the matrix first reaches

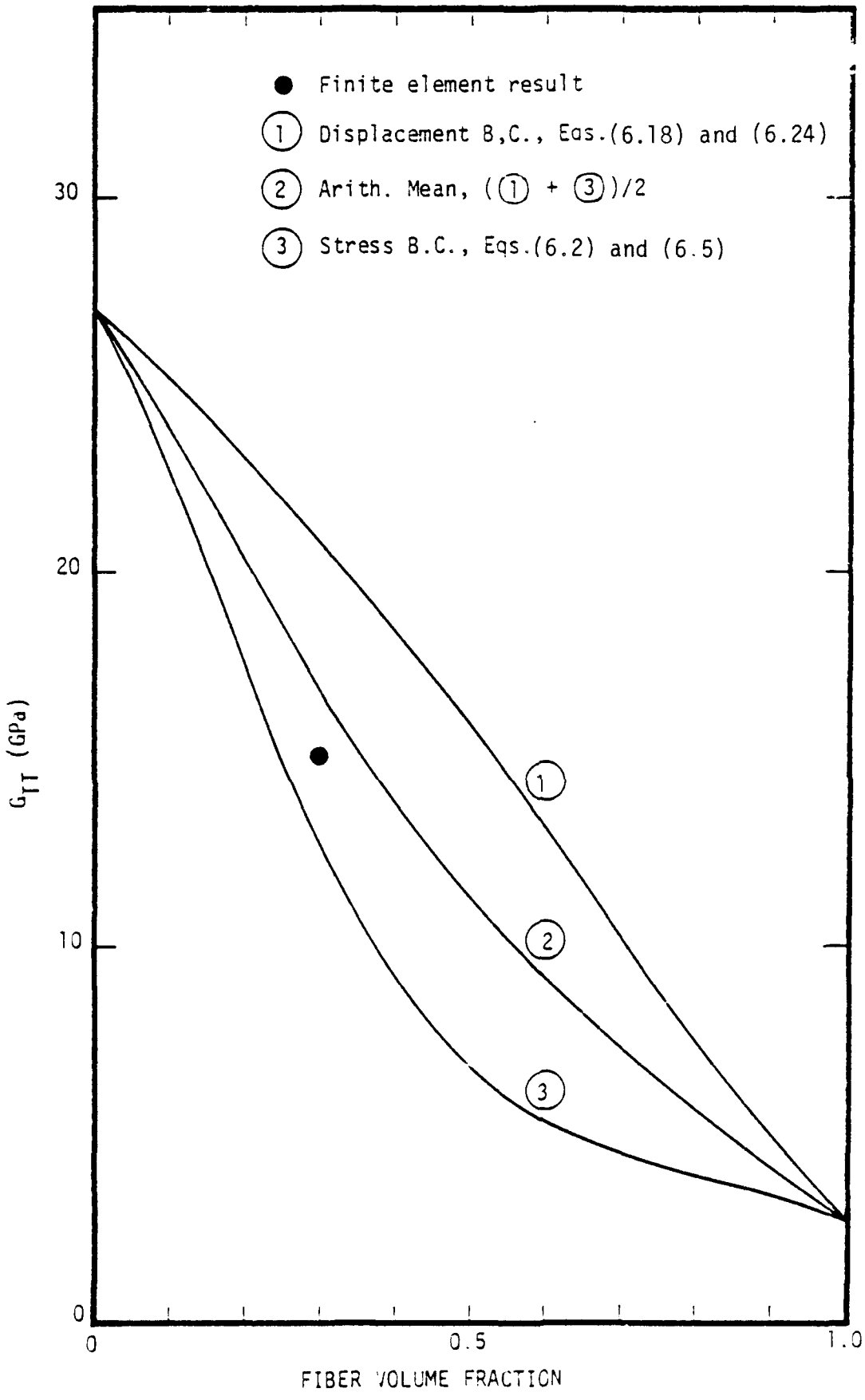

Figure 6.5. Comparison of the transverse shear modulus for a grapnite/aluminum composite as calculated with displacement boundary conditions and stress boundary conditions. Also shown is the finite element result of Hashin and Humphreys.[2]

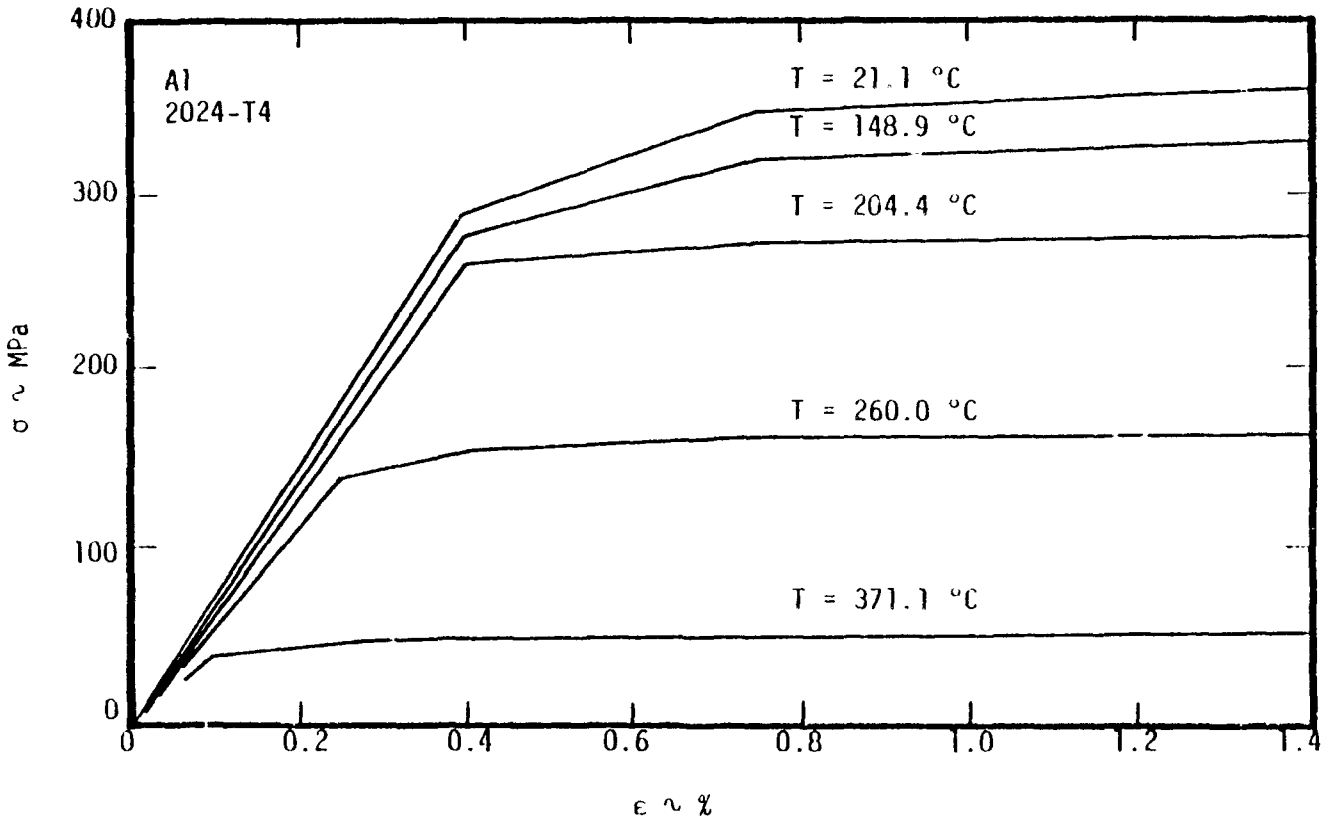

Figure 6.6. Isotropic hardening model used by Hashin and Humphreys, reproduced from Ref. 2.

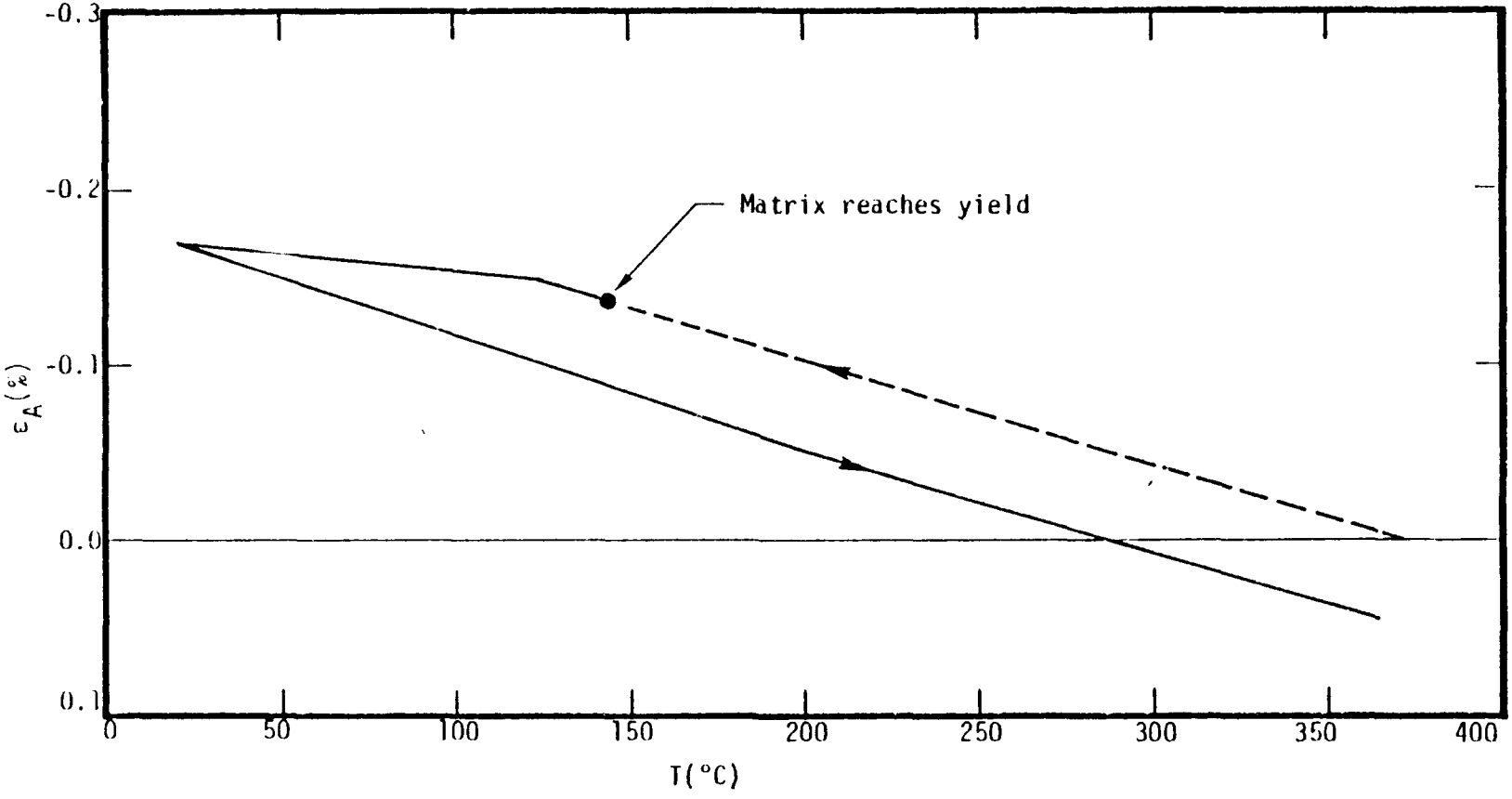

Figure 6.7. Axial strain as calculated with the S-CUBED residual stress model for a metal-matrix composite cooled from an initial stress-free state at 371°C. Results for the same process using a finite element method are given in Figure 6.8.

the yield surface at ~142°C. Upon reheating from room temperature, the matrix immediately falls off the yield surface and does not

TABLE 6.3

CALCULATED PROPERTIES USING THE REVISED PRUFC* CODE FOR A GRAPHITE/ALUMINUM COMPOSITE (30 percent by volume of fibers).

Elastic Constant	PRUFC*	Finite-Element Method
E_A(GPa)	167.18	167.14
E_T(GPa)	45.22	42.26
G_{TT}(GPa)	16.80	15.13
G_{AT}(GPa)	22.82	23.20
ν_{TT}	0.346	0.396
ν_{AT}	0.338	0.340
$\alpha_A(°C^{-1})$	6.29×10^{-6}	6.36×10^{-6}
$\alpha_T(°C^{-1})$	25.65×10^{-6}	25.69×10^{-6}

*Revised as per above.

reacn it again until about 350°C. The initial segment from 371°C to 142°C is snown as dashed because the present version of the S-CUBED code does not produce output for this interval. The results for the same process obtained by Hashin and Humphreys[2] using the finite element method and ANSYS code are given in Figure 6.8. The agreement between the two types of calculation appears to be quite satisfactory.

Calculated results for the transverse strain for the same tnermal cycle are given in Figures 6.9 and 6.10. Again the agreement is quite satisfactory. We conclude tnat, when their use is appropriate, the revised S-CUBED PRUFC code and concentric-cylinder residual-stress model(1) will give results for metal-matrix composites which are as satisfactory as those obtained with the more complex finite element metnod.

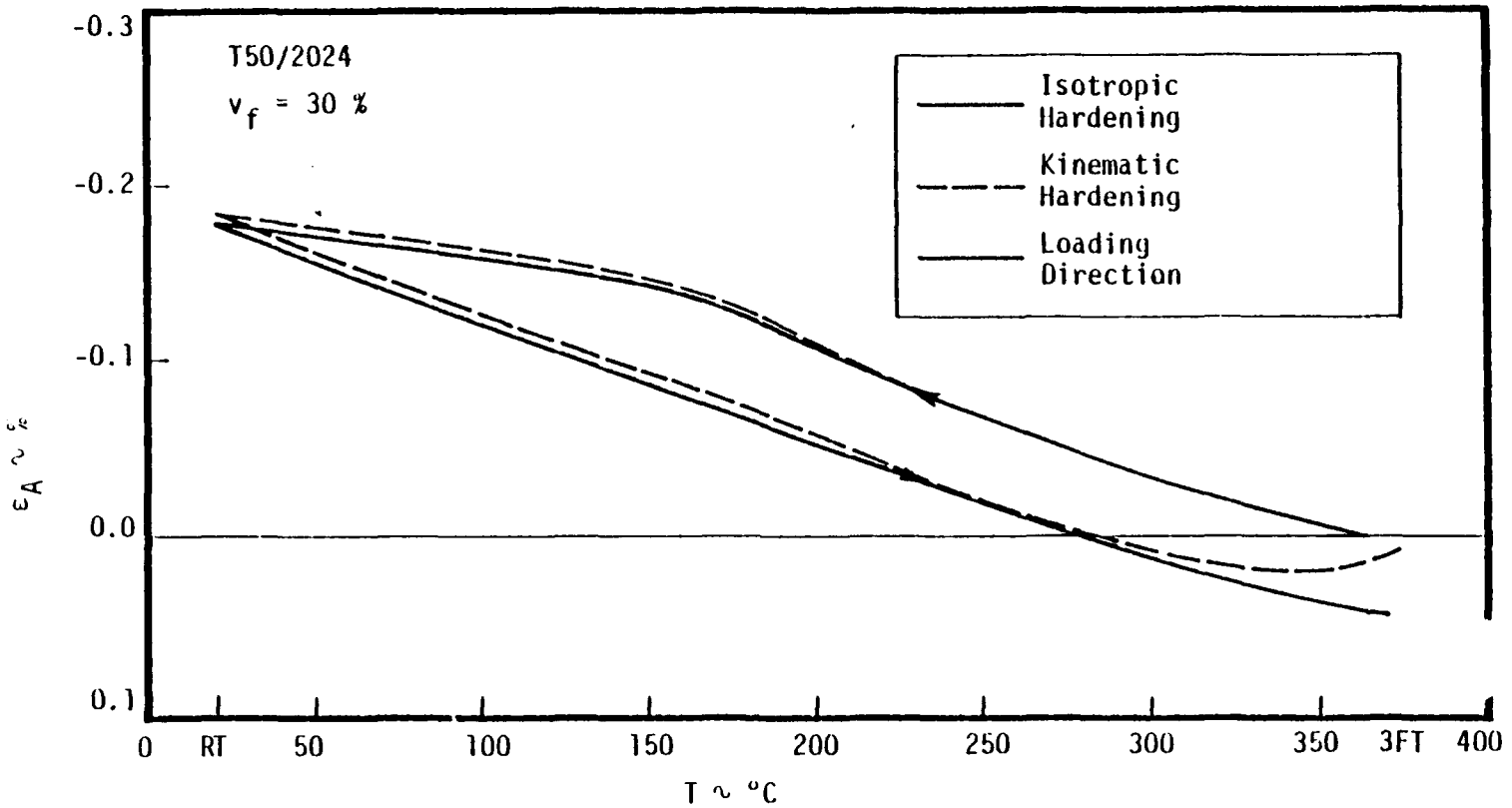

Figure 6.8. Hashin and Humphreys result for the axial strain of a metal-matrix composite, reproduced from Ref. 2. Compare with Figure 6.7.

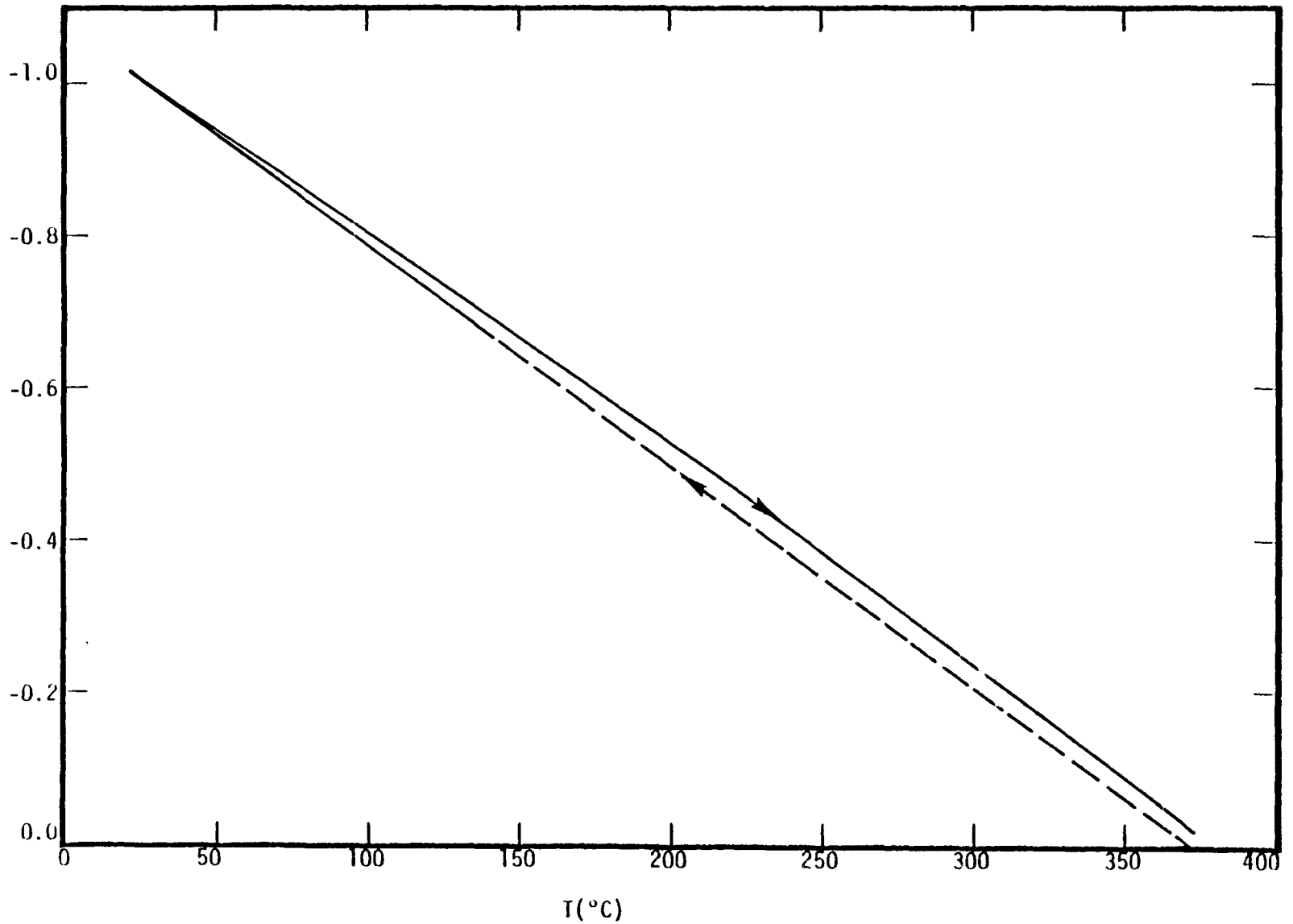

Figure 6.9. Transverse strain as calculated with the S-CUBED residual stress model for a metal-matrix composite cooled from an initial stress-free state at 371°C. Results for the same process using a finite element method are given in Figure 6.10.

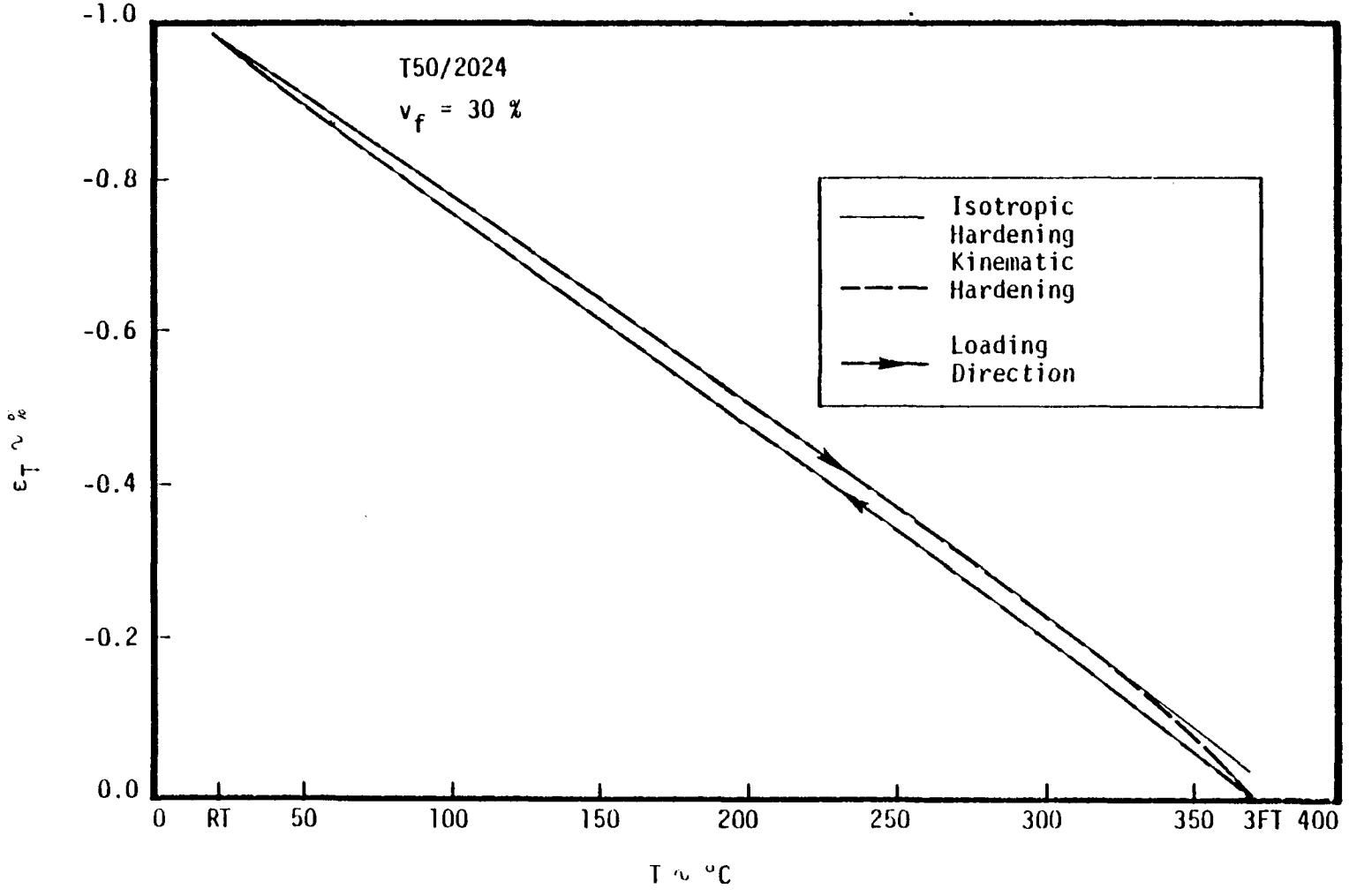

Figure 6.10. Hashin and Humphrey's result for the transverse strain of a metal-matrix composite, reproduced from Ref. 2. Compare with Figure 6.9.

(This Page Left Blank)

7. THERMAL DEFORMATIONS AND STRESSES IN AN ELASTIC PLATE UNDER AN ARBITRARY TEMPERATURE DISTRIBUTION

The material in this section has previously been submitted as a Progress Report to the Defense Supply Service (Ref. 10). It is reproduced here since it might prove useful in computing the permanent bending deformations of a metal-matrix composite under X-ray energy deposition.

The method of separation of variables is used to obtain the elastic displacements in a two-dimensional plate subject to an arbitrary transverse temperature distribution. The geometry is illustrated below:

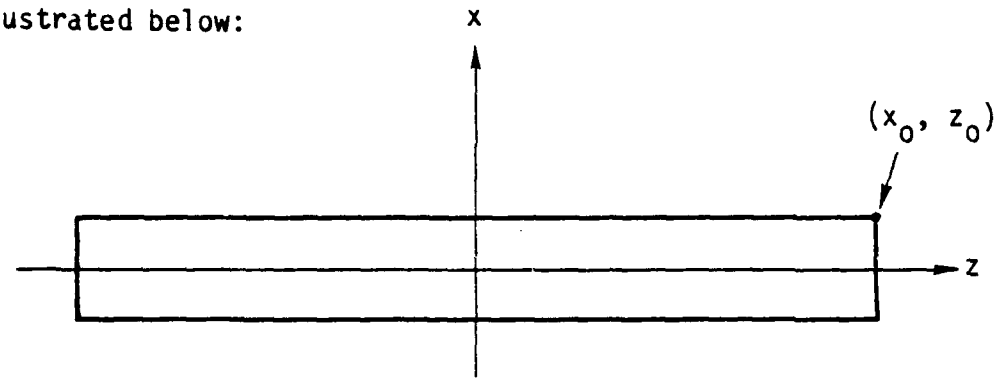

The plate, of width $2x_0$ and length $2z_0$, is assumed to be anisotropic-transversely isotropic with the xy plane being the plane of isotropy. The stresses are then given by

$$\sigma_{xx} = C_{11}\frac{\partial u_1}{\partial x} + C_{12}\frac{\partial u_2}{\partial y} + C_{13}\frac{\partial u_3}{\partial z} - \gamma_1 T(x)$$

$$\sigma_{yy} = C_{12}\frac{\partial u_1}{\partial x} + C_{11}\frac{\partial u_2}{\partial y} + C_{13}\frac{\partial u_3}{\partial z} - \gamma_1 T(x) \qquad (7.1)$$

$$\sigma_{zz} = C_{13}\frac{\partial u_1}{\partial x} + C_{13}\frac{\partial u_2}{\partial y} + C_{33}\frac{\partial u_3}{\partial z} - \gamma_3 T(x)$$

$$\sigma_{zx} = C_{44}\left(\frac{\partial u_1}{\partial z} + \frac{\partial u_3}{\partial x}\right)$$

where u_1, u_2, u_3 are the displacements in the x, y, and z directions, T(x) is the applied temperature distribution, and γ_1, γ_3 are the stress-temperature coupling coefficients, which are given in terms of the linear expansion coefficients β_1, β_3 by

$$\gamma_1 = (C_{11} + C_{12})\,\beta_1 + C_{13}\beta_3$$
$$\gamma_3 = 2C_{13}\beta_1 + C_{33}\beta_3 \quad . \tag{7.2}$$

With appropriate changes, as indicated below, the method presented here could be adapted to an isotropic plate.

In the case of plane strain, $\varepsilon_{yy} = 0$, the two-dimensional problem of interest here is

$$\sigma_{xx} = C_{11}\frac{\partial u_1}{\partial x} + C_{13}\frac{\partial u_3}{\partial z} - \gamma_1\,T(x)$$
$$\sigma_{zz} = C_{13}\frac{\partial u_1}{\partial x} + C_{33}\frac{\partial u_3}{\partial z} - \gamma_3\,T(x) \tag{7.3}$$
$$\sigma_{zx} = C_{44}\left(\frac{\partial u_1}{\partial z} + \frac{\partial u_3}{\partial x}\right) \quad .$$

The above relations are also valid for the case of plane stress, $\sigma_{yy} = 0$, provided that the actual elastic constants are replaced by

$$C_{11} \to C_{11} - \frac{C_{12}^2}{C_{11}} \quad , \quad C_{13} \to C_{13} - \frac{C_{12}C_{13}}{C_{11}}$$
$$C_{33} \to C_{33} - \frac{C_{13}^2}{C_{11}} \quad , \quad \gamma_1 \to \gamma_1\left(1 - \frac{C_{12}}{C_{11}}\right) \tag{7.4}$$
$$\gamma_3 \to \gamma_3 - \frac{C_{13}}{C_{11}}\gamma_1$$

The equations for elastic equilibrium,

$$\frac{\partial \sigma_{xx}}{\partial x} + \frac{\partial \sigma_{xz}}{dz} = 0$$
$$\frac{\partial \sigma_{zz}}{\partial z} + \frac{\partial \sigma_{xz}}{\partial x} = 0 \qquad (7.5)$$

become with the use of (7.3)

$$C_{11} \frac{\partial^2 u_1}{\partial x^2} + C_{44} \frac{\partial^2 u_1}{\partial z^2} + (C_{13} + C_{44}) \frac{\partial^2 u_3}{\partial x \partial z} = \gamma_1 \frac{\partial T}{\partial x}$$
$$C_{33} \frac{\partial^2 u_3}{\partial z^2} + C_{44} \frac{\partial^2 u_3}{\partial x^2} + (C_{13} + C_{44}) \frac{\partial^2 u_1}{\partial x \partial z} = 0 \quad . \qquad (7.6)$$

In the next two sections, we outline the solution of the set of equations (7.6) subject to the condition that the shear and normal stresses vanish at the surface of the plate. The formal solution itself is exact; the numerical evaluation, however, is approximate in the sense that the Fourier coefficients are obtained from the solution of a system of coupled equations of the form

$$C_{1m} = a_m + \sum_n b_{mn} A_{1n}$$
$$A_{1n} = f_n + \sum_m g_{nm} C_{1m} \quad , \qquad (7.7)$$

where A_{1n} and C_{1m} are the desired expansion coefficients, and a_m, f_n, b_{mn}, g_{nm} are constants. Thus, computational considerations limit one to the use of a few hundred terms.

In Section 7.1 we outline the solution for an applied temperature distribution which is an odd function of x, and in Section 7.2 the solution appropriate for an even function. The displacements corresponding to an arbitrary temperature function are obtained from a superposition of the two solutions.

Numerical results are presented in Section 7.3. In particular, we present calculated shear strains for a discontinuous applied temperature distribution of the form

$$T(x) = \begin{cases} 0 & , -x_o < x < 0.8\, x_o \\ 1 & , \quad 0.8x_o \leq x \leq x_o \end{cases}$$

This problem is mathematically equivalent to the uniform heating of two bonded plates which have the same elastic constants but different coefficients of thermal expansion.

7.1 ODD TEMPERATURE FUNCTION

This part of the solution has been reported in Reference 9, but in order that this report be self-contained, is repeated here. For an odd temperature distribution, the appropriate combination of functions to represent the elastic displacements is

$$\begin{aligned} u_1(x,z) &= \sum_n B_n(x) \cos kz + \sum_m D_m(z) \cos jx \\ u_3(x,z) &= \sum_n A_n(x) \sin kz + \sum_m C_m(z) \sin jx \end{aligned} \tag{7.9}$$

where

$$\begin{aligned} k &= (n + \tfrac{1}{2}) \frac{\pi}{z_o} \quad , n = 0, 1, 2, \ldots \\ j &= (m + \tfrac{1}{2}) \frac{\pi}{x_o} \quad , \quad m = 0, 1, 2, \ldots \end{aligned} \tag{7.10}$$

and $A_n(x)$ and $C_m(z)$ are odd functions of their respective variables, and $B_n(x)$ and $D_m(z)$ are even functions. The functions $A_n(x)$, $B_n(x)$, $C_m(z)$ and $D_m(z)$ are subject to the following constraints as determined from the boundary conditions:

1) Zero shear stress along (x_o, z)

$$A_n'(x_o) - kB_n(x_o) = 0 \tag{7.11}$$

2) Zero shear stress along (x,z_o)

$$jC_m(z_o) + D'_m(z_o) = -\frac{2}{x_o} \sum_n (-1)^n \int_0^{x_o} [A'_n(x) - kB_n(x)] \cos jx\,dx \qquad (7.12)$$

3) Zero normal stress along (x_o,z)

$$C_{13}kA_n(x_o) + C_{11}B'_n(x_o) = -\frac{2}{z_o} \sum_m (-1)^m \int_0^{z_o} \left[C_{13}C'_m(z) - jC_{11}D_m(z)\right] \cos kz\,dz + \frac{2}{z_o} \gamma_1 T(x_o) \frac{(-1)^n}{k} \qquad (7.13)$$

4) Zero normal stress along (x,z_o)

$$C_{33}C'_m(z_o) - C_{13}jD_m(z_o) = \frac{2}{x_o} \gamma_3 \int_0^{x_o} T(x) \sin jx\,dx \qquad (7.14)$$

The differential equations for $A_n(x)$, $B_n(x)$, $C_m(z)$, $D_m(z)$ are obtained from a substitution of equations (7.9) into equations (7.6). The resulting equations for $A_n(x)$ and $B_n(x)$ are

$$\begin{aligned} C_{44}A''_n(x) - C_{33}k^2A_n(x) - (C_{13} + C_{44})\,kB'_n(x) &= 0 \\ C_{11}B''_n(x) - C_{44}k^2B_n(x) + (C_{13} + C_{44})\,kA'_n(x) &= 0 \end{aligned} \qquad (7.15)$$

and for $C_m(z)$ and $D_m(z)$ are

$$\begin{aligned} C_{33}C''_m(z) - C_{44}j^2C_m(z) - (C_{13} + C_{44})\,jD'_m(z) &= 0 \\ C_{44}D''(z) - C_{11}j^2D_m(z) + (C_{13} + C_{44})\,jC'_m(z) &= \frac{2}{x_o} \gamma_1 \int_0^{x_o} \frac{\partial T}{\partial x} \cos jx\,dx \quad . \end{aligned} \qquad (7.16)$$

The appropriate solutions are

$$A_n(x) = A_{1n} \frac{\sinh(a_1 kx)}{\cosh(a_1 kx_o)} + A_{2n} \frac{\sinh(a_2 kx)}{\cosh(a_2 kx_o)}$$

$$B_n(x) = A_{1n}S_1 \frac{\cosh(a_1 kx)}{\cosh(a_1 kx_o)} + A_{2n}S_2 \frac{\cosh(a_2 kx)}{\cosh(a_2 kx_o)} \qquad (7.17)$$

and

$$C_m(z) = C_{1m} \frac{\sinh(b_1 jz)}{\cosh(b_1 jz_o)} + C_{2m} \frac{\sinh(b_2 jz)}{\cosh(b_2 jz_o)}$$

$$D_m(z) = C_{1m}R_1 \frac{\cosh(b_1 jz)}{\cosh(b_1 jz_o)} + C_{2m}R_2 \frac{\cosh(b_2 jz)}{\cosh(b_2 jz_o)} \qquad (7.18)$$

$$- \frac{2}{x_o} \frac{\gamma_1}{C_{11} j^2} \int_0^{x_o} \frac{\partial T}{\partial x} \cos jx dx \quad ,$$

where A_{1n}, A_{2n}, C_{1m}, C_{2m} are constant expansion coefficients to be determined from the boundary conditions (7.11 - 7.14). The hyperbolic cosines in the denominators were factored out to facilitate the avoidance of overflow during numerical evaluation. The quantities a_1, a_2 are the positive roots of the equation

$$C_{11}C_{44}a^4 - (C_{11}C_{33} - 2C_{13}C_{44} - C_{13}^2)a^2 + C_{33}C_{44} = 0 \qquad (7.19)$$

with

$$S_i = \frac{(C_{44}a_i^2 - C_{33})}{(C_{13} + C_{44})\, a_i} \quad , \quad i = 1,2$$

and b_1, b_2 are the positive roots of

$$C_{33}C_{44}b^4 - (C_{11}C_{33} - 2C_{13}C_{44} - C_{13}^2)b^2 + C_{11}C_{44} = 0 \qquad (7.20)$$

with

$$R_i = \frac{(C_{33}b_i^2 - C_{44})}{(C_{13} + C_{44})b_i}, \quad i = 1,2$$

Note that in the limit of isotropy, equation (7.19) has only one positive root, $a^2 = 1$, and the solution for $A_n(x)$ becomes a linear combination of sinh(kx) and x cosh(kx).

Substitution of (7.17) and (7.18) into the boundary conditions (7.11 - 7.14) yields the following equations for the expansion coefficients,

1) Zero shear stress along (x_o,z)

$$A_{1n}(a_1-S_1) + A_{2n}(a_2-S_2) = 0 \tag{7.21}$$

2) Zero shear stress along (x,z_o)

$$C_{1m}(1 + R_1b_1)\tanh(b_1jz_o) + C_{2m}(1 + R_2b_2)\tanh(b_2jz_o)$$
$$= -\frac{2}{x_o}(-1)^m \sum_n (-1)^n k \left[A_{1n}\frac{a_1 - S_1}{j^2 + a_1^2k^2} + A_{2n}\frac{a_2 - S_2}{j^2+a_2^2k^2}\right] \tag{7.22}$$

3) Zero normal stress along (x_o,z)

$$A_{1n}(C_{13} + C_{11}S_1a_1)\tanh(a_1kx_o) + A_{2n}(C_{13} + C_{11}S_2a_2)\tanh(a_2kx_o)$$
$$= -\frac{2}{z_o}(-1)^n \sum_m (-1)^m j\left[C_{1m}\frac{C_{13}b_1-C_{11}R_1}{k^2+b_1^2j^2} + C_{2m}\frac{C_{13}b_2-C_{11}R_2}{k^2 + b_2^2j^2}\right] \tag{7.23}$$

In arriving at (7.23) from (7.13), use has been made of the fact that T(x) is an odd function and that

$$T(x_o) = \frac{2}{x_o} \sum_m (-1)^m \int_0^{x_o} T(x) \sin jx\,dx \quad .$$

4) Zero normal stress along (x,z_o)

$$C_{1m}\,(C_{33}b_1 - C_{13}R_1) + C_{2m}(C_{33}b_2 - C_{13}R_2) \tag{7.24}$$

$$= \frac{2}{x_o}\left(\gamma_3 - \gamma_1 \frac{C_{13}}{C_{11}}\frac{1}{j}\right)\int_0^{x_o} T(x)\,\sin jx\,dx \quad .$$

From (7.24),

$$C_{2m} = -\,Q_2 C_{1m} + Q_1 \frac{1}{j}\int_0^{x_o} T(x)\,\sin jx\,dx \tag{7.25}$$

where

$$Q_1 \equiv \frac{2}{x_o}\,\frac{\left(\gamma_3 - \gamma_1 \dfrac{C_{13}}{C_{11}}\right)}{\left(C_{33}b_2 - C_{13}R_2\right)} \tag{7.26}$$

$$Q_2 \equiv \frac{C_{33}b_1 - C_{13}R_1}{C_{33}b_2 - C_{13}R_2} \tag{7.27}$$

Note that Q_1 above is defined differently than in Reference 9. From (7.21)

$$A_{2n} = -\,Q_3 A_{1n} \tag{7.28}$$

$$Q_3 \equiv \frac{a_1 - S_1}{a_2 - S_2} \tag{7.29}$$

Substitution of (7.25) and (7.28) into (7.22) and (7.23) gives two sets of coupled equations for the coefficients A_{1n} and C_{1m},

$$C_{1m}Q_{5m} = -\,Q_1 \frac{1}{j}\left[\int_0^{x_o} T(x)\,\sin jx\,dx\right](1 + R_2 b_2)\,\tanh\,(b_2 j z_o)$$

$$- \frac{2}{x_o}(-1)^m \sum_n (-1)^n\, k\left[\frac{a_1 - S_1}{j^2 + a_1^2 k^2} - Q_3\,\frac{a_2 - S_2}{j^2 + a_2^2 k^2}\right] A_{1n} \tag{7.30}$$

$$A_{1n}Q_{4n} = -\frac{2}{z_o}(-1)^n Q_1(C_{13}b_2-C_{11}R_2)\sum_m (-1)^m \frac{\int_o^{x_o} T(x)\sin jx\,dx}{k^2+b_{2j}^2}$$

$$-\frac{2}{z_o}(-1)^n \sum_m (-1)^m j\left[\frac{C_{13}b_1-C_{11}R_1}{k^2+b_{1j}^2}\right.$$

$$\left.-Q_2\frac{C_{13}b_2-C_{11}R_2}{k^2+b_{2j}^2}\right]C_{1m}\,, \qquad (7.31)$$

where

$$Q_{5m} \equiv (1+R_1b_1)\tanh(b_1jz_o) - Q_2(1+R_2b_2)\tanh(b_2jz_o)\,, \qquad (7.32)$$

$$Q_{4n} \equiv (C_{13}+C_{11}S_1a_1)\tanh(a_1kx_o) - Q_3(C_{13}+C_{11}S_2a_2)\tanh(a_2kx_o). \qquad (7.33)$$

The coupled sets of equations (7.30) and (7.31) are of the form

$$\begin{aligned} C_{1m} &= a_m + \sum_n b_{mn}A_{1n} \\ A_{1n} &= f_n + \sum_m g_{nm}C_{1m} \end{aligned} \qquad (7.34)$$

which can be solved with the following iteration procedure:

$$C_{1m}^{(0)} = a_m$$

$$A_{1n}^{(1)} = f_n + \sum_m g_{nm}C_{1m}^{(0)}$$

$$C_{1m}^{(1)} = a_m + \sum_n b_{mn}A_{1n}^{(1)}$$

$$A_{1n}^{(2)} = f_n + \sum_m g_{nm}C_{1m}^{(1)}\,, \text{ etc.}$$

7.2 EVEN TEMPERATURE FUNCTION

For an even temperature distribution, the appropriate combination of functions for the displacements is

$$u_1(x,z) = \sum_n B^*_n(x) \cos kz + \sum_m D^*_m(z) \sin jx$$
$$u_3(x,z) = \sum_n A^*_n(x) \sin kz + \sum_m C^*_m(z) \cos jx \,, \tag{7.36}$$

where as before,

$$k = (n + \tfrac{1}{2}) \frac{\pi}{z_o} \,, \quad n = 0, 1, 2, \ldots$$

$$j = (m + \tfrac{1}{2}) \frac{\pi}{x_o} \,, \quad m = 0, 1, 2, \ldots$$

amd $B^*_n(x)$ and $C^*_m(z)$ are odd functions of their respective variables, and $A^*_n(x)$ and $D^*_m(z)$ are even functions. The boundary conditions impose the following constraints:

1) Zero shear stress along (x_o,z)

$$A^{*\prime}_n(x_o) - kB^*_n(x_o) - \frac{2}{z_o} \sum_m (-1)^m \int_0^{z_o} \left[jC^*_m(z) - D^{*\prime}_m(z)\right] \sin kz\, dz \tag{7.36}$$

2) Zero shear stress along (x,z_o)

$$jC^*_m(z_o) - D^{*\prime}_m(z_o) = \frac{2}{x_o} \sum_n (-1)^n \int_0^{x_o} \left[A^{*\prime}_n(x) - kB^*_n(x)\right] \sin jx\, dx \tag{7.37}$$

3) Zero normal stress along (x_o,z)

$$C_{13} kA^*_n(x_o) + C_{11} B^{*\prime}_n(x_o) = \frac{2}{z_o} \gamma_1 T(x_o) \frac{(-1)^n}{k} \tag{7.38}$$

4) Zero normal stress along (x,z_o)

$$C_{33}C^{*\prime}_m(z_o) + C_{13}j\,D^*_m(z_o) = \frac{2}{x_o}\,\gamma_3 \int_0^{x_o} T(x)\,\cos jx\,dx \qquad (7.39)$$

The equations (7.6) for elastic equilibrium are unchanged, as are the equations (7.15) for $A^*_n(x)$ and $B^*_n(x)$. The equations for $C^*_m(z)$ and $D^*_m(z)$ become

$$C_{33}C^{*\prime\prime}_m(z) - C_{44}j^2C^*_m(z) + (C_{13} + C_{44})\,jD^{*\prime}_m(z) = 0$$

$$C_{44}D^{*\prime\prime}_m(z) - C_{11}j^2D^*_m(z) - (C_{13} + C_{44})\,jC^{*\prime}_m(z)$$

$$= \frac{2}{x_o}\,\gamma_1 \int_0^{x_o} \frac{\partial T}{\partial x}\,\sin jx\,dx \quad .$$

The functions $A^*_n(x)$ and $B^*_n(x)$ are now

$$A^*_n(x) = A^*_{1n}\,\frac{\cosh(a_1kx)}{\cosh(a_1kx_o)} + A^*_{2n}\,\frac{\cosh(a_2kx)}{\cosh(a_2kx_o)}$$

$$B^*_n(x) = A^*_{1n}S_1\,\frac{\sinh(a_1kx)}{\cosh(a_1kx_o)} + A^*_{2n}S_2\,\frac{\sinh(a_2kx)}{\cosh(a_2kx_o)} \qquad (7.40)$$

and $C^*_m(z)$ and $D^*_m(z)$ become

$$C^*_m(z) = C^*_{1m}\,\frac{\sinh(b_1jz)}{\cosh(b_1jz_o)} + C^*_{2m}\,\frac{\sinh(b_2jz)}{\cosh(b_2jz_o)}$$

$$D^*_m(z) = C^*_{1m}R^*_1\,\frac{\cosh(b_1jz)}{\cosh(b_1jz_o)} + C^*_{2m}R^*_2\,\frac{\cosh(b_2jz)}{\cosh(b_2jz_o)} \qquad (7.41)$$

$$- \frac{2}{x_o}\,\frac{\gamma_1}{C_{11}}\,\frac{1}{j^2} \int_0^{x_o} \frac{\partial T}{\partial x}\,\sin jx\,dx \quad .$$

The quantities a_1, a_2 are the positive roots of

$$C_{11}C_{33}a^4 - (C_{11}C_{33} - 2C_{13}C_{44} - C_{13}^2)\, a^2 + C_{33}C_{44} = 0$$

with

$$S_i = \frac{(C_{33}a_i^2 - C_{33})}{(C_{13} + C_{44})a_i}, \quad i = 1, 2 \tag{7.42}$$

the same as for the odd temperature function; and b_1, b_2 are the positive roots of

$$C_{33}C_{44}b^4 - (C_{11}C_{33} - 2C_{13}C_{44} - C_{13}^2)b^2 + C_{11}C_{44} = 0 \quad ,$$

but now

$$R_i^* = -\frac{(C_{33}b_i^2 - C_{44})}{(C_{13} + C_{44})b_i}, \quad i = 1, 2 \quad . \tag{7.43}$$

The boundary conditions give the following relations for the expansion coefficients,

1) Zero shear stress along (x_o, z)

$$A_{1n}^*(a_1 - S_1)\tanh(a_1 k x_o) + A_{2n}^*(a_2 - S_2)\tanh(a_2 k x_o) \tag{7.44}$$

$$= \frac{2}{z_o}\frac{(-1)^n}{k}\sum_m (-1)^m j^2\left[\frac{b_1(1-R_1^*b_1)}{k^2+b_1^2j^2}C_{1m}^* + \frac{b_2(1-R_2^*b_2)}{k^2+b_2^2j^2}C_{2m}^*\right]$$

2) Zero snear stress along (x, z_o)

$$C_{1m}^*(1-R_1^*b_1)\tanh(b_1 j z_o) + C_{2m}^*(1-R_2^*b_2)\tanh(b_2 j z_o) \tag{7.45}$$

$$= \frac{2}{x_o}\frac{(-1)^m}{j}\sum_n (-1)^n k^2\left[\frac{a_1(a_1-S_1)}{j^2+a_1^2k^2}A_{1n}^* + \frac{a_2(a_2-S_2)}{j^2+a_2^2k^2}A_{2n}^*\right]$$

3) Zero normal stress along $(x_o z)$

$$A^*_{1n}(C_{13} + C_{11}S_1a_1) + A^*_{2n}(C_{13} + C_{11}S_2a_2) = \frac{2}{z_o}\gamma_1 T(x_o)\frac{(-1)^n}{k^2} \tag{7.46}$$

4) Zero normal stress along (x, z_o)

$$C^*_{1m}(C_{33}b_1 + C_{13}R^*_1) + C^*_{2m}(C_{33}b_2 + C_{13}R^*_2) = \frac{2}{x_o}\frac{\gamma_3}{j}\int_o^{x_o} T(x)\cos jx\,dx + \frac{2}{x_o}\frac{\gamma_1 C_{13}}{C_{11}}\frac{1}{j^2}\int_o^{x_o}\frac{\partial T}{\partial x}\sin jx\,dx \tag{7.47}$$

From (7.46),

$$A^*_{2n} = -Q^*_1 A^*_{1n} + Q^*_2 T(x_o)\frac{(-1)^n}{k^2} \tag{7.48}$$

with

$$Q^*_1 \equiv \frac{(C_{13} + C_{11}S_1a_1)}{(C_{13} + C_{11}S_2a_2)} \tag{7.49}$$

$$Q^*_2 \equiv \frac{2\gamma_1}{z_o(C_{13} + C_{11}S_2a_2)}\quad , \tag{7.50}$$

and from (7.47),

$$C^*_{2m} = -Q^*_3 C^*_{1m} + Q^*_4\frac{1}{j}\int_o^{x_o} T(x)\cos jx\,dx + Q^*_5\frac{1}{j^2}\int_o^{x_o}\frac{\partial T}{\partial x}\sin jx\,dx \tag{7.51}$$

with

$$Q_3^* \equiv \frac{(C_{33}b_1 + C_{13}R_1^*)}{(C_{33}b_2 + C_{13}R_2^*)} \tag{7.52}$$

$$Q_4^* \equiv \frac{2\gamma_3}{x_o(C_{33}b_2 + C_{13}R_2^*)} \tag{7.53}$$

$$Q_5^* \equiv \frac{2\gamma_1 C_{13}}{x_o C_{11}(C_{33}b_2 + C_{13}R_2^*)} \tag{7.54}$$

Substitution into (7.44) and (7.45) yields the following coupled equations for A^*_{1n} and C^*_{1m}:

$$C^*_{1m}Q^*_{5m} = -(1-R_2^*b_2)\tanh(b_2 j z_o)\left[\frac{Q_4^*}{j}\int_0^{x_o} T(x)\cos jx\,dx + \frac{Q_5^*}{j^2}\int_0^{x_o}\frac{\partial T}{\partial x}\sin jx\,dx\right] \tag{7.55}$$

$$+\frac{2}{x_o}\frac{(-1)^m}{j}a_2(a_2-S_2)Q_2^*T(x_o)\sum_n \frac{1}{j^2+a_2^2k^2}$$

$$+\frac{2}{x_o}\frac{(-1)^m}{j}\sum_n (-1)^n k^2\left[\frac{a_1(a_1-S_1)}{j^2+a_2^2k^2} - Q_1^*\frac{a_2(a_2-S_2)}{j^2+a_2^2k^2}\right]A^*_{1n}$$

$$A^*_{1n}Q^*_{4n} = -Q_2^*T(x_o)(a_2-S_2)\tanh(a_2kx_o)\frac{(-1)^n}{k^2}$$

$$+\frac{2b_2(1-R_2^*b_2)}{z_o}\frac{(-1)^n}{k}\sum_m (-1)^m\frac{1}{k^2+b_2^2j^2}\left[jQ_4^*\int_0^{x_o} T(x)\cos jx\,dx\right. \tag{7.56}$$

$$\left. + Q_5^*\int_0^{x_o}\frac{\partial T}{\partial x}\sin jx\,dx\right]$$

$$+\frac{2}{z_o}\frac{(-1)^n}{k}\sum_m (-1)^m j^2\left[\frac{b_1(1-R_1^*b_1)}{k^2+b_1^2j^2} - Q_3\frac{b_2(1-R_2^*b_2)}{k^2+b_2^2j^2}\right]C^*_{1m}$$

where

$$Q^*_{5m} = (1-R^*_1 b_1) \text{ tann } (b_1 j z_o) - Q^*_3(1-R^*_2 b_2) \tanh (b_2 j z_o)$$
$$J^*_{4n} = (a_1-S_1) \tanh (a_1 k x_o) - Q^*_1(a_2-S_2) \tanh (a_2 k x_o) \quad . \tag{7.57}$$

Equations (7.55) and (7.56) are also of the form of (7.34) and can be solved with the same iteration procedure.

7.3 COMPUTATIONAL RESULTS

In this section we present calculated results for several discontinuous temperature distributions. The input, plane-stress elastic constants, the same as those used for the calculations reported in Reference 9, are appropriate to a 50 percent aluminum-graphite composite,

C_{11} = 3.187 Msi
C_{13} = 1.118 Msi
C_{33} = 55.401 Msi
C_{44} = 3.298 Msi
γ_1 = 5.033×10^{-5} Msi/°F
γ_3 = 3.705×10^{-5} Msi/°F.

The thermal expansion coefficients are

β_1 = 15.705×10^{-6} °F^{-1}
β_3 = 0.352×10^{-6} °F^{-1}

and the length to width ratio is 10,

x_o = 1
z_o = 10

Figure 7.1 is a plot of the shear strain as a function of z along x = 0 for the odd temperature distribution

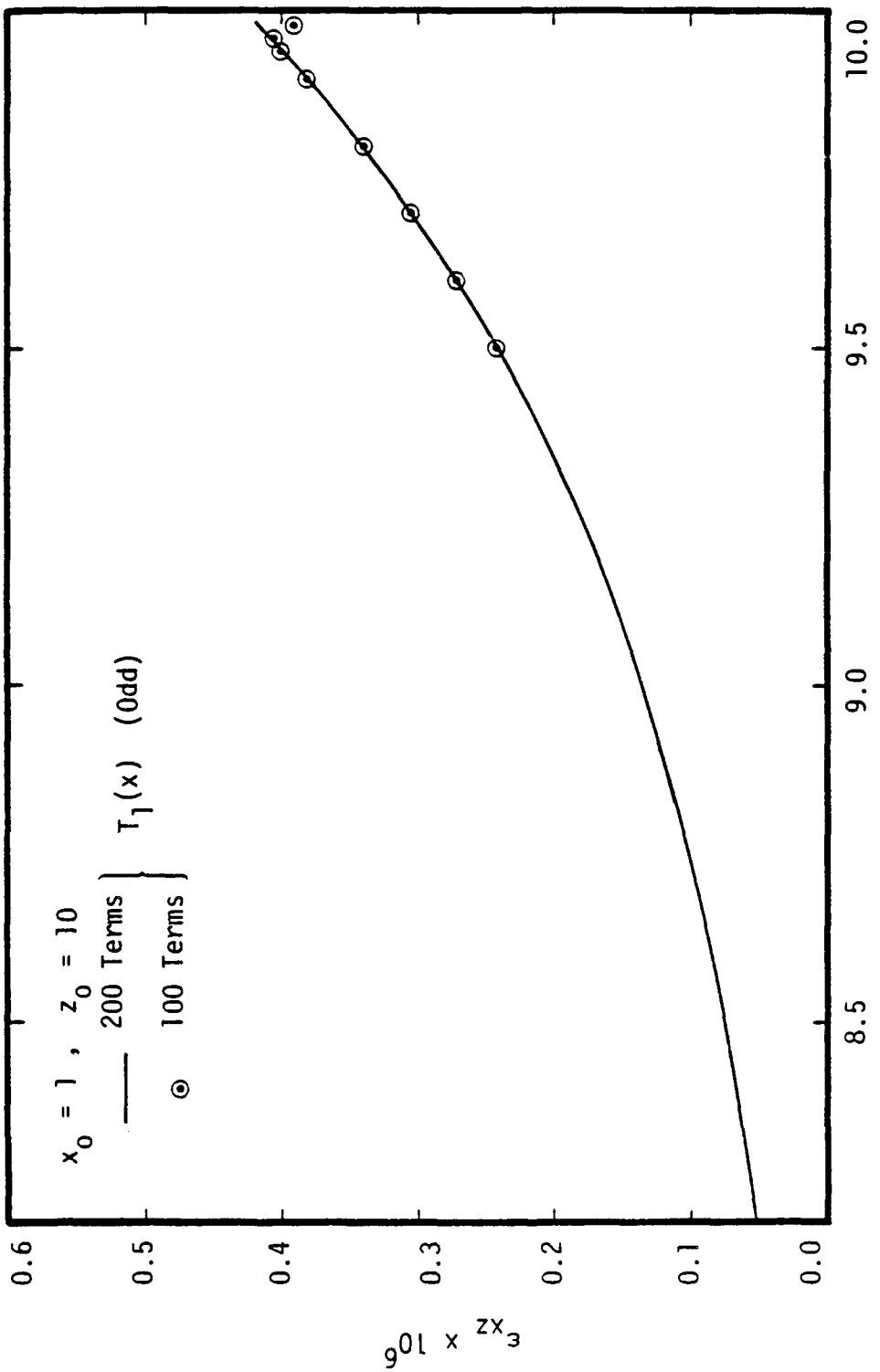

Figure 7.1. Shear strain along z = 0 for the odd temperature distribution $T_1(x)$.

$$T_1(x) = \begin{cases} -\frac{1}{2} , & -x_o \leq x < 0 \\ +\frac{1}{2} , & 0 < x \leq x_o \end{cases} \tag{7.58}$$

The solid line indicates the shear strain as calculated with 200 coefficients, and the dots indicate selected values as calculated with 100 coefficients. The numerical results give no indication of a singularity in the stress field; and, indeed, from Bogy's work on wedges (Reference 11), one would not expect one.

Figure 7.2 shows the results of two calculations for the shear strain as a function of z along $x = 0.8\ x_o$ for the odd and even temperature distributions.

$$T_2(x) = \begin{cases} -\frac{1}{2} , & -x_o < x < -0.8\ x_o \\ 0 , & -0.8\ x_o < x < +0.8\ x_o \\ -\frac{1}{2} , & 0.8\ x_o < x < x_o \end{cases} \tag{7.59}$$

and

$$T_3(x) = \begin{cases} +\frac{1}{2} , & -x_o < x < -0.8\ x_o \\ 0 , & -0.8\ x_o < x < +0.8\ x_o \\ +\frac{1}{2} , & 0.8\ x_o < x < x_o \end{cases} \tag{7.60}$$

The shape of the curve corresponding to the even temperature distribution $T_3(x)$ was unexpected, but so far no algebraic or coding errors have been found. In any case, it has been verified that the longitudinal force at $z = 0$,

$$\int_{0.8\ x_o}^{x_o} \sigma_{zz}(x,0)dx \ ,$$

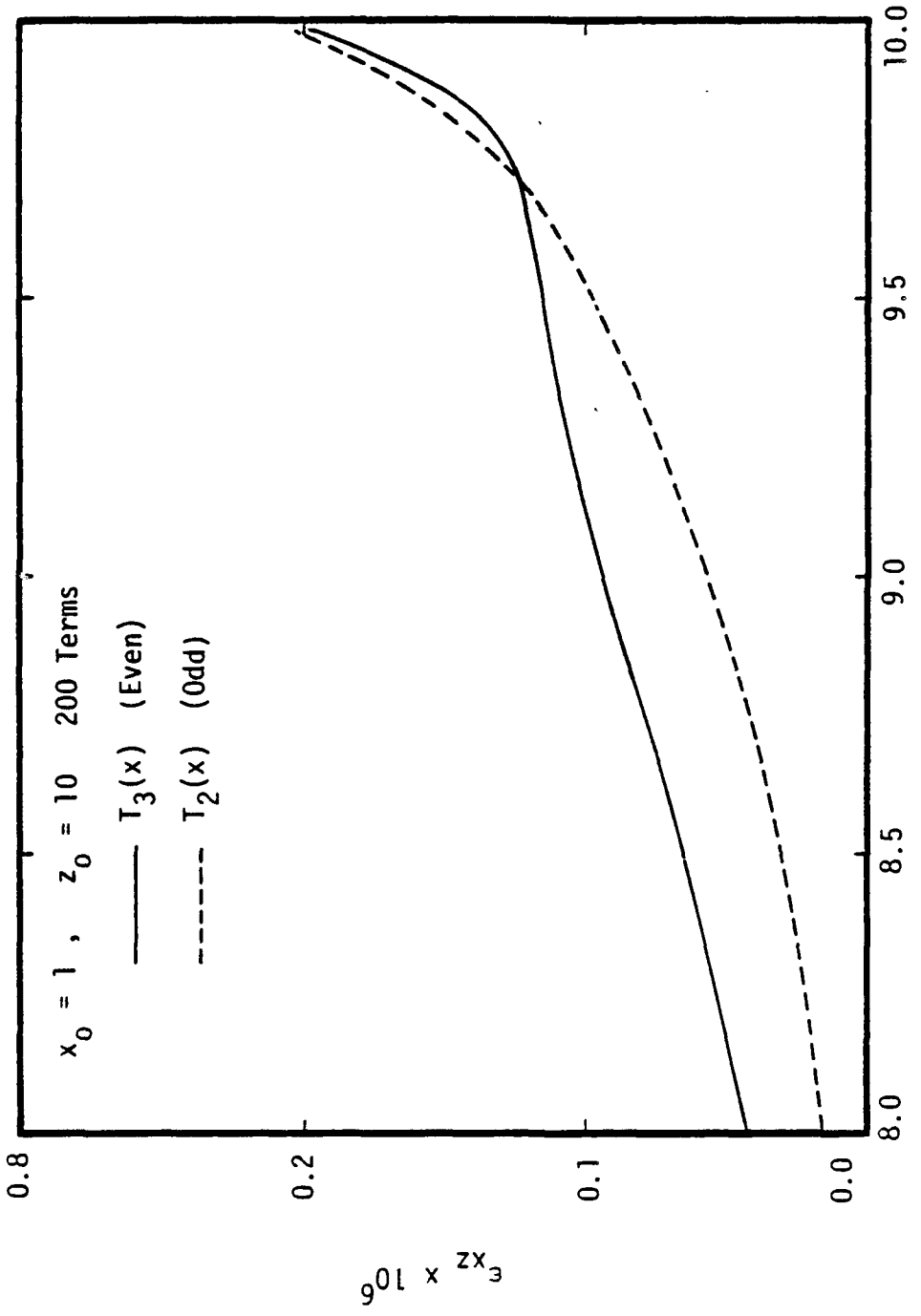

Figure 7.2. Shear strain along $x = 0.8x_o$ for the odd and even temperature distributions $T_2(x)$ and $T_3(x)$.

balances that of the shear stress,

$$\int_0^{z_0} \sigma_{xz}\,(0.8\,x_0, z)\,dz\ .$$

A plot of the longitudinal strain ε_{zz} as a function of z along $x = 0.8\,x_0$, corresponding to the temperature distributions $T_2(x)$ and $T_3(x)$, is given as Figure 7.3.

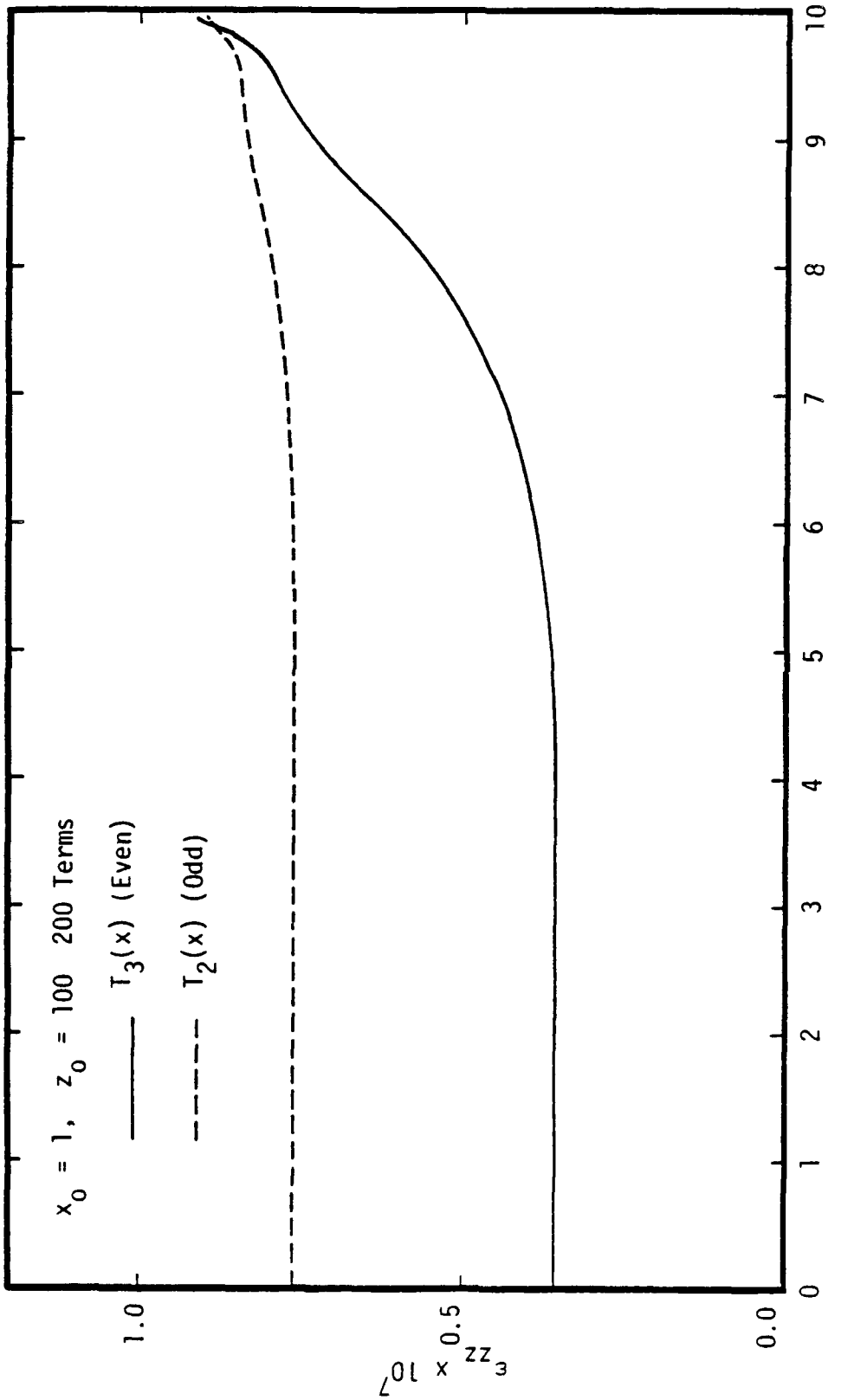

Figure 7.3. Longitudinal strain ε_{zz} along $x = 0.8x_o$ for the odd and even temperature distributions $T_2(x)$ and $T_3(x)$.

8. SUMMARY AND CONCLUSIONS

a. For G/Al where the matrix is in a T4 temper (rapid quench to -240°F):

Axial stresses in the aluminum at room temperature are tensile and lie in the range 30 to 40 ksi.

Subsequent reheating will lower the axial stress, and the matrix will remain elastic up to a temperature of approximately 600°F, at which point the axial stress will have become compressive.

Residual hoop stresses in the matrix are tensile and range from approximately 10 to 20 ksi for all cases in which the fibers' transverse coefficient of thermal expansion remains less than or equal to that of the matrix.

The interfacial radial stress is compressive and ranges from 2 to 10 ksi so long as the fibers' transverse coefficient of thermal expansion does not exceed that of the matrix. This would appear to be a most desirable result in maintaining the integrity of these materials, since they are currently limited by their ability to bear significant radial tensile stresses across this interface.

b. For G/Al where the matrix is in a T0 temper (slow quench to -240°F), the axial residual stresses are near zero at room temperature.

c. For G/Al in the T4 temper, a reduction of approximately 5 to 10 ksi in the room temperature axial residual stress could be expected if the composite was quenched to -320°F.

d. For the W/Al and SiC/Al composites, residual stress results are qualitatively similar to those of G/Al of equivalent temper.

e. Calculated axial stress strain behavior of SiC/Al using a yielded matrix material in the TO temper condition is in reasonable agreement with experimental data up to 200 ksi.

f. For a three-layer laminate of G/Al, minimum longitudinal coefficient of thermal expansion occurs at a ply angle of approximately 20 degrees (i.e., 20/0/20).

g. PRUFC yields G/Al thermoelastic properties in good agreement with those reported by Hashin and Humphries who used a finite element analysis (Ref.2).

h. The S-CUBED residual stress code yields results for G/Al which are in good agreement with the ANSYS finite element results reported by Hashin and Humphries (Ref. 2).

REFERENCES

1. Rice, M. H. and G. A. Gurtman, "Residual Stresses in Fiber Reinforced Metal Matrix Composites," S-CUBED Report SSS-R-82-5447, March 1982 (Submitted to DARPA).

2. Hashin, Z. and E. A. Humphreys, "Elevated Temperature Behavior of Metal-Matrix Composites," Materials Sciences Corporation Report MSC TFR 1214/1502, November 1981 (AFOSR-TR-82-0212).

3. Rice, M. H. and G. A. Gurtman, "PRUFC: A Computer Code to Calculate the Properties of Unidirectional Fibrous Composites," S-CUBED Report SSS-R-81-4940, April 1981.

4. Rice, M. H. and G. A. Gurtman, "Residual Stresses and Mechanical Properties of SiC/Al composites," S-CUBED Report SSS-R-83-5934, December 1982.

5. Appendix II of Silicon Carbide -- 1973, eds., R. C. Marshall, J. W. Faust, Jr., and C. E. Ryan, University of S. Carolina Press (1973).

6. Hill, R., The Mathematical Theory of Plasticity, Oxford University Press (1950).

7. Private communication from D. J. A. Cornie (AVCO-SMC) to G. A. Gurtman (S-CUBED).

8. Hashin, Z., "Theory of Fiber Reinforced Materials," NASA Contractor Report NASA CR-1974, March 1972.

9. Gurtman, G. A., M. H. Rice and A. Maewal, "Thermomechanical Analysis of Graphite/Metal Matrix Composites," S-CUBED Report SSS-R-81-4862, February 1981.

10. Rice, M. H. and G. A. Gurtman, "Thermal Deformation of an Elastic Plate," S-CUBED Progress Report SSS-R-81-5075, July 1981.

11. Bogy, D. B., "Two Edge-Bonded Elastic Wedges of Different Materials and Wedge Angles Under Surface Tractions," J. App. Mech, 38, 377(1971).

12. Metals Handbook, Ninth Edition, Volume 2, "Properties and Selection: Nonferrous Alloys and Pure Metals," American Society for Metals (1979).

13. Military Handbook, MIL-HDBK-5A, "Metallic Materials and Elements for Aerospace Vehicle Structures," February 1966.

(This Page Left Blank)

APPENDIX A
ALUMINUM PROPERTIES

Thermoelastic properties and yield-strength models for 6061 and 2024 aluminum alloys are summarized below.

A.1 6061 ALUMINUM

For the 6061 aluminum matrix, the elastic modulus was input as a function of temperature, linear interpolation being used between the following tabular points in Table A1:

TABLE A1
ELASTIC MODULUS FOR 6061 ALUMINUM

T(°F)	E(Msi)
-459	11.8
75	10.0
240	9.8
400	9.0
600	7.0
1100	0.0

The Poisson's ratio was also allowed to vary with temperature according to

$$\nu = 0.5 - E/58.823 \qquad (A.1)$$

where E is the elastic modulus in Msi as computed from the table above. The thermal expansion coefficient for the aluminum matrix was taken to be temperature dependent according to the tabulated points in Table A2:

TABLE A2

LINEAR COEFFICIENT OF THERMAL EXPANSION FOR

Al 6061 AND Al 2024

T(°F)	$\alpha(10^{-6}°F^{-1})$
- 400	0
- 300	5
- 200	9
0	12
1100	18.5

Residual stress calculations were done with two different yield strength models. A model appropriate to 6061 Al in the annealed state, or T0 temper, is depicted in Figure A1. The room-temperature yield stress at 0.2 percent offset if 8 ksi in accord with Ref. 12 (the elastic modulus at room temperature is taken as 10 Msi). A yield model appropriate to 6061 Al in the T4 temper (rapid quenching) is shown in Figure A2. Here the yield stress at room temperature at the 0.2 percent offset point is 21 ksi, as given in Ref. 12. The shapes of the room-temperature stress-strain curves for both tempers were scaled from that for Al 201 in the 0 temper, for which experimental data were available (see p. 25 of Ref. 1). The variation of yield stress with temperature is scaled proportionately to that of other aluminums (see, for example, Ref. 13).

A.2 2024 ALUMINUM

For the 2024 aluminum matrix, the elastic modulus as a function of temperature was given by the tabulated points in Table A3:

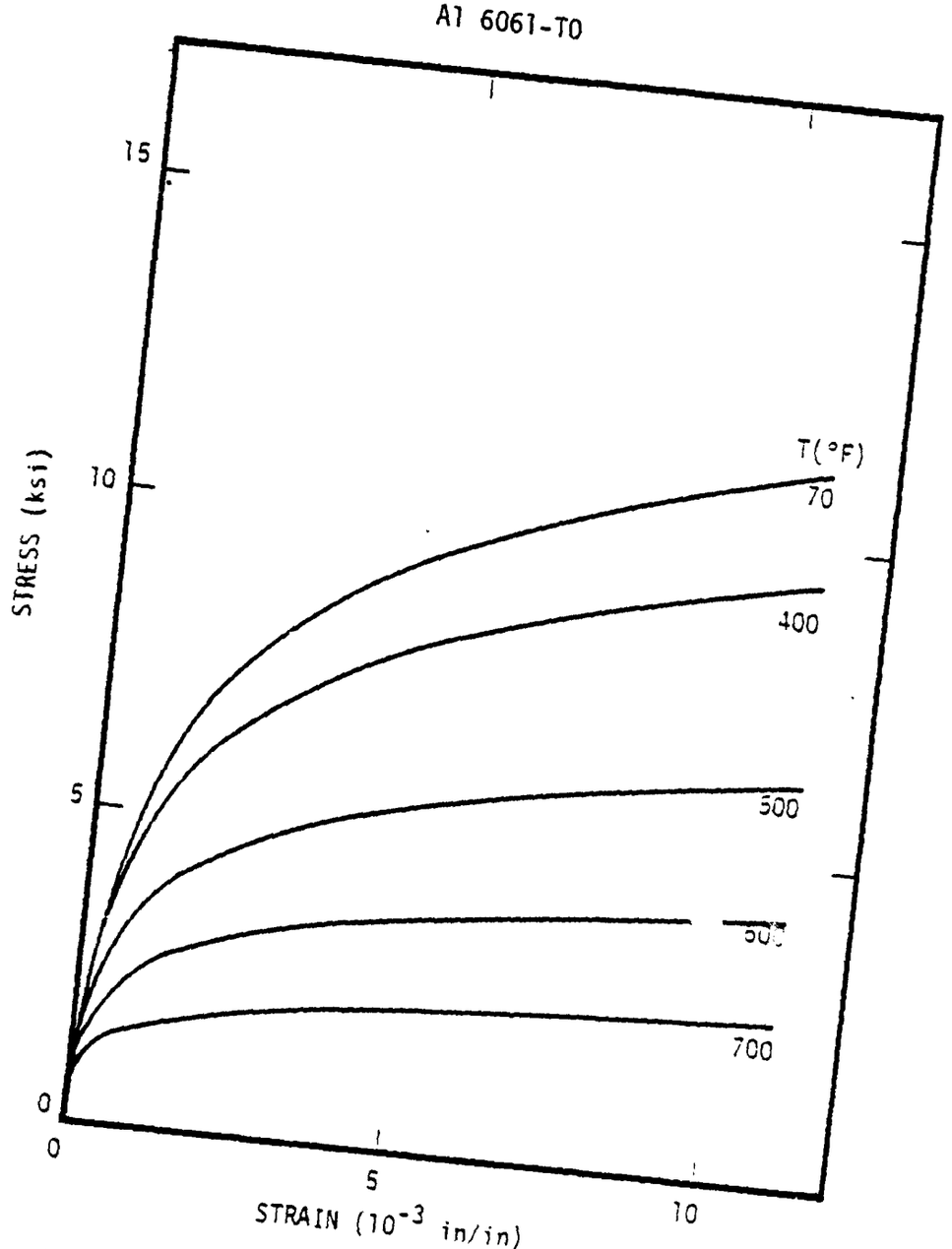

Figure A-1. Yield stress model for 6061 aluminum in the TO temper (annealed).

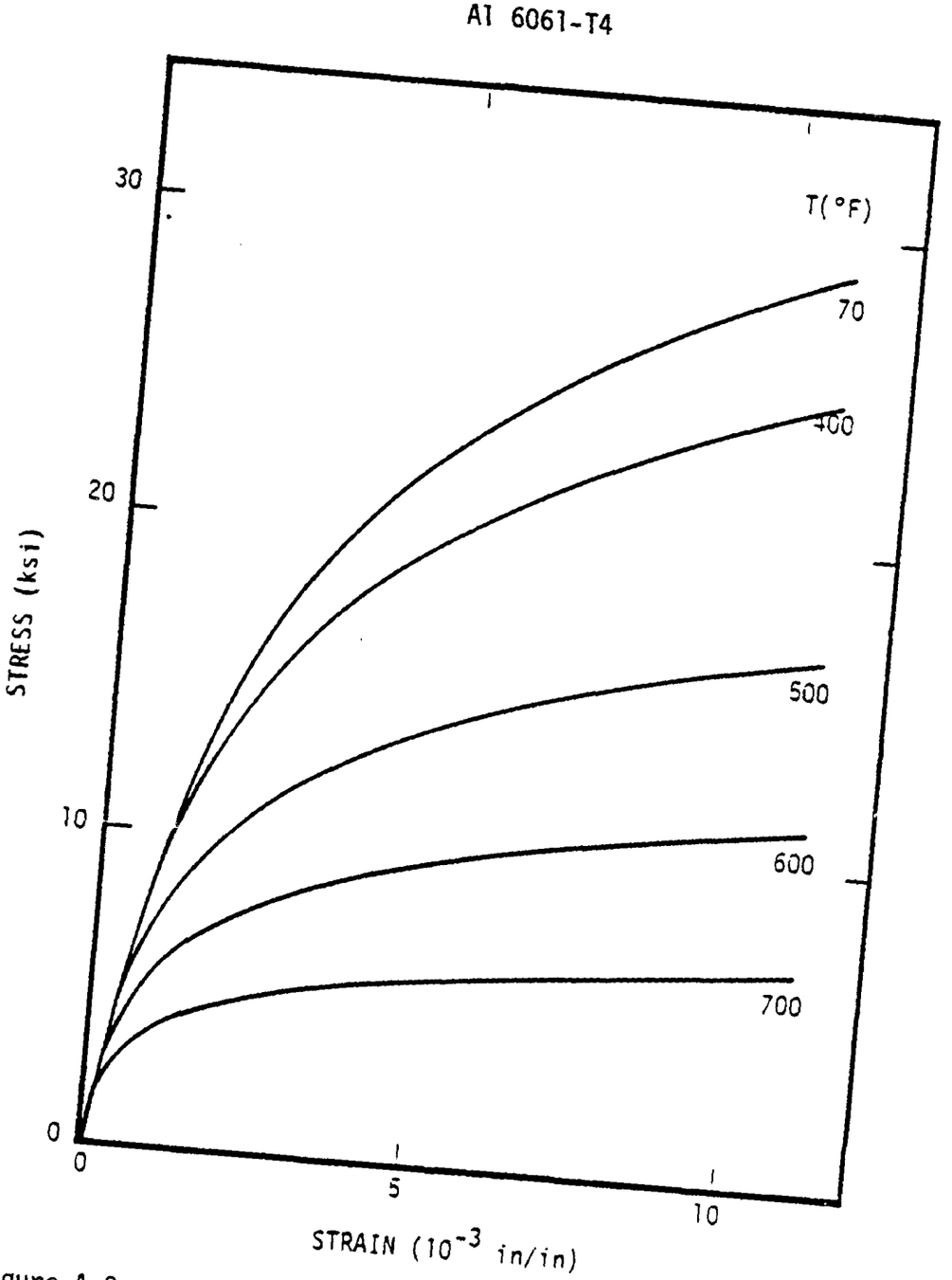

Figure A-2. Yield stress model for 6061 aluminum in the T4 temper.

TABLE A3

ELASTIC MODULUS FOR 2024 ALUMINUM

T(°F)	E(Msi)
- 459	12.39
75	10.5
240	10.29
400	9.45
600	7.35
1100	0

The Poisson's ratio was allowed to vary with temperature according to

$$\nu = 0.5 - E/61.765 \quad , \qquad (A.2)$$

where E is the elastic modulus in Msi from Table A3. The thermal expansion coefficient was taken to be the same as that for Al 6061 as given in Table A2.

The yield stress model for the T0 (annealed) and T4 tempers are shown in Figures A3 and A4.

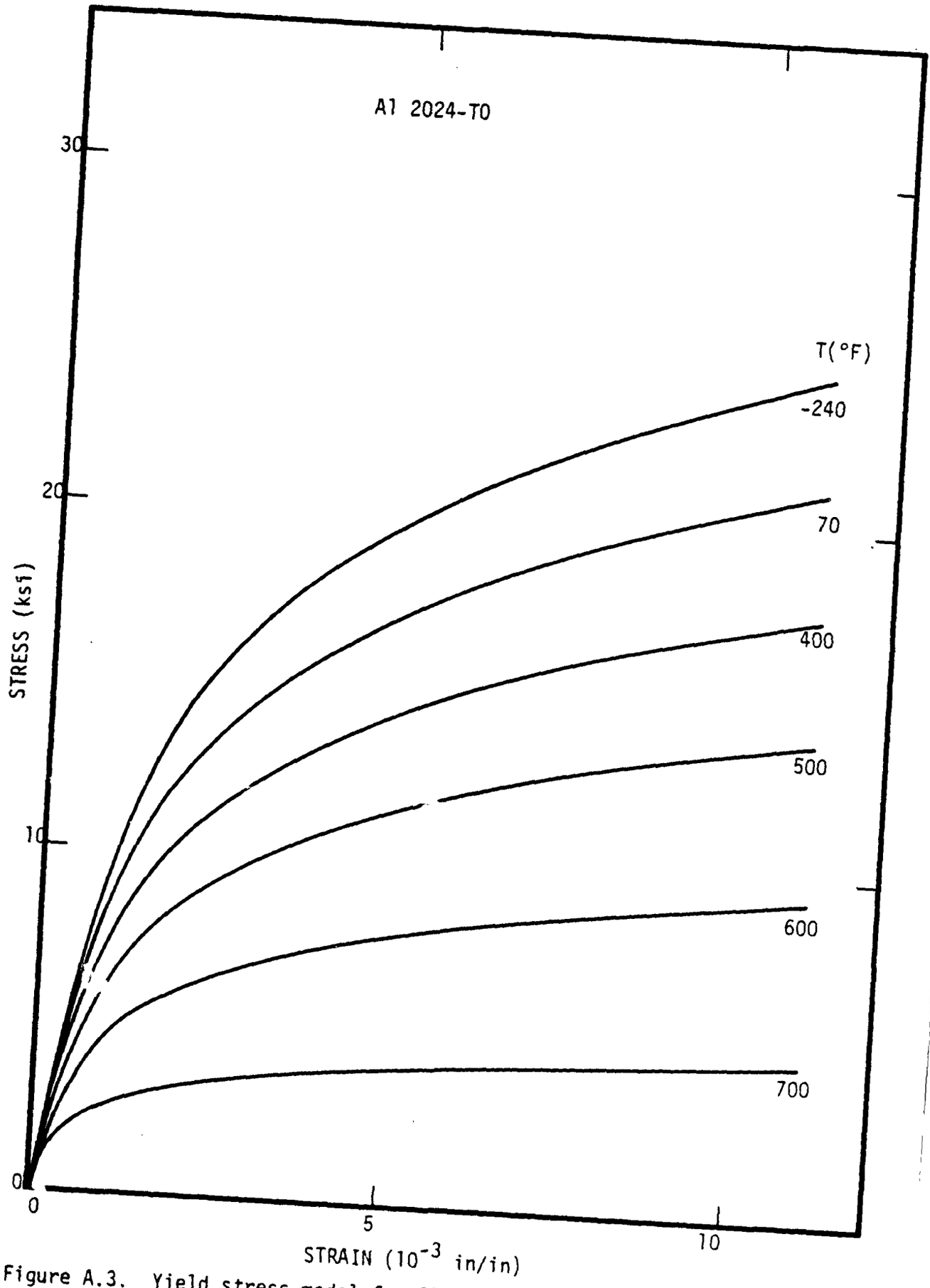

Figure A.3. Yield stress model for 2024 aluminum in the T0 temper (annealed).

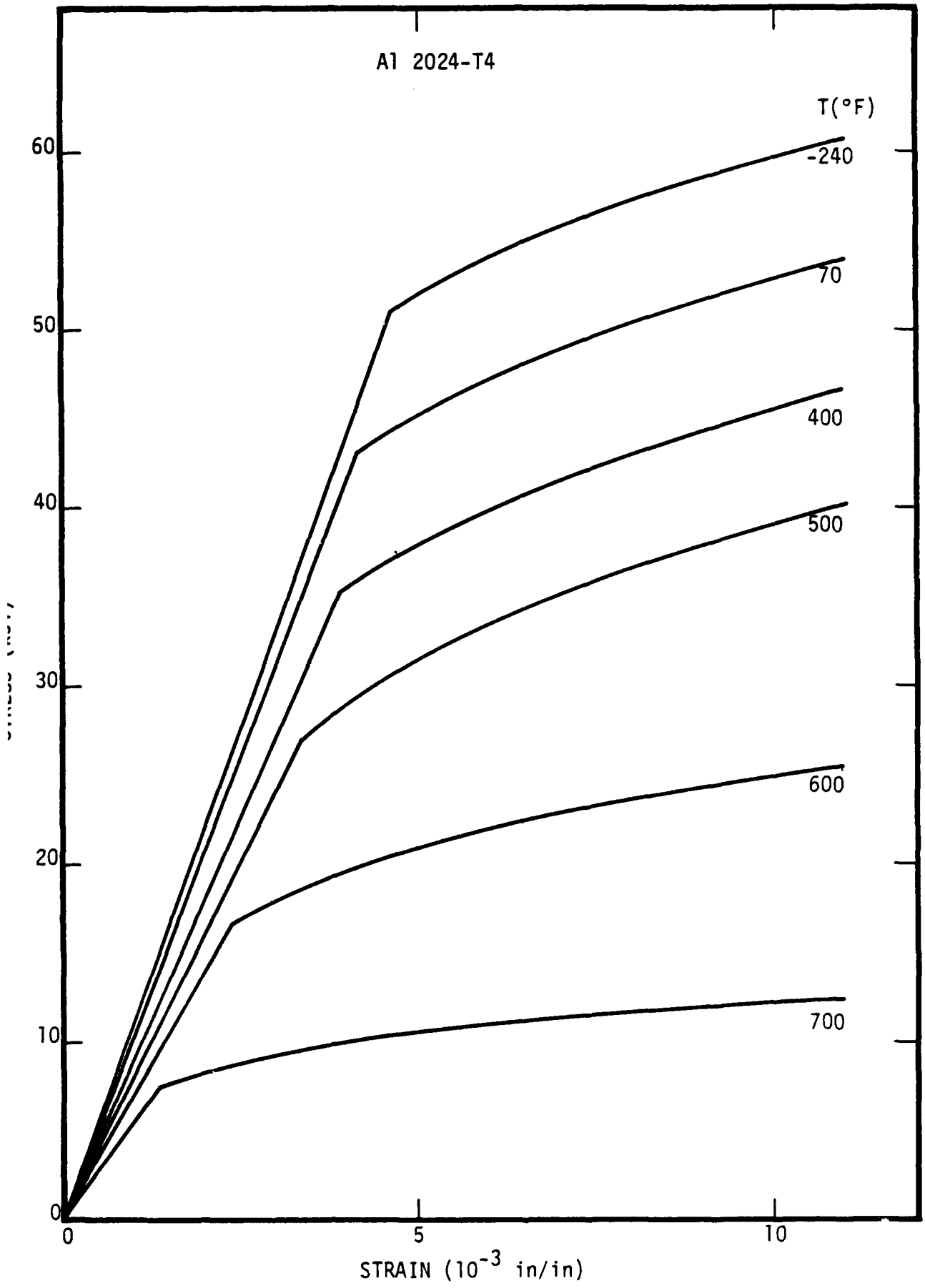

Figure A.4. Yield stress model for 2024 aluminum in the T4 temper.

(This Page Left Blank)

APPENDIX B
LAMINATE CODE

A description is given here of the code constructed at S-CUBED for calculating the thermoelastic properties of a cross-plied laminate whose individual plies may be anisotropic-transversely isotropic. The input properties may be either the overall elastic constants and thermal expansion coefficients of each type of ply (up to three types oriented in three different directions) or the corresponding quantities for the fiber and matrix constituents in each type of ply.

The required input deck is described in Section B1, a sample output is given in Section B2, and a FORTRAN listing of the code constitutes Section B3 below.

B.1 INPUT DATA DECK

Any consistent set of units may be used for the input parameters; the corresponding output will be in the same units.

Card No.	Format	Columns	Input Parameter	Description
1	I10	1-10	NPROB	Number of calculations
2	20A4	1-80	HEADER	User's problem description
3	8E10.0	1-10	VFRAC(J)	Volume fraction of first type of ply
		11-20	ANGLE(J)	Orientation of first type of ply with respect to laminate z-axis (degrees) (See discussion below).

Card No.	Format	Columns	Input Parameter	Description
		21-30	TYPE(J)	Type of input to follow. If TYPE>0 input for the individual fiber and matrix components is expected (2 additional cards) If TYPE<=0, input of overall ply properties is required (1 additional card).
3A	8E10.0	Ply properties		Card 3A is required if ply properties VFRAC>0 and TYPE<=0. Otherwise omit.
		1-10	ET(J)	Transverse elastic modulus for first type of ply
		11-20	EA(J)	Axial elastic modulus.
		21-30	NUTT(J)	Poisson's ratio: transverse contraction, transverse stress.
		31-40	NUTA(J)	Poisson's ratio: transverse contraction, axial stress.
		41-50	GA(J)	Inplane shear modulus
		51-60	ALFT(J)	Transverse linear coefficient of thermal expansion
		61-70	ALFA(J)	Axial linear coefficient of thermal expansion.
3B	8E10.0	Fiber Properties		Cards 3B and 3C are required if VFRAC>0 and TYPE>0. Otherwise omit.

Card No.	Format	Columns	Input Parameter	Description
		1-10	ETF(J)	Transverse elastic modulus of fiber in first ply.
		11-20	EAF(J)	Axial elastic modulus of fiber.
		21-30	NUTTF(J)	Transverse-transverse Poisson's ratio.
		31-40	NUTAF(J)	Poisson's ratio: transverse contraction, axial stress.
		41-50	GAF(J)	Transverse-axial shear modulus for fiber.
		51-60	ALFTF(J)	Transverse linear coefficient of thermal expansion.
		61-70	ALFAF(J)	Axial linear coefficient of thermal expansion.
		71-80	VF(J)	Fiber volume fraction in first type of ply.
3C	8E10.0		Matrix	Identical to Card 3B, except that the properties correspond to the matrix material in ply J.

The sets of data cards 2, 3, ... 3C are repeated as many times as specified on Card 1. For each set of data, Card 3 must appear three times, once for each of three different orientations of plies. However, if VFRAC is set to zero on Card 3, no further data for that type of ply is required.

If the orientation ANGLE(J) is set to 0.0 on all three of Cards 3, the code will run a series of calculations for orientations

+θ, -θ, 0.0 degrees of the three ply types, for increments in θ of 5 degrees from 0.0 degrees to 90 degrees. Otherwise the code will do one calculation of laminate properties for the ply orientations specified.

B.2 SAMPLE OUTPUT

A sample output is given below for the case of a laminate of SiC/Al plies, and in this case properties of the fiber and matrix constituents were input for each type of ply.

The first section of output is a printing of the user-supplied header followed by a reiteration of the input properties (fiber and matrix for each ply type in this case). The properties as calculated with the PRUFC code (ply coordinate system) are then given for the three ply types, and the stiffness coefficients and stress-temperature coupling coefficients are also printed.

The main output is then begun. In this example, the orientation angles ANGLE(J), J=1,2,3, were set to zero, so a series of output results at +θ, -θ, 0.0 degrees are printed, only one of which is included here for the +35, -35, 0.0 degree case corresponding to input volume fractions of 0.25, 0.25, and 0.50 respectively. The stiffness and compliance coefficients are listed followed by the thermal expansion coefficients. Finally the intraply stress-temperature derivatives (N.I. printed in this case) are given in both the laminate and ply coordinate systems.

The final bit of output is a summary for each of the orientations (5 degree increments) of the engineering elastic constants and thermal expansion coefficients for the laminate.

```
SIC/AL LAMINATE   MSI   DEG-F     ELASTIC MATRIX


CONSTITUENT INPUT PROPERTIES OF PLY 1     VOL FRAC= .25000   AT    .00 DEG TO LAMINATE Z-AXIS

FIBER PROPERTIES     VOL FRAC= .45000

ELASTIC MODULUS TRANSVERSE=  .5848D+02     AXIAL=  .6328D+02     AXIAL SHEAR MODULUS=  .2352D+02
POISSONS RATIO NUTT  .23700000     NUTA=  .26000000          THERM  EXP TRANSVERSE=  .2420D-05     AXIAL=  .2420D-05

MATRIX PROPERTIES     VOL FRAC= .55000

ELASTIC MODULUS TRANSVERSE=  .1000D+02     AXIAL=  .1000D+02     AXIAL SHEAR MODULUS=  .3759D+01
POISSONS RATIO NUTT  .33000000     NUTA=  .33000000          THERM  EXP TRANSVERSE=  .1310D-04     AXIAL=  .1310D-04


CONSTITUENT INPUT PROPERTIES OF PLY 2     VOL FRAC= .25000   AT    .00 DEG TO LAMINATE Z-AXIS

FIBER PROPERTIES     VOL FRAC= .45000

ELASTIC MODULUS TRANSVERSE=  .5848D+02     AXIAL=  .6328D+02     AXIAL SHEAR MODULUS=  .2352D+02
POISSONS RATIO NUTT  .23700000     NUTA=  .26000000          THERM  EXP TRANSVERSE=  .2420D-05     AXIAL=  .2420D-05

MATRIX PROPERTIES     VOL FRAC= .55000

ELASTIC MODULUS TRANSVERSE=  .1000D+02     AXIAL=  .1000D+02     AXIAL SHEAR MODULUS=  .3759D+01
POISSONS RATIO NUTT  .33000000     NUTA=  .33000000          THERM  EXP TRANSVERSE=  .1310D-04     AXIAL=  .1310D-04


CONSTITUENT INPUT PROPERTIES OF PLY 3     VOL FRAC= .50000   AT    .00 DEG TO LAMINATE Z-AXIS

FIBER PROPERTIES     VOL FRAC= .45000

ELASTIC MODULUS TRANSVERSE=  .5848D+02     AXIAL=  .6328D+02     AXIAL SHEAR MODULUS=  .2352D+02
POISSONS RATIO NUTT  .23700000     NUTA=  .26000000          THERM  EXP TRANSVERSE=  .2420D-05     AXIAL=  .2420D-05

MATRIX PROPERTIES     VOL FRAC= .55000

ELASTIC MODULUS TRANSVERSE=  .1000D+02     AXIAL=  .1000D+02     AXIAL SHEAR MODULUS=  .3759D+01
POISSONS RATIO NUTT  .33000000     NUTA=  .33000000          THERM  EXP TRANSVERSE=  .1310D-04     AXIAL=  .1310D-04
```

PROPERTIES OF PLY 1 AS CALCULATED WITH PRUFC

ET=	.17104+02	EA=	.33991+02	NUTT=	.43445	NUTA=	.29477
GAT=	.73956+01	GTT=	.59619+01	ALFT=	.89393-05	ALFA=	.42390-05

PROPERTIES OF PLY 2 AS CALCULATED WITH PRUFC

ET=	.17104+02	EA=	.33991+02	NUTT=	.43445	NUTA=	.29477
GAT=	.73956+01	GTT=	.59619+01	ALFT=	.89393-05	ALFA=	.42390-05

PROPERTIES OF PLY 3 AS CALCULATED WITH PRUFC

ET=	.17104+02	EA=	.33991+02	NUTT=	.43445	NUTA=	.29477
GAT=	.73956+01	GTT=	.59619+01	ALFT=	.89393-05	ALFA=	.42390-05

STIFFNESS COEFFICIENTS OF PLY 1

C11=	.23849+02	C12=	.11926+02	C13=	.10545+02	C33=	.40238+02
C44=	.73956+01	C66=	.59619+01	GAMMA1=	.36451-03	GAMMA3=	.35898-03

STIFFNESS COEFFICIENTS OF PLY 2

C11=	.23849+02	C12=	.11926+02	C13=	.10545+02	C33=	.40238+02
C44=	.73956+01	C66=	.59619+01	GAMMA1=	.36451-03	GAMMA3=	.35898-03

STIFFNESS COEFFICIENTS OF PLY 3

C11=	.23849+02	C12=	.11926+02	C13=	.10545+02	C33=	.40238+02
C44=	.73956+01	C66=	.59619+01	GAMMA1=	.36451-03	GAMMA3=	.35898-03

```
SIC/AL LAMINATE   MSI   DEG-F     ELASTIC MATRIX

**************************************************

PLIES AT +35.,-35., 0. DEG TO LAMINATE Z-AXIS

STIFFNESS COEFFICIENTS OF LAMINATE
     C11=  .23849+02     C12=  .11699+02     C13=  .10772+02     C14=  .00000
                         C22=  .25061+02     C23=  .12025+02     C24=  .00000
                                             C33=  .36038+02     C34=  .00000
                                                                 C44=  .88641+01
                         C55=  .71142+01     C56=  .00000        C66=  .61593+01

COMPLIANCE COEFFICIENTS FOR LAMINATE
     S11=  .57113-01     S12= -.21990-01     S13= -.97349-02     S14=  .00000
                         S22=  .55976-01     S23= -.12105-01     S24=  .00000
                                             S33=  .34698-01     S34=  .00000
                                                                 S44=  .28294-01
                         S55=  .35141-01     S56=  .00000        S66=  .40596-01

THERMAL EXPANSION COEFFICIENTS FOR LAMINATE
     ALF1=  .93192-05     ALF2=  .79810-05     ALF3=  .45376-05     ALF4=  .00000

PLY STRESS-TEMPERATURE DERIVATIVES (LAMINATE COORD SYSTEM)

     PLY 1     DSIGXXDT= -.72760-11     DSIGYYDT=  .15566-04     DSIGZZDT= -.55638-05     DSIGYZDT=  .40939-04
     PLY 2     DSIGXXDT= -.72760-11     DSIGYYDT=  .15566-04     DSIGZZDT= -.55638-05     DSIGYZDT= -.40939-04
     PLY 3     DSIGXXDT= -.72760-11     DSIGYYDT= -.15566-04     DSIGZZDT=  .55638-05     DSIGYZDT=  .00000

PLY STRESS-TEMPERATURE DERIVATIVES (PLY COORD SYSTEM)

     PLY 1     DSIGXXDT= -.72760-11     DSIGYYDT= -.29855-04     DSIGZZDT=  .39858-04     DSIGYZDT=  .23930-04
     PLY 2     DSIGXXDT= -.72760-11     DSIGYYDT= -.29855-04     DSIGZZDT=  .39858-04     DSIGYZDT= -.23930-04
     PLY 3     DSIGXXDT= -.72760-11     DSIGYYDT= -.15566-04     DSIGZZDT=  .55638-05     DSIGYZDT=  .00000

**************************************************
```

SIC/AL LAMINATE MSI DEG-F ELASTIC MATRIX

LAMINATE ENGINEERING ELASTIC CONSTANTS AND COEFFS OF THERMAL EXPANSION

PLY ANGLES	EX	EY	EZ	NUXZ	NUYZ	GYZ	ALFX	ALFY	ALFZ
• 0., 0., 0.	.17104•02	.17104•02	.33991•02	.29477•00	.29477•00	.73956•01	.89393-05	.89393-05	.42390-05
• 5., -5., 0.	.17113•02	.17103•02	.33846•02	.29379•00	.29729•00	.74457•01	.89482-05	.89216-05	.42413-05
•10.,-10., 0.	.17141•02	.17106•02	.33420•02	.29108•00	.30443•00	.75901•01	.89745-05	.88675-05	.42496-05
•15.,-15., 0.	.17186•02	.17125•02	.32747•02	.28724•00	.31492•00	.78114•01	.90179-05	.87748-05	.42670-05
•20.,-20., 0.	.17249•02	.17182•02	.31877•02	.28321•00	.32687•00	.80827•01	.90770-05	.86405-05	.42986-05
•25.,-25., 0.	.17326•02	.17304•02	.30881•02	.28008•00	.33797•00	.83715•01	.91497-05	.84623-05	.43507-05
•30.,-30., 0.	.17414•02	.17522•02	.29835•02	.27892•00	.34594•00	.86429•01	.92321-05	.82408-05	.44291-05
•35.,-35., 0.	.17509•02	.17865•02	.28820•02	.28056•00	.34886•00	.88641•01	.93192-05	.79810-05	.45376-05
•40.,-40., 0.	.17603•02	.18356•02	.27905•02	.28543•00	.34562•00	.90085•01	.94051-05	.76931-05	.46764-05
•45.,-45., 0.	.17690•02	.19006•02	.27137•02	.29346•00	.33605•00	.90587•01	.94837-05	.73921-05	.48408-05
•50.,-50., 0.	.17765•02	.19806•02	.26541•02	.30412•00	.32092•00	.90085•01	.95503-05	.70954-05	.50219-05
•55.,-55., 0.	.17823•02	.20728•02	.26118•02	.31658•00	.30171•00	.88641•01	.96023-05	.68191-05	.52080-05
•60.,-60., 0.	.17865•02	.21725•02	.25849•02	.32980•00	.28028•00	.86429•01	.96393-05	.65755-05	.53873-05
•65.,-65., 0.	.17893•02	.22734•02	.25701•02	.34278•00	.25859•00	.83715•01	.96632-05	.63716-05	.55497-05
•70.,-70., 0.	.17908•02	.23683•02	.25641•02	.35459•00	.23842•00	.80827•01	.96768-05	.62096-05	.56881-05
•75.,-75., 0.	.17916•02	.24505•02	.25633•02	.36450•00	.22125•00	.78114•01	.96834-05	.60884-05	.57979-05
•80.,-80., 0.	.17919•02	.25139•02	.25649•02	.37195•00	.20822•00	.75901•01	.96859-05	.60049-05	.58770-05
•85.,-85., 0.	.17919•02	.25539•02	.25668•02	.37657•00	.20010•00	.74457•01	.96865-05	.59564-05	.59246-05
•90.,-90., 0.	.17919•02	.25675•02	.25675•02	.37813•00	.19735•00	.73956•01	.96865-05	.59404-05	.59404-05

PLY ANGLES	GXZ	GXY
• 0., 0., 0.	.73956•01	.59619•01
• 5., -5., 0.	.73888•01	.59663•01
•10.,-10., 0.	.73689•01	.59794•01
•15.,-15., 0.	.73365•01	.60009•01
•20.,-20., 0.	.72930•01	.60303•01
•25.,-25., 0.	.72401•01	.60669•01
•30.,-30., 0.	.71798•01	.61100•01
•35.,-35., 0.	.71142•01	.61583•01
•40.,-40., 0.	.70456•01	.62106•01
•45.,-45., 0.	.69762•01	.62656•01
•50.,-50., 0.	.69082•01	.63215•01
•55.,-55., 0.	.68435•01	.63766•01
•60.,-60., 0.	.67838•01	.64293•01
•65.,-65., 0.	.67308•01	.64776•01
•70.,-70., 0.	.66857•01	.65199•01
•75.,-75., 0.	.66496•01	.65547•01
•80.,-80., 0.	.66232•01	.65805•01
•85.,-85., 0.	.66072•01	.65964•01
•90.,-90., 0.	.66018•01	.66018•01

FIN

B.3 CODE LISTING

A FORTRAN listing of the code is given below.

```
C     LAMINATE MAIN PROGRAM
      REAL N1,N2,N3,NUXZ,NUYZ,NUTT,NUTA,NUTTF,NUTAF,NUTTM,NUTAM
      DIMENSION S(6,6),SINV(6,6),AX(19),AY(19),AZ(19),GAA(19)
      DIMENSION HEADER(20), A(4), SIGDOT(4,3), PHI(3), SIGPLY(4,3)
      DIMENSION CIN(8,3),CPRIME(6,6),E1(19),E2(19),E3(19),NUXZ(19),
     .   NUYZ(19),GXY(19),GXZ(19),TYPE(3),COUM(8),GPRIME(4)
      COMMON/ONE/N1, N2, N3
      COMMON/TWO/C1(4,4), C2(4,4), C3(4,4)
      COMMON/THREE/GAMMA1(4), GAMMA2(4), GAMMA3(4)
      COMMON/FOUR/D1(2,2), D2(2,2), D3(2,2)
      COMMON/INPUT/VFRAC(3),ANGLE(3),ET(3),EA(3),NUTT(3),NUTA(3),GA(3),
     .ALFT(3),ALFA(3),ETF(3),EAF(3),NUTTF(3),NUTAF(3),GAF(3),ALFTF(3),
     .ALFAF(3),VF(3),ETM(3),EAM(3),NUTTM(3),NUTAM(3),GAM(3),ALFTM(3),
     .ALFAM(3),VM(3)
      DATA PI/3.1415927/
      READ(5,101) NPROB
      NNN=0
    1 CONTINUE
      READ(5,102) HEADER
      WRITE(6,100)
      WRITE(6,112) HEADER
      DO 11 J=1,3
      READ(5,103) VFRAC(J), ANGLE(J), TYPE(J)
      IF(VFRAC(J).LE.0.) GO TO 18
      IF(TYPE(J).GT.0.) GO TO 12
      READ(5,103) ET(J),EA(J),NUTT(J),NUTA(J),GA(J),ALFT(J),ALFA(J)
      WRITE(6,105) J, VFRAC(J), ANGLE(J)
      WRITE(6,106) ET(J), EA(J), GA(J)
      WRITE(6,107) NUTT(J), NUTA(J), ALFT(J), ALFA(J)
      GO TO 11
   18 DO 19 K=1,8
   19 CIN(K,J)=0.
      GO TO 11
   12 READ(5,103) ETF(J),EAF(J),NUTTF(J),NUTAF(J),GAF(J),ALFTF(J),ALFAF(
     .J),VF(J)
      READ(5,103) ETM(J),EAM(J),NUTTM(J),NUTAM(J),GAM(J),ALFTM(J),ALFAM(
     .J),VM(J)
      WRITE(6,108) J, VFRAC(J), ANGLE(J)
      WRITE(6,109) VF(J)
      WRITE(6,106) ETF(J), EAF(J), GAF(J)
      WRITE(6,107) NUTTF(J), NUTAF(J), ALFTF(J), ALFAF(J)
      WRITE(6,110) VM(J)
      WRITE(6,106) ETM(J), EAM(J), GAM(J)
      WRITE(6,107) NUTTM(J), NUTAM(J), ALFTM(J), ALFAM(J)
   11 CONTINUE
      N1=VFRAC(1)
      N2=VFRAC(2)
      N3=VFRAC(3)
      DO 13 J=1,3
      IF(VFRAC(J).LE.0.) GO TO 13
      IF(TYPE(J).LE.0.) GO TO 13
      CALL PRUFC(J,CIN)
   13 CONTINUE
      DO 14 J=1,3
      IF(VFRAC(J).LE.0.) GO TO 14
      IF(TYPE(J).GT.0.) GO TO 14
      CALL CCOEF(J,CIN)
   14 CONTINUE
      DO 22 J=1,3
      WRITE(6,115) J
      WRITE(6,116) (CIN(I,J),I=1,4)
   22 WRITE(6,117) (CIN(I,J),I=5,8)
      WRITE(6,100)
      WRITE(6,112) HEADER
      WRITE(6,132)
      ANGL=-5.
      KMAX=19
      IF((ABS(ANGLE(1))+ABS(ANGLE(2))+ABS(ANGLE(3))).GT.0.) KMAX=1
      DO 10 KK=1,KMAX
      ANGL=ANGL + 5.
      IF(KMAX.EQ.1) ANGL=ANGLE(1)
      THETA=ANGL*PI/180.
      DO 15 K=1,8
   15 COUM(K)=CIN(K,1)
      CALL CROT(CPRIME,GPRIME,COUM,THETA)
      DO 20 J=1,4
      DO 20 I=1,4
   20 C1(I,J)=CPRIME(I,J)
      DO 21 J=1,4
```

```
      21 GAMMA1(J)=GPRIME(J)
         DO 23 J=1,2
         DO 23 I=1,2
      23 D1(I,J)=CPRIME(I+4,J+4)
         THETA= - THETA
         IF(KMAX.EQ.1) THETA=ANGLE(2)*PI/180.
         DO 16 K=1,8
      16 COUM(K)=CIN(K,2)
         CALL CROT(CPRIME,GPRIME,COUM,THETA)
         DO 30 J=1,4
         DO 30 I=1,4
      30 C2(I,J)=CPRIME(I,J)
         DO 31 J=1,4
      31 GAMMA2(J)=GPRIME(J)
         DO 24 J=1,2
         DO 24 I=1,2
      24 D2(I,J)=CPRIME(I+4,J+4)
         THETA=0.
         IF(KMAX.EQ.1) THETA=ANGLE(3)*PI/180.
         DO 17 K=1,8
      17 COUM(K)=CIN(K,3)
         CALL CROT(CPRIME,GPRIME,COUM,THETA)
         DO 40 J=1,4
         DO 40 I=1,4
      40 C3(I,J)=CPRIME(I,J)
         DO 41 J=1,4
      41 GAMMA3(J)=GPRIME(J)
         DO 25 J=1,2
         DO 25 I=1,2
      25 D3(I,J)=CPRIME(I+4,J+4)
         CALL EX(S11,S21,S31,S41)
         CALL EY(S12,S22,S32,S42)
         CALL EZ(S13,S23,S33,S43)
         CALL GYZ(S14,S24,S34,S44)
         CALL GXZXY(S55,S56,S65,S66)
         DO 26 J=1,6
         DO 26 I=1,6
      26 S(I,J)=0.
         S(1,1)=S11
         S(1,2)=S12
         S(1,3)=S13
         S(1,4)=2.*S14
         S(2,1)=S21
         S(2,2)=S22
         S(2,3)=S23
         S(2,4)=2.*S24
         S(3,1)=S31
         S(3,2)=S32
         S(3,3)=S33
         S(3,4)=2.*S34
         S(4,1)=S41
         S(4,2)=S42
         S(4,3)=S43
         S(4,4)=2.*S44
```

```
134*            S(5,5)=S55*2.
135*            S(5,6)=S56*2.
136*            S(6,5)=S65*2.
137*            S(6,6)=S66*2.
138*            CALL INVRS(6,S,SINV)
139*            CALL THERML(A,SIGDOT)
140*            AX(KK)=A(1)
141*            AY(KK)=A(2)
142*            AZ(KK)=A(3)
143*            E1(KK)=1./S11
144*            E2(KK)=1./S22
145*            E3(KK)=1./S33
146*            NUXZ(KK)= - S13*E3(KK)
147*            NUYZ(KK)= - S23*E3(KK)
148*            GAA(KK)=.5*SINV(4,4)
149*            GXZ(KK)=.5*SINV(5,5)
150*            GXY(KK)=.5*SINV(6,6)
151*            ANGL2= - ANGL
152*            ANGL3=0.
153*            IF(KMAX.NE.1) GO TO 51
154*            ANGL2=ANGLE(2)
155*            ANGL3=ANGLE(3)
156*         51 CONTINUE
157*            WRITE(6,111) ANGL, ANGL2, ANGL3
158*            WRITE(6,118)
159*            WRITE(6,119) SINV(1,1),SINV(1,2),SINV(1,3),SINV(4,1)
160*            WRITE(6,121) SINV(2,2),SINV(2,3),SINV(4,2)
161*            WRITE(6,122) SINV(3,3),SINV(4,3)
162*            XX=.5*SINV(4,4)
163*            XY=.5*SINV(5,5)
164*            XYY=.5*SINV(5,6)
165*            XXY=.5*SINV(6,6)
166*            WRITE(6,123) XX
167*            WRITE(6,137) XY, XYY, XXY
168*            WRITE(6,124)
169*            WRITE(6,125) S11,S12,S13,S14
170*            WRITE(6,126) S22,S23,S24
171*            WRITE(6,127) S33,S34
172*            WRITE(6,128) S44
173*            WRITE(6,138) S55,S56,S66
174*            WRITE(6,129)
175*            WRITE(6,131) A
176*            WRITE(6,135)
177*            DO 42 J=1,3
178*            IF(SIGDOT(4,J).NE.0.) GO TO 43
179*            GO TO 42
180*         43 DO 44 I=1,3
181*         44 IF(ABS(SIGDOT(I,J)/SIGDOT(4,J)).LT.1.E-07) SIGDOT(I,J)=0.
182*         42 CONTINUE
183*            PHI(1)=ANGL*PI/180.
184*            PHI(2)=ANGL2*PI/180.
185*            PHI(3)=ANGL3*PI/180.
186*            DO 62 J=1,3
187*            SI=SIN(PHI(J))
```

```
188*          CO=COS(PHI(J))
189*          SI2=SI**2
190*          CO2=1. - SI2
191*          SIGPLY(1,J)=SIGDOT(1,J)
192*          SIGPLY(2,J)=SIGDOT(2,J)*CO2 - 2.*SIGDOT(4,J)*SI*CO + SIGDOT(3,J)
193*         .   *SI2
194*          SIGPLY(3,J)=SIGDOT(2,J)*SI2  2.*SIGDOT(4,J)*SI*CO + SIGDOT(3,J)
195*         .   *CO2
196*          SIGPLY(4,J)=SIGDOT(2,J)*SI*CO + SIGDOT(4,J)*(CO2 - SI2)
197*         .   - SIGDOT(3,J)*SI*CO
198*       62 CONTINUE
199*          DO 60 J=1,3
200*       60 WRITE(6,136) J, (SIGDOT(I,J),I=1,4)
201*          WRITE(6,141)
202*          DO 61 J=1,3
203*       61 WRITE(6,136) J, (SIGPLY(I,J),I=1,4)
204*          WRITE(6,132)
205*       10 CONTINUE
206*          WRITE(6,100)
207*          WRITE(6,112) HEADER
208*          WRITE(6,133)
209*          WRITE(6,134)
210*          ANGL=-5.
211*          DO 50 I=1,KMAX
212*          ANGL=ANGL + 5.
213*          ANGL2= - ANGL
214*          ANGL3=0.
215*          IF(KMAX.NE.1) GO TO 52
216*          ANGL=ANGLE(1)
217*          ANGL2=ANGLE(2)
218*          ANGL3=ANGLE(3)
219*       52 CONTINUE
220*       50 WRITE(6,130) ANGL,ANGL2,ANGL3,E1(I),E2(I),E3(I),NUXZ(I),NUYZ(I),
221*         .   GAA(I),AX(I),AY(I),AZ(I)
222*          WRITE(6,139)
223*          ANGL=-5.
224*          DO 27 I=1,KMAX
225*          ANGL=ANGL + 5.
226*          ANGL2= - ANGL
227*          ANGL3=0.
228*          IF(KMAX.NE.1) GO TO 53
229*          ANGL=ANGLE(1)
230*          ANGL2=ANGLE(2)
231*          ANGL3=ANGLE(3)
232*       53 CONTINUE
233*       27 WRITE(6,140) ANGL,ANGL2,ANGL3,GXZ(I),GXY(I)
234*          NNN=NNN + 1
235*          IF(NNN.LT.NPROB) GO TO 1
236*          STOP
237*      100 FORMAT(1H1)
238*      101 FORMAT(I10)
239*      102 FORMAT(20A4)
240*      103 FORMAT(8E10.0)
241*      104 FORMAT(1H ,20A4,//)
```

```
      105 FORMAT(///,' INPUT PROPERTIES OF PLY',I2,'     VOL FRAC=',F7.5,'
     . AT',F7.2,' DEG TO LAMINATE Z - AXIS',/)
      106 FORMAT(' ELASTIC MODULUS TRANSVERSE=',E11.5,'     AXIAL=',E11.5,'
     .    AXIAL SHEAR MODULUS=',E11.5)
      107 FORMAT(' POISSONS RATIO NUTT',F11.8,'     NUTA=',F11.8,10X,'THERM
     . EXP TRANSVERSE=',E11.5,5X,'AXIAL=',E11.5)
      108 FORMAT(///,' CONSTITUENT INPUT PROPERTIES OF PLY',I2,5X,'VOL FRAC=
     .',F7.5,'   AT',F7.2,' DEG TO LAMINATE Z-AXIS')
      109 FORMAT(/,' FIBER PROPERTIES',5X,'VOL FRAC=',F7.5,/)
      110 FORMAT(/,' MATRIX PROPERTIES',5X,'VOL FRAC=',F7.5,/)
      111 FORMAT(' PLIES AT +',F3.0,',',F4.0,',',F3.0,' DEG TO LAMINATE Z-AX
     .IS',/)
      112 FORMAT(1H ,20A4)
      113 FORMAT(/,1H ,4E16.8)
      114 FORMAT(1H ,8E14.5)
      115 FORMAT(/,' STIFFNESS COEFFICIENTS OF PLY',I2)
      116 FORMAT(1H ,5X,'C11=',E11.5,5X,'C12=',E11.5,5X,'C13=',E11.5,5X,'C33
     .=',E11.5)
      117 FORMAT(1H ,5X,'C44=',E11.5,5X,'C66=',E11.5,5X,'GAMMA1=',E11.5,5X,'
     .GAMMA3=',E11.5)
      118 FORMAT(' STIFFNESS COEFFICIENTS OF LAMINATE')
      119 FORMAT(1H ,5X,'C11=',E11.5,5X,'C12=',E11.5,5X,'C13=',E11.5,5X,'C14
     .=',E11.5)
      121 FORMAT(1H ,25X,'C22=',E11.5,5X,'C23=',E11.5,5X,'C24=',E11.5)
      122 FORMAT(1H ,45X,'C33=',E11.5,5X,'C34=',E11.5)
      123 FORMAT(1H ,65X,'C44=',E11.5)
      124 FORMAT(/,' COMPLIANCE COEFFICIENTS FOR LAMINATE')
      125 FORMAT(1H ,5X,'S11=',E11.5,5X,'S12=',E11.5,5X,'S13=',E11.5,5X,'S14
     .=',E11.5)
      126 FORMAT(1H ,25X,'S22=',E11.5,5X,'S23=',E11.5,5X,'S24=',E11.5)
      127 FORMAT(1H ,45X,'S33=',E11.5,5X,'S34=',E11.5)
      128 FORMAT(1H ,65X,'S44=',E11.5)
      129 FORMAT(/,' THERMAL EXPANSION COEFFICIENTS FOR LAMINATE')
      131 FORMAT(1H ,5X,'ALF1=',E11.5,5X,'ALF2=',E11.5,5X,'ALF3=',E11.5,5X,'
     .ALF4=',E11.5)
      120 FORMAT(1H ,4E16.8)
      130 FORMAT(' +',F3.0,',',F4.0,',',F3.0,9E12.5)
      132 FORMAT(/,' **************************************************',/)
      133 FORMAT(//,' LAMINATE ENGINEERING ELASTIC CONSTANTS AND COEFFS OF T
     .HERMAL EXPANSION')
      134 FORMAT(/,'   PLY ANGLES ',5X,'EX',10X,'EY',10X,'EZ',9X,'NUXZ',8X,'
     .NUYZ',9X,'GYZ',8X,'ALFX',8X,'ALFY',8X,'ALFZ',/)
      135 FORMAT(/,' PLY STRESS-TEMPERATURE DERIVATIVES (LAMINATE COORD SYST
     .EM)',/)
      136 FORMAT(1H ,5X,'PLY',I2,5X,'DSIGXXDT=',E11.5,5X,'DSIGYYDT=',E11.5,5
     .X,'DSIGZZDT=',E11.5,5X,'DSIGYZDT=',E11.5)
      137 FORMAT(1H ,25X,'C55=',E11.5,5X,'C56=',E11.5,5X,'C66=',E11.5)
      138 FORMAT(1H ,25X,'S55=',E11.5,5X,'S56=',E11.5,5X,'S66=',E11.5)
      140 FORMAT(' +',F3.0,',',F4.0,',',F3.0,2E12.5)
      139 FORMAT(/,'   PLY ANGLES ',5X,'GXZ',9X,'GXY',/)
      141 FORMAT(/,' PLY STRESS-TEMPERATURE DERIVATIVES (PLY COORD SYSTEM)',
     ,/)
          END
```

```
      SUBROUTINE CCOEF(J,CIN)
      REAL NUTT,NUTA,NUAT,NUTTF,NUTAF,NUTTM,NUTAM
      DIMENSION CIN(8,3)
      COMMON/INPUT/VFRAC(3),ANGLE(3),ET(3),EA(3),NUTT(3),NUTA(3),GA(3),
     .ALFT(3),ALFA(3),ETF(3),EAF(3),NUTTF(3),NUTAF(3),GAF(3),ALFTF(3),
     .ALFAF(3),VF(3),ETM(3),EAM(3),NUTTM(3),NUTAM(3),GAM(3),ALFTM(3),
     .ALFAM(3),VM(3)
      NUAT=ET(J)*NUTA(J)/EA(J)
      DELTA=1. - NUTT(J)**2 - 2.*NUTA(J)*NUAT - 2.*NUTT(J)*NUTA(J)*NUAT
      CIN(1,J)=ET(J)*(1. - NUTA(J)*NUAT)/DELTA
      CIN(2,J)=ET(J)*(NUTT(J) + NUTA(J)*NUAT)/DELTA
      CIN(3,J)=ET(J)*(1. + NUTT(J))*NUTA(J)/DELTA
      CIN(4,J)=EA(J)*(1. - NUTT(J)**2)/DELTA
      CIN(5,J)=GA(J)
      CIN(6,J)=.5*(CIN(1,J) - CIN(2,J))
      CIN(7,J)=(CIN(1,J) + CIN(2,J))*ALFT(J) + CIN(3,J)*ALFA(J)
      CIN(8,J)=2.*CIN(3,J)*ALFT(J) + CIN(4,J)*ALFA(J)
      RETURN
      END

END OF COMPILATION:        NO  DIAGNOSTICS.
```

```
      SUBROUTINE CROT(CPRIME,GPRIME,CIN,THETA)
C     SEE MEMO 13 OCT 82 RICE TO GURTMAN
C     COMPUTES CPRIME(I,J) ELASTIC CONSTANTS IN ROTATED COORD SYSTEM
C     FROM THE CIN ELASTIC CONSTANTS IN THE FIBER SYSTEM
C     CIN(1)=C11,  CIN(2)=C12,  CIN(3),C13,  CIN(4)=C33,  CIN(5)=C44,
C     CIN(6)=C66 = .5*(C11 - C12) IF MATERIAL IS TRANSVERSELY ISOTROPIC
C     COORD SYSTEM ROTATED BY ANGLE THETA ABOUT THE X(=1) AXIS,  WHERE
C     THE FIBER DIRECTION IS THE OLD Z(=3) AXIS
C     CIN(7) = GAMAX,   CIN(8) = GAMAZ
      DIMENSION CPRIME(6,6), CIN(8), GPRIME(4)
      X=SIN(THETA)
      Y=COS(THETA)
      X2=X**2
      Y2=Y**2
      X4=X2*X2
      Y4=Y2*Y2
      X3=X2*X
      Y3=Y2*Y
      CPRIME(1,1)=CIN(1)
      CPRIME(1,2)=Y2*CIN(2) + X2*CIN(3)
      CPRIME(1,3)=X2*CIN(2) + Y2*CIN(3)
      CPRIME(1,4)=X*Y*(CIN(3) - CIN(2))
      CPRIME(1,5)=0.
      CPRIME(1,6)=0.
      CPRIME(2,1)=CPRIME(1,2)
      CPRIME(2,2)=Y4*CIN(1) + X4*CIN(4) + 2.*X2*Y2*CIN(3)
     .   + 4.*X2*Y2*CIN(5)
      CPRIME(2,3)=X2*Y2*(CIN(1) + CIN(4)) + (X4 + Y4)*CIN(3)
     .   - 4.*X2*Y2*CIN(5)
      CPRIME(2,4)= - X*Y3*CIN(1) + (X*Y3 - X3*Y)*CIN(3) + X3*Y*CIN(4)
     .   + 2.*(X*Y3 - X3*Y)*CIN(5)
      CPRIME(2,5)=0.
      CPRIME(2,6)=0.
      CPRIME(3,1)=CPRIME(1,3)
      CPRIME(3,2)=CPRIME(2,3)
      CPRIME(3,3)=Y4*CIN(4) + X4*CIN(1) + 2.*X2*Y2*CIN(3) + 4.*X2*Y2
     .   *CIN(5)
      CPRIME(3,4)= - X3*Y*CIN(1) + X*Y3*CIN(4) + (X3*Y - X*Y3)*CIN(3)
     .   + 2.*(X3*Y - X*Y3)*CIN(5)
      CPRIME(3,5)=0.
      CPRIME(3,6)=0.
      CPRIME(4,1)=CPRIME(1,4)
      CPRIME(4,2)=CPRIME(2,4)
      CPRIME(4,3)=CPRIME(3,4)
      CPRIME(4,4)=X2*Y2*(CIN(1) + CIN(4)) - 2.*X2*Y2*CIN(3)
     .   + ((Y2 - X2)**2)*CIN(5)
      CPRIME(4,5)=0.
      CPRIME(4,6)=0.
      CPRIME(5,1)=0.
      CPRIME(5,2)=0.
      CPRIME(5,3)=0.
      CPRIME(5,4)=0.
      CPRIME(5,5)=Y2*CIN(5) + X2*CIN(6)
      CPRIME(5,6)=X*Y*(CIN(5) - CIN(6))
      CPRIME(6,1)=0.
      CPRIME(6,2)=0.
      CPRIME(6,3)=0.
      CPRIME(6,4)=0.
      CPRIME(6,5)=CPRIME(5,6)
      CPRIME(6,6)=Y2*CIN(6) + X2*CIN(5)
      GPRIME(1)=CIN(7)
      GPRIME(2)=Y2*CIN(7) + X2*CIN(8)
      GPRIME(3)=X2*CIN(7) + Y2*CIN(8)
      GPRIME(4)=(CIN(8) - CIN(7))*X*Y
      RETURN
      END

END OF COMPILATION:        NO  DIAGNOSTICS.
```

```
      SUBROUTINE EX(S11,S21,S31,S41)
      DIMENSION X(6)
      REAL N1, N2, N3, K
      COMMON/ONE/N1, N2, N3
      COMMON/TWO/C1(4,4), C2(4,4), C3(4,4)
      COMMON/COEF/K(6,7)
      K(1,1)=C1(1,1)
      K(1,2)=0.
      K(1,3)=0.
      K(1,4)=C1(1,2)
      K(1,5)=C1(1,3)
      K(1,6)=2.*C1(1,4)
      K(1,7)=1.
      K(2,1)=0.
      K(2,2)=C2(1,1)
      K(2,3)=0.
      K(2,4)=C2(1,2)
      K(2,5)=C2(1,3)
      K(2,6)=2.*C2(1,4)
      K(2,7)=1.
      K(3,1)=0.
      K(3,2)=0.
      K(3,3)=C3(1,1)
      K(3,4)=C3(1,2)
      K(3,5)=C3(1,3)
      K(3,6)=2.*C3(1,4)
      K(3,7)=1.
      K(4,1)=N1*C1(1,2)
      K(4,2)=N2*C2(1,2)
      K(4,3)=N3*C3(1,2)
      K(4,4)=N1*C1(2,2) + N2*C2(2,2) + N3*C3(2,2)
      K(4,5)=N1*C1(2,3) + N2*C2(2,3) + N3*C3(2,3)
      K(4,6)=2.*(N1*C1(2,4) + N2*C2(2,4) + N3*C3(2,4))
      K(4,7)=0.
      K(5,1)=N1*C1(1,3)
      K(5,2)=N2*C2(1,3)
      K(5,3)=N3*C3(1,3)
      K(5,4)=N1*C1(2,3) + N2*C2(2,3) + N3*C3(2,3)
      K(5,5)=N1*C1(3,3) + N2*C2(3,3) + N3*C3(3,3)
      K(5,6)=2.*(N1*C1(3,4) + N2*C2(3,4) + N3*C3(3,4))
      K(5,7)=0.
      K(6,1)=N1*C1(1,4)
      K(6,2)=N2*C2(1,4)
      K(6,3)=N3*C3(1,4)
      K(6,4)=N1*C1(2,4) + N2*C2(2,4) + N3*C3(2,4)
      K(6,5)=N1*C1(3,4) + N2*C2(3,4) + N3*C3(3,4)
      K(6,6)=2.*(N1*C1(4,4) + N2*C2(4,4) + N3*C3(4,4))
      K(6,7)=0.
      CALL ROOT(6,X)
      EPSX=N1*X(1) + N2*X(2) + N3*X(3)
      S11=EPSX
      S21=X(4)
      S31=X(5)
      S41=X(6)
      RETURN
      END

END OF COMPILATION:        NO  DIAGNOSTICS.
```

```
      SUBROUTINE EY(S12,S22,S32,S42)
      DIMENSION X(6)
      REAL N1, N2, N3, K
      COMMON/ONE/N1, N2, N3
      COMMON/TWO/C1(4,4), C2(4,4), C3(4,4)
      COMMON/COEF/K(6,7)
      K(1,1)=C1(1,1)
      K(1,2)=0.
      K(1,3)=0.
      K(1,4)=C1(1,3)
      K(1,5)=2.*C1(1,4)
      K(1,6)= - C1(1,2)
      K(2,1)=0.
      K(2,2)=C2(1,1)
      K(2,3)=0.
      K(2,4)=C2(1,3)
      K(2,5)=2.*C2(1,4)
      K(2,6)= - C2(1,2)
      K(3,1)=0.
      K(3,2)=0.
      K(3,3)=C3(1,1)
      K(3,4)=C3(1,3)
      K(3,5)=2.*C3(1,4)
      K(3,6)= - C3(1,2)
      K(4,1)=N1*C1(1,3)
      K(4,2)=N2*C2(1,3)
      K(4,3)=N3*C3(1,3)
      K(4,4)=N1*C1(3,3) + N2*C2(3,3) + N3*C3(3,3)
      K(4,5)=2.*(N1*C1(3,4) + N2*C2(3,4) + N3*C3(3,4))
      K(4,6)= - (N1*C1(2,3) + N2*C2(2,3) + N3*C3(2,3))
      K(5,1)=N1*C1(1,4)
      K(5,2)=N2*C2(1,4)
      K(5,3)=N3*C3(1,4)
      K(5,4)=N1*C1(3,4) + N2*C2(3,4) + N3*C3(3,4)
      K(5,5)= 2.*(N1*C1(4,4) + N2*C2(4,4) + N3*C3(4,4))
      K(5,6)= - (N1*C1(2,4) + N2*C2(2,4) + N3*C3(2,4))
      CALL ROOT(5,X)
      SIGY1=C1(1,2)*X(1) + C1(2,2) + C1(2,3)*X(4) + 2.*C1(2,4)*X(5)
      SIGY2=C2(1,2)*X(2) + C2(2,2) + C2(2,3)*X(4) + 2.*C2(2,4)*X(5)
      SIGY3=C3(1,2)*X(3) + C3(2,2) + C3(2,3)*X(4) + 2.*C3(2,4)*X(5)
      SIGY=N1*SIGY1 + N2*SIGY2 + N3*SIGY3
      EPSX=N1*X(1) + N2*X(2) + N3*X(3)
      S12=EPSX/SIGY
      S22=1./SIGY
      S32=X(4)/SIGY
      S42=X(5)/SIGY
      RETURN
      END

END OF COMPILATION:        NO  DIAGNOSTICS.
```

```
      SUBROUTINE EZ(S13,S23,S33,S43)
      DIMENSION X(6)
      REAL N1, N2, N3, K
      COMMON/ONE/N1, N2, N3
      COMMON/TWO/C1(4,4), C2(4,4), C3(4,4)
      COMMON/COEF/K(6,7)
      K(1,1)=C1(1,1)
      K(1,2)=0.
      K(1,3)=0.
      K(1,4)=C1(1,2)
      K(1,5)=2.*C1(1,4)
      K(1,6)= - C1(1,3)
      K(2,1)=0.
      K(2,2)=C2(1,1)
      K(2,3)=0.
      K(2,4)=C2(1,2)
      K(2,5)=2.*C2(1,4)
      K(2,6)= - C2(1,3)
      K(3,1)=0.
      K(3,2)=0.
      K(3,3)=C3(1,1)
      K(3,4)=C3(1,2)
      K(3,5)=2.*C3(1,4)
      K(3,6)= - C3(1,3)
      K(4,1)=N1*C1(1,2)
      K(4,2)=N2*C2(1,2)
      K(4,3)=N3*C3(1,2)
      K(4,4)=N1*C1(2,2) + N2*C2(2,2) + N3*C3(2,2)
      K(4,5)=2.*(N1*C1(2,4) + N2*C2(2,4) + N3*C3(2,4))
      K(4,6)= - (N1*C1(2,3) + N2*C2(2,3) + N3*C3(2,3))
      K(5,1)=N1*C1(1,4)
      K(5,2)=N2*C2(1,4)
      K(5,3)=N3*C3(1,4)
      K(5,4)=N1*C1(2,4) + N2*C2(2,4) + N3*C3(2,4)
      K(5,5)=2.*(N1*C1(4,4) + N2*C2(4,4) + N3*C3(4,4))
      K(5,6)= - (N1*C1(3,4) + N2*C2(3,4) + N3*C3(3,4))
      CALL ROOT(5,X)
      SIGZ1=C1(1,3)*X(1) + C1(2,3)*X(4) + C1(3,3) + 2.*C1(3,4)*X(5)
      SIGZ2=C2(1,3)*X(2) + C2(2,3)*X(4) + C2(3,3) + 2.*C2(3,4)*X(5)
      SIGZ3=C3(1,3)*X(3) + C3(2,3)*X(4) + C3(3,3) + 2.*C3(3,4)*X(5)
      SIGZ=N1*SIGZ1 + N2*SIGZ2 + N3*SIGZ3
      EPSX=N1*X(1) + N2*X(2) + N3*X(3)
      S13=EPSX/SIGZ
      S23=X(4)/SIGZ
      S33=1./SIGZ
      S43=X(5)/SIGZ
      RETURN
      END
```

END OF COMPILATION: NO DIAGNOSTICS.

```
 1*            SUBROUTINE GXZXY(S55,S56,S65,S66)
 2*            DIMENSION X(6)
 3*            REAL N1,N2,N3,K
 4*            COMMON/ONE/N1, N2, N3
 5*            COMMON/FOUR/D1(2,2), D2(2,2), D3(2,2)
 6*            COMMON/COEF/K(6,7)
 7*            DO 10 J=1,7
 8*            DO 10 I=1,6
 9*         10 K(I,J)=0.
10*            K(1,1)=D1(1,1)
11*            K(1,2)=D1(1,2)
12*            K(1,7)=.5
13*            K(2,3)=D2(1,1)
14*            K(2,4)=D2(1,2)
15*            K(2,7)=.5
16*            K(3,5)=D3(1,1)
17*            K(3,6)=D3(1,2)
18*            K(3,7)=.5
19*            K(4,1)=D1(1,2)
20*            K(4,2)=D1(2,2)
21*            K(5,3)=D2(1,2)
22*            K(5,4)=D2(2,2)
23*            K(6,5)=D3(1,2)
24*            K(6,6)=D3(2,2)
25*            CALL ROOT(6,X)
26*            EPS13=N1*X(1) + N2*X(3) + N3*X(5)
27*            EPS12=N1*X(2) + N2*X(4) + N3*X(6)
28*            S55=.5*EPS13
29*            S65=.5*EPS12
30*            K(1,7)=0.
31*            K(2,7)=0.
32*            K(3,7)=0.
33*            K(4,7)=.5
34*            K(5,7)=.5
35*            K(6,7)=.5
36*            CALL ROOT(6,X)
37*            EPS13=N1*X(1) + N2*X(3) + N3*X(5)
38*            EPS12=N1*X(2) + N2*X(4) + N3*X(6)
39*            S56=.5*EPS13
40*            S66=.5*EPS12
41*            RETURN
42*            END

END OF COMPILATION:        NO  DIAGNOSTICS.
```

```
      SUBROUTINE GYZ(S14,S24,S34,S44)
      DIMENSION X(6)
      REAL N1, N2, N3, K
      COMMON/ONE/N1, N2, N3
      COMMON/TWO/C1(4,4), C2(4,4), C3(4,4)
      COMMON/COEF/K(6,7)
      K(1,1)=C1(1,1)
      K(1,2)=0.
      K(1,3)=0.
      K(1,4)=C1(1,2)
      K(1,5)=C1(1,3)
      K(1,6)= - 2.*C1(1,4)
      K(2,1)=0.
      K(2,2)=C2(1,1)
      K(2,3)=0.
      K(2,4)=C2(1,2)
      K(2,5)=C2(1,3)
      K(2,6)= - 2.*C2(1,4)
      K(3,1)=0.
      K(3,2)=0.
      K(3,3)=C3(1,1)
      K(3,4)=C3(1,2)
      K(3,5)=C3(1,3)
      K(3,6)= - 2.*C3(1,4)
      K(4,1)=N1*C1(1,2)
      K(4,2)=N2*C2(1,2)
      K(4,3)=N3*C3(1,2)
      K(4,4)=N1*C1(2,2) + N2*C2(2,2) + N3*C3(2,2)
      K(4,5)=N1*C1(2,3) + N2*C2(2,3) + N3*C3(2,3)
      K(4,6)= - 2.*(N1*C1(2,4) + N2*C2(2,4) + N3*C3(2,4))
      K(5,1)=N1*C1(1,3)
      K(5,2)=N2*C2(1,3)
      K(5,3)=N3*C3(1,3)
      K(5,4)=N1*C1(2,3) + N2*C2(2,3) + N3*C3(2,3)
      K(5,5)=N1*C1(3,3) + N2*C2(3,3) + N3*C3(3,3)
      K(5,6)= - 2.*(N1*C1(3,4) + N2*C2(3,4) + N3*C3(3,4))
      CALL ROOT(5,X)
      SIGYZ1=C1(1,4)*X(1) + C1(2,4)*X(4) + C1(3,4)*X(5) + 2.*C1(4,4)
      SIGYZ2=C2(1,4)*X(2) + C2(2,4)*X(4) + C2(3,4)*X(5) + 2.*C2(4,4)
      SIGYZ3=C3(1,4)*X(3) + C3(2,4)*X(4) + C3(3,4)*X(5) + 2.*C3(4,4)
      SIGYZ=N1*SIGYZ1 + N2*SIGYZ2 + N3*SIGYZ3
      EPSX=N1*X(1) + N2*X(2) + N3*X(3)
      S14=.5*EPSX/SIGYZ
      S24=.5*X(4)/SIGYZ
      S34=.5*X(5)/SIGYZ
      S44=.5/SIGYZ
      RETURN
      END

END OF COMPILATION:        NO  DIAGNOSTICS.
```

```
      SUBROUTINE INVERT                                                      INV00100
C     INVERTS 3 X 3 MATRIX                                                   INV00200
      COMMON/MIX2/C(3,3), D(3), XX                                           INV00300
      COMMON/SOUT/S(3,3)                                                     INV00400
      D=C(1,1)*(C(2,2)*C(3,3) - C(3,2)*C(2,3)) - C(1,2)*(C(2,1)*C(3,3)       INV00500
     .  - C(3,1)*C(2,3)) + C(1,3)*(C(2,1)*C(3,2) - C(3,1)*C(2,2))           INV00600
      S(1,1)=(C(2,2)*C(3,3) - C(3,2)*C(2,3))/D                               INV00700
      S(1,2)=- (C(1,2)*C(3,3) - C(3,2)*C(1,3))/D                             INV00800
      S(1,3)=(C(1,2)*C(2,3) - C(2,2)*C(1,3))/D                               INV00900
      S(2,1)=- (C(2,1)*C(3,3) - C(3,1)*C(2,3))/D                             INV01000
      S(2,2)=(C(1,1)*C(3,3) - C(3,1)*C(1,3))/D                               INV01100
      S(2,3)=- (C(1,1)*C(2,3) - C(2,1)*C(1,3))/D                             INV01200
      S(3,1)=(C(2,1)*C(3,2) - C(3,1)*C(2,2))/D                               INV01300
      S(3,2)=- (C(1,1)*C(3,2) - C(3,1)*C(1,2))/D                             INV01400
      S(3,3)=(C(1,1)*C(2,2) - C(2,1)*C(1,2))/D                               INV01500
      RETURN                                                                 INV01600
      END                                                                    INV01700
```

END OF COMPILATION: NO DIAGNOSTICS.

```
      SUBROUTINE INVRS(N,XIN,XOUT)
C     COMPUTES INVERSE XOUT OF INPUT MATRIX  XIN
      DIMENSION C(6,7), XIN(6,6), XOUT(6,6), X(6)
      COMMON/COEF/C
      DO 30 J=1,6
      DO 30 I=1,6
   30 C(I,J)=XIN(I,J)
      DO 10 J=1,N
      DO 20 K=1,N
      C(K,N+1)=0.
      IF(K.EQ.J) C(K,N+1)=1.
   20 CONTINUE
      CALL ROOT(N,X)
      DO 40 L=1,N
   40 XOUT(L,J)=X(L)
   10 CONTINUE
      RETURN
      END
```

END OF COMPILATION: NO DIAGNOSTICS.

```
 1*            SUBROUTINE MIX                                                    MIX00100
 2*      C     COMPUTE EFFECTIVE ELASTIC CONSTANTS FROM THOSE OF CONSTITUENTS,   MIX00200
 3*      C     C11 , C12, C13, C33, GAMMA1, GAMMA3                               MIX00300
 4*            REAL N1, N2, K(2), KE                                             MIX00400
 5*            COMMON/ELAST/N1, C11(2), C12(2)                                   MIX00500
 6*            COMMON/MIX1/C1(3,3), C2(3,3), GAMMA1(3), GAMMA2(3), BETA1(3),     MIX00600
 7*           .            BETA2(3)                                             MIX00700
 8*            COMMON/MIX2/CE(3,3), GAMMAE(3), KE                                MIX00800
 9*            K(1)=C1(1,1) + C1(1,2)                                            MIX00900
10*            K(2)=C2(1,1) + C2(1,2)                                            MIX01000
11*            N2=1. - N1                                                        MIX01100
12*            H=N2*K(1) + N1*K(2) + C2(1,1) - C2(1,2)                           MIX01200
13*            KE=N1*K(1) + N2*K(2) - (K(1) - K(2))**2*N1*N2/H                   MIX01300
14*            CE(1,3)=N1*C1(1,3) + N2*C2(1,3) - (K(1) - K(2))*(C1(1,3) -        MIX01400
15*           .   C2(1,3))*N1*N2/H                                               MIX01500
16*            CE(3,3)=N1*C1(3,3) + N2*C2(3,3) - 2.*(C1(1,3) - C2(1,3))**2*N1*N2/MIX01600
17*           .   H                                                              MIX01700
18*            GAMMAE(1)=N1*GAMMA1(1) + N2*GAMMA2(1) - (GAMMA1(1) - GAMMA2(1))   MIX01800
19*           .   *(K(1) - K(2))*N1*N2/H                                         MIX01900
20*            GAMMAE(3)=N1*GAMMA1(3) + N2*GAMMA2(3) - 2.*(C1(1,3) - C2(1,3))*   MIX02000
21*           .   (GAMMA1(1) - GAMMA2(1))*N1*N2/H                                MIX02100
22*            CE(2,3)=CE(1,3)                                                   MIX02200
23*            CE(3,1)=CE(1,3)                                                   MIX02300
24*            CE(3,2)=CE(1,3)                                                   MIX02400
25*            GAMMAE(2)=GAMMAE(1)                                               MIX02500
26*            RETURN                                                            MIX02600
27*            END                                                               MIX02700

END OF COMPILATION:        NO  DIAGNOSTICS.
```

```
      SUBROUTINE MIXCC                                                  MXC001
C     CALCULATE COMPOSITE C11 AND C12 SEPARATELY                        MXC002
      REAL N1, K(6,7), KE                                               MXC003
      DIMENSION X(6)                                                    MXC004
      COMMON/ELAST/N1, C11(2), C12(2)                                   MXC005
      COMMON/MIX1/C1(3,3), C2(3,3), GAMMA1(3), GAMMA2(3), BETA1(3),     MXC006
     .            BETA2(3)                                             MXC007
      COMMON/MIX2/CE(3,3), GAMMAE(3), KE                                MXC008
      COMMON/COEF/K                                                     MXC009
      C11(1)=C1(1,1)                                                    MXC010
      C11(2)=C2(1,1)                                                    MXC011
      C12(1)=C1(1,2)                                                    MXC012
      C12(2)=C2(1,2)                                                    MXC013
      IF(N1.LE.0) N1=1.E-05
      CALL SETUP(1)
      CALL ROOT(6,X)                                                    MXC015
      SUM=X(1) + X(2) + X(3) + X(4)                                     MXC016
      ETA=C12(2)/C11(2)                                                 MXC017
      H=-X(1) - .5*(3. + ETA)*X(2)/ETA - .5*(1. - ETA)*X(3) + X(4)      MXC018
      SUM=SUM/3. - 2.*H/3.
      Y1=1./SUM
      IF(N1.LE.0) N1=1.E-05
      CALL SETUP(2)
      CALL ROOT(6,X)
      SIGRO=C11(2)*(X(1) + 3.*X(2) - X(3) - 3.*X(4)) - C12(2)
      C66= .5*(C11(2) - C12(2))
      SIGRTO=C66*(-X(1) - 1.5*(3. + ETA)*X(2)/ETA + .5*(1. - ETA)*X(3)
     .    - 3.*X(4) - 1.)
      Y2=SIGRO/3. - 2.*SIGRTO/3.
      Y=.5*(Y1 + Y2)
      CE(1,1)=.5*(Y + KE)                                               MXC021
      CE(1,2)=.5*(KE - Y)                                               MXC022
      CE(2,2)=CE(1,1)                                                   MXC023
      CE(2,1)=CE(1,2)                                                   MXC024
      RETURN                                                            MXC025
      END                                                               MXC026

END OF COMPILATION:        NO  DIAGNOSTICS.
```

```
      SUBROUTINE PRUFC(J,CIN)
      REAL NUXY(2), NUXZ(2), NUZX(2), N1                                PRU00400
      REAL NUTT,NUTA,NUTTF,NUTAF,NUTTM,NUTAM
      REAL NUCXYC,NUCXZC,NUCZXC
      REAL KX(2), KZ(2), KXE, KZE, KE                                   PRU00600
      DIMENSION CIN(8,3)
      DIMENSION BETAE(3), EX(2), EZ(2), RHO(2), G(2)
      COMMON/MIX1/C1(3,3), C2(3,3), GAMMA1(3), GAMMA2(3), BETA1(3),     PRU01200
     .     BETA2(3)                                                     PRU01300
      COMMON/MIX2/CE(3,3), GAMMAE(3), KE                                PRU01400
      COMMON/ELAST/N1,C11(2), C12(2)                                    PRU01500
      COMMON/SOUT/S(3,3)                                                PRU01600
      COMMON/INPUT/VFRAC(3),ANGLE(3),ET(3),EA(3),NUTT(3),NUTA(3),GA(3),
     .ALFT(3),ALFA(3),ETF(3),EAF(3),NUTTF(3),NUTAF(3),GAF(3),ALFTF(3),
     .ALFAF(3),VF(3),ETM(3),EAM(3),NUTTM(3),NUTAM(3),GAM(3),ALFTM(3),
     .ALFAM(3),VM(3)
      EX(1)=ETF(J)
      EZ(1)=EAF(J)
      NUXY(1)=NUTTF(J)
      NUXZ(1)=NUTAF(J)
      BETA1(1)=ALFTF(J)
      BETA1(3)=ALFAF(J)
      KX(1)=1.
      KZ(1)=1.
      RHO(1)=1.
      G(1)=GAF(J)
      EX(2)=ETM(J)
      EZ(2)=EAM(J)
      NUXY(2)=NUTTM(J)
      NUXZ(2)=NUTAM(J)
      BETA2(1)=ALFTM(J)
      BETA2(3)=ALFAM(J)
      KX(2)=1.
      KZ(2)=1.
      RHO(2)=1.
      G(2)=GAM(J)
C     CALCULATE CSUBIJ'S FOR FIBER                                      PRU03400
      NUZX(1)=(EX(1)*NUXZ(1))/EZ(1)                                     PRU03500
      DELTA=1. - NUXY(1)**2 - 2.*NUXZ(1)*NUZX(1) - 2.*NUXY(1)*NUXZ(1)   PRU03600
     .   *NUZX(1)                                                       PRU03700
      C1(1,1)=EX(1)*(1. - NUXZ(1)*NUZX(1))/DELTA                        PRU03800
      C1(1,2)=EX(1)*(NUXY(1) + NUXZ(1)*NUZX(1))/DELTA                   PRU03900
      C1(1,3)=EX(1)*(1. + NUXY(1))*NUXZ(1)/DELTA                        PRU04000
      C1(3,3)=EZ(1)*(1. - NUXY(1)**2)/DELTA                             PRU04100
      C1(2,1)=C1(1,2)                                                   PRU04200
      C1(2,2)=C1(1,1)                                                   PRU04300
      C1(2,3)=C1(1,3)                                                   PRU04400
      C1(3,1)=C1(1,3)                                                   PRU04500
      C1(3,2)=C1(1,3)                                                   PRU04600
C     CALCULATE CSUBIJ'S FOR MATRIX                                     PRU04700
      NUZX(2)=(EX(2)*NUXZ(2))/EZ(2)                                     PRU04800
      DELTA=1. - NUXY(2)**2 - 2.*NUXZ(2)*NUZX(2) - 2.*NUXY(2)*NUXZ(2)   PRU04900
     .   *NUZX(2)                                                       PRU05000
      C2(1,1)=EX(2)*(1. - NUXZ(2)*NUZX(2))/DELTA                        PRU05100
      C2(1,2)=EX(2)*(NUXY(2) + NUXZ(2)*NUZX(2))/DELTA                   PRU05200
      C2(1,3)=EX(2)*(1. + NUXY(2))*NUXZ(2)/DELTA                        PRU05300
      C2(3,3)=EZ(2)*(1. - NUXY(2)**2)/DELTA                             PRU05400
```

```
      C2(2,1)=C2(1,2)                                                   PRU05500
      C2(2,2)=C2(1,1)                                                   PRU05600
      C2(2,3)=C2(1,3)                                                   PRU05700
      C2(3,1)=C2(1,3)                                                   PRU05800
      C2(3,2)=C2(1,3)                                                   PRU05900
C     CALCULATE THERMAL STRESS COEFFS                                   PRU07900
      BETA1(2)=BETA1(1)                                                 PRU08000
      BETA2(2)=BETA2(1)                                                 PRU08100
      DO 30 I=1,3                                                       PRU08200
      GAMMA1(I)=0.                                                      PRU08300
      DO 30 JJ=1,3
   30 GAMMA1(I)=GAMMA1(I) + C1(I,JJ)*BETA1(JJ)
      DO 40 I=1,3
      GAMMA2(I)=0.                                                      PRU08700
      DO 40 JJ=1,3
   40 GAMMA2(I)=GAMMA2(I) + C2(I,JJ)*BETA2(JJ)
C     CALCULATE ELASTIC AND THERMAL STRESS COEFFS FOR COMPOSITE AS      PRU09200
C     FUNCTION OF FIBER VOLUME FRACTION, C11 + C12, C13, C33, GAMMA1,   PRU09300
C     GAMMA3                                                            PRU09400
      N1=VF(J)
      CALL MIX                                                          PRU09800
C     CALCULATE THERMAL EXPANSION COEFFS FOR COMPOSITE                  PRU09900
      BETAE(1)=.5*(GAMMAE(1)*CE(3,3) - GAMMAE(3)*CE(1,3))/(.5*KE       PRU10000
     .   *CE(3,3) - CE(1,3)**2)                                         PRU10100
      BETAE(3)=(.5*KE*GAMMAE(3) - CE(1,3)*GAMMAE(1))/(.5*KE             PRU10200
     .   *CE(3,3) - CE(1,3)**2)                                         PRU10300
      BETAE(2)=BETAE(1)                                                 PRU10400
      SAVEX=BETAE(1)
      SAVEZ=BETAE(3)
      CIN(7,J)=GAMMAE(1)
      CIN(8,J)=GAMMAE(3)
C     THERM COND FOR COMPOSITE                                          PRU10700
      KZE=N1*KZ(1) + (1. - N1)*KZ(2)                                    PRU10800
      Q=(KX(2) - KX(1))/(KX(1) + KX(2) + N1*(KX(2) - KX(1)))            PRU10900
      KXE=N1*KX(1)*(1. + (1. -N1)*Q) + (1. - N1)*KX(2)*(1. - N1*Q)      PRU11000
C     COMPOSITE DENSITY                                                 PRU11100
      RHOC=N1*RHO(1) + (1. - N1)*RHO(2)                                 PRU11200
C     COMPUTE C11 AND C12 FOR COMPOSITE                                 PRU11400
      CALL MIXCC                                                        PRU11500
      CALL INVERT                                                       PRU11600
      CIN(1,J)=CE(1,1)
      CIN(2,J)=CE(1,2)
      CIN(3,J)=CE(1,3)
      CIN(4,J)=CE(3,3)
C     COMPOSITE INPLANE SHEAR MODULUS                                   PRU12200
      CIN(5,J)=G(2)*(2.*N1*G(1) + (1. - N1)*(G(1) + G(2)))/(2.*N1*G(2)
     .   + (1. - N1)*(G(1) + G(2)))
      CIN(6,J)=.5*(CE(1,1) - CE(1,2))
C     CALCULATE COMPOSITE ENGINEERING MODULI AND SAVE FOR PRINTING      PRU12600
      ECXC=1./S(1,1)
      ECZC=1./S(3,3)
      NUCXYC= - S(1,2)*ECXC
      NUCXZC= - S(1,3)*ECZC
      NUCZXC=NUCXZC*ECXC/ECZC
      CALL STRESS(SIGZ1,SIGZ2,SIGR,SIGH11,SIGH21,SIGH22,SAVEX,SAVEZ)
      WRITE(6,103)
      WRITE(6,100) J
  100 FORMAT(/,' PROPERTIES OF PLY',I2,' AS CALCULATED WITH PRUFC')
      WRITE(6,101) ECXC,ECZC,NUCXYC,NUCXZC
  101 FORMAT(1H ,5X,'ET=',E11.5,5X,'EA=',E11.5,5X,'NUTT=',F8.5,5X,'NUTA=
     .',F8.5)
      WRITE(6,102) CIN(5,J),CIN(6,J),BETAE(1),BETAE(3)
  102 FORMAT(1H ,5X,'GAT=',E11.5,5X,'GTT=',E11.5,5X,'ALFT=',E11.5,5X,'AL
     .FA=',E11.5)
  103 FORMAT(//)
      RETURN
      END                                                               PRU22400
```

END OF COMPILATION: NO DIAGNOSTICS.

```
 1*            SUBROUTINE ROOT(N,XOUT)                                    R0000100
 2*      C     SOLVES N LINEAR SIMULTANEOUS EQUATIONS,  N.LE.6  UNLESS    R0000200
 3*      C     DIMENSIONS ARE CHANGED                                     R0000300
 4*            IMPLICIT DOUBLE PRECISION(A-H,O-Z)                         R0000400
 5*            REAL XOUT(6), XKIN(6,7)                                    R0000500
 6*            DIMENSION X(6), XK(6,7)                                    R0000600
 7*            COMMON/COEF/XKIN                                           R0000700
 8*            NP1=N + 1                                                  R0000800
 9*            NM1=N - 1                                                  R0000900
10*            NI=0                                                       R0001000
11*            DO 10 I=1,N                                                R0001100
12*            DO 10 J=1,NP1                                              R0001200
13*         10 XK(I,J)=XKIN(I,J)                                          R0001300
14*         20 NI=NI + 1                                                  R0001400
15*            IF(NI.GT.NM1) GO TO 80                                     R0001500
16*            NIP1=NI + 1                                                R0001600
17*            A=XK(NI,NI)                                                R0001700
18*            IM=NI                                                      R0001800
19*            DO 30 I=NIP1,N                                             R0001900
20*            IF(DABS(XK(I,NI)).LE.DABS(A)) GO TO 30                     R0002000
21*            A=XK(I,NI)                                                 R0002100
22*            IM=I                                                       R0002200
23*         30 CONTINUE                                                   R0002300
24*            IF(IM.LE.NI) GO TO 50                                      R0002400
25*            DO 40 J=NI,NP1                                             R0002500
26*            A=XK(IM,J)                                                 R0002600
27*            XK(IM,J)=XK(NI,J)                                          R0002700
28*         40 XK(NI,J)=A                                                 R0002800
29*         50 CONTINUE                                                   R0002900
30*            A=XK(NI,NI)                                                R0003000
31*            DO 60 J=NI,NP1                                             R0003100
32*         60 XK(NI,J)=XK(NI,J)/A                                        R0003200
33*            DO 70 I=NIP1,N                                             R0003300
34*            DO 70 J=NIP1,NP1                                           R0003400
35*         70 XK(I,J)=XK(I,NI)*XK(NI,J) - XK(I,J)                        R0003500
36*            GO TO 20                                                   R0003600
37*         80 CONTINUE                                                   R0003700
38*            X(N)=XK(N,NP1)/XK(N,N)                                     R0003800
39*            NX=N                                                       R0003900
40*         90 NX=NX - 1                                                  R0004000
41*            NXP1=NX + 1                                                R0004100
42*            IF(NX.LT.1) GO TO 110                                      R0004200
43*            X(NX)=XK(NX,NP1)                                           R0004300
44*            DO 100 K=NXP1,N                                            R0004400
45*        100 X(NX)=X(NX) - XK(NX,K)*X(K)                                R0004500
46*            X(NX)=X(NX)/XK(NX,NX)                                      R0004600
47*            GO TO 90                                                   R0004700
48*        110 CONTINUE                                                   R0004800
49*            DO 120 I=1,N                                               R0004900
50*        120 XOUT(I)=X(I)                                               R0005000
51*            RETURN                                                     R0005100
52*            END                                                        R0005200

NO OF COMPILATION:        NO  DIAGNOSTICS.
```

```
      SUBROUTINE SETUP(N)                                                SET00200
C     SETS UP MATRIX OF COEFFS USED BY SUBROUTINE MIXCC TO OBTAIN        SET00300
C     C11 AND C12                                                        SET00400
      REAL N1, K(6,7)                                                    SET00500
      DIMENSION ETA(2), C66(2)                                           SET00600
      COMMON/ELAST/N1, C11(2), C12(2)                                    SET00700
      COMMON/COEF/K
      IF(N.EQ.2) GO TO 10                                                SET00800
      R1=SQRT(N1)                                                        SET00900
      R12=R1**2                                                          SET01000
      R14=R12**2                                                         SET01100
      R16=R12**3                                                         SET01200
      ETA(1)=C12(1)/C11(1)                                               SET01300
      ETA(2)=C12(2)/C11(2)                                               SET01400
      C66(1)=.5*(C11(1) - C12(1))                                        SET01500
      C66(2)=.5*(C11(2) - C12(2))                                        SET01600
      K(1,1)=R14                                                         SET01700
      K(1,2)=R16                                                         SET01800
      K(1,3)=R12                                                         SET01900
      K(1,4)=1.                                                          SET02000
      K(1,5)=-R14                                                        SET02100
      K(1,6)=-R16                                                        SET02200
      K(1,7)=0.                                                          SET02300
      K(2,1)=-ETA(1)*ETA(2)*R14                                          SET02400
      K(2,2)=-.5*ETA(1)*(3. + ETA(2))*R16                                SET02500
      K(2,3)=-.5*ETA(1)*ETA(2)*(1. - ETA(2))*R12                         SET02600
      K(2,4)=ETA(1)*ETA(2)                                               SET02700
      K(2,5)=ETA(1)*ETA(2)*R14                                           SET02800
      K(2,6)=.5*ETA(2)*(3. + ETA(1))*R16                                 SET02900
      K(2,7)=0.                                                          SET03000
      K(3,1)=R14*(C11(2) - C12(2))                                       SET03100
      K(3,2)=0.                                                          SET03200
      K(3,3)=-R12*(C11(2) - ETA(2)*C12(2))                               SET03300
      K(3,4)=-3.*(C11(2) - C12(2))                                       SET03400
      K(3,5)=-R14*(C11(1) - C12(1))                                      SET03500
      K(3,6)=0.                                                          SET03600
      K(3,7)=0.                                                          SET03700
      K(4,1)=-2.*ETA(1)*ETA(2)*R14*C66(2)                                SET03800
      K(4,2)=-C66(2)*R16*ETA(1)*3.*(1. + ETA(2))                         SET03900
      K(4,3)=-C66(2)*ETA(1)*ETA(2)*(1. + ETA(2))*R12                     SET04000
      K(4,4)=-6.*C66(2)*ETA(1)*ETA(2)                                    SET04100
      K(4,5)=2.*C66(1)*ETA(1)*ETA(2)*R14                                 SET04200
      K(4,6)=3.*C66(1)*ETA(2)*(1. + ETA(1))*R16                          SET04300
      K(4,7)=0.                                                          SET04400
      K(5,1)=C11(2) - C12(2)                                             SET04500
      K(5,2)=0.                                                          SET04600
      K(5,3)=-C11(2) + ETA(2)*C12(2)                                     SET04700
      K(5,4)=-3.*(C11(2) - C12(2))                                       SET04800
      K(5,5)=0.                                                          SET04900
      K(5,6)=0.                                                          SET05000
      K(5,7)=1.                                                          SET05100
      K(6,1)=-2.*ETA(2)*C66(2)                                           SET05200
      K(6,2)=-3.*C66(2)*(1. + ETA(2))                                    SET05300
      K(6,3)=-C66(2)*ETA(2)*(1. + ETA(2))                                SET05400
      K(6,4)=-6.*ETA(2)*C66(2)                                           SET05500
      K(6,5)=0.                                                          SET05600
      K(6,6)=0.                                                          SET05700
      K(6,7)=-ETA(2)
      RETURN
   10 CONTINUE
      ETA(2)=C12(2)/C11(2)
      K(5,1)=1.
      K(5,2)=1.
      K(5,3)=1.
      K(5,4)=1.
      K(5,5)=0.
      K(5,6)=0.
      K(5,7)=1.
      K(6,1)= - ETA(2)
      K(6,2)= - .5*(3. + ETA(2))
      K(6,3)= - .5*(1. - ETA(2))*ETA(2)
      K(6,4)=ETA(2)
      K(6,5)=0.
      K(6,6)=0.
      K(6,7)= - ETA(2)
      RETURN                                                             SET05800
      END                                                                SET05900
```

```
 1*            SUBROUTINE STRESS(SIGZ1,SIGZ2,SIGR,SIGH11,SIGH21,SIGH22,BETAX,    STR00100
 2*           .   BETAZ)                                                          STR00200
 3*      C    CALCULATES INTERIOR FIBER AND MATRIX STRESSES                       STR00300
 4*           REAL N1                                                            STR00400
 5*           COMMON/MIX1/C1(3,3), C2(3,3), GAMMA1(3), GAMMA2(3), BETA1(3),      STR00500
 6*           .           BETA2(3)                                               STR00600
 7*           COMMON/ELAST/N1, C11(2), C12(2)                                    STR00700
 8*           A2=(C2(1,3)*BETAZ + (C2(1,1) + C2(1,2))*BETAX - GAMMA2(1))/        STR00800
 9*           .   (N1*2.*C2(1,1))                                                STR00900
10*           B2=BETAX - A2*N1                                                   STR01000
11*           B1=A2 + B2                                                         STR01100
12*           SIGZ1=2.*C1(1,3)*B1 + C1(3,3)*BETAZ - GAMMA1(3)                    STR01200
13*           SIGZ2=2.*C2(1,3)*B2 + C2(3,3)*BETAZ - GAMMA2(3)                    STR01300
14*           SIGR=(C1(1,1) + C1(1,2))*B1 + C1(1,3)*BETAZ - GAMMA1(1)            STR01400
15*           SIGH11=SIGR                                                        STR01500
16*           SIGH21=C2(1,2)*(-A2 + B2) + C2(1,1)*(A2 + B2) + C2(1,3)*BETAZ      STR01600
17*           .   - GAMMA2(1)                                                    STR01700
18*           SIGH22=C2(1,2)*(-A2*N1 + B2) + C2(1,1)*(A2*N1 + B2) + C2(1,3)      STR01800
19*           .   *BETAZ - GAMMA2(1)                                             STR01900
20*           RETURN                                                             STR02000
21*           END                                                                STR02100

) OF COMPILATION:        NO  DIAGNOSTICS.
```

```
      SUBROUTINE THERML(ALF,SIGDOT)
      DIMENSION X(6), ALF(4), SIGDOT(4,3)
      REAL N1, N2, N3, K
      COMMON/ONE/N1, N2, N3
      COMMON/TWO/C1(4,4), C2(4,4), C3(4,4)
      COMMON/COEF/K(6,7)
      COMMON/THREE/GAMMA1(4), GAMMA2(4), GAMMA3(4)
      K(1,1)=C1(1,1)
      K(1,2)=0.
      K(1,3)=0.
      K(1,4)=C1(1,2)
      K(1,5)=C1(1,3)
      K(1,6)=2.*C1(1,4)
      K(1,7)=GAMMA1(1)
      K(2,1)=0.
      K(2,2)=C2(1,1)
      K(2,3)=0.
      K(2,4)=C2(1,2)
      K(2,5)=C2(1,3)
      K(2,6)=2.*C2(1,4)
      K(2,7)=GAMMA2(1)
      K(3,1)=0.
      K(3,2)=0.
      K(3,3)=C3(1,1)
      K(3,4)=C3(1,2)
      K(3,5)=C3(1,3)
      K(3,6)=2.*C3(1,4)
      K(3,7)=GAMMA3(1)
      K(4,1)=N1*C1(1,2)
      K(4,2)=N2*C2(1,2)
      K(4,3)=N3*C3(1,2)
      K(4,4)=N1*C1(2,2) + N2*C2(2,2) + N3*C3(2,2)
      K(4,5)=N1*C1(2,3) + N2*C2(2,3) + N3*C3(2,3)
      K(4,6)=2.*(N1*C1(2,4) + N2*C2(2,4) + N3*C3(2,4))
      K(4,7)=N1*GAMMA1(2) + N2*GAMMA2(2) + N3*GAMMA3(2)
      K(5,1)=N1*C1(1,3)
      K(5,2)=N2*C2(1,3)
      K(5,3)=N3*C3(1,3)
      K(5,4)=N1*C1(2,3) + N2*C2(2,3) + N3*C3(2,3)
      K(5,5)=N1*C1(3,3) + N2*C2(3,3) + N3*C3(3,3)
      K(5,6)=2.*(N1*C1(3,4) + N2*C2(3,4) + N3*C3(3,4))
      K(5,7)=N1*GAMMA1(3) + N2*GAMMA2(3) + N3*GAMMA3(3)
      K(6,1)=N1*C1(1,4)
      K(6,2)=N2*C2(1,4)
      K(6,3)=N3*C3(1,4)
      K(6,4)=N1*C1(2,4) + N2*C2(2,4) + N3*C3(2,4)
      K(6,5)=N1*C1(3,4) + N2*C2(3,4) + N3*C3(3,4)
      K(6,6)=2.*(N1*C1(4,4) + N2*C2(4,4) + N3*C3(4,4))
      K(6,7)=N1*GAMMA1(4) + N2*GAMMA2(4) + N3*GAMMA3(4)
      CALL ROOT(6,X)
      EPSX=N1*X(1) + N2*X(2) + N3*X(3)
      ALF(1)=EPSX
      ALF(2)=X(4)
      ALF(3)=X(5)
      ALF(4)=X(6)
      SIGDOT(1,1)=C1(1,1)*X(1) + C1(1,2)*X(4) + C1(1,3)*X(5)
     .   + 2.*C1(1,4)*X(6) - GAMMA1(1)
      SIGDOT(2,1)=C1(1,2)*X(1) + C1(2,2)*X(4) + C1(2,3)*X(5)
     .   + 2.*C1(2,4)*X(6) - GAMMA1(2)
      SIGDOT(3,1)=C1(1,3)*X(1) + C1(2,3)*X(4) + C1(3,3)*X(5)
     .   + 2.*C1(3,4)*X(6) - GAMMA1(3)
      SIGDOT(4,1)=C1(1,4)*X(1) + C1(2,4)*X(4) + C1(3,4)*X(5)
     .   + 2.*C1(4,4)*X(6) - GAMMA1(4)
      SIGDOT(1,2)=C2(1,1)*X(2) + C2(1,2)*X(4) + C2(1,3)*X(5)
     .   + 2.*C2(1,4)*X(6) - GAMMA2(1)
```

```
66*            SIGDOT(2,2)=C2(1,2)*X(2) + C2(2,2)*X(4) + C2(2,3)*X(5)
67*           .   + 2.*C2(2,4)*X(6) - GAMMA2(2)
68*            SIGDOT(3,2)=C2(1,3)*X(2) + C2(2,3)*X(4) + C2(3,3)*X(5)
69*           .   + 2.*C2(3,4)*X(6) - GAMMA2(3)
70*            SIGDOT(4,2)=C2(1,4)*X(2) + C2(2,4)*X(4) + C2(3,4)*X(5)
71*           .   + 2.*C2(4,4)*X(6) - GAMMA2(4)
72*            SIGDOT(1,3)=C3(1,1)*X(3) + C3(1,2)*X(4) + C3(1,3)*X(5)
73*           .   + 2.*C3(1,4)*X(6) - GAMMA3(1)
74*            SIGDOT(2,3)=C3(1,2)*X(3) + C3(2,2)*X(4) + C3(2,3)*X(5)
75*           .   + 2.*C3(2,4)*X(6) - GAMMA3(2)
76*            SIGDOT(3,3)=C3(1,3)*X(3) + C3(2,3)*X(4) + C3(3,3)*X(5)
77*           .   + 2.*C3(3,4)*X(6) - GAMMA3(3)
78*            SIGDOT(4,3)=C3(1,4)*X(3) + C3(2,4)*X(4) + C3(3,4)*X(5)
79*           .   + 2.*C3(4,4)*X(6) - GAMMA3(4)
80*            RETURN
81*            END

END OF COMPILATION:        NO  DIAGNOSTICS.
```